

NUREG/CR-5646
EGG-2655

Piping System Response During High-Level Simulated Seismic Tests at the Heissdampfreaktor Facility (SHAM Test Facility)

Prepared by
R. Steele, Jr., M. E. Nitzel

Idaho National Engineering Laboratory
EG&G Idaho, Inc.

Prepared for
U.S. Nuclear Regulatory Commission

AVAILABILITY NOTICE

Availability of Reference Materials Cited in NRC Publications

Most documents cited in NRC publications will be available from one of the following sources:

1. The NRC Public Document Room, 2120 L Street, NW., Lower Level, Washington, DC 20555
2. The Superintendent of Documents, U.S. Government Printing Office, P.O. Box 37082, Washington, DC 20013-7082
3. The National Technical Information Service, Springfield, VA 22161

Although the listing that follows represents the majority of documents cited in NRC publications, it is not intended to be exhaustive.

Referenced documents available for inspection and copying for a fee from the NRC Public Document Room include NRC correspondence and internal NRC memoranda; NRC bulletins, circulars, information notices, inspection and investigation notices; licensee event reports; vendor reports and correspondence; Commission papers; and applicant and licensee documents and correspondence.

The following documents in the NUREG series are available for purchase from the GPO Sales Program: formal NRC staff and contractor reports, NRC-sponsored conference proceedings, international agreement reports, grant publications, and NRC booklets and brochures. Also available are regulatory guides, NRC regulations in the *Code of Federal Regulations*, and *Nuclear Regulatory Commission Issuances*.

Documents available from the National Technical Information Service include NUREG-series reports and technical reports prepared by other Federal agencies and reports prepared by the Atomic Energy Commission, forerunner agency to the Nuclear Regulatory Commission.

Documents available from public and special technical libraries include all open literature items, such as books, journal articles, and transactions. *Federal Register* notices, Federal and State legislation, and congressional reports can usually be obtained from these libraries.

Documents such as theses, dissertations, foreign reports and translations, and non-NRC conference proceedings are available for purchase from the organization sponsoring the publication cited.

Single copies of NRC draft reports are available free, to the extent of supply, upon written request to the Office of Administration, Distribution and Mail Services Section, U.S. Nuclear Regulatory Commission, Washington, DC 20555.

Copies of industry codes and standards used in a substantive manner in the NRC regulatory process are maintained at the NRC Library, 7920 Norfolk Avenue, Bethesda, Maryland, for use by the public. Codes and standards are usually copyrighted and may be purchased from the originating organization or, if they are American National Standards, from the American National Standards Institute, 1430 Broadway, New York, NY 10018.

DISCLAIMER NOTICE

This report was prepared as an account of work sponsored by an agency of the United States Government. Neither the United States Government nor any agency thereof, or any of their employees, makes any warranty, expressed or implied, or assumes any legal liability of responsibility for any third party's use, or the results of such use, of any information, apparatus, product or process disclosed in this report, or represents that its use by such third party would not infringe privately owned rights.

Piping System Response During High-Level Simulated Seismic Tests at the Heissdampfreaktor Facility (SHAM Test Facility)

Manuscript Completed: June 1992
Date Published: July 1992

Prepared by
R. Steele, Jr., M. E. Nitzel

G. H. Weidenhamer, NRC Technical Monitor

Idaho National Engineering Laboratory
Managed by the U.S. Department of Energy

EG&G Idaho, Inc.
Idaho Falls, ID 83415

Prepared for
Division of Engineering
Office of Nuclear Regulatory Research
U.S. Nuclear Regulatory Commission
Washington, DC 20555
NRC FIN A6857
Under DOE Contract No. DE-AC07-76ID01570

ABSTRACT

The SHAM seismic research program studied the effects of increasing levels of seismic excitation on a full-scale, in situ nuclear piping system containing a naturally aged United States (U.S.) 8-in. motor-operated gate valve. The program was conducted by Kernforschungszentrum Karlsruhe at the Heissdampfreaktor near Frankfurt, Germany. Participants included the United States, Germany, and England. Fifty-one experiments were conducted, with the piping supported by six different piping support systems, including a typical stiff U.S. piping support system of snubbers and rigid struts. This report specifically addresses the tests conducted with the U.S. system. The piping system withstood large displacements caused by overload snubber failures and local piping strains. Although some limit switch chatter was observed, the motor operator and valve functioned smoothly throughout the tests. The results indicate that sufficient safety margins exist when commonly accepted design methods are applied and that piping systems will likely maintain their pressure boundary in the presence of severe loading and the loss of multiple supports.

FIN No. A6857—Seismic tests of U.S. 8-in. motor-operated gate valve and stiff U.S. piping support system.

CONTENTS

ABSTRACT	iii
LIST OF FIGURES	vii
LIST OF TABLES	viii
EXECUTIVE SUMMARY	ix
ACKNOWLEDGMENTS	xiii
ACRONYMS, ABBREVIATIONS, AND DEFINITIONS	xv
1. INTRODUCTION	1
1.1 Background	1
1.2 Objectives	3
1.3 Qualification Standards and Regulatory Guides	3
2. TEST FACILITY AND SYSTEM DESCRIPTION	5
2.1 Heissdampfreaktor (HDR)	5
2.2 Versuchskreislauf (VKL) Piping System	5
2.3 Seismic Simulation	5
2.4 Versuchskreislauf (VKL) Piping Support Systems	8
2.5 Gate Valve	10
2.6 Instrumentation	10
3. PRETEST DESIGN ANALYSES	11
3.1 General Information	11
3.2 Design Criteria	11
3.3 Piping Material Data	11
3.4 Versuchskreislauf (VKL) Piping System Test Operating Conditions	11
3.5 Analysis Procedure	13
3.5.1 Computer Code Used	13
3.5.2 Load Cases Considered	13
3.5.3 Method of Calculation	13
3.5.4 Damping Values Used	14

3.5.5	Modeling of Supports	14
3.5.6	Finite Element Model	14
3.5.7	Stress Evaluation Methodology	14
3.6	Design Analysis Results	14
4.	TEST RESULTS	18
4.1	General Information	18
4.2	Data Conversion	18
4.3	Piping System Dynamic Response	19
4.3.1	Test T41.81.1	19
4.3.2	Test T41.81.2	23
4.3.3	Test T41.81.3	25
4.4	Dynamic Support Performance	29
4.4.1	Tests Prior to T41.81.1	29
4.4.2	Test T41.81.1	30
4.4.3	Test T41.81.2	33
4.4.4	Test T41.81.3	37
4.5	Performance of Other Support Components	41
4.6	Gate Valve Performance	41
5.	CONCLUSIONS	45
5.1	Piping System Dynamic Response	45
5.2	Dynamic Support Performance	46
5.3	Gate Valve Performance	47
5.4	General Conclusions	47
6.	REFERENCES	49
Appendix A—Design Report: Servohydraulic Excitation of Mechanical Equipment HDR		
Test Group SHAM vs. No. T41		A-1
Appendix B—Determination of Allowable Stress Values Used on the VKL Piping		
Analysis for the SHAM Test Series		B-1
Appendix C—Power Spectral Density Curves for Selected Points—SHAM Tests		
T41.81.1, T41.81.2, and T41.81.3		C-1

LIST OF FIGURES

1-1. VKL piping system with NRC support configuration	2
2-1. Simplified view of the HDR facility showing VKL room	6
2-2. Design response spectrum used in the VKL piping system analysis	7
3-1. NUPIPE-II finite element model of the VKL piping system	15
4-1. 200% SSE PVRC response spectrum, Test T41.81.1, H-25 location	20
4-2. 200% SSE PVRC response spectrum, Test T41.81.1, H-5 location	20
4-3. 600% SSE response spectrum, Test T41.81.2, ES3011, PVRC damping	23
4-4. 600% SSE response spectrum, Test T41.81.2, ES3021, PVRC damping, H-25 location	24
4-5. 800% SSE response spectrum, Test T41.81.3, ES3011, PVRC damping, H-5 location	25
4-6. 800% SSE response spectrum, Test T41.81.3, ES3021, PVRC damping, H-25 location	26
4-7. Circumferential strain at Elbow 1 (Test T41.81.3)	27
4-8. Longitudinal strain at Elbow 1 (Test T41.81.3)	27
4-9. Circumferential strain at Elbow 2 (Test T41.81.3)	28
4-10. Longitudinal strain at Elbow 2 (Test T41.81.3)	28
4-11. Force time history plot for H-8 (Test T41.81.2)	34
4-12. Displacement time history for H-8 (Test T41.81.2)	34
4-13. Force time history plot for H-22 (Test T41.81.2)	35
4-14. Displacement time history for H-22 (Test T41.81.2)	35
4-15. Force time history plot for H-12 (Test T41.81.2)	36
4-16. Displacement time history for H-12 (Test T41.81.2)	36
4-17. Photographs of failed H-22 (PSA-1/4) snubber components	38
4-18. Force time history plot for H-7 (Test T41.81.2)	39
4-19. Displacement time history for H-7 (Test T41.81.2)	39
4-20. Photographs of failed H-7 (PSA-1) snubber components	40

4-21. Force time history plot for H-6 (Test T41.81.3)	42
4-22. Displacement time history for H-6 (Test T41.81.2)	42
4-23. Valve current history for the 800% SSE test	43

LIST OF TABLES

2-1. VKL piping and material data	7
2-2. U.S. support configuration and design loads	9
2-3. Participants support configurations for the SHAM test series	9
3-1. VKL piping material correlations	12
3-2. ASME Code allowable stresses used for design analysis	12
3-3. VKL piping system maximum design analysis stresses	16
3-4. U.S. Support configuration component information	17
4-1. U.S. stiff support system test matrix	19
4-2. VKL piping system ASME Code Equation 9 stress comparisons	21
4-3. Summary of predicted vibrational modes below 12 Hz	22
4-4. Snubber installation matrix for U.S. stiff support system	30
4-5. U.S. stiff support configuration maximum dynamic support loads	31
4-6. U.S. stiff support configuration maximum snubber displacement	32
4-7. Gate valve accelerations	44

EXECUTIVE SUMMARY

This report describes the analysis and results from the Servohydraulische Anregung Maschinetchnik (SHAM), an international seismic research program in which the U.S. Nuclear Regulatory Commission (USNRC) and the Idaho National Engineering Laboratory (INEL) participated. The program was conducted by Kernforschungszentrum Karlsruhe (KfK) at the decommissioned Heissdampfreaktor (HDR) located near Frankfurt, Germany. Participating countries were the United States, Germany, and England. The SHAM experiments at HDR consisted of the direct excitation of a piping system called the Versuchskreislauf (VKL) by using two large 40-ton servohydraulic shakers mounted to the HDR containment building and attached to the piping system at two different locations. The research program included the study of the effects of increasing levels of seismic excitation on a full-scale, in situ nuclear piping system containing a naturally aged U.S. 8-in. motor-operated gate valve.

Earthquake-like displacement histories were input to the servohydraulic shakers. Inputs to the piping system started with a magnitude of 0.6 g ZPA for the baseline load case (hereafter referred to as 1 SSE or 100% SSE) and were stepped up, using the same frequency content, to a maximum of 800 percent of the baseline load (8 SSE). In all, 51 experiments were conducted, with the piping supported by six different piping support systems. These included support configurations typical of those commonly used in European power plants, a typical stiff U.S. piping support system made up of snubbers and rigid struts, support systems containing snubber replacement devices, and a very flexible system. This report will address the tests performed with the U.S. stiff support configuration.

The objectives of the INEL portion of the research program were to

- Measure the effects of increasingly greater dynamic loadings on gate-valve operability and determine, if possible, the loadings

where the U.S. gate valve would sustain structural damage

- Determine the safety margins and failure modes of nuclear-grade snubbers, rigid supports, trunion attachments, and concrete anchors when subjected to dynamic excitation
- Determine the effects of individual support and multiple support failures on piping response in a simulated seismic event
- Obtain data that could be used to compare the performance of stiff, flexible, very flexible, and snubber replacement piping support systems.

The results of this testing will contribute to the technical basis used for development of equipment qualification standards and will help establish the seismic safety margins in piping and piping support system components.

With these servohydraulic shakers, the input loads could be adjusted independently of the excitation frequency to balance the input to the entire piping system. This offers the possibility of simulating a wide range of time histories. Two excitation points were used for all the tests reported here. Both of these shakers provided input in the horizontal plane in the global X direction. While actual seismic input is applied to piping systems through all their dynamic supports (snubbers and rigid struts) and anchor points, program scope limitations and the physical limitations of the facility made this approach impractical. Since the test objectives deal with the ability of the piping and supports to withstand extremely high level loads, the two points of dynamic excitation used in the SHAM test series were sufficient to deliver the level of loading that will enable the test objectives to be realized.

Based on the pretest information, a model of the piping and support system was developed and analyzed. Commonly accepted nuclear industry design practices were used in the analysis effort.

By agreement among the test participants, all piping in the VKL system was assumed to be ASME Code Class 2, Section III, Division I, Subsection NC (Class 2) of the ASME Boiler and Pressure Vessel Code was used to define the allowable stress criteria for analyses of the piping system and the derivation of support loads that were used to design the piping supports. The test loads were analyzed using Service Level C values to define the maximum allowable stresses. Analysis of the VKL piping system considered the effects of weight, pressure, thermal expansion, and the dynamic input intended to simulate the seismic event. Dynamic analyses were performed using the response spectrum technique in conjunction with ASME Code Case N-411 damping. Maximum design loads for the piping supports were obtained from the computer analysis and used to select appropriate sizes of support components. Components commonly used throughout the nuclear industry were selected for use. Piping support substructures linking component supports (snubbers, struts, spring hangers, etc.) to their grounding points on the facility walls or other major structures were analyzed in accordance with ASME Code rules and commonly accepted industry practices.

Only the U.S. stiff piping support system components (snubbers, struts, and anchors) were sized to determine safety margins and failure modes. All other participants' support system components were sized for much higher loads, in an effort to avoid support failures in these configurations. The design loads for each dynamic pipe support in the U.S. stiff configuration were calculated from seismic analyses based on 100% SSE excitation levels. The supports were then sized for each location, using the support manufacturer's published ASME Code, Level C Allowables. The reason for the reduced conservatism in sizing the supports was so that support safety margins and failure modes could be determined in the lower level tests and the effects of multiple support failures could be investigated at the higher loadings.

While each piping system includes its own specific details regarding materials, geometry, and

support configuration, the VKL system with the U.S. stiff support configuration can be considered typical of seismically designed piping systems found throughout the U.S. nuclear industry. The VKL piping system was exposed to significant simulated seismic loadings, and the specific results from tests at input levels of 200% SSE, 600% SSE, and 800% SSE were examined.

The 200% SSE test results, with all dynamic supports operable, were most comparable to the analytical predictions. Snubber overload failures in the early tests of the U.S. stiff support configuration delayed characterization of the piping system, so the final 200% SSE test was performed with snubbers larger than those called for by the design calculations to ensure completion of the test without snubber failures. These results showed that the post-test design analysis predicted maximum stresses at most of the same locations where the maximum strains were recorded during the tests. Similarly, the PSDs calculated from acceleration histories show that the piping responses were generally in the same frequency bands as the natural frequencies and mode shapes predicted by computer.

Loadings in excess of 600 and 800% SSE were applied to the U.S. system, resulting in significant piping system responses and the overload failure of several individual snubbers. The piping system sustained multiple adjacent support failures, with measured strains greater than yield, yet no significant piping system damage occurred. With the failure of the snubbers at four locations, a major portion of the piping system was left without dynamic supports in the vertical (Y) direction. The displacement and the strain data also reflect a decrease in the response frequency, which was expected as multiple snubber failures occurred and the piping system became more flexible. The timing of the failures of three of the snubbers and the force and displacement data for these three snubbers indicate that a zipper effect failure phenomenon occurred. However, in spite of the large increases in displacements and strains, no physical failure of the piping occurred.

When the analytically predicted support loads are compared to test loads scaled to the 100%

SSE level it is observed that about half of the support loads were overpredicted while about half were underpredicted. Except for two cases, all snubber failures occurred at loads well above their design ratings. In one case, a load of 8.67 times the design rating was sustained prior to failure. The test data show that most snubbers operated within their performance specifications, such as dead band travel, until a failure occurred.

The U.S. 8-in. motor-operated gate valve operated smoothly during all tests in the SHAM series. In the highest level tests, some limit switch chatter was observed; however, the limit switch

contacts did not stay open long enough to cause the motor controller circuit to interrupt current flow to the motor. The data show that even under the most severe structural loading experienced during any of the 51 tests, the valve operated smoothly.

The test results indicate that sufficient safety margins exist when commonly accepted design methods and criteria are applied and that piping systems will likely maintain their pressure boundary in the presence of severe loading and the loss of multiple supports.

ACKNOWLEDGMENTS

The efforts of many people and organizations were required to successfully complete the SHAM test series. The authors wish to thank Hr. Dr. L. Malcher and Hr. Schrammel from KfK and Herren L. Löhr and R. Machad from HDR. Drs. G. H. Weidenhamer and J. F. Costello, the U.S. Nuclear Regulatory Commission program managers provided direction throughout the program. Dr. C. Kot of Argonne National Laboratory also contributed to the success of this effort. The authors wish to thank Drs. J. G. Arendts and A. G. Ware of the Idaho National Engineering Laboratory for their consultation and assistance in completing this work. We would also like to thank Hr. Schrammel, Mr. H. L. Magleby, and Drs. Weidenhamer and Kot for the valuable review of the draft report.

ACRONYMS, ABBREVIATIONS, AND DEFINITIONS

ANL	Argonne National Laboratory
ASME/ANSI	American Society of Mechanical Engineers/American National Standards Institute, Standard B16.41
ASME Code	The American Society of Mechanical Engineers Boiler and Pressure Vessel Code, Section III, Subsection NC-3650, 1980 Addition.
Baseline Functional	A functional test performed without dynamic loading to establish a normal measurement
Bechtel	Bechtel Power Corporation
CEGB	Central Electricity Generating Board of the United Kingdom
Cloud	Robert L. Cloud Associates, Inc.
DIN	Deutsche Institute für Norming
EPRI	Electric Power Research Institute
HDR	Heissdampfreaktor (superheated steam reactor)
HDU	Heissdampfumformer (steam convertor)
INEL	Idaho National Engineering Laboratory
ISM	independent support motion
KfK	Kernforschungszentrum Karlsruhe (Nuclear Research Center)
kip	Unit of measure equal to 1000 lbs dead weight
ksi	kips per square inch, common indicator of stress
KWU	Kraftwerk Union AG (German architect-engineer)
LBF	Fraunhofer Institut für Betriebsfestigkeit Darmstadt (research institute)
Nupipe-II	Piping analysis computer code developed by the Quadrex Corporation, Campbell, California
PSD	power spectral density
SHAG	Shakergebäude (building shaker)
SHAM	Servohydraulische Anregung Maschinetechnik (Servo Hydraulic Shaker Technology)
SMACS	Seismic Methodology Analysis Chain with Statistics Computer Code

SSE	Safe Shutdown Earthquake (IEEE 344)
S_c	Piping material allowable at room temperature (cold)
S_h	Piping material allowable at operating temperature (hot)
S_u	Material ultimate strength
S_y	Material yield strength
NRC	U.S. Nuclear Regulatory Commission
VKL	Versuchskreislauf (experimental piping system)
ZPA	zero period acceleration (IEEE 344)

Piping System Response During High-Level Simulated Seismic Tests at the Heissdampfreaktor Facility (SHAM Test Series)

1. INTRODUCTION

1.1 Background

During the spring of 1988, the Idaho National Engineering Laboratory (INEL) and the Argonne National Laboratory (ANL), under sponsorship of the U.S. Nuclear Regulatory Commission (NRC), participated in the Kernforschungszentrum Karlsruhe (KfK)-designated Servohydraulische Anregung Maschinetchnik (SHAM) test series. KfK, Kraftwerk Union (KWU), the Electric Power Research Institute (EPRI), the Fraunhofer Institut für Betriebsfestigkeit (LBF) in Darmstadt, and the Central Electricity Generating Board of the United Kingdom (CEGB) also took part in the series. This test program was conducted at the Heissdampfreaktor (HDR), a decommissioned experimental reactor facility located near Frankfurt, Germany.

Each of the multinational participants had different objectives for participation in the SHAM Test Program.

The U.S. NRC sponsored the participation of the INEL and ANL. The INEL participation is reported in this report. ANL's participation is reported in NUREG/CR-5841 *Verification of Non-linear Piping Response Calculation with Data from Seismic Testing of an In-plant Piping System*.

EPRI sponsored two companies, Bechtel and Cloud, who were developing snubber replacement devices. We do not know if EPRI reported on this work.

KfK and KWU were performing confirmation work for the German Nuclear Seismic Program. KfK has put out Technical Report PHDR 96-90 September, 1990 (Structural Dynamics Investiga-

tion at the HDR) Evaluation Report. Only the summary is in English.

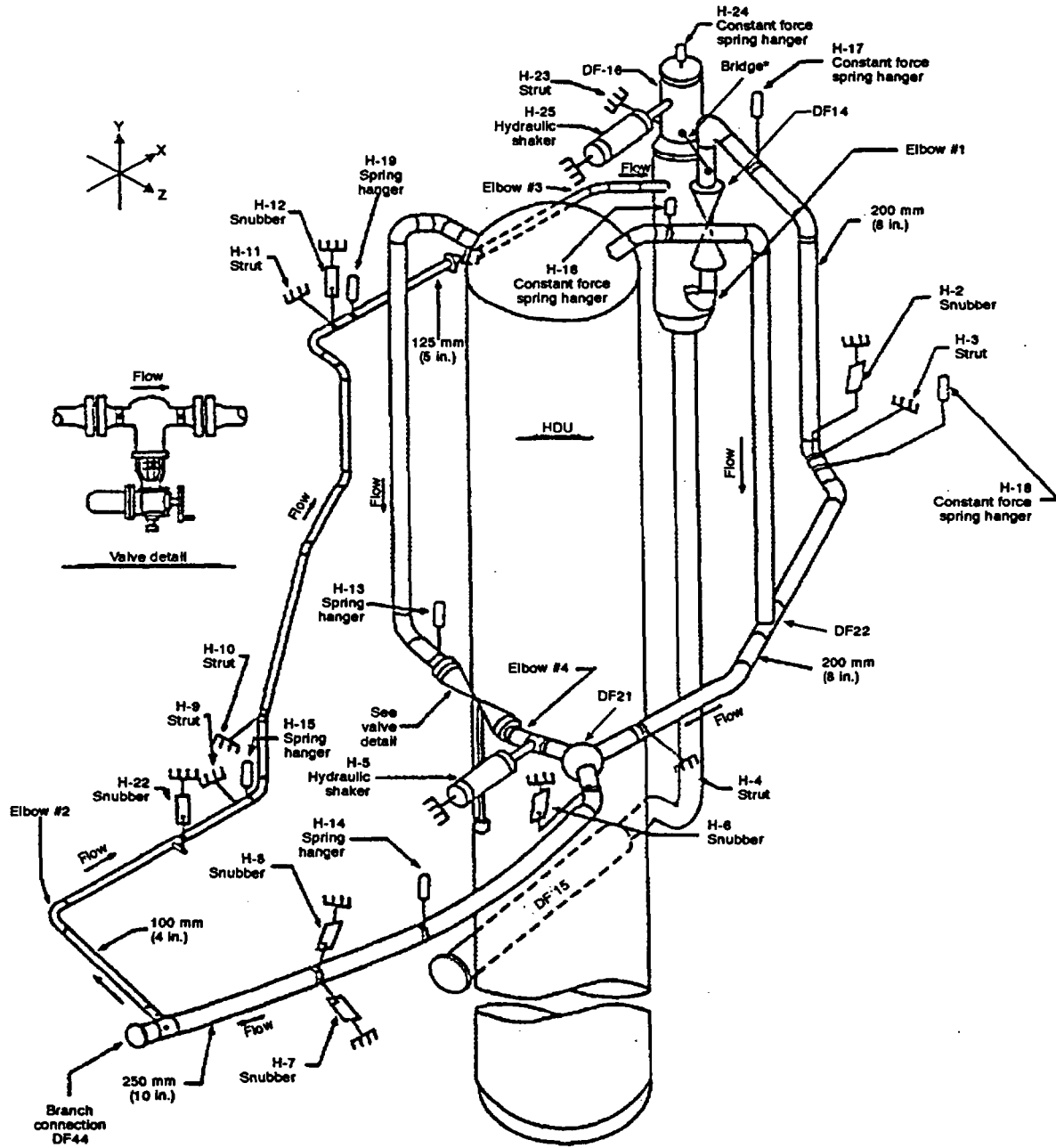
CEGB was performing confirmation work for England's first PWR, Sizewell B.

LBF designed and operated the Hydraulic Shaker System.

The SHAM experiments consisted of the direct excitation of a piping system called the Versuchskreislauf (VKL) (Figure 1-1). This was accomplished by using two large 40-ton servohydraulic shakers mounted to the HDR containment building and attached to the piping system. The research program studied the effects of increasing levels of seismic excitation on a full-scale in situ nuclear piping system containing a naturally aged U.S. 8-in. motor-operated gate valve.

Earthquake-like displacement histories were input to the servohydraulic shakers. Inputs to the piping system started with a magnitude of 0.6 g zero periodic acceleration (ZPA) for the baseline load case [hereafter referred to as 1 safe shutdown earthquake (SSE) or 100% SSE] and were stepped up, using the same frequency content, to a maximum of 800% of the baseline load (8 SSE). In all, 51 experiments were conducted, with the piping supported by six different piping support systems. These included support configurations typical of those commonly used in European power plants, a typical stiff U.S. piping support system made up of snubbers and rigid struts, support systems containing snubber replacement devices, and a very flexible system.

This report presents a general overview of the SHAM test program and a specific review of the U.S. stiff support system response at 200, 600, and 800% SSE loadings.



* Bridge between DF16 and DF14 installed for NRC high level tests only

M638 rs-0692-01

Figure 1-1. VKL piping system with NRC support configuration.

1.2 Objectives

Objectives of the INEL's participation in this multinational program were to

- Measure the effects of increasingly greater dynamic loadings on gate valve operability, and determine, if possible, the loadings where the valve would sustain structural damage
- Determine the safety margins and failure modes of nuclear-grade snubbers, rigid supports, trunion attachments, and concrete anchors when subjected to dynamic excitation
- Determine the effects of individual and multiple support failures on piping response in a simulated seismic event
- Obtain data that could be used as a basis for comparing the performance of stiff, flexible, very flexible, and snubber replacement piping support systems.

1.3 Qualification Standards and Regulatory Guides

The results of this testing will contribute to the technical basis used for supporting and developing equipment qualification standards and will help establish the seismic safety margins in piping and piping support system components. The following equipment qualification standards and regulatory guides may be affected by the HDR research results:

- American Society of Mechanical Engineers, "Functional Qualification Requirements for Power Operated Active Valve Assemblies for Nuclear Power Plants," ANSI/ASME B16.41, currently being revised as QME-QV
- American Society of Mechanical Engineers, "Self-Operated and Power-Operated Safety-Related Valves Safety Specification Standard," ANSI/ASME N278.1-1975
- Institute of Electrical and Electronic Engineers, "Recommended Practices for Seismic Qualification of Class 1E Equipment for Nuclear Power Generating Stations," IEEE Standard 344, 1987
- Institute of Electrical and Electronic Engineers, "Qualification of Safety-Related Valve Actuators," IEEE Standard 382, 1980
- Institute of Electrical and Electronic Engineers, "Design Qualification of Safety Systems Equipment Used in Nuclear Power Generating Stations," IEEE Standard 627, 1980
- NRC, "Development of Floor Design Spectra for Seismic Design of Floor-Supported Equipment or Components," Regulatory Guide 1.122
- NRC, "Damping Values for Seismic Design of Nuclear Power Plants," Regulatory Guide 1.61
- NRC, "Functional Specification for Active Valve Assemblies in Systems Important to Safety in Nuclear Power Plants," Regulatory Guide 1.148
- NRC, "Seismic Qualification of Electric Equipment for Nuclear Power Plants," Regulatory Guide 1.100
- NRC, "Qualification Tests of Electric Valve Operators Installed Inside the Containment of Nuclear Power Plants," Regulatory Guide 1.73
- NRC, "USNRC Standard Review Plan, Section 3.9.3., ASME Code Class 1, 2, and 3 Components," Component Supports, and Core Support Structures, NUREG-0800, 1981
- NRC, "Qualification and Acceptance Tests for Snubbers Used in Systems Important to Safety," Draft Regulatory Guide SC 708-4, Revision 1, 1981

Introduction

- American Society of Mechanical Engineers, "Examination and Performance Testing of Nuclear Power Plant Dynamic Restraints (Snubbers)," ANSI ASME OM4, 1982
- American Society of Mechanical Engineers, *Boiler and Pressure Vessel Code, Section XI, Subsection IWF, Requirements for Class 1, 2, 3 and MC Component Supports of Light-Water Cooled Power Plants.*

2. TEST FACILITY AND SYSTEM DESCRIPTION

2.1 Heissdampfreaktor (HDR)

The HDR is a decommissioned experimental reactor facility located near Frankfurt, Germany. A simplified cross section of the facility is shown in Figure 2-1. The facility has been used for several other testing programs such as the Shakergebäude (SHAG) test series.¹

2.2 Versuchskreislauf (VKL) Piping System

The VKL piping system is constructed of stainless steel in four metric pipe sizes equivalent to 10-, 8-, 5-, and 4-in. nominal pipe size. The majority of the piping is 8-in. (200-mm) nominal size. The system is located between the 18- and 24-m elevations in the HDR facility, as shown in Figure 2-1. The system consists of two parallel flow loops connected to a large vessel called the Heissdampfumformer (HDU) and a manifold header (DF 16). Figure 1-1 shows a general arrangement of the VKL piping system, major components, and pipe sizes. Further information regarding piping sizes and materials is included in Table 2-1. The VKL system is capable of operating under high temperature and high pressure; however, for the SHAM tests, the fluid remained pressurized at 1000 psig (70 bar) and ambient temperature to avoid the risk of damaging the sensitive instrumentation in the event of a test-induced line rupture. Seismic tests were conducted without fluid flow through the system; valve functional tests were conducted with flow through the valve.

2.3 Seismic Simulation

We accomplished the seismic excitation of the VKL piping system by using two large 40-ton servohydraulic shakers mounted to the HDR containment building and attached to the piping system. With these shakers, the input loads could be adjusted independently of the excitation frequency. This offers the possibility of simulating a

wide range of seismic time histories with a uniform input to the piping system. We used two excitation points for all the tests reported here. One point was located between the spherical tee and the 8-in. gate valve replacing the horizontal strut at the H5 support attachment point. The second shaker was attached to the 12-in. (300-mm) nominal size piping directly above the DF16 component. Both of these shakers provided input in the horizontal plane in the global X direction. The shaker locations and the directions of input can be visualized in relation to the complete VKL piping system by referring to Figure 1-1. Further details regarding the individual components making up the shaker system can be found in Appendix A.

Except for the tests of the CEGB support system, all test configurations used the same earthquake history. Differences in the displacement magnitudes were used to amplify the input to simulate the various seismic levels (1 SSE, 6 SSE, etc.) desired for each test. Inputs to the piping system started with a magnitude of 0.6 g ZPA for the 1 SSE baseline load case and were stepped up, using the same frequency content, to a maximum of 800% (8 SSE) of the baseline load.

The nominal 100% SSE input is shown in Figure 2-2 in the response spectra format. The spectrum is representative of U.S. earthquake spectra in the frequencies associated with piping response. Each earthquake test was 15 seconds in duration, with approximately 12 seconds of strong motion. Tests that imposed higher loadings used the same frequency content, but with a linear increase in the amplitude of the displacement history input to the shakers. CEGB used two other displacement histories in their lower level tests, one for the Sizewell B location and the other based on a generic all-sites spectrum. In their high-level tests, they used a sine burst format. The CEGB inputs are very different from the ones used by other participants. Therefore, a comparison of these results is not possible.

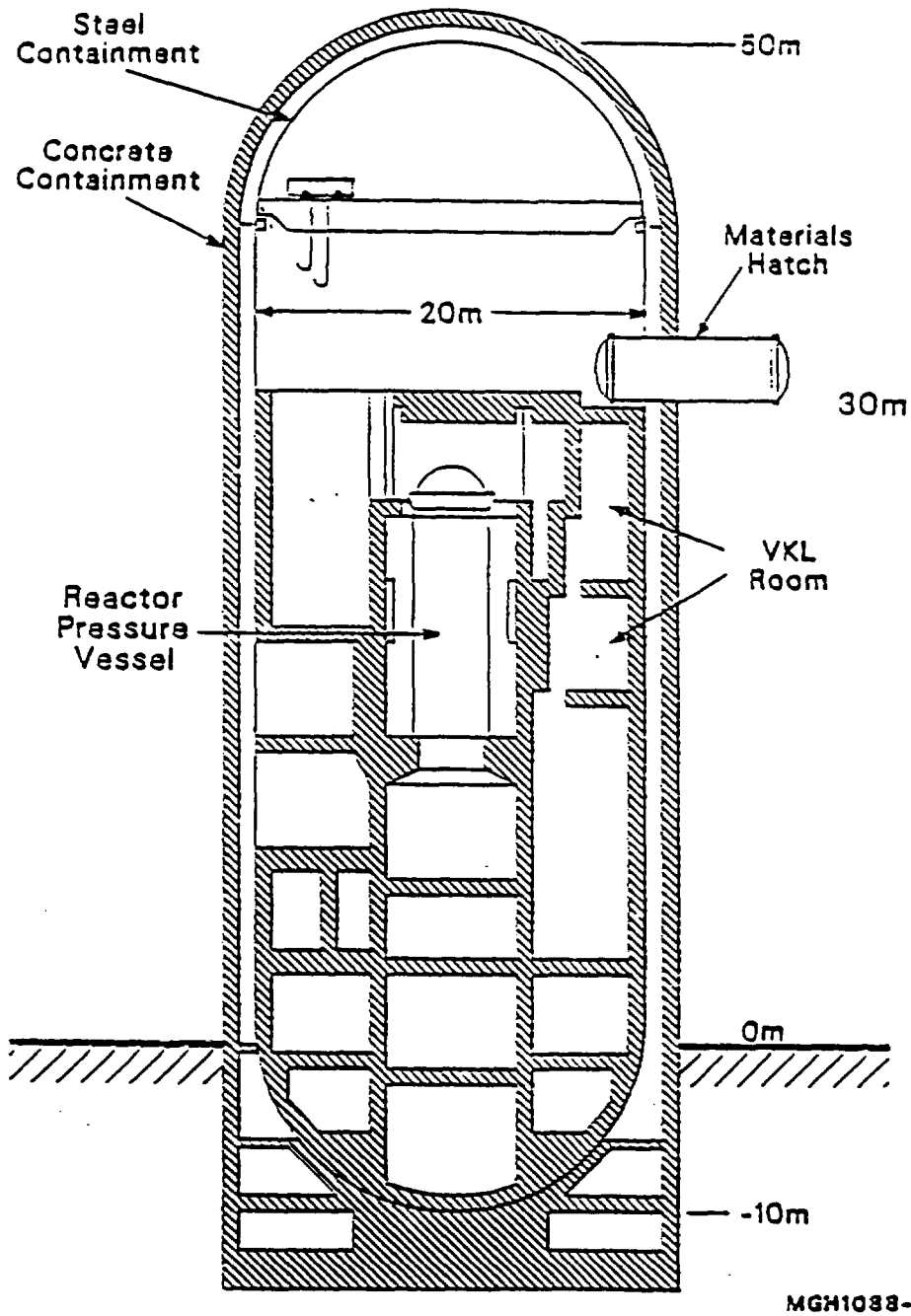


Figure 2-1. Simplified view of the HDR facility showing VKL room.

Table 2-1. VKL piping and material data.

Pipe designation	Nominal size (mm)	DIN standard material	From component	To component
DR108	200	1.4961	D14	DF16
DR109	125	1.4961	D15	DF16
VN-R23	100	1.4550	DF44	D15
DR201	200	1.4550	HDU-II 135	DF21
DR202	200	1.4550	HDU-II 305	DF21
DR203	250	1.4550	DF21	DF44
DR205	200	1.4961	DF22	D14

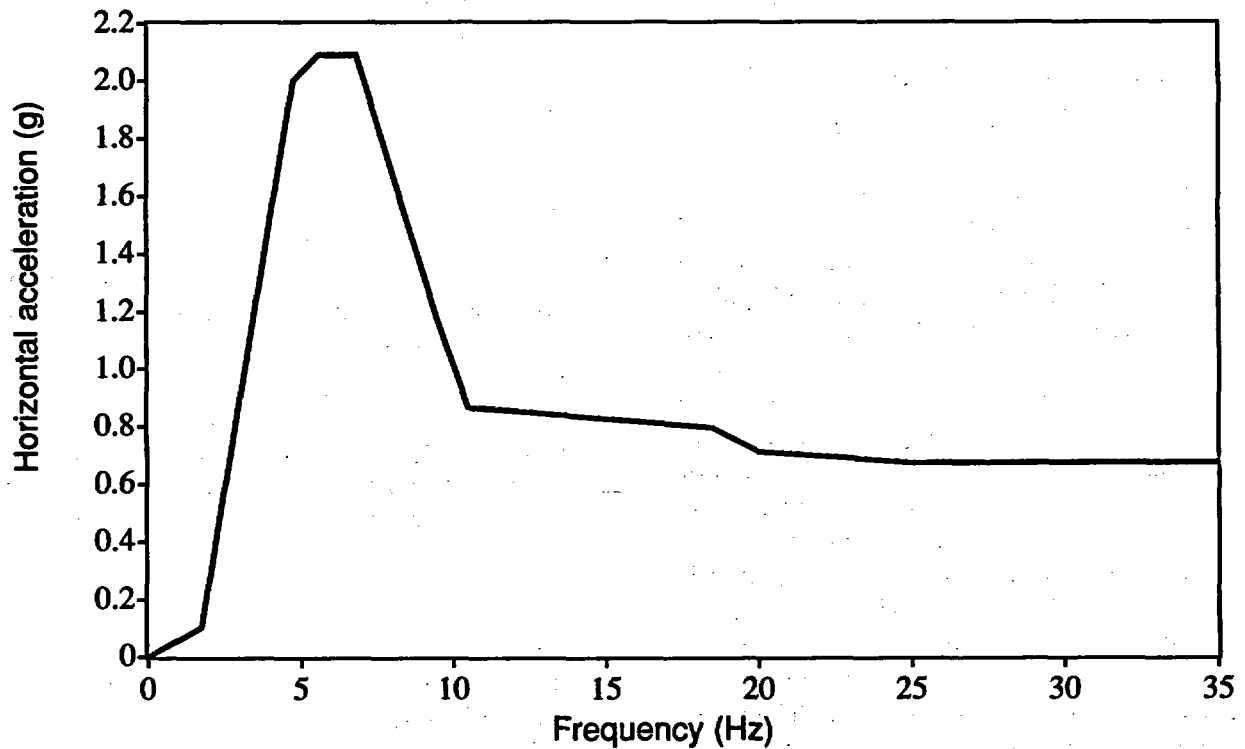


Figure 2-2. Design response spectrum used in the VKL piping system analysis.

Test Facility and System Description

During an actual earthquake, the seismic input is applied to piping systems through each of their dynamic supports (snubbers and rigid struts) and anchor points. Program scope limitations and the physical limitations of the facility made this approach impractical. In the previous test series (SHAG), the HDR containment building was excited and the piping system response was monitored. During the SHAG tests, the highest measured inputs to the piping system were from the HDU and the H-5 support. For the SHAM tests, we decided to input the motion as close as possible to these two points and to compromise by having the other support positions provide only restraint. Since the major test objectives deal with the ability of the piping and supports to withstand extremely high-level loads, the two points of dynamic excitation used in the SHAM test series are sufficient to deliver the level of loading that will enable the objectives to be realized. The exact duplication of actual seismic excitation is not required to satisfy the objectives of the test series.

2.4 Versuchskreislauf (VKL) Piping Support Systems

The piping system and facility were modified from the SHAG configuration before the SHAM testing began. We replaced a reducing elbow with a tee (DF44 in Figure 1-1) at the same location, and installed the previously discussed servo-hydraulic shakers, new piping, and the U.S. support system. The design and operation of the shakers were the responsibility of LBF. The other participants were responsible for the design of their respective piping support systems. These piping support systems were based on the U.S. stiff pipe support system, which was the responsibility of the INEL. Each participant removed or replaced one or more components from the U.S. stiff support system and, in some cases, replaced them with components of their own. The result was generally a more flexible support system. The dead weight supports and the rigid struts at locations H-4 and H-23 remained in place in all six systems.

Dead weight supports H-4 and H-23 were used to help control the hydraulic shakers at H-5 and H-25. Thus they were sized for the highest anticipated loads. They were not considered part of the experimental piping system for safety margins purposes.

Only the U.S. stiff piping support system components (snubbers, struts, and anchors) were sized to determine safety margins and failure modes. All other participants' support system components were sized for much higher loads in an effort to avoid support failures in these configurations. The design loads for each dynamic pipe support in the U.S. stiff configuration were calculated from seismic analyses based on 100% SSE excitation levels. The supports were then sized for each location, using the support manufacturer's published American Society of Mechanical Engineers (ASME)² Code, Level C Allowables. We reduced the conservatism in sizing the supports to determine the support safety margins and failure modes in the lower-level tests and to investigate the effects of multiple support failures at the higher loadings. Table 2-2 lists the support type, the predicted 1 SSE design load, and the manufacturers' ASME Code Level C rated load for the U.S. stiff support configuration. Note that H-6 is slightly underrated. The pretest as-built calculations increased the load slightly above the Level C rated load after the support was built. The pretest as-built calculations also do not reflect the bridge between DF16 and DF14 which was installed for the high-level NRC tests only. For the two hydraulic shakers, Table 2-2 defines output loads. Further details regarding the support design and analytical predictions are contained in Section 3.

As previously mentioned, 51 tests were performed, using a total of six different piping support configurations. Table 2-3 lists the supports used in each of the six systems. Since the primary focus of this report is on the performance of the system with the U.S. support configuration, Table 2-3 is provided for information only.

Table 2-2. U.S. support configuration and design loads.

Support number	Support type ^a	Design load 1 SSE [kip (kN)]	Level C rated support load [kip (kN)]	Support designation
H-2	S	1.39 (6.20)	2.10 (9.34)	PSA1
H-3	RS	0.85 (3.80)	2.00 (8.92)	211-13
H-4	RS	N/A	45.0 (200.0)	NPS-20
H-5	HS	3.39 (15.2) ^b	87.05 (390.0)	N/A
H-6	S	0.94 (4.20)	0.87 (3.85)	PSA 1/2
H-7	S	0.77 (3.50)	2.0 (8.90)	A/D 150
H-8	S	0.43 (1.90)	0.93 (4.15)	A/D 70
H-9	RS	0.45 (2.00)	0.87 (3.85)	211-A
H-10	RS	0.29 (1.30)	0.87 (3.85)	211-A
H-11	RS	0.40 (1.80)	0.87 (3.85)	211-A
H-12	S	0.27 (1.20)	0.53 (2.30)	A/D 40
H-13	S	0.32 (1.40)	0.52 (2.30)	PSA 1/2
H-14	RS	N/A	90.0 (400)	NPS-20 ^c
H-15	HS	5.38 (24.1) ^b	87.05 (390.0)	N/A

a. S = snubber, RS = rigid strut, HS = hydraulic shaker.

b. Calculated force at 1 SSE.

c. Two each in parallel.

Table 2-3. Participants support configurations for the SHAM test series.

Support number	KfK ^a	KWU ^a	U. S. ^a	EPRI/ Bechtel ^a	EPRI/ Cloud ^a	CEGB ^a
H-2			S		SS	
H-3			RS	RS	RS	
H-4	RS	RS	RS	RS	RS	RS
H-5	HS	HS	HS	HS	HS	HS
H-6			S		SS	
H-7			S	EA	SS	RS
H-8			S	EA	SS	RS
H-9		RS	RS	RS	RS	RS
H-10		RS	RS	RS	RS	
H-11		RS	RS	RS	RS	
H-12			S		SS	RS
H-22			S	EA	SS	
H-23	RS	RS	RS	RS	RS	RS
H-25	HS	HS	HS	HS	HS	HS

a. S = snubber, RS = rigid strut, HS = hydraulic shaker, EA = energy absorber, SS = seismic stop.

2.5 Gate Valve

The NRC provided a naturally aged Limitorque, motor-operated Crane gate valve from the decommissioned Shippingport Atomic Power Station for installation in the VKL. The valve was 25 years old when it was refurbished and installed in the VKL for the SHAG test series in 1986. The valve experienced some operational problems during the SHAG testing that were not related to the seismic portion of the test program. Following SHAG, the motor operator was removed and refurbished for the SHAM test. The valve remained in the VKL, blocked open, until 1988 when the refurbished motor operator was reinstalled and functionally checked out. The motor operator refurbishment included replacing the original dc motor with a new ac motor, a new torque spring and torque switch, and subjecting the motor operator to dynamometer testing at the Limitorque Test Laboratory. The valve was installed in the VKL, motor operator down because of overhead obstructions. This is the second most desirable installation option. For seismic concerns it does not make any difference whether the motor operator is up or down, but for packing leakage it does. Ours was not a permanent installation, so long-term packing leakage problems were not a concern.

2.6 Instrumentation

Three hundred and one data-gathering instruments of various types were used during the

SHAM test program to measure both test input and piping system and valve response. Measurements included: acceleration, displacement, strain, and force on the piping system and supports; and acceleration, strain, stem position, current, voltage, pressure, differential pressure, and flow through the valve. The following numbers and types of instruments were used:

- 90 acceleration transducers
- 29 displacement transducers
- 143 strain gages
- 28 force transducers
- 11 other transducers (pressure, temperature, etc.).

Instrument locations are shown in Figures 3.1-1 through 3.1-22 of the KfK report included as Appendix A.

For each experiment, KfK collected the data from all instruments through a central data-acquisition system. The data-acquisition system was computer coupled and allowed instrument calibrating, data filtering, and offset and drift correction. The report included as Appendix A includes a detailed discussion of the application of the data-acquisition system. The recorded data were stored on magnetic tape and shared with all test program participants.

3. PRETEST DESIGN ANALYSES

3.1 General Information

The following information summarizes the analytical work performed by the INEL for the VKL piping system installed at the HDR facility. The objective of this effort was to arrive at a support configuration representative of that resulting from commonly accepted design practices and analysis techniques used throughout the U.S. nuclear power generation industry. General design philosophy applicable to commercial nuclear power plants built in the United States during the mid-1970s to early 1980s was employed in performing the analysis.

As with most piping support design analyses, the VKL piping analysis was an iterative process. Several different support configurations were investigated and discarded because of their failure to satisfy the acceptance criteria. The support configuration referred to as the U.S. stiff support configuration or, alternatively, the NRC support configuration, enabled all ASME Code acceptance criteria to be satisfied and, therefore, was used as the basic piping support configuration for the SHAM test series. The information described below deals only with the U.S. stiff support configuration. The results discussed in this chapter are all calculated with a seismic input at the 1 SSE level.

3.2 Design Criteria

By agreement among the test participants, all piping in the VKL system was assumed to be ASME Code Class 2. Therefore, Section III, Division I, Subsection NC (Class 2), of the ASME Boiler and Pressure Vessel Code (hereafter referred to as the "ASME Code") was used to define the allowable stress criteria and applicable load cases for the analyses of the piping system and the derivation of support loads that were used to design the piping supports.

As specified in the ASME Code, the piping was analyzed for sustained loads (weight + pressure) and thermal expansion loads, using Service

Level A values to define the maximum allowable stresses. The test loads simulating seismic input were analyzed using Service Level C values to define the maximum allowable stresses.

3.3 Piping Material Data

The VKL piping system uses materials designated by Deutsche Institut für Norming (DIN) Standards 1.4961, 1.5415, and 1.4550. Since detailed U.S. equivalent material property information needed in the piping analysis was not provided directly, we used the following procedure to determine equivalent U.S. materials listed in the ASME Code:

1. Determine the equivalent material listed in the ASME Code tables by comparing chemical analysis data
2. Obtain the allowable values of S_c and S_h from the appropriate tables in the ASME Code for the equivalent materials
3. Determine the allowable stress values as defined in the ASME Code, Subsection NC-3600 for Class 2 components.

Using the procedure described above, we determined the material correlations shown in Table 3-1. The corresponding ASME Code allowable stresses are included in Table 3-2. Further details regarding the derivation of the allowable values are contained in Appendix B.

3.4 Versuchskreislauf (VKL) Piping System Test Operating Conditions

The temperatures and pressures used in the analysis are

Design temperature	550°F (288°C)
Operating temperature	550°F (288°C)
Design pressure	1600 psi (11 MPa)
Operating pressure	1000 psi (7 MPa)

Pretest Design Analyses

Table 3-1. VKL piping material correlations.

DIN designation	ASME Code material
1.4691	SA-312, TP316H
1.5415 ^a	SA-355, P1
1.4550	SA-312, TP321H

a. This material was used only in the DF44 tee.

Table 3-2. ASME Code allowable stresses used for design analysis.

Piping system model area			Allowable stresses for model points [ksi (MPa)]				
From	To	Material	Eq. 8	Eq. 9	Eq. 10	Eq. 11	Eq. 12
D14	DF16	SA-312, TP316H (1.4691)	17.5 (121)	31.5 (217)	27.9 (192)	56.4 (389)	45.4 (313)
D15	DF16	SA-312, TP316H (1.4691)	17.5 (121)	31.5 (217)	27.9 (192)	56.4 (389)	45.4 (313)
F44	D15	SA-335, P1 (1.5415)	13.8 (95.1)	24.8 (171)	20.7 (143)	41.4 (286)	34.5 (238)
HDU (135)	DF21	SA-312, TP321H (1.4550)	16.8 (116)	30.2 (208)	27.6 (190)	56.1 (387)	44.4 (306)
HDU (305)	DF21	SA-312, TP321H (1.4550)	16.8 (116)	30.2 (208)	27.6 (190)	56.1 (387)	44.4 (306)
DF21	F44	SA-312, TP321H (1.4550)	16.8 (116)	30.2 (208)	27.6 (190)	56.1 (387)	44.4 (306)
DF22	D14	SA-312, TP321H (1.4550)	16.8 (116)	30.2 (208)	27.6 (190)	56.1 (387)	44.4 (306)

S_h
 \uparrow
 level c
 $= 1.8 S_h$
 \uparrow
 level
 \circ
 $3 S_h$

3.5 Analysis Procedure

3.5.1 Computer Code Used. The piping system was analyzed using the computer code NUPIPE-II a proprietary code developed by Quadrex Corporation.^a NUPIPE-II is well known throughout the U.S. nuclear power generation industry and is widely used for analyzing all classes of piping systems.

The NUPIPE-II computer program performs linear elastic analyses of three-dimensional piping systems subject to static and dynamic loads. The NUPIPE-II program was also written to perform Class 1, 2, and 3 stress and fatigue analyses in accordance with various editions of the ASME Code and the ANSI B31.1 and B31.3 piping codes. Piping systems of more than one classification can be analyzed in the same computer run. Multiple loadings (both static and dynamic) and multiple stress passes may be analyzed in a single execution of NUPIPE-II.

NUPIPE-II uses the finite-element method of analysis, with special features incorporated to accommodate the specific requirements of piping system analyses. In accordance with the finite-element method, the continuous piping system is mathematically idealized as an assembly of elastic structural members connecting discrete nodal points. Nodal points are placed to define particular types of piping elements, such as straight runs of pipe, elbows, valves, etc. Nodal points are also placed at all discontinuities, such as pipe supports, concentrated weights, branch lines, and changes in cross section. System loads such as weight, pressure, thermal, seismic, and force or acceleration history loadings can be applied to the piping. For the weight and dynamic (time-history and response spectra) analyses, distributed weight properties of the piping, as well as concentrated weights such as valves, flanges, or supports, can be considered. A lumped mass model

a. Mention of specific products and/or manufacturers in this document implies neither endorsement, preference, nor disapproval by the U.S. Government, any of its agencies, or EG&G Idaho, Inc., of the use of a specific product for any purpose.

of the piping system is used for all dynamic analyses. Both translational and rotational degrees of freedom may be considered. A wide variety of pipe support types are available for user input, including rigid (user-specified stiffnesses), constant force or spring hanger preloads, and snubbers.

The INEL program module V4AGINL (Version 1.4 of NUPIPE-I) was used for all computer runs performed in the pretest phase for determining support design loads. This module was run on a CDC Cyber 176 computer system. After the SHAM tests had been performed, additional computer runs were made to compare analytical results. These subsequent runs were made using INEL program module CRAY21S (Version 1.8.1 of NUPIPE-II) executed on the INEL Cray X-MP computer system. Both versions of the code have been verified by the INEL Applied Mechanics Group personnel using a comprehensive set of benchmark problems. Both versions of the code were also verified for correctness by the Quadrex Corporation before their release.

3.5.2 Load Cases Considered. The analysis of the VKL piping system considered the effects of weight, pressure, thermal expansion, and the dynamic input intended to simulate the seismic event. Pressure effects are considered by their inclusion in the appropriate ASME Code equations.

3.5.3 Method of Calculation. Sustained loads from the weight of the piping, fluid, and insulation were applied to the model as static loads at the appropriate node points. Dynamic analyses were performed, using the response spectrum technique. A detailed explanation of this method is beyond the scope of this report. Simply stated, in this approach, the natural frequencies of the piping system are determined and static loads are applied at system support points, based on the accelerations from the response spectrum at the calculated system frequencies. The response spectrum technique has been widely used in the design of piping systems throughout the nuclear industry for many years. An independent support motion (ISM) approach was used in the piping analysis to facilitate the two-point input of the

hydraulic shakers. One response spectrum representing the test input was applied at the two shaker input points, while a second spectrum of essentially zero magnitude was input at all other support points in the analytical model. The response spectrum shown in Figure 2-2 was used at the shaker input points. As prescribed in Paragraph NC-3652.4 of the ASME Code, the components of bending moment in all three directions are included in the calculation of the resultant moments. The guidelines contained in U.S. Nuclear Regulatory Guide 1.92 were used to consider closely spaced modes in the dynamic load case.

3.5.4 Damping Values Used. ASME Code Case N-411 damping (also known as PVRC damping) values were used throughout the analysis. KfK, LBF, and KWU used 4% damping. Direct comparisons of their response spectra curves and analysis results with ours will differ at some frequencies because of the different damping values used.

3.5.5 Modeling of Supports. Accurate spring stiffnesses and set loads were used to represent the spring hangers attached to the piping system. All dynamic supports (snubbers and rigid struts) were modeled using stiffness values representative of the appropriate size of the support component (snubber or strut) anticipated to be installed.

3.5.6 Finite Element Model. The finite element model that was developed for use with the NUPIPE-II computer program contained 190 node points and 191 elements. The model contained 1140 static degrees of freedom and 507 dynamic degrees of freedom. Figure 3-1 contains a plot of the finite element model. As can be seen by comparing Figures 1-1 and 3-1, all important features of the piping system and attached major components, such as the HDU vessel, are included in the model.

3.5.7 Stress Evaluation Methodology. All stress evaluations were based on the rules stated in Paragraph NC-3650 of Section III, Division I, Subsection NC (Class 2) of the ASME Code.² The analysis of the VKL piping system consid-

ered the effects of weight, pressure, thermal expansion, and the dynamic input intended to simulate seismic input. Pressure effects are considered by their inclusion in the appropriate ASME Code equations. Resultant moments caused by the loads described above were combined according to the appropriate ASME Code equations listed in Subsection NC-3650. The calculated stresses were compared to the allowable values as defined by the ASME Code and displayed in Table 3-2.

3.6 Design Analysis Results

Analysis of the U.S. stiff support configuration showed that all piping stresses were below the ASME Code allowable limits for the 1 SSE case. Table 3-3 shows the five maximum code stresses that were calculated. Table 3-3 results are for the occasional load case with seismic input at the two hydraulic shaker attachment points. The occasional load case includes the effects of pressure, weight, and the simulated seismic loads. All of the nodes listed in Table 3-3 are located in the section of piping between the DF14 and DF16 components (see Figure 1-1).

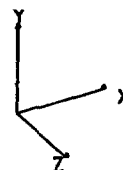
The modal analysis performed for the dynamic load case showed that 27 natural frequencies were calculated below the 33-Hz cutoff point. It is commonly assumed in piping analyses that the system response beyond 33-Hz is essentially rigid; therefore, the 33-Hz cutoff is used to conserve computational time. NUPIPE-II includes the capability to estimate the effect of the "rigid body" modes that are not calculated directly and include them in the results. This feature was used in the design analysis and is included in the results shown in Table 3-3. The results discussed in this chapter are all calculated with a seismic input at the 1 SSE level.

Maximum design loads for the piping supports were obtained from the computer analysis and used to select appropriate sizes of support components. Components commonly used throughout the nuclear industry were selected. Piping support substructures linking component supports (snubbers, struts, spring hangers, etc.) to their

VKL LOOP, TYP U.S. SUPT., SHAM SUPT
 UPT DESIGN, 1-29-88, 2 PT. PVRC INPU
 NUPIPE MATHEMATICAL MODEL (V 2.0.3)

LEGEND

- / - NODE LOCATION
- O - MASSPOINT LOCATION
- ←--- SPRING HANGER
- SNUBBER
- ↑--- RIGID SUPPORT
- ANCHOR
- X - ELASTO JOINT
- FLEXIBLE ANCHOR
- VALVE



ROTATION ABOUT Y-AXIS - -29 DEG.
 X-Z PLANE TILT - -30 DEG.

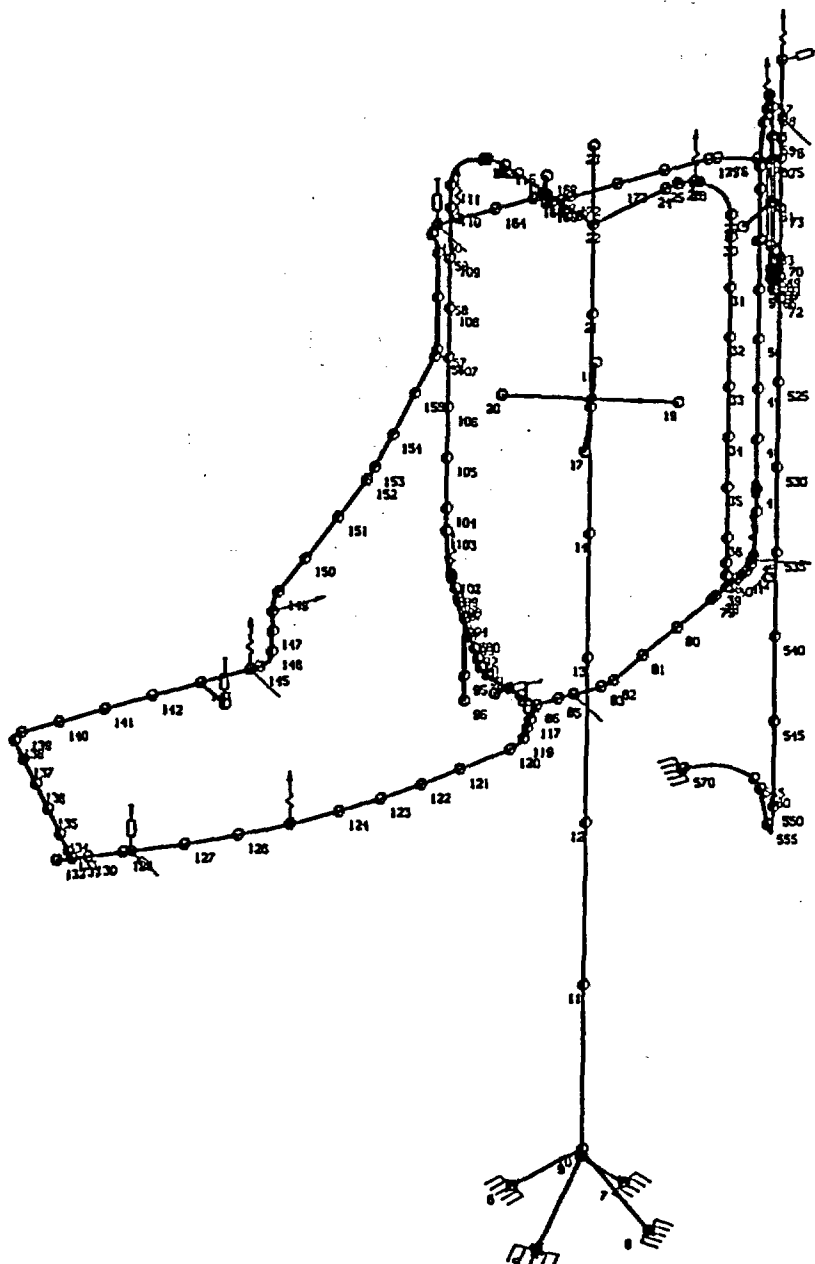


Figure 3-1. NUPIPE-II finite element model of the VKL piping system.

Table 3-3. VKL piping system maximum design analysis stresses.

Node	Stress [ksi (MPa)]	Allowable [ksi (MPa)]
64	14.81 (102)	31.5 (217)
65	16.98 (117)	31.5 (217)
66	19.89 (137)	31.5 (217)
67	18.44 (127)	31.5 (217)
68	18.44 (127)	31.5 (217)

grounding points on the facility walls or other major structures were analyzed in accordance with ASME Code rules and commonly accepted industry practices. Table 3-4 summarizes information pertinent to the U.S. support system as initially installed on the VKL piping.

The support loads that were calculated by the computer analysis and used for design purposes are shown in Table 2-2. Since the performance of the dynamic supports was one of the primary interests of this test series, Table 2-2 includes only information regarding these support types.

Table 3-4. U.S. support configuration component information.

Support number	Support type ^a	Manufacturer initial	Replacement	Manufacturer's designation initial	Replacement
H-2	S	Pacific Scientific		PSA 1	
H-3	RS	ITT Grinnell		Size B	
H-4	RS	NPS Industries		Size 20	
H-6	S	Pacific Scientific		PSA 1/2	PSA 1
H-7	S	Anchor Darling	Pacific Scientific	A/D 150	PSA 1
H-8	S	Anchor Darling	Pacific Scientific	A/D 70	PSA 1/2
H-9	RS	ITT Grinnell		Size A	
H-10	RS	ITT Grinnell		Size A	
H-11	RS	ITT Grinnell		Size A	
H-12	S	Anchor Darling	Pacific Scientific	A/D 40	PSA 1/4
H-13	SP	ITT Grinnell		Size 16	
H-14	SP	ITT Grinnell		Size 13	
H-15	SP	ITT Grinnell		Size 6	
H-16	CF	ITT Grinnell		GR12, Type 81H-A	
H-17	CF	ITT Grinnell		GR22, Type 81H-A	
H-18	CF	ITT Grinnell		GR10, Type 81H-A	
H-19	SP	ITT Grinnell		GR12, Type 81H-A	
H-22	S	Pacific Scientific		PSA 1/4	
H-23	RS	NPS Industries		Size 20	
H-24	CF	ITT Grinnell		GR21, Type 81H-A	

- a. S = Snubber
 RS = Rigid strut
 SP = Spring hanger
 CF = Constant force support

4. TEST RESULTS

4.1 General Information

Nine of the 51 tests were conducted with the U.S. Stiff Support System (see Figure 1-1, Tables 2-2 and 4-1). The overload snubber failures in the earlier tests (T41.35.2 through T41.31.5, 300% SSE) prevented a true characterization of the piping system we analyzed. A shortage of snubbers caused us to suspend the NRC testing while we shipped additional snubbers from the U.S. In the meantime, we tested the other support system shown in Table 2-3. The strains in Elbow 1 were very high, particularly in the CEGB tests. We did not want to fail Elbow 1 until the last high-level test if possible. So, before the U.S. stiff system was reinstalled for our high-level tests, we built a special support (bridge) between DF16 and DF14 (see Figure 1-1). This bridge helped reduce the response in Elbow 1. The bridge was installed for our tests (T41.81.1 through T41.81.3) (see Table 4-1). While the system containing the bridge was not the system we analyzed for design purposes, we still wanted to characterize the system response without support failures. Reanalysis with the bridge could be performed post-test if necessary. Therefore, for the T41.81.1 test, we repeated the 200% SSE test and temporarily replaced the smaller snubbers at locations H-6, H-8, H-12, and H-22 with larger snubbers PSA-1s. For the final two tests (T41.81.2 and T41.81.3, the 600 and 800% SSE tests, with the exception of H-6), we reinstalled the smaller snubbers at the locations stated above. H-6 was slightly undersized in one as-built analysis and the actual loads from the earlier test confirmed that to be the case, so H-6 was resized to a PSA-1 for all three of the final tests.

The earlier tests through T41.31.5 must be categorized as a learning experience. We can report the history of what happened and quantify the loads at which it happened, but the continuous snubber failures did not provide a system that could be compared with the design analysis. The T41.81.1 system with the bridge cannot be

directly compared, so we performed a post-test analysis with the bridge and the actual T41.81.1 input spectra. Remarks about performance versus design throughout the results will be referring to this comparison, scaled up or down accordingly.

Sufficient data were obtained to satisfy most of the program objectives. The one exception may be pipe failure modes. Strains in excess of 0.5% were experienced in tests with the U.S. stiff support system, without significant visible physical damage. Indications of plastic response were visually observed after Test T41.81.3, between the branch connection DF44 and Elbow No. 2 and DF16 and Elbow 1, after the bridge broke. In tests of other, more flexible, support configurations, strains up to approximately 0.9% were recorded, and indications of plastic response were observed between the branch connection DF44 and Elbow No. 2.

4.2 Data Conversion

For each experiment, KfK collected the data from all instruments through a central data acquisition system. The recorded data were stored on magnetic tapes and shared with all test program participants. Further processing of the data was required for post-test analysis.

The data were recorded during the tests at a frequency of approximately 200 Hz, with a 100-, and 60-Hz filtering, which resulted in 6,875 time steps over the length of time the data acquisition system was actively recording. Since 301 instruments were installed on the VKL piping system, a large amount of data was obtained from each test. Several specialized computer programs and command procedures were developed by INEL engineers to handle the data. These programs read the data tapes, correlated the data and time information to separate files for the individual instruments, and arranged the data in the proper format for subsequent processing with the DADiSP software.³

Table 4-1. U.S. stiff support system test matrix.

Test number	Load type	Load level
T41.35.2	Checkout	0.2g
T41.30.2	Random	0.3g
T41.30.1	Random	0.3g
T41.31.0	SSE	100% SSE ^a
T41.31.1	SSE	100% SSE
T41.31.2	SSE	100% SSE
T41.31.3	SSE	200% SSE
T41.31.4	SSE	300% SSE ^b
T41.31.5	SSE	300% SSE
T41.81.1	SSE	200% SSE
T41.81.2	SSE	600% SSE
T41.81.3	SSE	800% SSE

a. 100% SSE = 0.6g ZPA input.

b. Incomplete test, malfunction of test equipment.

The DADiSP software uses a multi-windowed screen format (termed a worksheet) to facilitate data series processing. Typically, one window is used to display raw data, with other windows used to show the results of processed data. A variety of built-in functions are available, along with the capability to develop custom macros to perform specific tasks. In addition to the quality control measures used by the program authors, the DADiSP software has been verified for accuracy by INEL personnel.

4.3 Piping System Dynamic Response

4.3.1 Test T41.81.1. This test was conducted at an input level of 200% SSE. Because of snubber failures in earlier tests, the 200% SSE test was used as the benchmark test of the U. S. stiff support system configuration. The output acceleration time histories of the hydraulic shakers were converted to response spectra for

comparison to the original design spectrum curve. As shown in Figures 4-1 and 4-2, the SHAM output spectra envelope the design spectra curves for this 2 SSE test. Good correlation exists between the SHAM output and the design curves, except in the 20- to 40-Hz range, where the test input curves show a secondary peak. These secondary peaks are most probably caused by such things as support connection gaps (pin slop) and other inevitable differences between the idealized mathematical model and the actual (as tested) piping system. These peaks are in the frequency range where rigid response is normally assumed in design analyses.

The actual 2 SSE test spectra curves were used as input to the NUPIPE-II finite-element model of the as-built VKL piping system. This model was then reanalyzed with the test spectra input, using a cutoff frequency of 60-Hz to include any effects of the secondary peaks. The ASME Code stress results for these analyses are compared to the allowable values in Table 4-2. The 60 Hz

Test Results

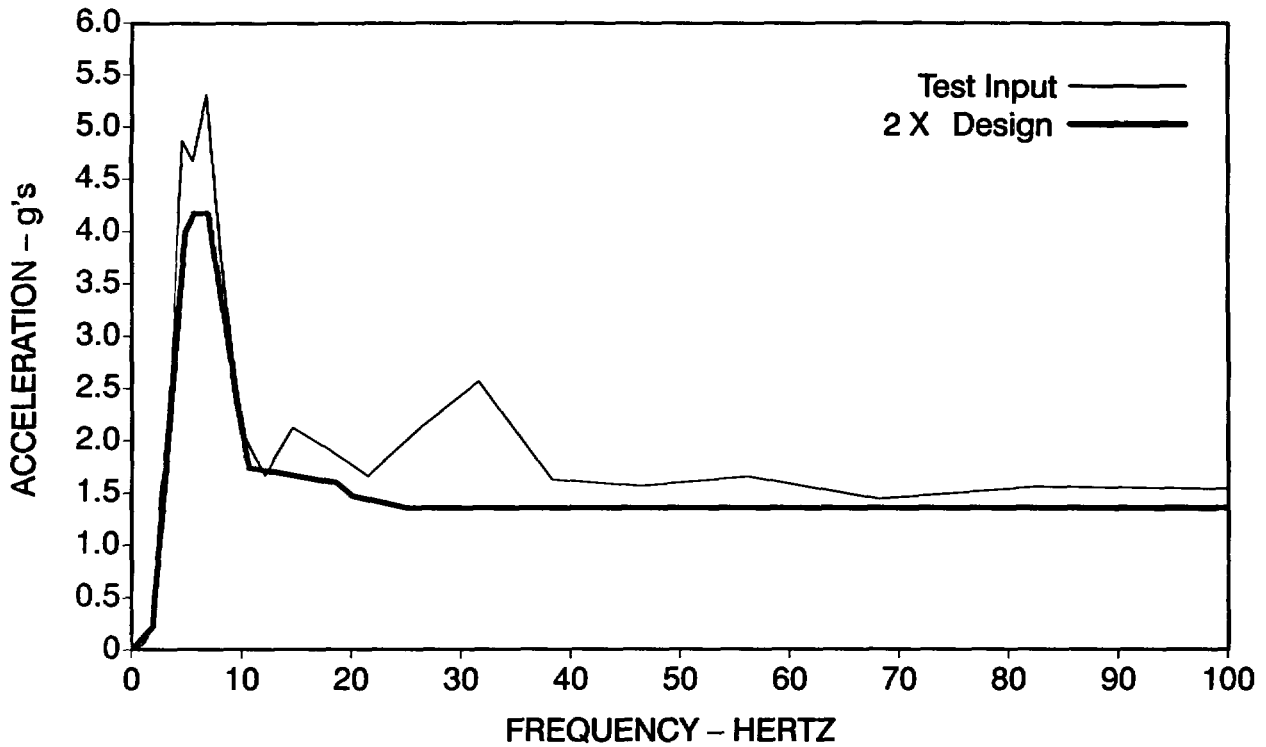


Figure 4-1. 200% SSE PVRC response spectrum, Test T41.81.1, H-25 location.

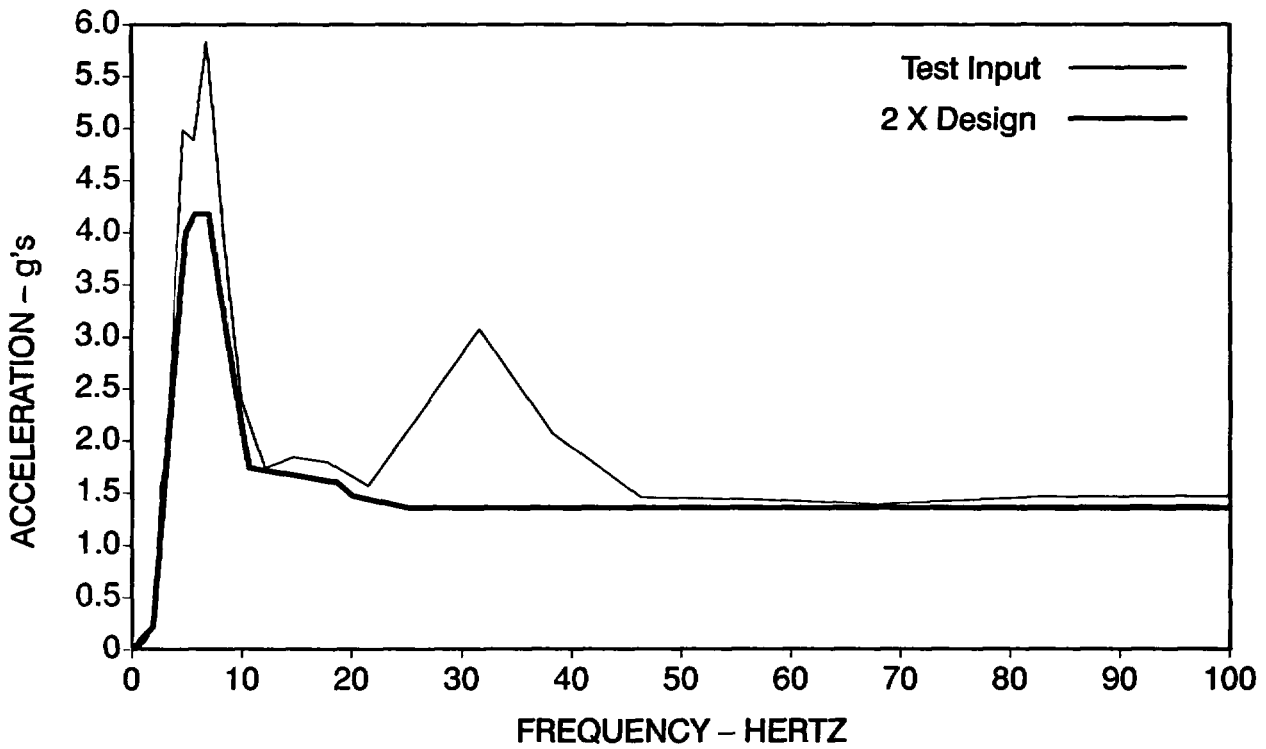


Figure 4-2. 200% SSE PVRC response spectrum, Test T41.81.1, H-5 location.

Table 4-2. VKL piping system ASME Code Equation 9 stress comparisons (2 SSE).

Node	As-tested 2 SSE stress ^a ksi (MPa)	Allowable ^b ksi (MPa)
176	30.89 (213)	31.5 (217)
175	30.46 (210)	31.5 (217)
160	22.77 (157)	24.8 (171)
174	22.63 (156)	31.5 (217)
162	22.63 (156)	24.8 (171)

a. Response spectra curves from test T41.81.1 used as input.

b. Service Level C stress allowable values ($1.8S_H$).

cut-off frequency allowed the computer code to calculate the natural frequencies of the model in the range of the secondary peaks. Using this cut-off value, 45 natural frequencies were calculated. The fundamental model frequency was calculated to be 6.10 Hz. The natural frequencies were fairly evenly distributed between the 6.10-Hz first mode and the 60-Hz cutoff value so that all areas of the response spectra curves would have been used to define loads. Table 4-2 shows that the ASME Code Equation 9 stresses calculated with the test input spectra (2 SSE) did not exceed the allowable stresses. All of the points listed in Table 4-2 are located in the VN-R23 section of piping between support H-11 and DF16 (see Figure 1-1).

Table 4-2 shows that seismic input levels of 200% SSE resulted in stresses very near the ASME Code allowables for the as-tested piping configuration with the bridge. Predictions without the bridge showed that ASME Code stresses were exceeded. One would not expect structural failure of the piping system at these stress levels. The strains measured during this test reinforce this view. Of the piping strain data for this test that were examined, the maximum longitudinal and circumferential values (0.051% and 0.039%, respectively) occurred at Elbow 1. These strains are well below the 0.3% strain value used to

define yield in the stainless steel materials used in piping.

Since the strain gages were reset to a zero value before each test, only strains resulting from the dynamic test loads were recorded. However, it should be remembered that the test dynamic loads contributed approximately 80% of the total Equation 9 stresses for the 2 SSE load case. Thus, the observations regarding the locations of the maximum total strain location would remain valid.

Observing the general shape of the response spectra curves for the seismic input (see Figures 4-1 and 4-2) would indicate that the most severe loading would be expected from those vibrational modes below approximately 12 Hz. The computer analysis determined seven vibrational modes with natural frequencies in this range. These seven modes occurred in three general areas of the piping system, as described in Table 4-3.

One of the more useful techniques for examining frequency domain behavior of a dynamic system such as a piping system is the mean-square spectral density or Power Spectral Density (PSD) method. This method was used to examine the piping system response characteristics. The DADiSP software described earlier was used to calculate and display the PSDs for the selected

Test Results

Table 4-3. Summary of predicted vibrational modes below 12 Hz.

Mode	Frequency (Hz)	Mode shape description
1	6.10	X and Z direction displacement in DR205 piping from H-2 through DF14 and DF16 (see Figure 1-1) (model nodes 150-158)
2	6.26	X and Z direction displacement between H-10 and H-11 (see Figure 1-1) (largest displacement between model nodes 150-158)
3	6.53	X and Z direction displacement between H-10 and H-11 (see Figure 1-1) (largest displacement between model nodes 150-158)
4	7.50	Y direction displacement in area of Elbow 2 (see Figure 1-1) (model nodes 134-145)
5	9.05	X, Y and Z direction displacement between DF14 and DF15 (see Figure 1-1) (model nodes 61-550)
6	9.22	X displacement between DF14 and DF15 (see Figure 1-1) (model nodes 63-555)
7	11.9	Predominantly Y direction displacement (some X and Z direction displacement also) in area of Elbow 2 (see Figure 1-1) (model nodes 134-155)

data points. PSD plots calculated from acceleration time histories taken from instruments located throughout the VKL piping system were examined. Considering such things as support connection gaps (pin slop) and other inevitable differences between the idealized mathematical model and the actual, as-tested, piping system, analysis of the PSD results shows generally good agreement with predicted frequencies from the computer analysis. The PSDs of selected points on the piping and the gate valve are contained in Appendix C.

Figures C1 through C9 show PSDs for all three global directions for the three areas of the piping system described in Table 4-3. The PSDs shown in Figures C1, C2, and C3 correspond to data channels QB1101, QB1102, and QB1103. These channels recorded accelerometer data in the area between the DF22 and DF16 components (see Figure 1-1) and are applicable to modes 1, 5, and 6 described in Table 4-3. The PSDs shown in Figures C4, C5, and C6 correspond to data channels RS7610, RS7610, and RS7610. These channels recorded accelerometer data in the area between pipe supports H-10 and H-11 (see Figure 1-1) and are applicable to modes 2 and 3, described in Table 4-3. The PSDs shown in Figures C7, C8, and C9 correspond to data channels

QB1011, QB1012, and QB1013. These channels recorded accelerometer data in the area between the DF44 component (tee) and pipe support H-9 (see Figure 1-1). The Figures C7-C9 PSDs are applicable to modes 4 and 7 described in Table 4-3.

The information presented in Table 4-3 shows that the computer analysis predicted a fundamental frequency at 6.10 Hz with a mode shape of predominantly horizontal motion. The PSDs shown in Figures C1-C3 indicate this same behavior. Figure C1 shows response in the band from approximately 4 Hz to 8 Hz with the largest magnitude at approximately 6.5 Hz. The frequencies predicted for modes 5 and 6 are also near the frequency bands of the response shown in the PSDs of Figures C1-C3. One difference between the predicted dynamic behavior and that demonstrated by Figures C1-C3 is in the vertical (global Y) direction. While the X and Z direction responses were predicted to be the main contributors, some Y direction motion was also predicted to occur in mode 5. Figure C2 shows no discernible response in this direction. There are many possible reasons for this difference. Based upon both analytical and field experience, it is likely that such things as differences in damping, differences in actual versus the nominal material and

geometric properties of the piping, etc., would contribute to the differences in actual-versus-predicted piping response. The scope of this project did not allow for further investigation into additional contributors to the differences between analytical predictions and actual test response.

The PSDs shown in Figures C4–C6 were calculated from data taken in the general area of the piping system, where vibration modes 2 and 3 were expected to occur. The data shown in these figures support the analytical predictions, in that the frequency bands are in general agreement with predictions and the magnitudes indicate predominant contributions in the X and Z directions.

Vibration mode 4 described in Table 4-3 is predominantly Y direction motion. The PSDs shown in Figures C7–C9 also clearly indicate this behavior in the 7.5-Hz range. The analytical predictions for vibration mode 7 include motion in all three directions. Figures C7–C9 show that the test results also confirm this behavior. Figure C9 indicates a larger magnitude response at approximately 14.5 Hz. This is beyond the 6.0- to

12.0-Hz band under discussion; however, review of the analytical predictions shows that this generally corresponds to mode 9, which was predicted to occur at approximately 13.6 Hz. Generally, there was good agreement between the analytical predictions and the actual response with respect to mode shapes.

4.3.2 Test T41.81.2. This test was conducted at an input level of 6 SSE (600% SSE). The output acceleration time histories of the hydraulic shakers were converted to response spectra for comparison to the original 6 SSE design spectrum curve. As can be seen in Figures 4-3 and 4-4, the test input spectra envelope the amplified design spectra curves. Figures 4-3 and 4-4 show good correlation between the test input and the design curves. As in the 2 SSE test, secondary peaks are evident in the higher frequency ranges of the spectra curves.

Since the primary purpose of the original design analytical predictions was to confirm an acceptable support configuration for the design load case, no computer predictions were

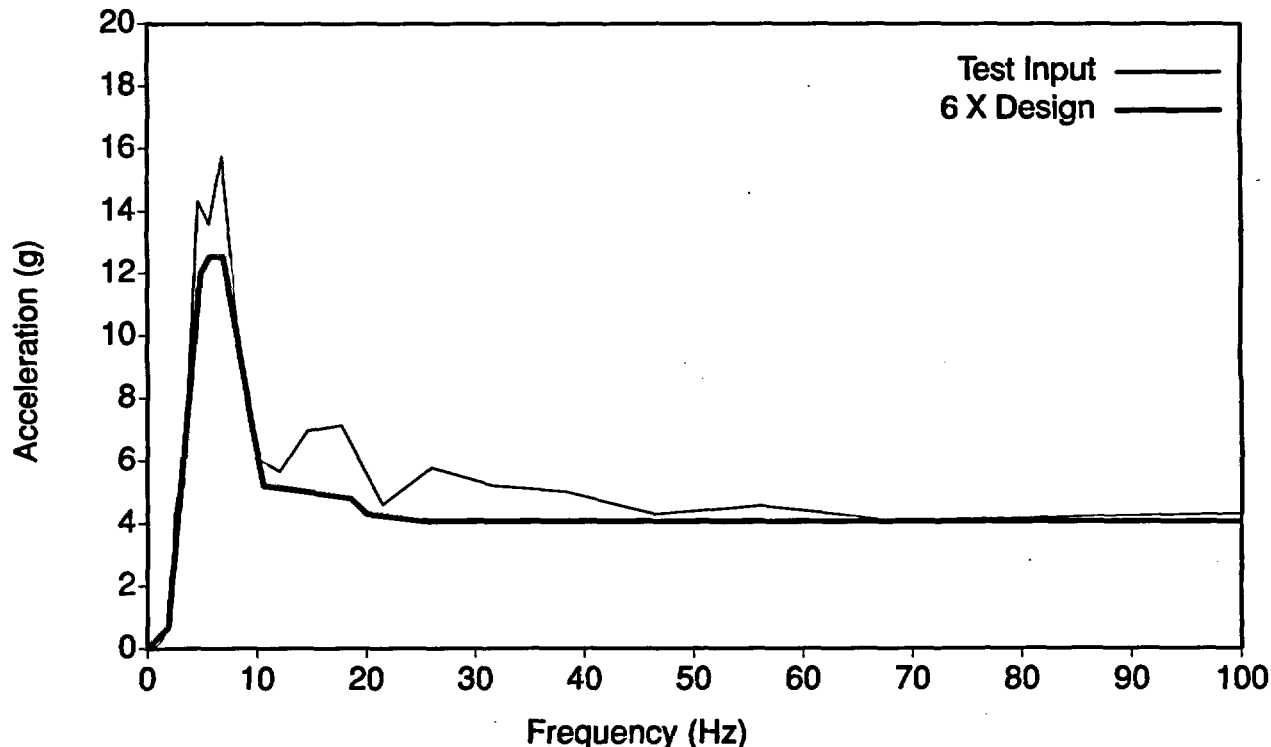


Figure 4-3. 600% SSE response spectrum, Test T41.81.2, ES3011, PVRC damping.

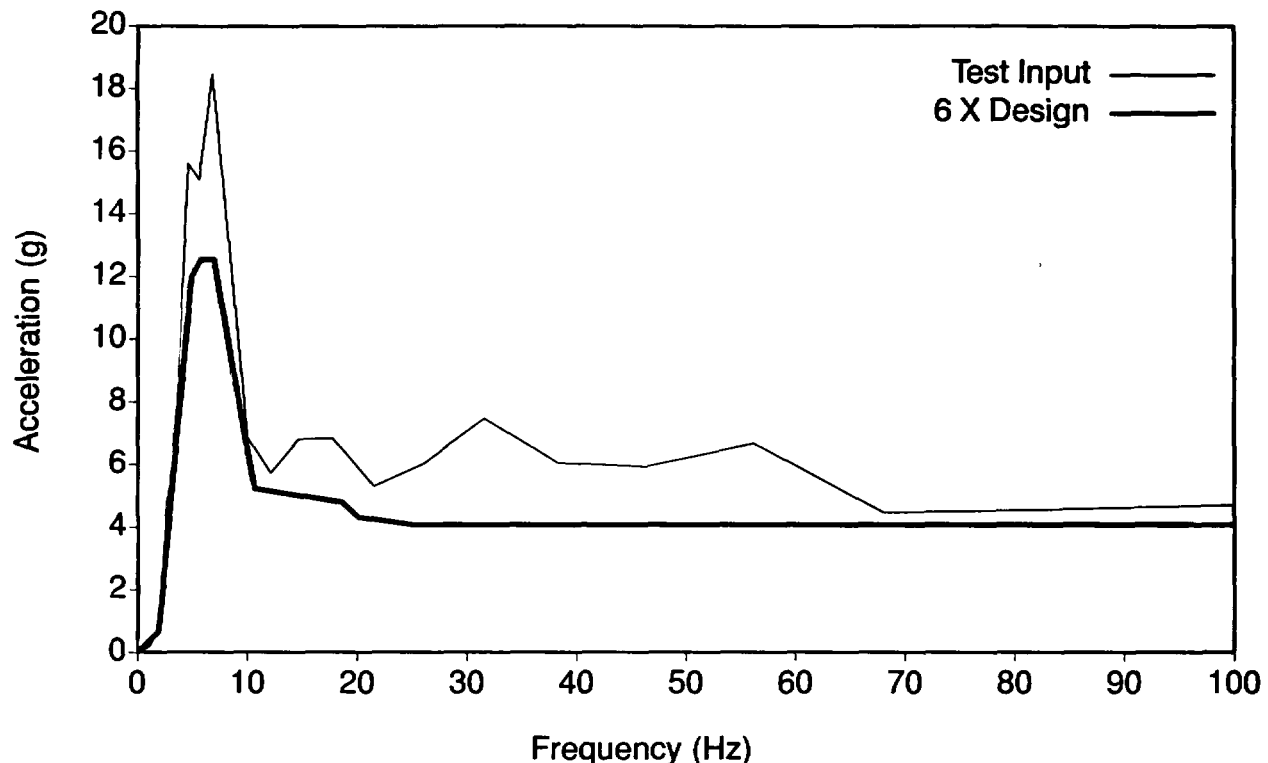


Figure 4-4. 600% SSE response spectrum, Test T41.81.2, ES3021, PVRC damping, H-25 location.

performed for the 600% and 800% load levels. Obviously, higher stresses in the piping are expected at these levels. ASME Code stresses nearly exceeding the allowable values were determined by the analytical predictions for the 200% SSE input level. Thus, one would expect that the Code stress allowables would be exceeded at the 600% SSE input level. Analytically, the higher seismic inputs would simply be linearly scaled from the design curve. The seismic results from linear-elastic calculations (such as performed by NUPIPE-II) would also then be multiples of the design curve results.

The strain data for this test show that the highest strains occurred, even with the bridge, at the component labeled Elbow 1 in Figure 1-1. This is the same point where the highest strains occurred in the 200% SSE test (T41.81.1). The maximum longitudinal and circumferential values were 0.197 and 0.150%, respectively. Remember that only the dynamic strains were measured in this test series. The maximum strains are higher than those that would be extrapolated from simply linearly scaling the 200% SSE

results. This is primarily a result of the failure of supports H-8, H-12, and H-22 during this test. Thus, larger displacements and strains were experienced throughout the system. The maximum dynamic strains are slightly below the 0.3% strain used to define yield in stainless steel material. When strains contributed by the weight and thermal conditions are considered, it is likely that the 0.3% value was exceeded. However, examination of the strain data shows no apparent plastic activity that would be evidenced by an offset of the final portions of the strain plots from their initial values. Also, no visual plastic deformations were observed in the post-test inspections of the piping system at this or other high strain locations.

The DADiSP software described earlier was used to calculate PSDs for the various points throughout the piping system, where acceleration time history data were available. Figures C-10 through C-18 show PSDs for all three global directions for the same three areas of the piping system discussed in Section 4.3.1 for the 200% SSE test (T41.81.1). The PSD plots for the 600% SSE test (T41.81.2) show a broader frequency content and

much greater magnitude than the plots for the same areas from the previous test. A higher magnitude is what would be expected considering the higher level of input. A broader frequency content of the PSDs is also expected since the support failures will generally make the system less stiff and allow system response over a broader frequency range.

4.3.3 Test T41.81.3. This test was conducted at an input level of 8 SSE (800% SSE). As before, the acceleration time histories of the hydraulic shakers were converted to response spectra for comparison to the original design spectrum curve. As can be seen in Figures 4-5 and 4-6, the test input spectra envelope the amplified design spectra curves. Figures 4-5 and 4-6 show good correlation between the test input and the design curves. As in the previous tests, secondary peaks are evident in the higher frequency ranges of the spectra curves.

No computer predictions were made for the 800% SSE load level. One would expect stresses

calculated with the procedures used in the design analysis to be well beyond the limits allowable in the ASME Code.

The strain data for this test show that the highest strains occurred at the components labeled Elbow 1, particularly after a weld on the bridge between DF16 and DF14 failed at the 10-second mark, and Elbow 2 in Figure 1-1. The maximum longitudinal and circumferential values were 0.534 and 0.413%, respectively, at Elbow 1, and 0.323 and 0.570%, respectively, for Elbow 2. Once again, these strains are only those for the dynamic load. This test was run without replacing the supports (H-8, H-12, and H22) that failed in the previous test. The snubber at support H7 failed during this test. Thus, the piping support configuration for this test was significantly different than the design configuration. With these supports gone, the piping was much more flexible, especially in the vertical (Y) direction. In fact, no dynamic supports were available in the Y direction on that part of the system beginning with the DF21 spherical tee and extending through the

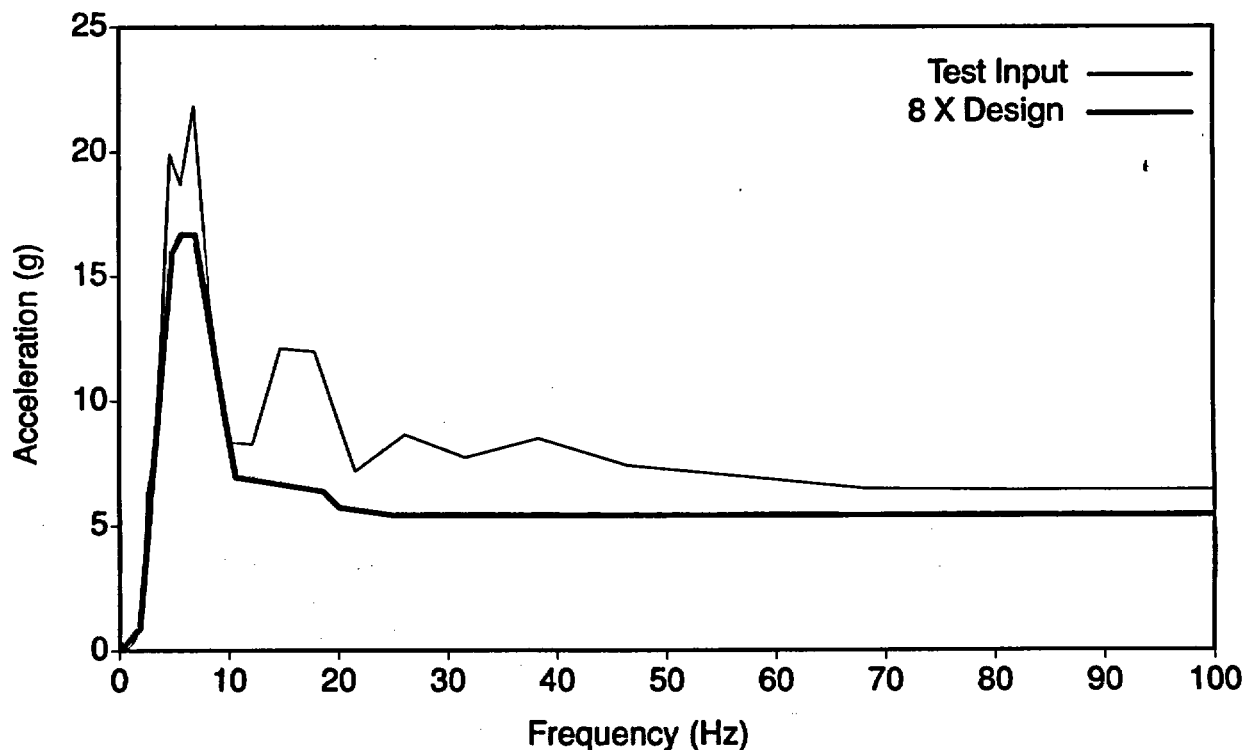


Figure 4-5. 800% SSE response spectrum, Test T41.81.3, ES3011, PVRC damping, H-5 location.

Test Results

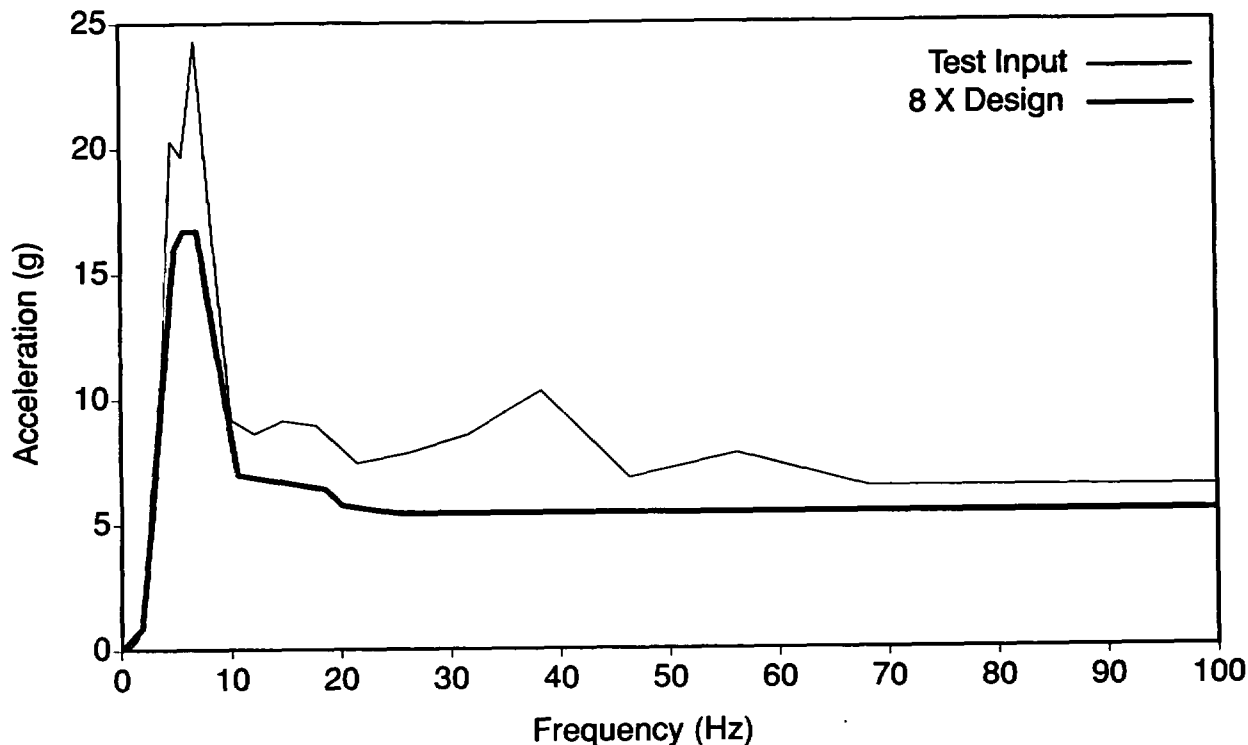


Figure 4-6. 800% SSE response spectrum, Test T41.81.3, ES3021, PVRC damping, H-25 location.

DF44 tee to the manifold section at DF16 (see Figure 1-1). Given this support configuration and the higher level of dynamic input, larger displacements and strains would be expected throughout the system. The maximum dynamic strains are greater than the 0.3% strain used to define yield in stainless steel. The strain plots in Figures 4-7 through 4-10 clearly show the offset indicative of plastic action. Plastic deformation of the piping system was observed during the inspection subsequent to this test.

The DADiSP software described earlier was used to calculate PSDs for the various points throughout the piping system where acceleration time history data were available. Figures C-19 through C-27 show PSDs for all three global directions for the same three areas of the piping system discussed in Subsections 4.3.2 and 4.3.3. The PSD plots for this test show greater magnitude than the plots for the same areas from the previous test. The higher magnitude is what would be expected considering the higher level of input. The PSDs for this test exhibit about the

same frequency content as those for the previous test (600% SSE). The frequency band for the vertical (Y axis) direction PSD plot shown in Figure C-26 is somewhat narrower than those for the same point in previous tests; however, the magnitude of this plot is much greater. This indicates significant response in the vertical direction and is what one would expect, considering the lack of dynamic support for the piping in this area of the system.

The project scope did not include a detailed investigation of the piping system structural damping experienced during the various tests. Previous research results indicate that increases in damping would be expected as some threshold level of system response is passed.⁴ Given the high level of system response, including plastic behavior, increases in piping system damping during the higher level tests is very likely. The expected increases in damping would also affect the overall response of the system and would influence the changes observed in the PSD plots.

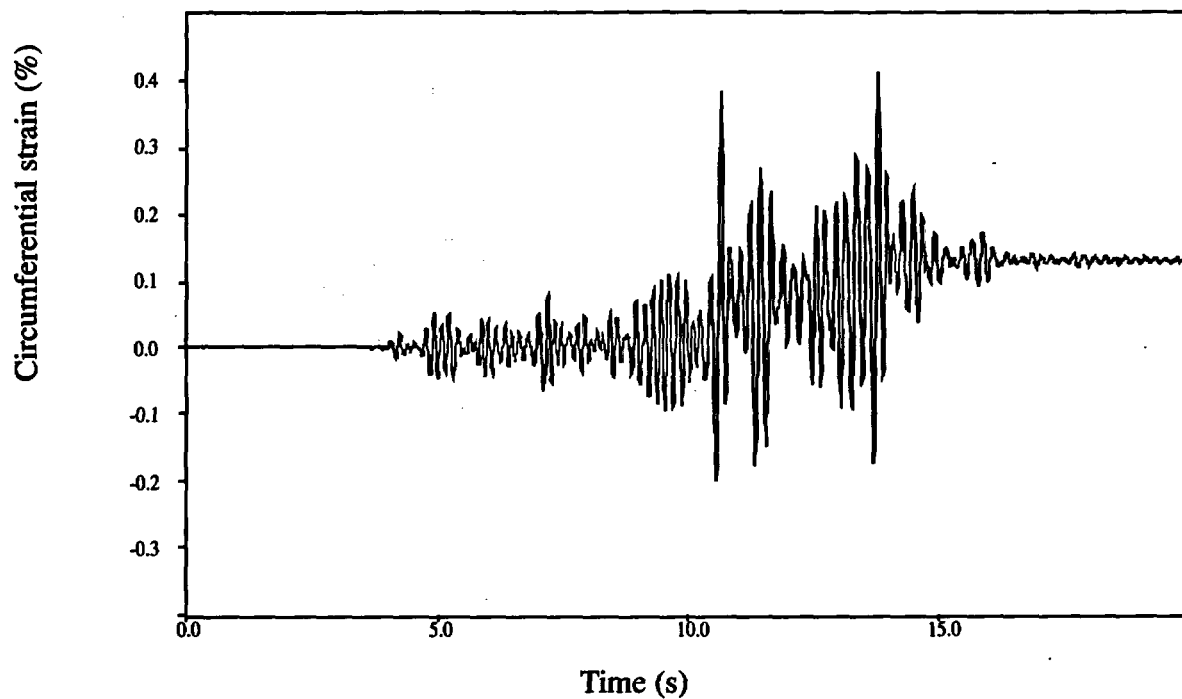


Figure 4-7. Circumferential strain at Elbow 1 (Test T41.81.3).

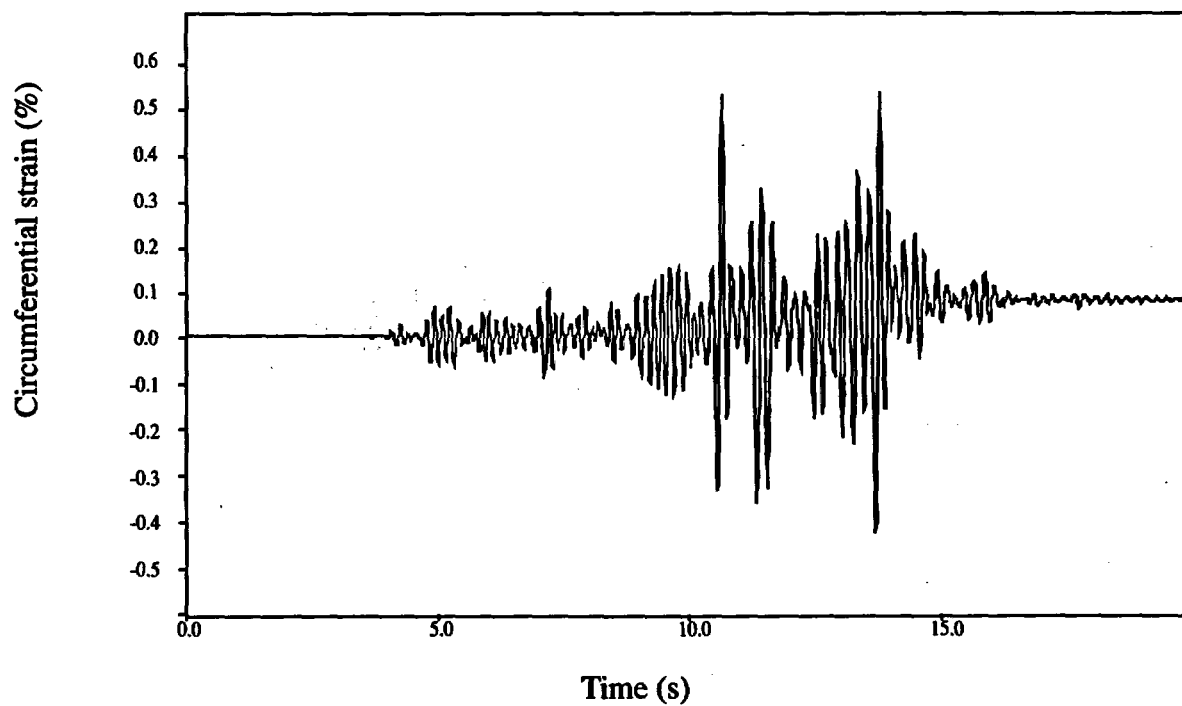


Figure 4-8. Longitudinal strain at Elbow 1 (Test T41.81.3).

Test Results

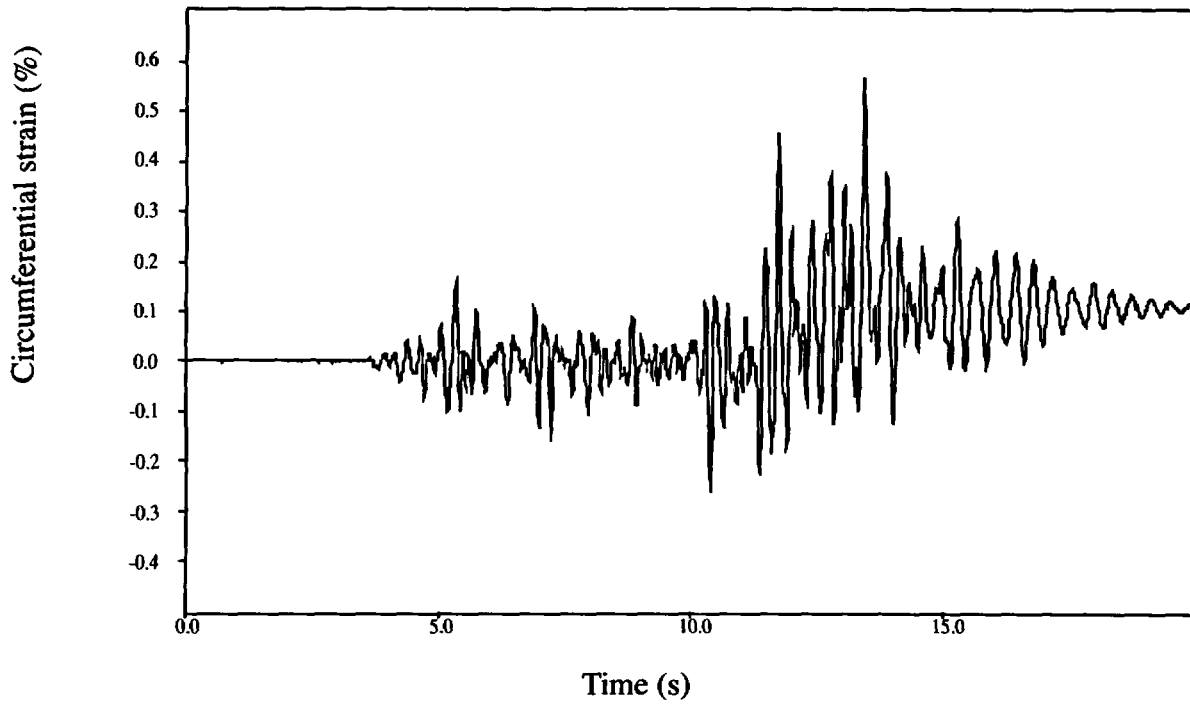


Figure 4-9. Circumferential strain at Elbow 2 (Test T41.81.3).

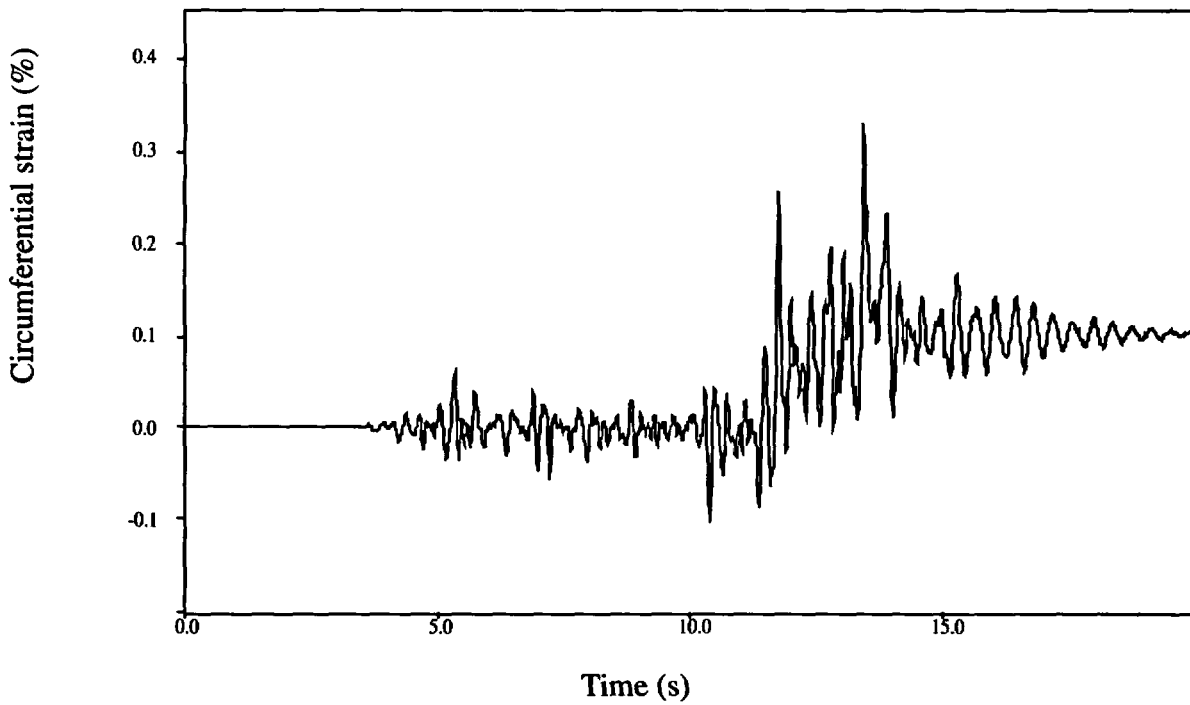


Figure 4-10. Longitudinal strain at Elbow 2 (Test T41.81.3).

4.4 Dynamic Support Performance

The U.S. stiff piping support system components (snubbers, struts, and anchors) were sized using commonly accepted industry design practices and design loads based upon the 1 SSE dynamic input and analysis techniques described in Section 3. This approach was taken to enable the observation of support component performance while subjected to loads and system excitation well beyond design levels. The performance of these components was expected to yield information about support component safety margins and failure modes. All other participants' support system components were sized for much higher loads; thus, no support failures in these systems were anticipated and none were realized except for CEGBs, whose inputs were not comparable to the other five systems.

The HDR data acquisition system required four to six hours to process the data and make quick-look plots from each test. This work was typically performed at night following each day's testing. The test schedule required that two to four tests be performed each day. The piping system was visually inspected after each test. Any faults detected by the inspections were repaired before the next test. Internally failed snubbers could not be detected visually. As many snubbers as possible were disconnected and tested between tests; however, several tests were performed with failed snubbers in place.

4.4.1 Tests Prior to T41.81.1. The majority of support performance anomalies experienced during the SHAM test series involved snubbers. Numerous snubber failures were experienced with the U.S. stiff support system in the tests before Test T41.81.1. Table 4-4 provides a matrix describing the snubbers installed for each test of the U.S. stiff support system. The test numbers correlate to the input levels shown in Table 4-1. While these snubber failures delayed a true characterization of the response of the piping system, they did provide useful information regarding performance of individual components. The following paragraphs provide further narra-

tive on the performance of the snubbers in the tests before T41.81.1.

During Test T41.35.2, the snubber at support location H-7 failed at approximately one second and at a load of 0.393 kip. The design load given for this component in the vendor's catalog is 1.50 kip.

The snubber at location H-7 that failed during Test T41.35.2 was replaced for Test T41.31.0. This snubber again failed at approximately one second into the test. The failure load was not accurately determined; however, it appeared to be small in magnitude. It appeared that the snubber failed at the first application of load. Brittle fracture of a connecting component appeared to be the failure mode for both of these premature failures. Both the snubbers installed at location H-7 during Tests T41.35.2 and T41.31.0 were returned to the manufacturer for inspection and analysis. No further information regarding these units has been received to date.

The snubbers at locations H-8 and H-22 failed during Test T41.31.1. The H-8 unit failed at four seconds into the test, at a load of 1.798 kip. The design load listed in the vendor's catalog for this unit is 0.700 kip. The snubber at H-22 failed at approximately 2.5 seconds into the test at a load of 0.674 kip. The vendor's data for this unit lists a design load (ASME Code Service Levels A and B) of 0.350 kip. This same unit successfully resisted a load of 0.899 kip during Test T41.31.0. Although no failure occurred, anomalous behavior was also noted in the snubber at location H-6 during this test. This unit resisted a load of 1.461 kip, while the vendor design load (ASME Code Service Levels A and B) is listed as 0.650 kip. This particular snubber did fail in Test T41.31.2.

Subsequent to the failure of the snubber at H-8 during Test T41.31.1, the unit was replaced with an alternate model from another vendor. The replacement unit then failed during Test T41.31.3 at approximately 11 seconds into the test. The load at failure was 1.798 kip. While the vendor's catalog lists a design load of 0.650 kip, this same snubber resisted loads as high as 2.248 kip during Test T41.31.2.

Test Results

Table 4-4. Snubber installation matrix for U.S. stiff support system.

Test No.	Snubber installed ^a					
	H-2	H-6	H-7	H-8	H-22	H-12
T41.35.2	PSA-1	PSA-1/2	A/D 150 ^b	A/D 70	PSA-1/4	A/D 40
T41.30.2	PSA-1	PSA-1/2	A/D 150 ^c	A/D 70	PSA-1/4	A/D 40
T41.30.1	PSA-1	PSA-1/2	A/D 150 ^c	A/D 70	PSA-1/4	A/D 40
T41.31.0	PSA-1	PSA-1/2	A/D 150 ^d	A/D 70	PSA-1/4	A/D 40
T41.31.1	PSA-1	PSA-1/2	A/D 150 ^c	A/D 70 ^b	PSA-1/4 ^b	A/D 40
T41.31.2	PSA-1	PSA-1/2 ^b	PSA-1	PSA-1/2	PSA-1/4 ^c	PSA-1/4
T41.31.3	PSA-1	PSA-1/2 ^c	PSA-1	PSA-1/2 ^b	PSA-1/4 ^c	PSA-1/4
T41.31.4	PSA-1	PSA-1/2 ^c	PSA-1	PSA-1/2 ^c	PSA-1/4 ^c	PSA-1/4
T41.31.5	PSA-1	PSA-1/2 ^c	PSA-1	PSA-1/2 ^c	PSA-1/4 ^c	PSA-1/4
T41.81.1	PSA-1	PSA-1	PSA-1	PSA-1	PSA-1	PSA-1
T41.81.2	PSA-1	PSA-1	PSA-1	A/D 70 ^b	PSA-1/4 ^b	A/D 40 ^b
T41.81.3	PSA-1	PSA-1	PSA-1 ^b	A/D 70 ^c	— ^c	A/D 40 ^c

a. PSA denotes a snubber provided by the Pacific Scientific Corporation while A/D denotes a snubber provided by Anchor/Darling Industries.

b. Snubber failed during this test.

c. Snubber in place but previously failed.

d. Snubber replaced for this test and failed again during this test.

e. Snubber removed—failed in previous test T41.81.2.

4.4.2 Test T41.81.1. Because of snubber failures in earlier tests, the 200% SSE test was used as the benchmark test of the U.S. stiff support system configuration. Overload snubber failures in the earlier tests prevented a true characterization of the U.S. system exposed to the dynamic loading. It was decided to repeat the 200% SSE test and to temporarily replace the smaller snubbers at locations H-6, H-8, H-12, and H-22. These snubbers did not have as much load safety margin as the larger snubbers at locations H-2 and H-7 (refer to Figure 1-1). The smaller mechanical snubbers were replaced with larger Pacific Scientific mechanical snubbers Size 1

(PSA-1), which were the same size as those installed at the other two locations.

Dynamic support load summaries for Tests T41.81.1, T41.81.2, and T41.81.3 are compared to the post-test load predictions in Table 4-5. The predicted loads are all positive because of the mathematical methods used in their calculation. The predicted loads would have the same magnitude in both tension (positive) and compression (negative). The maximum loads shown from the test results include the indication of whether the load was in tension or compression when the magnitude was recorded.

Table 4-5. U.S. stiff support configuration maximum dynamic support loads.

Support number	Node	Support type ^a	Global dir. ^b	Support loads—kip (kN)				
				Rated ^c	As-tested	Test 81.1 ^g	Test 81.2 ^g	Test 81.3 ^g
H-2	46	S	Y	2.10 (9.34)	2.61(11.6)	-1.69 (-7.53)	5.04 (22.4)	4.73 (21.0)
H-3	44	RS	HL ^d	2.10 (9.34)	3.05(13.6)	3.47 (15.4)	10.3 (45.8)	13.5 (59.9)
H-4	84	RS	Z	24.73 (110)	3.57(15.9)	N/A	N/A	N/A
H-6	118	S	Y	2.10 (9.34)	1.27(5.64)	1.36 (6.05)	5.64 (25.1)	9.17 (40.8)
H-7	128	S	Z	2.10 (9.34)	1.80(8.01)	4.19 (18.6)	9.75 (43.4)	-26.4 ^e (-118.)
H-8	128	S	Y	0.87 (3.85)	0.85(3.78)	-1.32 (-5.85)	1.87 ^e (8.30)	-10.5 ^f (-46.8)
H-9	144	RS	Z	0.87 (3.85)	1.28(5.68)	-0.62 (-2.75)	2.12 (9.44)	4.02 (17.9)
H-10	148	RS	X	0.87 (3.85)	0.77(3.43)	-0.94 (-4.17)	-2.97 (-13.2)	4.85 (21.6)
H-11	162	RS	Z	0.87 (3.85)	1.78(7.94)	-1.27 (-5.64)	-3.23 (-14.4)	-4.36 (-19.4)
H-12	162	S	Y	0.52 (2.30)	0.71(3.17)	-0.55 (-2.44)	1.07 ^e (4.78)	-5.72 ^f (-25.5)
H-22	213	S	Y	0.52 (2.30)	0.52(2.35)	-0.47 (-2.11)	-1.75 ^e (-7.80)	Removed ^f
H-23	77	RS	Z	49.5 (220)	9.09(40.4)	N/A	N/A	N/A

a. S = Snubber RS = Rigid Strut

b. Directions are in model global coordinate system.

c. Loads are Service Level C maximum loads—applies to tests 81.2 and 81.3 only.

d. HL = horizontal-lateral. This is a support located in the horizontal plane, perpendicular to the axis of the pipe.

e. Snubber failed during this test (see Table 4-4 also)

f. Snubber failed during previous test (see Table 4-4 also)

g. Negative signs imply compressive loads.

N/A = Not Applicable.

Test Results

The test data show that the snubbers allowed less than 0.03 in. of dead band travel (the distance a snubber travels from resisting the load in one direction to resisting in the other direction). The manufacturer specifies that this distance will be no more than 0.1 in. at design load and at frequencies above 3 Hz. If the Table 4-5 data for the T41.81.1 are compared with the predicted (200% SSE) values, it is observed that about half of the support loads were overpredicted, while about half were under predicted. The existence of gaps (pin slop), snubber dead band travel, and other differences between the idealized mechanical model and the actual system contribute to some of the over- and under-predictions. However, the analysis model is also sensitive to support changes. The addition of the bridge altered the

predicted dynamic response so that the first mode occurred at a frequency of 6.10 Hz. The predicted loads at H-7 increased from the design predictions to the as-tested predictions, but not enough to compensate for the as-measured load. H-7 is the most under-predicted support. Without running sensitivity studies we cannot determine the exact cause of the underprediction at H-7, but a good guess is that it probably could be improved by optimization of support location. Review of the Table 4-5 data for the other tests shows that some of the snubbers resisted loads far in excess of their rated loadings. The rigid struts also resisted loads far in excess of their ratings without any failures.

Displacements in the direction of the snubber restraint force are summarized in Table 4-6 for

Table 4-6. U.S. stiff support configuration maximum snubber displacement.

Support Number	Node	Global Dir. ^a	Design	Displacements [in. (mm)]		
				Test 81.1	Test 81.2	Test 81.3
H-2	46	Y	0.00	0.038 (0.978)	-0.102 (-2.602)	-0.069 (-76)
H-6	118	Y	0.00	0.052 (1.314)	-0.067 (-1.708)	-0.123 (-3.13)
H-7	128	Z	0.00	0.132 (3.362)	0.104 (2.646)	-0.688 ^b (-17.48)
H-8	128	Y	0.00	0.036 (0.912)	0.588 ^b (14.93)	-0.622 ^c (-15.79)
H-12	162	Y	0.00	0.048 (1.224)	-1.363 ^b (-34.63)	-2.23 ^c (-56.58)
H-22	213	Y	0.00	0.031 (0.800)	-0.504 ^b (-12.82)	NA ^d

a. Directions are in model global coordinates.

b. Snubber failed during this test (also see Table 4-4).

c. Snubber failed during previous test (also see Table 4-4).

d. Not applicable-snubber failed during previous test and was removed.

all snubber locations for Tests T41.81.1, T41.81.2, and T41.81.3. The data in this table for Test T41.81.1 show that the snubbers restrained piping motion to minimal values. Larger displacements were recorded in the other tests as the individual snubber failures occurred. Where no snubber failures occurred, displacements were minimized. It should be noted that the snubbers that were installed were either velocity- or acceleration-limiting types. That is, they are not designed to "lock" into a rigid restraint. Rather they are intended to supply the required force (within their design load limitations) to limit either the perceived velocity or acceleration to the threshold level. The displacement values for the design case were calculated to be essentially zero, as would be expected considering the mathematical idealization of the model and the approximate stiffness values used in the representation of the snubbers. In addition, the repeat 200% SSE test provided a characterization of stiff system performance, at significant loading, to which comparisons with predicted values and other test results could be made.

4.4.3 Test T41.81.2. The objectives of the 600 and 800% SSE tests were to study multiple support failures and possible damage to the piping system resulting from these failures. For the 600% SSE test (T41.81.2), the smaller snubbers sized for the predicted loads at 100% SSE were reinstalled at locations H-8, H-12, and H-22. These were mechanical snubbers manufactured by Pacific Scientific and Anchor/Darling Industries. The snubbers at the H-2, H-6, and H-7 locations were PSA-1. H-2 and H-7 were also sized for the predicted loads at 100% SSE. H-6 was resized for the T41.81 series because of the observed loadings from the earlier test series.

During the 600% SSE test, the snubbers at H-8, H-12, and H-22 failed on overload. Figures 4-11 and 4-12 are plots of the force and displacement histories, respectively, for H-8. These are typical examples of snubber force and displacement histories, showing the loads at which the snubbers failed and the resulting displacements. It should be noted that these time histories began when the

data acquisition system was started. Typically, the data acquisition system was started about three seconds before the shaker input was initiated. The tests were considered to have begun when the shaker input was initiated. Therefore, an event that is described as occurring at three seconds into the test will be located at six seconds on the time scale of the time histories.

Figure 4-11 shows the Anchor/Darling mechanical snubber at H-8 failing after resisting 1.80 kip (8 kN) loading at approximately three seconds into the test (six seconds on the plot time scale). This snubber was a size A/D-70, with a rated load of 0.700 kip (ASME Code Service Level B). Thus, the snubber failed at 2.5 times its rated load. This snubber did not resist any load after it failed. As can be seen in Figure 4-12, increased displacement was experienced after the failure. We use the Level B load for comparison to failure, as most industry applications would be sized for Level B.

Figures 4-13 and 4-14 show the force and displacement histories for the Pacific Scientific snubber size 1/4 at the H-22 location. At approximately 7.5 seconds into the test (10.5 seconds on the time history time scale), the snubber resisted a 1.6-kip (7.2-kN) loading; at this point, the displacement increased significantly. Large displacements continued, but the snubber also continued to resist some loading as shown in the force history. The Pacific Scientific size 1/4 snubber is rated for 0.350 kip (ASME Code Service Level B). The snubber failed at 4.6 times its rated load.

The snubber at H-12 failed at five seconds into the transient (eight seconds on the time history time scale), after resisting loads up to about 1.1 kips (4.8 kN). Figures 4-15 and 4-16 show the force and displacement time histories for this unit. This Anchor/Darling snubber (size AD-40) had an ASME Code Service Level B rating of 0.400 kip. The snubber failed at more than 2.5 times its rated load. As shown in Figure 4-15, the snubber did not resist load after the failure.

Test Results

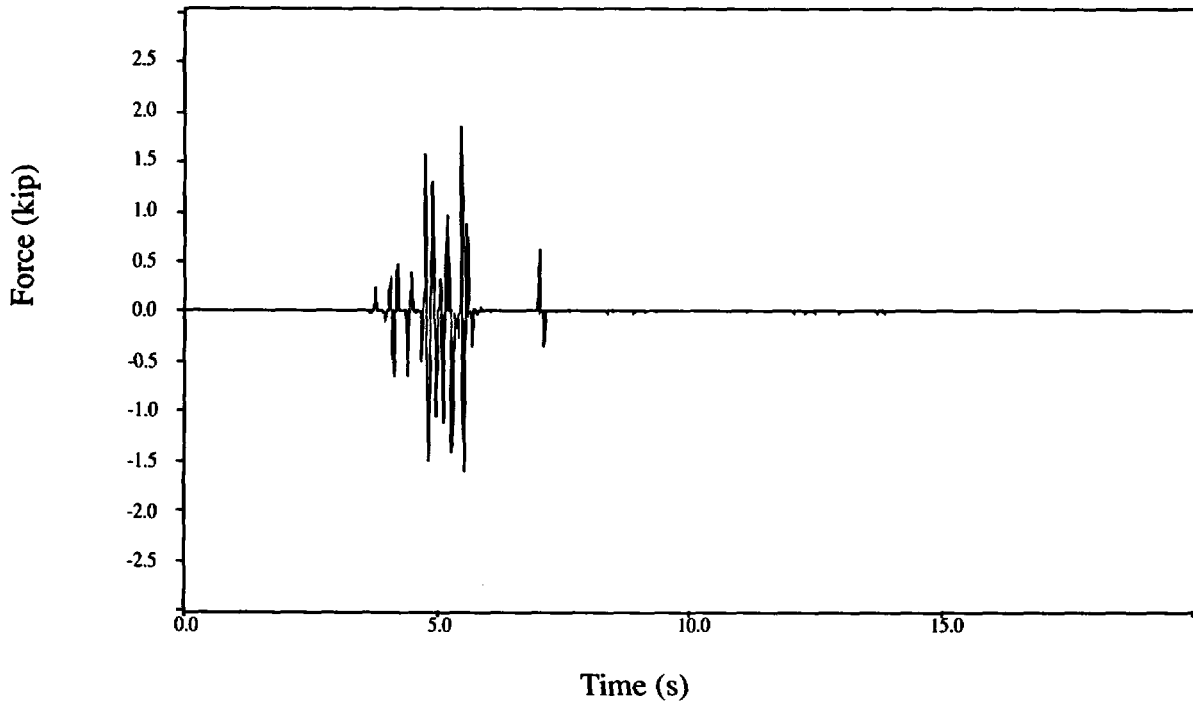


Figure 4-11. Force time history plot for H-8 (Test T41.81.2).

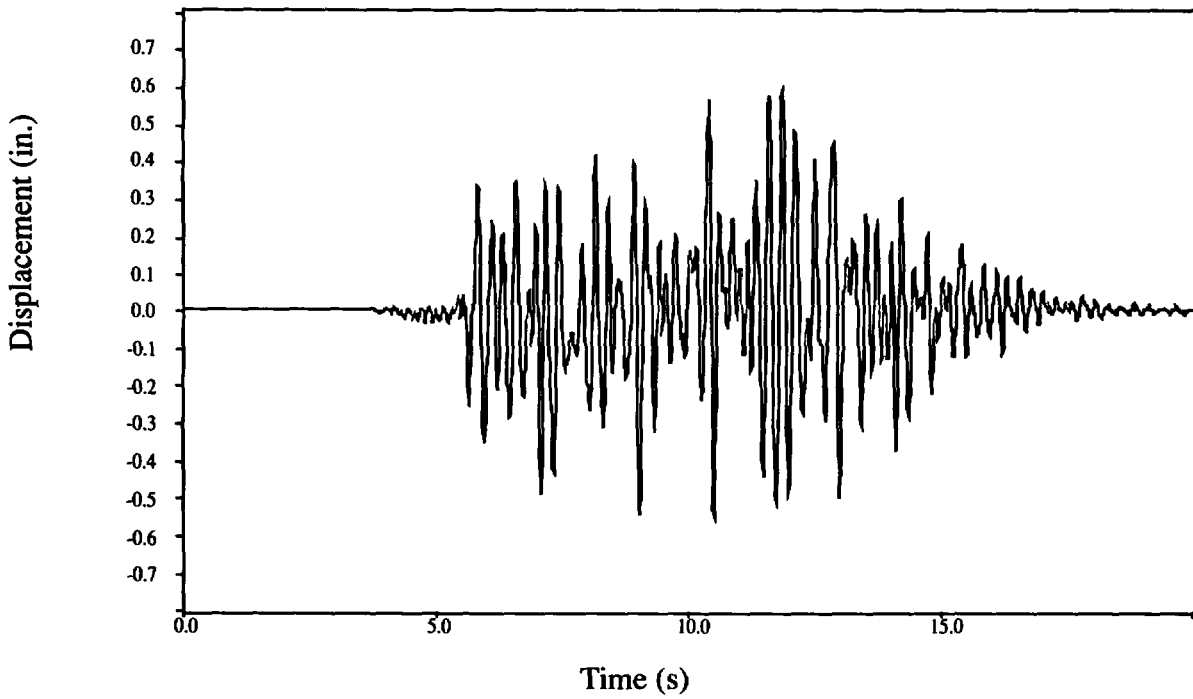


Figure 4-12. Displacement time history for H-8 (Test T41.81.2).

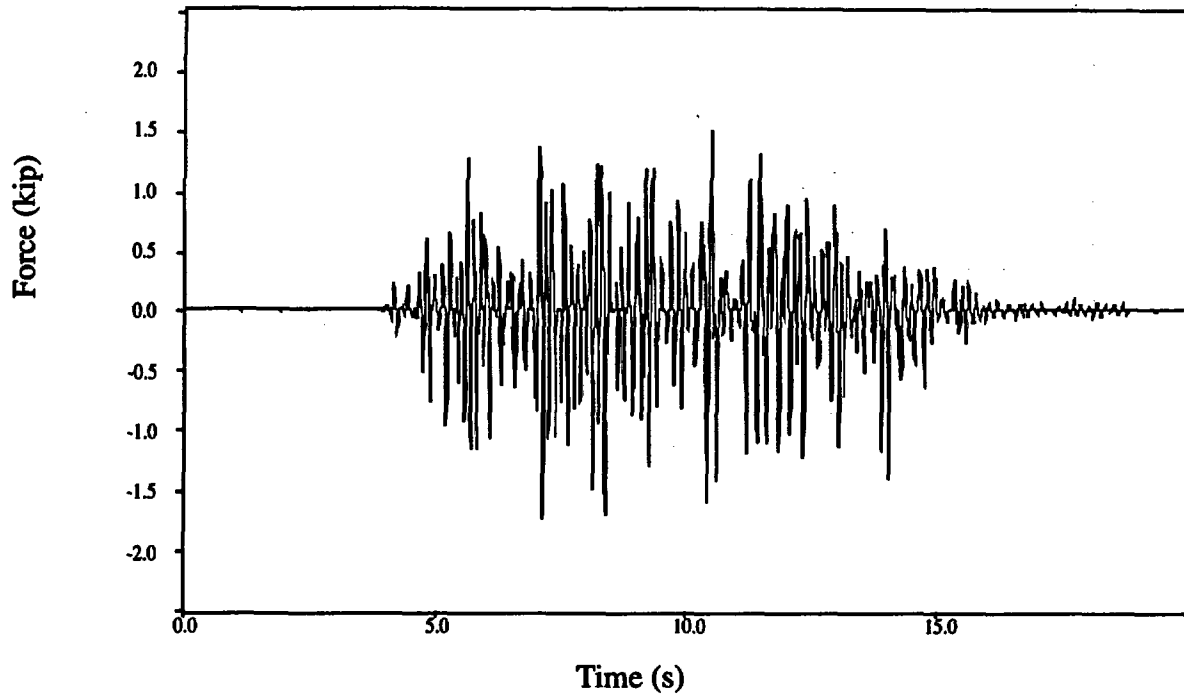


Figure 4-13. Force time history plot for H-22 (Test T41.81.2).

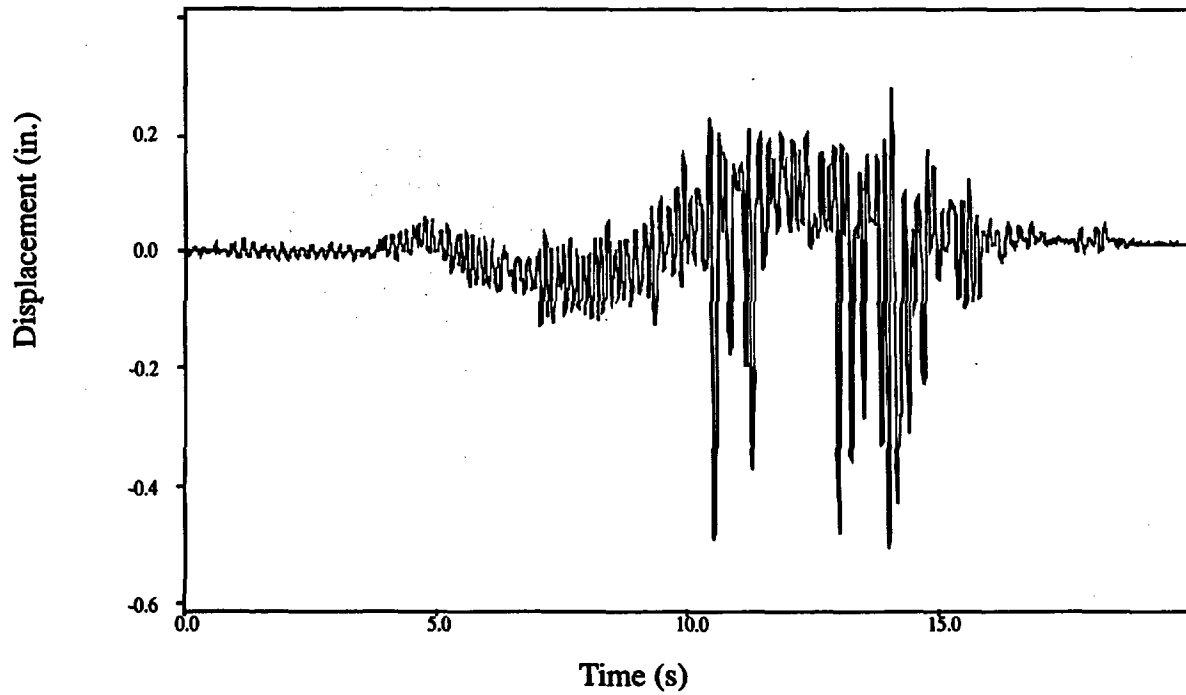


Figure 4-14. Displacement time history for H-22 (Test T41.81.2).

Test Results

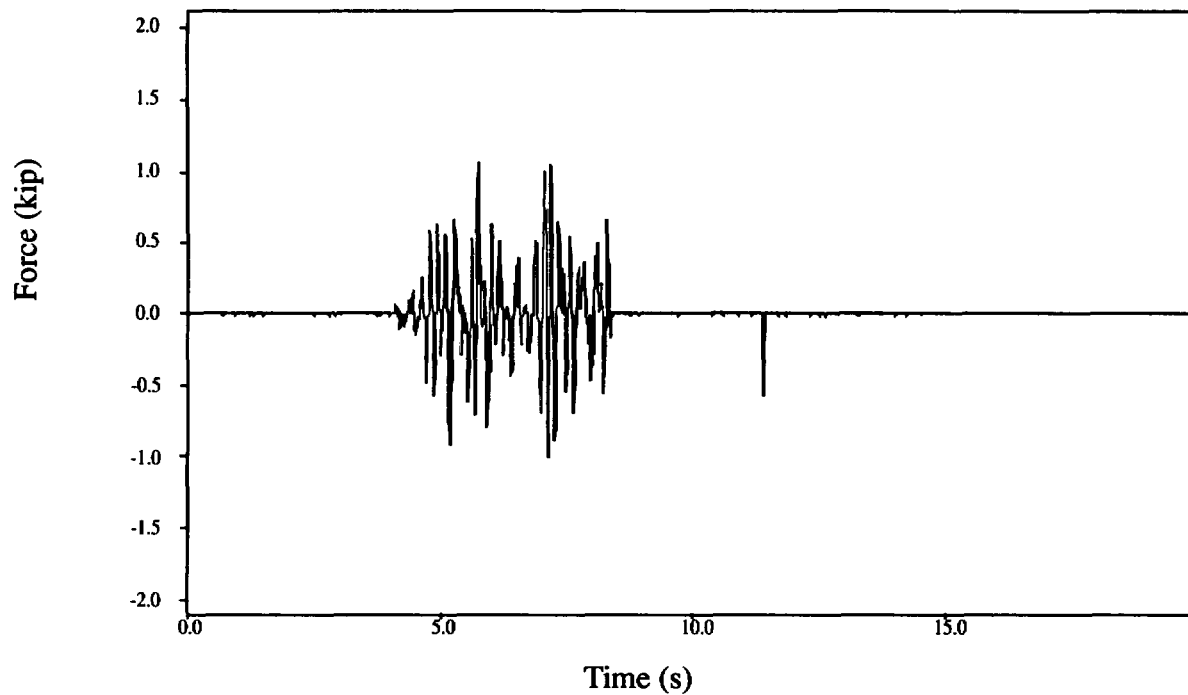


Figure 4-15. Force time history plot for H-12 (Test T41.81.2).

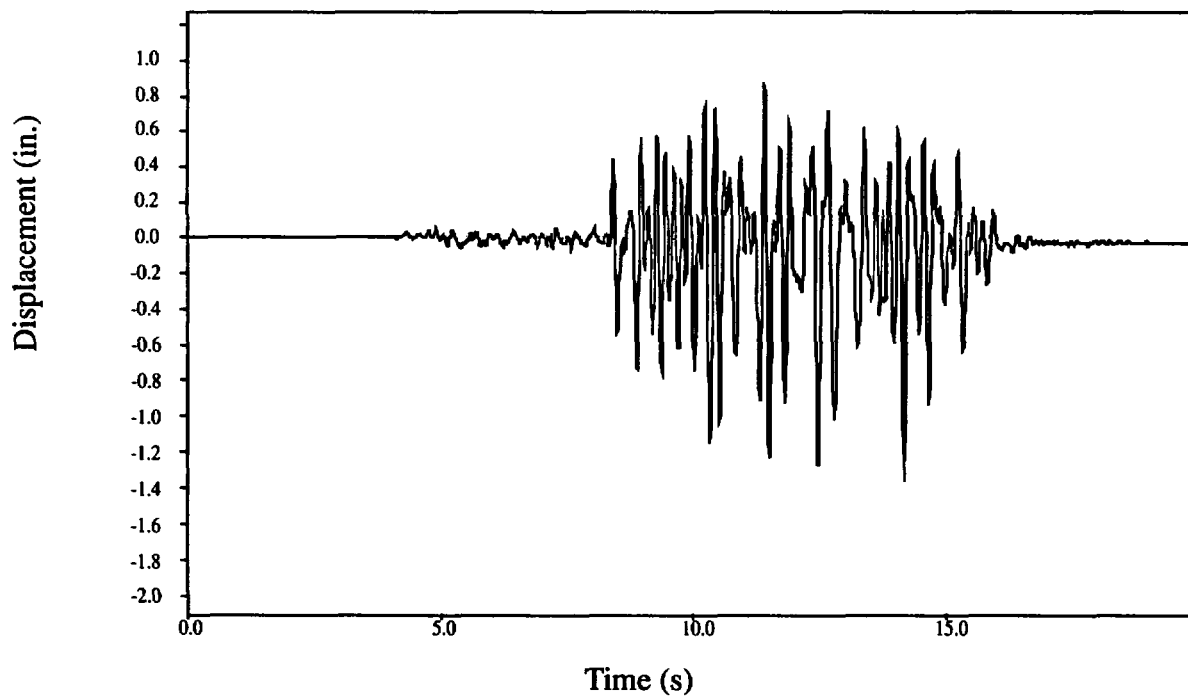


Figure 4-16. Displacement time history for H-12 (Test T41.81.2).

Figure 1-1 shows that snubber locations H-8, H-22, and H-12 are all vertical locations and control the vertical response of the 4-in. branch connection and the 4-in. loop. A further review of the data for this test shows that the snubber failures can be observed in the strain time history plots. The strains at the critical points on the piping system (Elbow 1, Elbow 2, and the DF44 tee shown in Figure 1-1) generally increase at the times of the snubber failures. No physical damage was observed on the piping system, and no permanent piping offsets were observed at the failed snubber locations. Photographs included in Figure 4-17 show the disassembled H-22 snubber and the damaged ball screw shaft. The failure of the ball screw shaft resulted in a "rigid mode" failure, in a thermal expansion sense, that rendered the unit incapable of normal movement while still able to resist some load. A rigid mode failure such as this may be beneficial during a dynamic event but could be very detrimental during normal operating conditions when movement is necessary to prevent large stresses resulting from thermal movements.

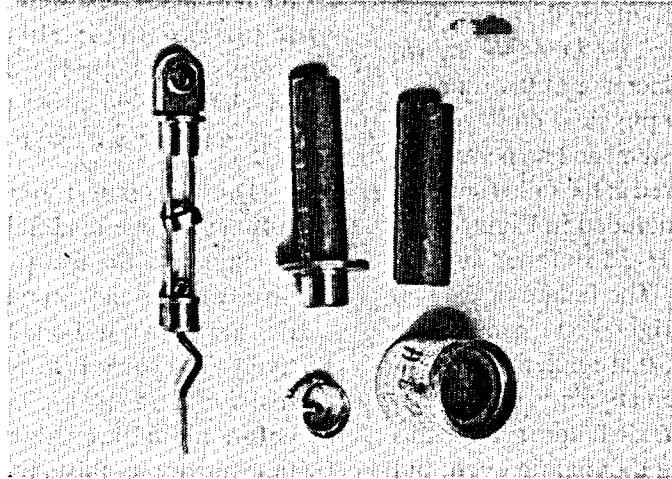
Zipper effect failures of piping supports and the associated performance of the piping system to which the supports were attached are subjects that have drawn much attention within the nuclear industry. In this scenario, the failure of one piping support results in a redistribution of loads to the remaining supports, which, in turn, subsequently fail from the increased loads. The timing of the failures of H-8, H-12, and H-22 at 3, 5, and 7.5 seconds, respectively, into the test transient show this behavior. The data plotted in Figures 4-11 through 4-16 show that, after the failure of H-8, the loads on both H-22 and H-12 increased to near the maximum levels that were sustained by each. Further information is given in the displacement histories of these snubber locations (Figures 4-12, 4-14, and 4-16). The displacements at the H-8 location increased in magnitude sequentially after the failures of H-12 and H-22. Likewise, the displacements at H-12 increased after the failure of the H-22 snubber. The displacement data show the increasingly flexible response that would be expected as the snubbers sequentially failed. In spite of the large

increases in displacements and strains, no physical failure of the piping occurred.

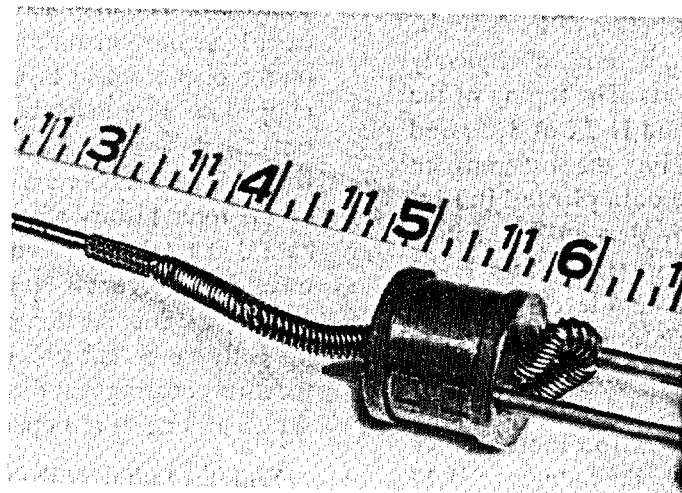
4.4.4 Test T41.81.3. For the 800% SSE test, the objectives changed slightly, the snubbers that failed (at locations H-8, H-12, and H-22) during the 600% SSE test were not replaced, in an effort to increase the likelihood that further piping stress could be induced. The snubber at H-22, which failed with resistance, was removed to simulate a failure without resistance.

During this test, the snubber located at H-7 suffered an overload failure at approximately six seconds into the test (nine seconds on the time history time scale). Force and displacement histories are shown in Figures 4-18 and 4-19, respectively. The force history shows that the snubber resisted loads as high as 13.0 kips (57.8 kN) before the failure. An examination of the force time history for this unit for Test T41.81.2 (600% SSE) shows that this unit resisted loads up to 11.0 kips (48.9 kN) during that test without failure. Since the ASME Code Service Level B load rating for this snubber is given in the vendor's catalog as 1.50 kip, loads up to 8.67 times the rated load were successfully resisted. The force time history shows the resisted force dropping to zero after the failure, then subsequently spiking to very large values. This is indicative of impacting as the snubber internal components were destroyed. The displacement history also indicates large movements after the failure. The peaks on the displacement history after the failure are clipped because displacements were beyond the range of the instrument. The nominal travel limits for a PSA-1 snubber are 4.0 in.; thus, the spikes on the force history after the failure would indicate that total movement exceeded the 4.0-in. travel limit. Figure 4-20 includes photographs of some of the snubber components. As can be seen, the ball screw shaft suffered severe deformation, the thrust bearing was destroyed, and the ball nut shows the effects of impacting.

With the failure of the snubber at location H-7 in this test and those at H-8, H-12, and H-22 in the previous test, the loop from snubber H-6 (see Figure 1-1) downstream to back the DF-16 is unsupported in the vertical (Y) direction, unsupported from H-4 to H-9 in the horizontal (Z) direction,



a. Disassembled PSA-1/4 snubber.



b. Close-up view of failed ball screw shaft.

Figure 4-17. Photographs of failed H-22 (PSA-1/4) snubber components.

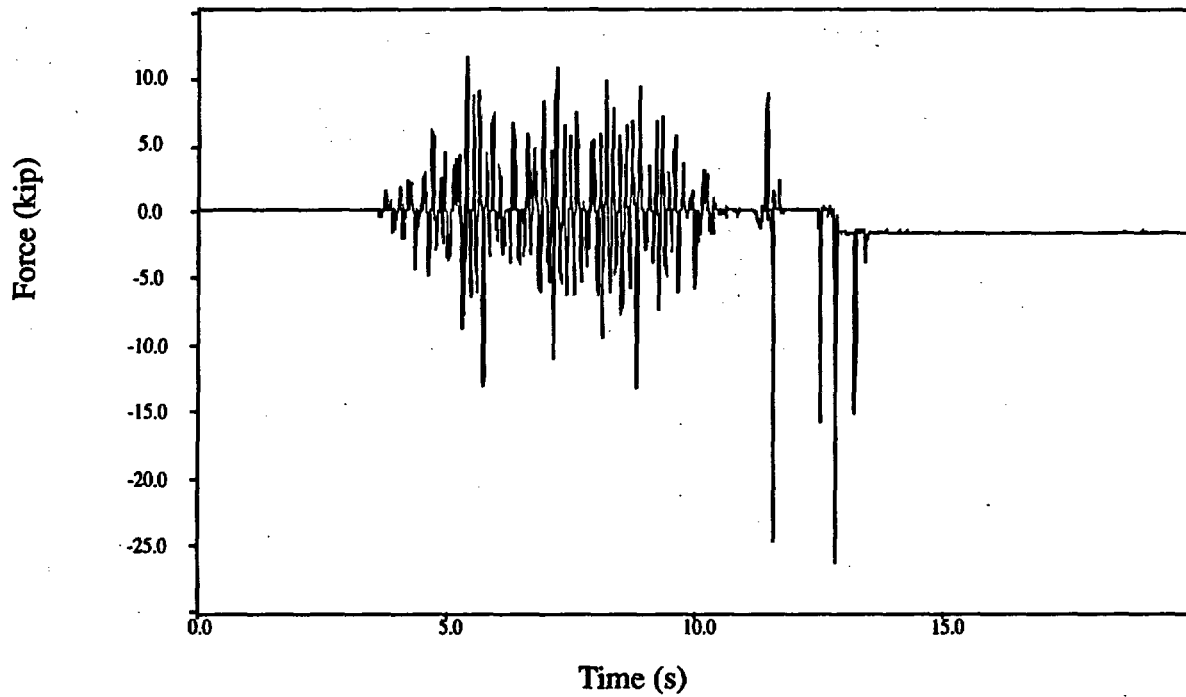


Figure 4-18. Force time history plot for H-7 (Test T41.81.2).

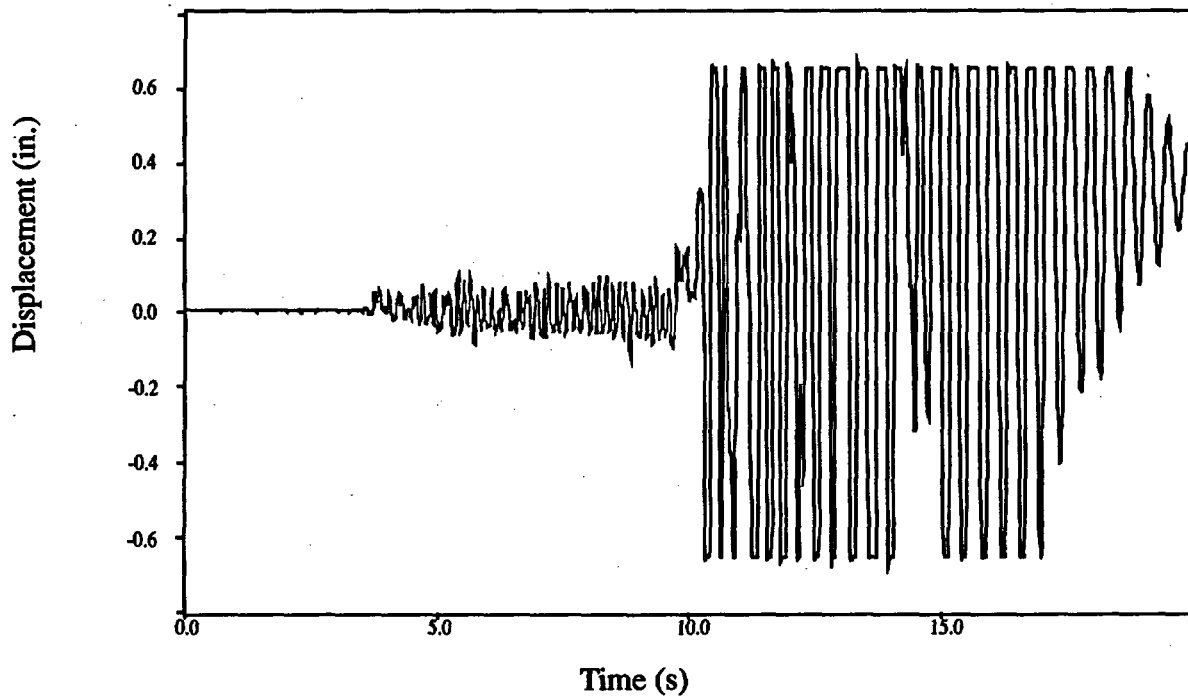
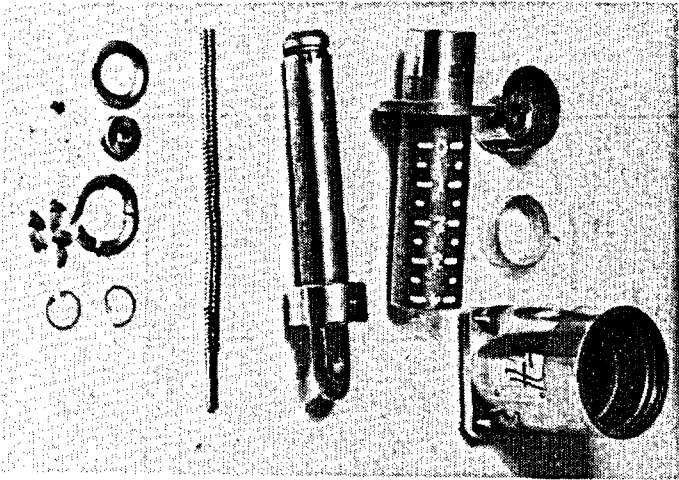
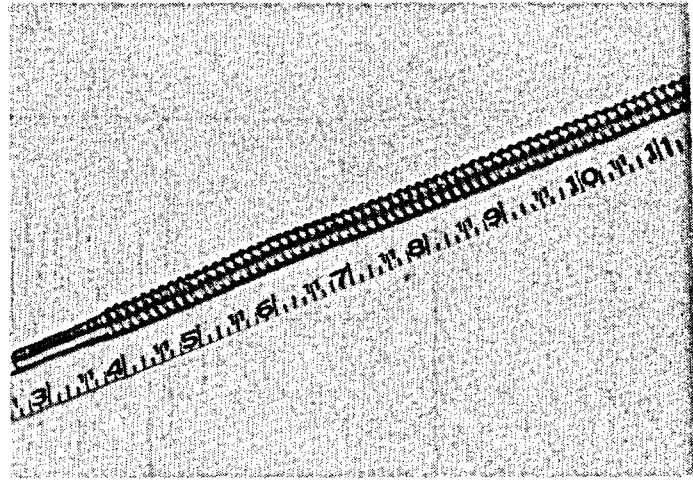


Figure 4-19. Displacement time history for H-7 (Test T41.81.2).

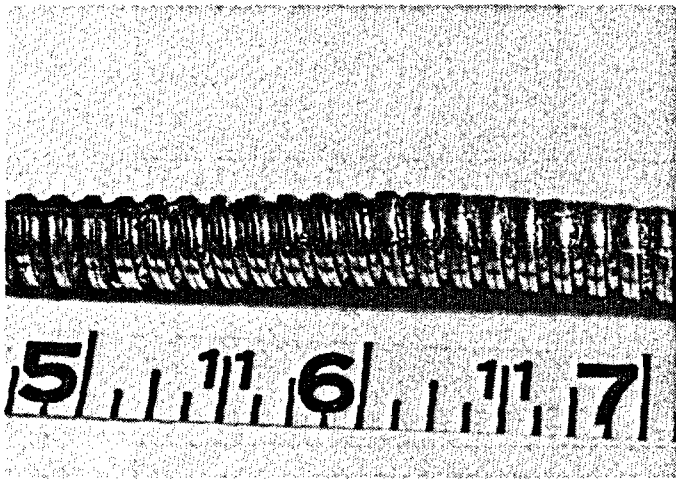
Test Results



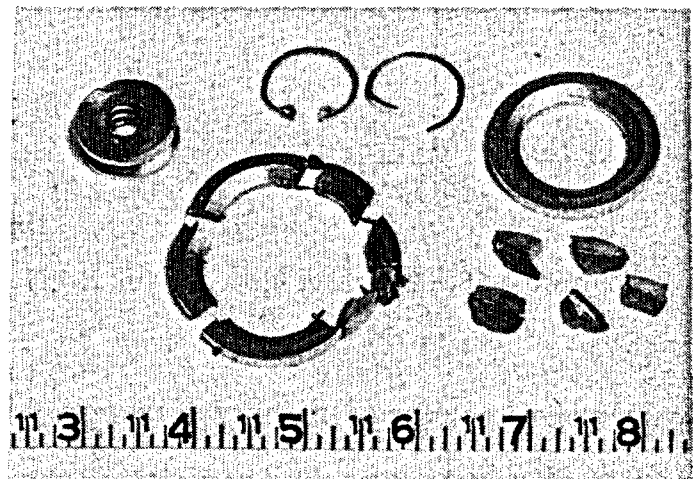
a. Disassembled snubber



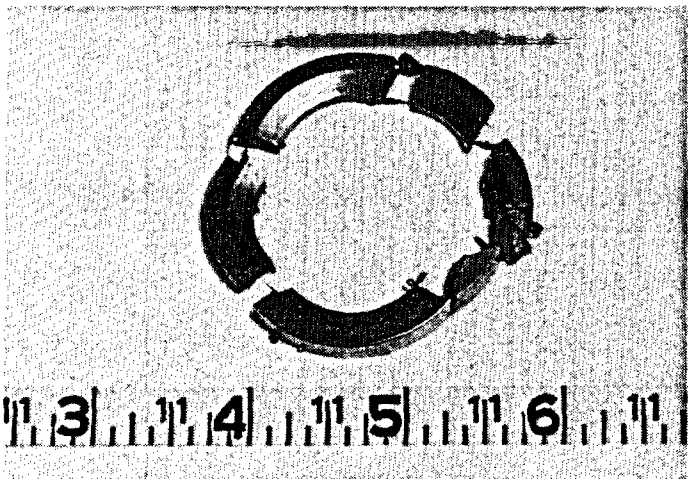
b. Failed ball screw shaft



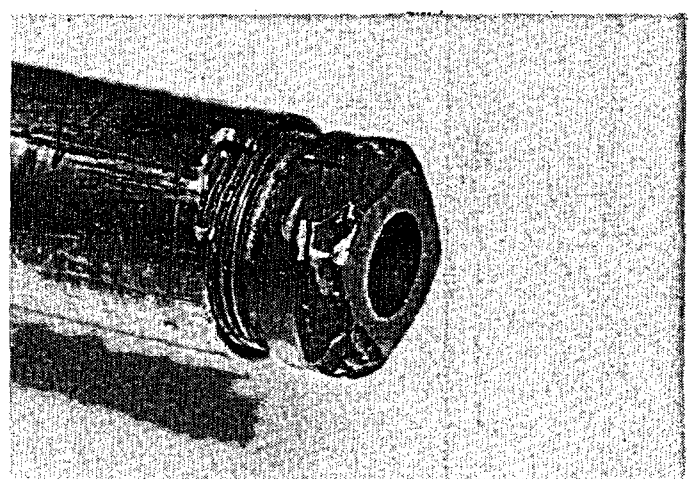
c. Close-up of ball screw shaft



d. Thrust bearing components



e. Failed thrust bearing



f. Damaged ball nut

Figure 4-20. Photographs of failed H-7 (PSA-1) snubber components.

and unsupported from H-5 to H-10 in the horizontal (X) direction. Examination of the displacement history for the H-8 location for these tests shows that the vertical and horizontal responses increased after the failure of H-7, but this is clouded by the fact that the bridge between DF-16 and DF-14 failed at nearly the same time. H-7 totally failed by 10.17 seconds and the bridge by 10.47 seconds. The videotape shot at the DF-16 location shows the bridge in what appears to be anti-resonant plastic behavior just prior to complete failure. The failures of H-7 and the bridge can be seen in the strain response at Elbows 1 and 2 (see Figure 1-1 and Figures 4-7 through 4-10). Plastic behavior is also evident by the strain measurements not returning to the 0.0 line after the test. The strain data for the DF-44 tee branch connection also show the corresponding increase in strain and the onset of plastic behavior. The displacements and the strains also reflect a decrease in the response frequency. This is expected because, after the final snubber failure, the piping system became more flexible in this area. The change in frequency is clearly seen in the strain plots of Figures 4-9 and 4-10.

Figures 4-21 and 4-22 show the force and displacement histories for H-6, a vertical snubber location. Both histories show the effect of the H-7 snubber failure. They also show the lower frequency response of the piping system. After the H-7 failure, the PSA-1 snubber at H-6 resisted loads up to approximately 9.0 kip, which is six times its ASME Code Service Level B design load. Dead band travel within the manufacturer's specified tolerance was maintained by the H-6 snubber. The snubbers installed at locations H-2 and H-6 were tested for proper function after the SHAM test series was completed. Both of these snubbers passed the design functional test required of new units.

4.5 Performance of Other Support Components

Obtaining data regarding the safety margins and failure modes of other piping support components was also one of the objectives of this

project. The performance of rigid struts, trunion attachments, and concrete anchors was observed throughout the test series.

All the rigid strut type supports performed well. Loads in excess of five times the design ratings were sustained, with no failures or other anomalous behavior.

Trunion attachments performed well throughout the test series. No structural failures of the trunions were sustained and no adverse local effects on the piping were observed.

Wedge-type concrete anchors were used to secure some of the piping support base plates to the facility walls. No concrete anchors failed; however, during inspections after the high-level tests, it was observed that several of the anchors had loosened. There were no cases where a pipe support substructure was incapacitated because of the inability of the anchors to transfer load.

4.6 Gate Valve Performance

The U.S. 8-in. motor-operated gate valve operated smoothly during all tests in the SHAM series. Some limit switch chatter was observed; however, the limit switch did not stay open long enough during chatter to cause the motor controller circuit to interrupt current flow to the motor. Figure 4-23 is a valve operator motor current history during the 800% SSE test. The histories for Tests T41.81.1 and T41.81.2 are similar, with variations only in opening time. The example history shown in Figure 4-23 shows that the valve operated smoothly under the most severe structural loading experienced during testing of the U.S. stiff support system.

Acceleration time histories were recorded at the valve body, the valve/operator center of gravity (c.g.), and at the motor operator. PSDs were calculated from the acceleration histories and are included in Appendix C as Figures C-28 through C-54. The frequency bands and shapes of these PSDs are consistent between tests, indicating no significant shift in response. Since the valve/operator assembly is relatively stiff in comparison to the piping system, this behavior is what one would expect. While the most significant contributions to the valve/operator response

Test Results

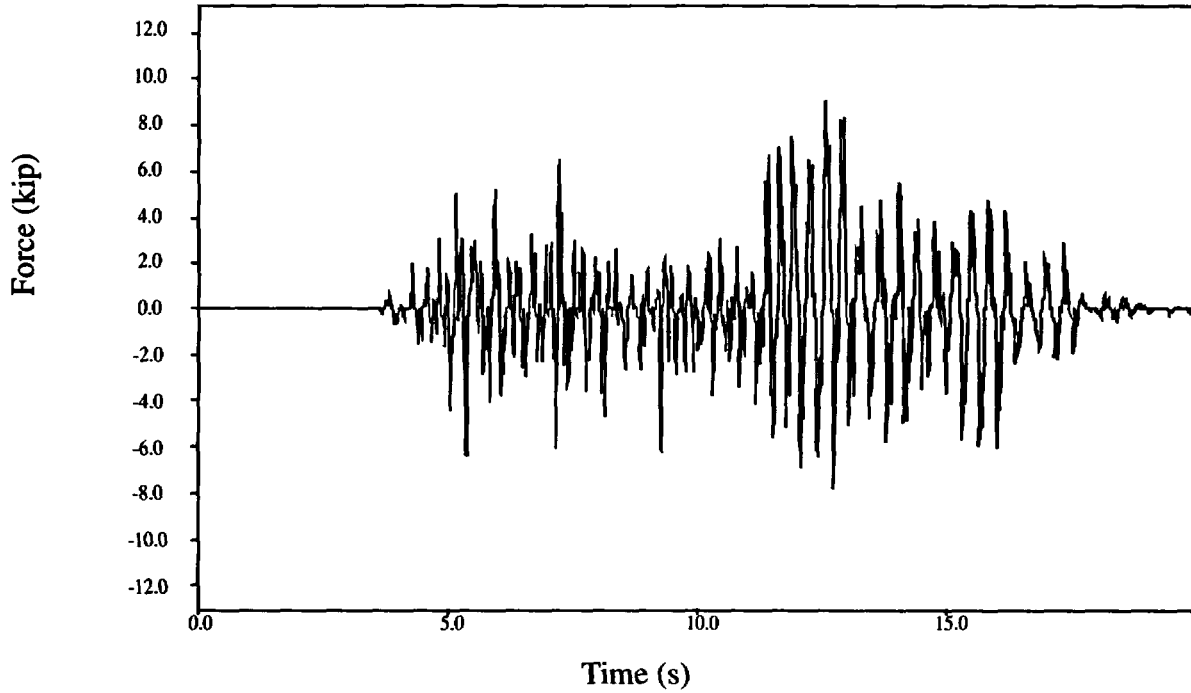


Figure 4-21. Force time history plot for H-6 (Test T41.81.3).

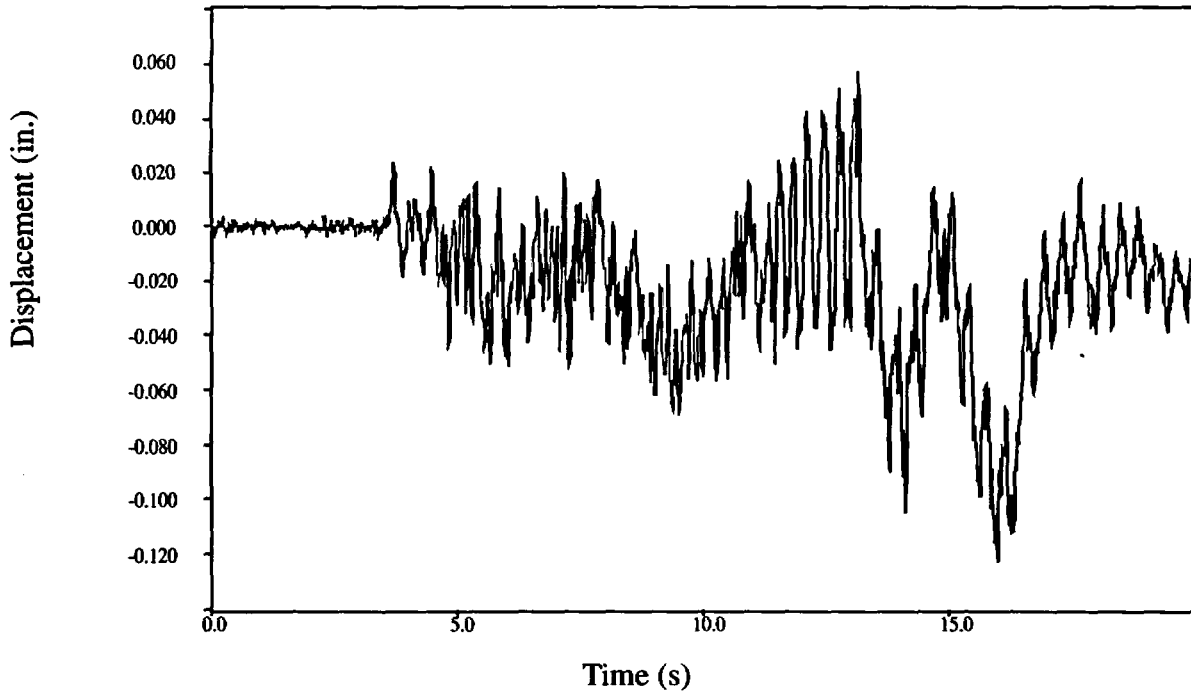


Figure 4-22. Displacement time history for H-6 (Test T41.81.2).

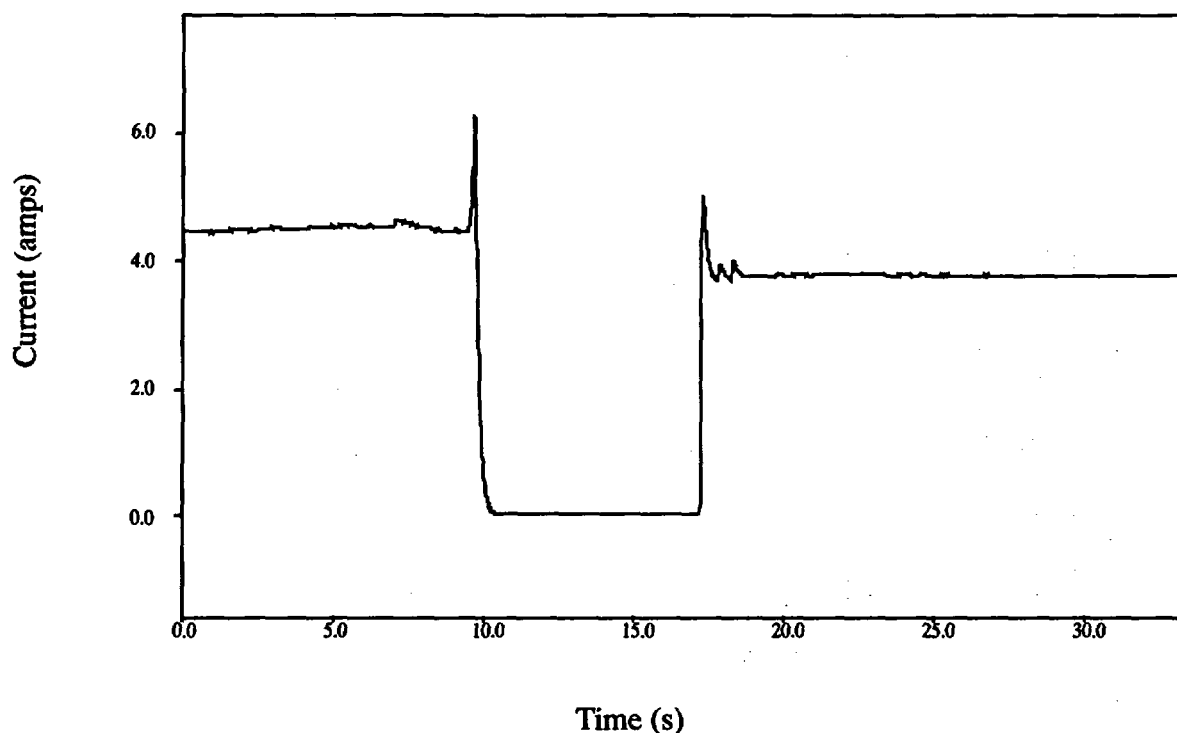


Figure 4-23. Valve current history for the 800% SSE test.

occur at the lower frequencies, the PSDs also show some higher frequency response in the 30- to 40-Hz range. This is higher frequency response than is normally considered in seismic qualification of valves. While this is not typically important to the structural response of valves subjected to seismic loads, it can be important to electrical components such as switches and relays located in valve operators. Responses in this frequency range did contribute to operator relay and switch chatter. However, the open portion of the switch chatter was not long enough to open the motor controller. The maximum accelerations of the valve/operator assembly were experienced at the motor operator. Since the motor operator is a significant mass essentially cantilevered off the relatively stiff valve body, this is where the largest accelerations would be expected. Table 4-7 includes both the accelerations measured during

Tests T41.81.1, T41.81.2, and T41.81.3 and those predicted by the system design analysis. A maximum acceleration of approximately 12 g was sustained in the 800% SSE test without apparent damage or malfunction. As can be seen in Table 4-7, the accelerations predicted by the design analysis differ from those that would be obtained by scaling the accelerations measured during the 200% SSE test (T41.81.1). Small differences in the actual stiffness of the valve/operator assembly versus that used in the finite element representation and actual versus idealized mass distribution would contribute to the differing results. Also, actual input for each test enveloped the design values (refer to Figures 4-1 through 4-6). The higher magnitude of the actual test input would also contribute to the larger accelerations experienced during the tests.

Table 4-7. Gate valve accelerations.

Location	Instrument	Global dir. ^a	Accelerations—g's							
			Design (1 SSE)		Test 41.81.1 (2 SSE)		Test 41.81.2 (6 SSE)		Test 41.81.3 (8 SSE)	
			Positive	Negative	Positive	Negative	Positive	Negative	Positive	Negative
Body	QB9401	X	0.51	0.51	1.45	1.44	5.43	4.57	7.61	7.19
Body	QB9402	Y	0.23	0.23	0.43	0.39	1.03	1.24	1.69	1.71
Body	QB9403	Z	0.30	0.30	0.65	0.67	2.56	3.07	3.58	5.20
C.G.	QB9411	X	0.73	0.73	1.51	1.50	6.58	6.00	9.13	7.97
C.G.	QB9412	Y	0.23	0.23	0.42	0.37	1.07	1.55	2.03	1.96
C.G.	QB9413	Z	0.88	0.88	0.49	0.56	2.25	2.47	3.29	4.87
Operator	QB9421	X	0.89	0.89	2.25	2.21	9.10	9.80	11.38	12.03
Operator	QB9422	Y	0.23	0.23	0.67	0.59	1.62	1.83	2.85	2.59
Operator	QB9423	Z	1.25	1.25	1.91	1.51	4.11	4.18	7.16	10.30

a. Directions are in model global coordinate system.

5. CONCLUSIONS

While each piping system includes its own specific details regarding materials, geometry, and support configuration, the VKL system with the U.S. stiff support configuration can be considered typical of those of similar size found throughout the U.S. nuclear industry. The VKL piping system was exposed to significant dynamic loadings and the specific results from tests at input levels of 200% SSE, 600% SSE, and 800% SSE were examined. These tests were numbered T41.81.1, T41.81.2, and T41.81.3, respectively, in the SHAM series. Analyses of the results were generally divided into three categories: piping system dynamic response, dynamic support performance, and gate valve performance.

5.1 Piping System Dynamic Response

The comparison of the scaled results from the 200% SSE test (T41.81.1) was not expected to exactly match the analytical predictions. Generally speaking, piping system analyses using the ASME Code rules and procedures that were followed will not provide information describing the exact state of stress. Rather, satisfaction of the Code rules provides assurance that piping system function and performance with an acceptable safety margin will be maintained.

The 200% SSE test results with all dynamic supports operable would be most comparable to the analytical predictions. Snubber overload failures in the early tests of the U.S. stiff support configuration delayed characterization of the piping system. Therefore, the 200% SSE test was performed with snubbers larger than those called for by the design calculations in order to ensure completion of the test without snubber failures. The post-test analyses with the bridge installed showed that the design analysis predicted maximum stresses at the same locations where the maximum strains were recorded during the tests. Similarly, the PSDs calculated from acceleration histories show that the piping responses were generally in the same frequency bands as the computer-predicted natural frequencies and mode shapes.

The 600% SSE and 800% SSE test results showed that, as the different snubbers failed, leaving a large portion of the piping system without vertical dynamic support, the frequency response shifted, as one would expect for a more flexible system. The piping system was able to sustain dynamic loads in excess of eight times the baseline seismic input that was used for the design analysis, without violation of the piping pressure boundary.

The test results summarized above support the following conclusions regarding piping system dynamic response:

- The observed test results for the support configuration, closely resembling those used in the analytical predictions, showed that predicted behavior generally agreed with the system behavior when subjected to similar loading.
- Application of commonly accepted good design practice and use of the ASME Code rules resulted in a conservative prediction of the piping system behavior under high-level dynamic loading.
- Actual failure of the piping and loss of pressure boundary retention was not observed, even under dynamic loads in excess of eight times the baseline seismic input. The actual margin to failure of this specific system is not known.
- Piping system behavior reinforced observations made in post-seismic-event inspections of piping systems in fossil-fuel-powered plants. Specifically, the piping was able to maintain the pressure boundary throughout the event. Piping displacement was accommodated by the failure of individual supports.
- Behavior of the system with several failed dynamic supports indicates that revised design practices resulting in a less stiff support configuration could still include acceptable safety margins.

5.2 Dynamic Support Performance

The U.S. stiff piping support system was designed using commonly accepted industry practices and sized for a 100% SSE loading. Loadings in excess of 800% SSE were applied, resulting in significant piping system responses and the overload failure of several individual snubbers. The piping system sustained multiple adjacent support failures, with measured strains greater than yield, yet no significant damage occurred.

Two snubbers failed before reaching their rated loads in tests previous to Test T41.81.1. These two snubbers were the same size and supplied by the same manufacturer. Brittle fracture of a connecting component was the apparent failure mode for both of the premature failures. Except for these two cases, all snubber failures occurred at loads well above their design ratings. In one case, a load of 8.67 times the design rating was sustained before failure. The test data show that the snubbers operated within their performance specifications, such as dead band travel, until a failure occurred.

The snubber failures can be observed in the strain time history plots. The strains at the critical points on the piping system (Elbow 1, Elbow 2, and the DF44 tee shown in Figure 1-1) generally increase at the times of the snubber failures. With the failure of the snubbers at locations H-8, H-12, and H-22, the loop from the snubber at H-6 near the spherical tee (refer to Figure 1-1) through the branch connection (DF44) and terminating at the DF16 manifold was left with no dynamic supports in the vertical (Y) direction. The displacement history for the H-8 location shows that the vertical displacements increased after the H-7 snubber failure. This was accompanied by the large increases in strain and plastic behavior. The displacements and the strains also reflect a decrease in the response frequency, which is expected, because after the final snubber failure, the piping system became more flexible in this area.

The timing of the failures of H-8, H-12, and H-22 and the force and displacement data for these three snubbers show that a zipper effect failure phenomenon occurred. However, in spite of

the large increases in displacements and strains, no physical failure of the piping occurred.

When the analytically predicted support loads are compared to test loads scaled to the 100% SSE level, we observe that about half of the support loads were over-predicted, while about half were under-predicted.

The results discussed in Section 4.4 and summarized above support the following conclusions regarding dynamic support performance:

- The rigid strut type supports performed well throughout the test series. While loads in excess of five times the design ratings were sustained, no failure or anomalous behavior was observed.
- Trunion attachments performed well throughout the test series. No structural failures of the trunions were sustained and no adverse local effects on the piping were observed.
- Concrete anchors securing the piping supports to the facility walls performed well throughout the tests. No concrete anchors failed; however, during inspections after the high-level tests, we observed that several of the anchors had loosened. There were no cases where a pipe support substructure was incapacitated from the inability of the anchors to transfer load.
- The zipper effect failure phenomenon was demonstrated during Test T41.81.2. The severity of this effect will vary for individual piping and support configurations; however, these test results indicate that this zipper effect may not be the problem it is currently considered to be in the performance of probabilistic risk analyses (PRAs), and other safety evaluations.
- The rigid mode failure of one snubber, in our opinion, highlights the continuing need for ongoing snubber inspection and test programs. This type of failure has been observed many times elsewhere throughout the nuclear industry. While a rigid mode failure may be acceptable during a dynamic

event, the failure of a snubber to allow the required thermal movements could be highly detrimental.

- Further research on the ability to accurately predict support loads would be warranted. For the piping system used in this test series, the analytical predictions were accurate for only one dynamic support. About half of the loads were over-predicted while about half were under-predicted. As industry initiatives to reduce the number of snubbers installed in nuclear power plants progress, the ability to accurately predict the loads on the remaining supports will become more critical to ensuring that adequately sized components are installed.

5.3 Gate Valve Performance

The U.S. 8-in. motor-operated gate valve operated smoothly during all tests in the SHAM series. Some limit switch chatter was observed; however, the limit switch did not stay open long enough during the chatter event to cause the motor controller circuit to interrupt current flow to the motor. The data show that the valve operated smoothly, even under the most severe structural loading experienced during testing of the U.S. stiff support system.

The valve performance data support the following conclusions:

- The valve/operator assembly performed well during all tests, sustaining a maximum acceleration of slightly greater than 12 g without adverse effect.
- Higher frequency response than is normally considered in seismic qualification was observed. While this is not typically important to the seismic performance of mechanical devices, it can be important to electrical components such as switches and relays.
- Further investigation into existing research literature or additional testing to determine the threshold level where limit switch chatter would cause current interruption would

be useful. This information would help in identifying methods to mitigate this potential problem. Such information would also be useful for possible future revisions to the rules for qualifying valve operators, contained in the IEEE-382 standard. This standard currently allows a cutoff frequency below the range of the high-frequency effects that were observed in these tests.

5.4 General Conclusions

The analytical and test efforts described in Sections 3 and 4 show that, in general, all program objectives were satisfied. The load level where structural damage to the valve or operator occurred was not established in these tests. However, the test results showed that increasing seismic loading up to eight times the baseline seismic input had no serious effect on the operation of the gate valve and operator. Much useful information regarding the safety margins of piping and supports was gained from these tests. We saw that most of the snubbers sustained loads well in excess of their design ratings, with one unit carrying a load 8.67 times its design rating before failure. At dynamic input levels of eight times the baseline design SSE loading, no piping structural failures occurred. Some plastic behavior was observed at Elbows 1 and 2, but pressure boundary integrity was maintained in all cases. The effects of individual and multiple support failures were observed throughout the tests, and it was found that, while system response changed, no loss of function of the piping system occurred. Additionally, the test results will add to the body of data available for comparing and assessing piping systems with differing support configurations and design philosophies.

Further analysis of the available data by ANL and KfK may yield additional insights into piping system and support component behavior. However, according to the results described above, sufficient safety margins exist when commonly accepted design methods are applied, and piping systems will likely maintain their pressure boundary, even in the presence of severe loading and the loss of multiple supports.

Conclusions

6. REFERENCES

1. R. Steele, Jr. and J. G. Arendts, *SHAG Test Series Seismic Research on an Aged United States Gate Valve and on a Piping System in the Decommissioned Heissdampfreaktor (HDR), Volumes I and II*, NUREG/CR-4977, EGG-2505, July 1989.
2. "Boiler and Pressure Vessel Code," Section III, Division I, Subsection NC, Class 2 Components, 1980 edition, American Society of Mechanical Engineers.
3. DADiSP, Version 2.01C, *DSP Development Corporation*, July 1991.
4. A. G. Ware, and G. L. Thinnes, *Damping Test Results for Straight Sections of 3-inch and 8-inch Unpressurized Pipe*, NUREG/CR-3722, EGG-2305, April 1984.

Appendix A

**Design Report:
Servohydraulic Excitation of Mechanical
Equipment HDR Test Group Sham
vs. No. T41**

PHDR Work Report No. 4.338/88

HDR Safety Program

Individual Project 4000: Structural Dynamic Investigations

DESIGN REPORT
**Servohydraulic Excitation
of Mechanical Equipment**
HDR Test Group SHAM
VS. No. T41

PHDR Work Report No. 4.338/88
March 1988

Vibration Behavior of Mechanical Installations Under High Dynamic Load

Authors: L. Malcher, PHDR
H. Steinhilber, LBF
D Schrammel, PHDR

Publisher: Kernforschungszentrum Karlsruhe GmbH
Project HDR safety program (PHDR)

Commissioned by the Federal Minister for Research and Technology
(Project RS 1500 123 C5)

The authors want to thank Dr.Ch.A. Kot (ANL), Dr. P.T. George (CEGB) and their staff for the translation of this report.

Distribution:

Fraunhofer Institut für Betriebsfestigkeit (LBF), Darmstadt
Argonne National Laboratory (ANL), Argonne, IL, U.S.A.

Bayerisches Staatsministerium für Landesentwicklung und Umweltfragen, München

Bechtel Power Corporation, San Francisco, CA, U.S.A.

Central Electricity Generating Board (CEGB), Knutsford
Chesh., U.K.

Cloud Associates, Berkeley, CA, U.S.A.

Electric Power Research Institut (EPRI), Palo Alto,
CA, U.S.A.

Idaho National Engineering Laboratory (INEL),
Idaho Falls, ID, U.S.A.

Gerb, Essen und Berlin

Gesellschaft Für Reaktorsicherheit/Forschungsbetreuung, Köln

Jarret, Oberhausen

Lisega, Zeven

Siemens Unternehmensbereich KWU, Offenbach

TÜV - Rheinland, Köln

TÜV - Bayern, München

United States Nuclear Regulatory Commission (USNRC)

Wolfel Beratende Ingenieure, Würzburg

Internal distribution:

Müller-Dietsche	PHDR
Dr. Katzenmeier	PHDR
Dr. Jehlicka	PHDR
Dr. Malcher	PHDR
Schrammel	PHDR
Wenzel	HDR
Löhr	HDR
Grimm	HDR
Huber	HDR
Dr. Jansen	HDR
Reserve (5x)	

Preliminary remarks:

The design report describes the technical test set-up, the planned test program, and the planned measurements for a test or test group. It shall contain the basic information to enable advance calculation of the test and evaluation of the results.

The test report, the supplementary report, and to a limited extent also the quick look report and further technical reports build on the design report and do not repeat its information. Summaries, important extracts and deviations from the design report will be forwarded according to circumstances.

The design report is an internal work report and is distributed only to the parties participating in the test series.

Not to be circulated outside the organization of the recipient without the prior written consent of the publisher.

CONTENTS

Page

1.	OBJECTIVE OF THE TEST SERIES	
2.	EXPERIMENTAL FACILITY	
2.1	Investigated structures	
2.2	Pre-test weld seam examination	
2.3	Excitation systems	
3.	INSTRUMENTATION	
3.1	Measurement plan	
3.2	Stress coating instrumentation	
3.3	Brief description of the central measurement data acquisition system ZMA	
3.3.1	Introduction	
3.3.2	Signal processing	
3.3.3	Data recording	
3.3.4	Data processing and evaluation	
3.3.5	Form of representation of the data	
4.	TEST PROCEDURE	
4.1	General observations	
4.2	Load functions	
4.2.1	Random excitation	
4.2.2	Earthquake histories	
4.3	Accuracy requirements for the excitation systems	
5.	CALCULATIONS	
5.1	Design calculations	
5.1.1	Objectives of the design calculations	
5.1.2	Calculation models	

5.1.3 Calculations performed

5.1.4 Summary of results

6. REFERENCES

1. OBJECTIVE OF THE TEST SERIES

The tests with servohydraulic excitation of the mechanical equipment (SHAM) are related directly to the seismic design of nuclear power stations and have the overall aim of investigation of the behavior of pipes and tanks under very high to extreme dynamic loads. This investigation is conducted firstly by suitable experiments on the VKL (Versuchskreislauf) pipe system, which is connected to the HDU (Heissdampfuraformer, now pressurizer) and to the primary steam header, and secondly by accompanying calculations (design, advance and supplementary calculations), the latter being made on the basis of measured load time functions, but without a knowledge of the measured vibration responses.

In all earthquake or structural dynamic experiments so far conducted the stresses on the mechanical installations have intentionally been kept in the linear-elastic range. In the SHAM experiments the aim is to achieve local plasticization of the pipe with earthquake-type or dynamic excitation.

Upon completion of the SHAM test program, in already the second test series of Phase III of the HDR safety program, it is planned to insert damaged pipe sections (with selectively introduced, quasi-natural fatigue cracks) at the most highly stressed pipe bend and straight pipe run of the VKL system and to load the piping with internal pressure and a superimposed dynamic load until failure [Phase III, Test Series E32].

The SHAM tests serve the following purposes:

- evaluation of different pipe support concepts, using both highly flexible as well as very rigid hanger configurations,
- determination of the shifting of natural frequencies or
- determination of the increase in damping in the system as a result of different load stages up to local plastic deformation,

- evaluation of the capability of the calculation models or correctness of the assumptions made for dominant Parameters and boundary conditions, i.e., in general terms to verify the calculation methods, taking cognizance of the anticipated high excitations, and
- from the point of view of "equipment qualification" for the performance test on one valve under operating pressure and superimposed earthquake loads of various magnitudes (up to 10-fold Safe Shutdown Earthquake (SSE) technically attainable).

2. EXPERIMENTAL FACILITY

2.1 Investigated structures

The VKL (Versuchskreislaff) pipe system investigated in the SHAM experiments is located in compartment 1.704 of the HDR between the heights 14.25 m and 30.05 m (see Figure 2.1-1). The VKL system (Figure 2.1-2) is doubly connected to the HDU (Heissdampfumformer) vessel (previously superheated steam heat exchanger, now pressurizer) and the primary steam header (DF15), branched several times and contains pipes with nominal diameters of 300, 250, 200, 125, or 100 mm. The predominant part of the VKL consists of austenitic stainless steel material No. 1.4550 or 1.4961; only the subsequently inserted part DF44 as well as some caps are fabricated from ferritic stainless steel (15MO3/1.5,15). The exact dimensions of the VKL are contained in the table in Figure 2.1-3 as well as in the plan view in Figure 2.1-4 and the elevation view in Figure 2.1-5. The entire VKL pipe is insulated with mats 100 mm thick and with a density of 100 kg/m³; consequently different weights per meter result according to the nominal pipe size. In all SHAM experiments, the pipes and HDU will be filled with water, be cold, and be pressurized to 70 bar.

Hanger configurations used in the SHAM tests will be similar to those already used in the SHAG tests (configurations 1-5). Newly added are the configurations 6 and 7 represented by CEGB, where 7 is obtained from 6 by removal or addition of a strut/snubber. A survey of the different hanger configurations is presented in Figure 2.1-6. Figure 2.1-7 shows the assignment of the dynamic hangers to the individual positions. The technical

details of these hangers are summarized in Figures 2.1-8 and 2.1-9 (Refs. 1, 2).

The HDU - a slender, approx. 14 m high vessel with an outside diameter of 1855 mm and a wall thickness of 45 mm - stands on an 0.77 m high support skirt at building level + 14.25 m. Besides an electric heater (m approx. 325 kg) it contains a thermal shield (see Figure 2.1-10), its weight when empty is about 35 tonnes, 30 tonnes being added when it is completely filled with water. A deflection limiter consisting of double T-sections is located at building level 24.95 m (see Figure 2.1-11). The HDU is wedged in this deflection limiter as in the SHAG tests, so that the excitation energy is introduced essentially into the piping.

The annular support skirt of the HDU supports the vessel via 4 bearing zones, viz. 1 fixed bearing, 2 sliding bearings, and 1 roller bearing (see Figure 2.1-12), which are designed to essentially suppress thermal stresses.

The entire vessel is insulated with 100 mm thick foam; the insulation layer is held in position by a 1 mm thick sheet metal casing. The density of the insulation without the sheet metal casing is 100 kg/m^3 .

The VKL pipes are attached to the two cover nozzles II on the HDU. Figure 2.1-13 shows the connection of the pipes to the HDU. The pipe from the central cover nozzle I was removed for the SHAM tests.

During the SHAG-test the fitting DF16 (see Figure 2.1-14) was secured to the outer wall of compartment 1.704 to provide a further VKL "fixed point." During the SHAM test the components securing the DF16 were again removed and one of the two load application points was provided above the DF16 at the 27.6 m height. The pipe DR107 (nominal pipe size 300) leaving DF16 horizontally must be cut off for this purpose. Likewise, pipe DR105 (nominal pipe size 300) leaving DF16 vertically at the top is cut off above the excitation location. All cut locations are closed pressure tight by caps. The pipe (nominal pipe size 300) leaving DF16 downwards leads into the primary steam header, which now is changed to a fixed point (see Figure 2.1-15).

The NRC Valve of the Shipping Port reactor already installed during the SHAG-tests will also be installed during the SHAM-tests in the VKL system (see Figure 2.1-16).

2.2 Pre-test weld seam examination

In the regions most highly stressed during the tests as indicated by the design calculations, the weld seams will be subjected to different methods of nondestructive examination prior to the start of the experiments. Applied will be:

- X-ray examination
- Surface crack examination
- Ultrasonic examination

A survey of the individual measurement locations and the test methods applied there is presented in Figures 2.2-1 and 2.2-2.

Minor defects in the weld seams observed during this inspection will be documented but not repaired. Larger defects will either be repaired prior to the tests or will be monitored during the test performance.

A renewed inspection of the same weld seams and documentation of changes is planned after the performance of all tests.

2.3 Excitation systems

It is planned to excite the VKL piping system to the order of magnitude of several Safe Shutdown Earthquakes (SSE) (a maximum 10-fold SSE is technically possible) in the course of the SHAM experiments. Imbalance exciters of a suitable order of magnitude for direct excitation of the mechanical installations can no longer be used here, because their size would already falsify the dead weight of the investigated structures too much, quite apart from the unwieldiness during operation.

Hence servohydraulic cylinders, with which the deflection distance or load, for example, can be varied independently of the excitation frequency during an experimental run, will be used. In addition predetermined distance or load time curves can be realized within wide limits. The dependence of natural frequencies or damping on load can be investigated in an experimental run. Frequency ranges of interest can be directly approached selectively.

Two excitation points are planned for the hydraulic cylinder (see Figure 2.3-1). One point is located between the spherical fitting and the NRC valve. Here the excitation cylinder replaces a horizontal strut (H5), acting in the overall x direction, included in all hanger configurations in SHAG. Overstressing of the pipe section at the load application point is eliminated according to corresponding safety considerations.

The second excitation point is located on the nominal pipe size 300 pipe line leaving DF16 vertically upwards. Here too the excitation direction is the overall x direction.

The excitation systems include essentially the following:

A) Hydraulic Actuator (Cylinder)

Two hydraulic actuators (see Figure 2.3-2) each with a rated force of + or - 400 kN (40t) and a rated stroke of + or - 125 mm will be used. Special types for large oil flows, in this case 1000 l/min, are involved. The operating pressure is 280 bar. The actuators are each equipped with a servo block, differential pressure transducer, 3-stage servo valve, remote controlled multi-valve, and distance transducer installed in the actuator. Operating diagram DPP3 268, see Figure 2.3-3, applies to these. Construction details of the load application at H5 and DF16 are to be taken from Figures 2.3-4 and 2.3-5.

B) Suction pumps

These are required to remove the leakage oil from the hydraulic actuators and return it to the hydraulic unit.

C) Supply valves

The supply valves are used for the pressurized oil supply to the actuators, each cylinder requiring its own valve. In the case of system fails, the valves block the oil supply within milliseconds and relieve the lines and systems on the pressurized oil side.

D) Piston/accumulator systems

A piston/accumulator storage system (see Figures 2.3-6 and 2.3-7) serving as energy storage system or intermediate buffer (see Figure 2.3-8) in conjunction with corresponding amounts of nitrogen is required for each actuator both on the pressurized oil and return oil side.

E) Electronic control systems

An electronic system containing generators of the specified input values and control elements as well as connections for control signals generated by a computer for the actuators is required for each of the two cylinders (or control circuits).

The specified input value can be predetermined directly or indirectly with the aid of a magnetic tape device by the Genrad system of the LBF. In this way excitation frequency and actuator displacement are controlled for stochastic excitation (RANDOM) and optional earthquake displacement history functions (ETH). If required, SINE SWEEP or SINE BEAT excitation can be provided without difficulty.

F) Hydraulic unit

The hydraulic unit at hand for the drive of the MK16 shaker, with its delivery of 840 l/min at a system pressure of 200 bar, is not adequate for the operation of the servo-hydraulic actuators. It was therefore rebuilt for a delivery of 350 l/min at a system pressure of 280 bar, at which time there were made different additional alterations, such as for instance fill and ventilation filters, filters to separate the clean oil side (3 micron), check valves, diaphragm reservoir for pulsation damping, etc. Such a unit is adequate to supply only one actuator; therefore the construction of a new second unit was required.

Figure 2.3-9 shows the connection diagram of the hydraulic unit, Figure 2.3-10 a schematic of the entire excitation system.

3. INSTRUMENTATION

3.1 Measurement plan

The number of measurement locations agreed upon in the meantime by all participants is 301 channels. Essentially

90	acceleration transducers (BA)
29	displacement transducers (WA)
143	strain gages (ES)
28	force transducers (FC)
11	other transducers (trigger, pressures, temperatures, etc.)

are used to determine the excitation load histories, the structural dynamic reaction, and the stresses. The operating measurement locations for monitoring the functional behavior of the American valve are included with 26 channels in the above number.

A total survey of the measurement locations is presented in Figures 3.1-1 to 3.1-22. In Figure 3.1-23 to 3.1-35 these measurement locations are orderly

arranged according to relevant aspects, listed according to individual PCM-tracks (see Section 3.3) as well as supplied with coordinates, measurement range information, and transducer sensitivities.

If forces or displacements are measured by one and the same transducers on different hangers, for example, only one measurement location name is allocated. If different transducers are used at the same location, different measurement location names are allocated.

3.2 Stress coating instrumentation

During the SHAM-test stress coating instrumentation will be used additionally for the first time.

With the stress coating method regions of high strain can be recognized without knowledge of the exact position and orientation. The surface of the pipe section to be examined is sprayed with the stress coating lacquer, which, after the hardening period, cracks at a certain limit strain. The strain, at which the coating cracks, can be selected within limits by the selection of different coatings.

The stress coating used is "STRESSCOAT" by the firm Fischer-Pierce & Waldburg, Nondestructive Material Testing with the type code ST 50F/10C.

The coating is selected in such a way that for the environmental conditions during the SHAM-tests (20°C and 70% relative air humidity) the coatings cracks at a strain of 0.15%. The value still lies below the 0.2% strain, which is defined as a significant plasticization, so that there is a safety margin in case the crack strain cannot be exactly provided and the surrounding conditions in the reactor building vary somewhat.

Selected as measurement location (see Figure 3.2-1) were the two VKL-nozzles on DF16, the T-Section DF-44, and the load application location H5, which constitute the most highly stressed locations besides the elbows. The most highly stressed elbows are already sufficiently instrumented with strain gages and receive no stress coating covering.

The tests will be conducted for one configuration at a time with load increase. Therefore, the stress coating lacquer will be applied before it is tested to each new configuration at the measurement locations (undamaged measurement locations of a previous configuration will be taken over unchanged) and will not be renewed again during this test series.

The further procedure will depend on when the cracks occur in the stress coating.

- If the cracks appear before the last load increase, then these will be made distinctly visible with a contrasting substance and documented photographically with a reference scale. At the recognized locations of highest stress, strain gages, which measure the strain for the next tests of this configuration, will be mounted. The stress coating will be renewed only for the next configuration, at which time the then mounted strain gages will be removed again.
- If cracks occur at the last load increase, the reference specimen, which was sprayed at the same time as the measurement location, will be loaded and the crack strain unambiguously determined. With that one has a measure of the minimum strain that occurred at the measurement location. The measurement location proper will be photographically documented - as mentioned above.
- If no cracks occur at the last load increase, then the reference specimen will be loaded nevertheless and the crack strain determined. With that one has a measure of what maximum strain was not reached.

3.3 Brief description of the central measurement data acquisition system (ZMA)

3.3.1 Introduction

In the ZMA (Zentrale Messwerterfassungsanlage) the many electrical transducer signals are amplified and converted via an analog/digital converter system to pulse code modulated binary signals (PCM).

This binary signal form is used because of the high assurance against interference during storage. The high processing speed (max. 26 M bit/sec) requires intermediate storage on PCM tapes. During evaluation of the test data these high processing speed data are transformed back to physical data by serial processing at low bit rates/sec in the computer. Output on magnetic tapes and in diagrams is possible.

3.3.2 Signal processing

It is necessary to use three types of amplifiers due to the application of different measurement principles.

1. DC-coupled amplifiers

A Bell and Howell amplifier is used as pure voltage amplifier, which both prepares the transducer signals and also provides the supply of the transducers. A supply voltage of 5 V or 10 V is applied to the transducers, which are controlled "on line" via "sense lines". Each amplifier has its own power supply; consequently electrical isolation of the measuring chains from each other is assured. The limit frequency of these amplifiers is 20 kHz. The amplification is infinitely variable between 1 and 10000.

The following operating conditions can be adjusted for investigations on the measuring chains:

Measurement: the transducer voltage is amplified.

Zero: the transducer is not disconnected and the amplifier short-circuited at the input.

- Cal: the transducer is disconnected and a calibration voltage accurate to within 0.1% is switched to the input.
- Test: the transducer bridge is adjusted by auxiliary resistors.

2. Carrier-frequency amplifier

The carrier-frequency method (5 kHz) is used to measure with inductive displacement transducers. The transducers can likewise be supplied via "sense lines". Change-over from full to half bridge is possible. Mutual influencing of adjacent displacement transducers by cross-talk is largely avoided by synchronous operation of the 5 kHz generators of the individual amplifiers.

These amplifiers likewise have facilities for remote operation for Cal, Measurement, Test, and Zero.

3. Charge amplifier

These amplifiers are already integrated in the transducers. The output signal is transmitted to the DC amplifiers.

3.3.3 Data recording

1. Analog/digital conversion

The outputs of all amplifiers are led potential-free to a plug board, where the amplifier position and PCM recording are freely assigned according to track and channel. 29 measurement channels are combined to form a PCM track in each case.

Digitalization is effected by analog/digital conversion of the 29 channels one after the other via analog multiplexers and "sample and hold" electronic systems. The analog range from -10V to +10V is divided into 2048 steps (11 bits). If 29 channels are converted, time code and synchronisation bits are attached to the associated bit flow (serial form), so that defined access to a channel and a time is possible during the evaluation.

Each analog channel is interrogated 5000 times per second and converted. Consequently a serial bit flow of about 1.8 Mbit/sec is formed. As 14 digital tracks are present, a total of 14 x 29 analog measuring channels can be processed.

The electric coupling of the analog channels is first effected only in the multiplexers. The digital section is electrically isolated from the analog section via optical couplers.

2. PCM recording

The binary signals of the 14 commutators are each recorded on a separate magnetic tape track (PCM high-density tape units with 1" tapes). For reasons of reliability the recording is made redundant on two magnetic tape units.

3. Data recording with higher scanning rate

For transducers, for which the scanning rate of the ZMA (max. 5 kHz) is not sufficient, a transient recorder with a max. scanning rate of 1 MHz is available for supplementary recording. With this recorder, the signals branched off before the ZMA amplifiers are, independent of the ZMA, amplified, filtered, and digitally recorded.

There are 16 channels at disposal, whereby on one a reference signal should be recorded. The maximum 1 MHz scanning rate can be reduced in steps to 0.1 Hz. For each measurement channel up to 64000 measurement values can be stored, i.e. the recording period depends on the scanning rate. The data recording is initiated by means of a trigger, which can be defined by means of logic connections, and can provide a defined time period before the trigger instant. The filter cut-off frequency of the low pass filter can be freely selected within the range of the selected scanning frequency.

After testing, the recorded values are stored again into the ZMA and with the help of the reference signal an unambiguous time matching is performed.

3.3.4 Data preparation and evaluation

Upon termination of recording, evaluation can follow. For this purpose the data are read track by track from the tape into a decommutator, converted from the serial form into 16 bit parallel form, and transferred to the computer by DMA (175 kbyte/sec).

Assignment to the individual channels is effected in the computer. The data can be displayed as voltage values as a function of time on the screen only in the first stage. The time resolution is freely selectable (the smallest practical resolution is 88 ms = 440 scan values). In the second stage the electrical values are converted into physical values and quantities.

Principle: As a calibration reference, which describes the relationship between physical load and electrical output voltage, is stored in the computer for each individual measurement transducer, it is first necessary to calculate back from the electrical output voltages of the amplifiers to the associated input voltages. This input voltage is then at the same time the output voltage of the measurement transducer and the physical value can then be determined via the calibration reference.

The amplifier condition (offset and amplification) can be determined in the computer with the stored values Cal, Zero, and Measurement, so that drift and accidental false setting of the amplifier can be recognized and corrected by calculation. In addition an amplifier can be changed during preparation for a test without the need for totally new adjustment of the measuring chain. The strict separation of transducer and amplifier thus results in simple handling in the case of intended modifications and location of faults. The physical values determined in the computer are recorded on digital tape, whereby a maximum of 29 channels of a track can be recorded on a tape. The conversion is normally made only for predetermined time ranges to limit the data quantity.

3.3.5 Form of representation of the data

The normal form is plotting in diagrams of physical value versus time. Both axes are freely selectable within logical limits. A maximum of 6 series of measured data can be superimposed in a diagram to facilitate comparisons.

Multiplex operation, which may involve a difference of max. 170 micro-seconds in the sampling time even when a greater accuracy is pretended on the plot (channel 29 is scanned 29 x 5.7 microseconds later than channel 1), should be taken into account in the case of extreme time resolutions.

For purposes of evaluation the measurement values are provided on digital tape at the central evaluation facility (ZAW).

4. TEST PROCEDURE

4.1 General observations

As was the case with SHAG, several external institutions will again participate in the SHAM tests. These institutions or their subcontractors are designing or developing various hanger configurations for the VKL pipe system. Tests with identical excitation will be conducted for five of the different hanger configurations to enable weighting and evaluation of the operating principle of the respective solution in a direct comparison. Only the hanger configurations of CEGB will be operated with special, English excitation functions.

A test matrix, which presents the present stage of planning of the experiments, is shown in Figure 4.1-1.

Basically it should be noted that the SHAM tests will be conducted with the mechanical installations in the cold condition. All systems, VKL, HDU, DF15 will be filled with water; no throughflow of the systems will be generated. However, a static internal pressure of 70 bar will be applied.

In the test matrix a distinction should be made between the following:

- Random tests for system identification, i.e. tests that serve for the identification of natural frequencies, mode shapes, and damping values of the tested piping system for the then used hanger configurations. The excitation is a gray noise (2-40 Hz) of relatively uniform intensity.
- Seismic tests in the linear-elastic stress range. During these tests, the limit of the load increase will be fixed on the basis of measurement stresses in such a manner, that at the measurement locations strains of 0.1% are reached but 0.2% are not exceeded.
- Earthquake tests with plasticization.

These tests, during which the region of linear-elastic material behavior shall be exceeded so that permanent deformation of the VKL system or its components can occur, shall be performed for at most 3 of the tested hanger configurations (NRC, CEGB, HDR).

If no plasticization effects are achieved on the pipe by the highest load that can be applied by the cylinders, which may be of the approx. 10-fold order of magnitude of SSE, (except CEGB), it is possible that this condition can be achieved by so-called SINE BEAT or SINE BURST test procedures.

Although tests conducted with previous damage selectively introduced into the VKL and designed to lead to failure of the pipe, will be conducted with the same test set-up, they are no longer part of the planned scope of test group SHAM, but are planned as test series E32 of Phase III and as such will not be described here.

After leaving the elastic range the effects of the permanent set should be determined after the tests. The changes in cross-section at the most highly stressed locations will be recorded. It is currently assumed that smaller plastic deformations will not inadmissibly change the overall rigidity of the pipe system after readjustment of the hanger elements and thus it will be

unnecessary to change slightly deformed sections. Such a change should be considered in the case of greater plasticization:

- Parts of the piping will only be exchanged, if irreparable cracks occurred or if the permanent deformation of a pipe section leads to a distinct alteration of the boundary conditions of the pipe line system.
- In all cases damaged parts of the support system (hangers, frames, anchors) will be exchanged or repaired after a test. Each of the participating institutions will keep the corresponding spare parts ready for this purpose.

4.2 Load functions

The following different functions are planned:

1. RANDOM excitation
2. Earthquake histories corresponding to predetermined spectra
3. SINE BEAT or SINE BURST

Remark: Should plasticization not be attained with earthquake histories for any hanger configuration, it is planned to perform supplementary tests with SINE BEAT/SINE BURST.

4.2.1 RANDOM-excitation

A gray noise (2-40 Hz), that was additionally filtered with a low pass of 1 Hz and 6 dB cut-off slopes, see Figures 4.2-1 and 4.2-2, shall be input for the path of the piston. This provides for the piston velocity to have a constant effective magnitude of 5 cm/sec for the entire excited bandwidth.

The time history is stored on magnetic tape and identical for all configurations.

- Excitation location: H5 and DF16, individually.
- Total excitation time: 2 min
- Recording time: -5 to +200 sec
- Conversion time: -5 to +150 sec
- Scanning: 625 (during data acquisition and conversion)
- Filter frequency: 100 Hz
- Immediate evaluation: for an acceleration measurement location (3 directions) and excitation pre-determination with LBF GENRAD system.

4.2.2 Earthquake histories

For all hanger configurations, except for those of CEGB, a common earthquake history will be used. This is an artificially generated displacement-time function of 15 sec duration, see Figure 4.2-3, fitted to a predetermined SSE-floor-response spectrum (D=4%). It was agreed to define a Zero-Period-Acceleration (ZPA) of 0.6 g in the pertinent spectrum as 100% excitation level corresponding with 1-fold potential Safe Shutdown Earthquake (SSE) on the floor of the VKL room.

For the tests with CEGB-hanger systems there will be used two different displacement histories of 20 seconds duration, see Figures 4.2-4 and 4.2-5, which were generated suitable to a spectrum for a specific location (Sizewell B) or to a covering spectrum for all possible English locations. Figure 4.2-6 provides a comparison of all 3 spectra used.

- Excitation location: H5 and DF16, synchronized

- Total excitation time: 15 or 20 sec
- Recording time: -5 to 50 sec
- Conversion time: -3 to 30 sec
- Scanning: 62.5 Hz (during data acquisition and conversion)
- Filter frequency: 100 Hz
- Immediate evaluation: Response-spectra of the piston acceleration with LBF Genrad-System.

Further details for the handling of the measured data are contained in Figures 4.2-7 and 4.2-8.

4.3 Accuracy requirements for the excitation systems

The excitation systems used for the tests and described in chapter 2.3 require perfect coordination of all electrical, mechanical, hydraulic, and electronic components in order to accurately follow the desired load functions. As for the three first-mentioned types are concerned, there are few possibilities to influence these during the test period. Their tuning to each other and to the test requirements occurs during the planning phase on the basis of the design calculations (see Section 5). By contrast, the electronic components i.e. the control electronics and the computer for the predetermined excitation, still offer possibilities to fit the load functions experienced during the test to the predetermined values.

The optimal setting of the control electronics depends principally on the hydraulic parameters (oil flow, opening and closing behavior of the servo valves) and is only in second order influenced by the dynamic forces (i.e. from reactions of the excited piping). This is true for majority of the planned tests, for which the demands on the excitation system are below its performance limits. Thus, the control setting, due to the cooperation of the

electronics with cylinder, servo valve, storage facility, and hydraulic unit, can be separated for each cylinder and optimized without load application at the piping (because 2 completely separate servo hydraulic systems are available). This setting is made for the initial operational acceptance test prior to the beginning of testing with help of the transfer function between specified and actual value, whose value in the 2 to 10 (40) frequency range should differ as little as possible from 1. Subsequently, the thus considered optimal setting shall be kept for all tests.

For each configuration with pipe support initial, individual tests for each cylinder will be driven with noise excitation. These take place at a lower excitation level and serve for the identification of the modal parameters of the pipe system in the corresponding configuration. Since the identification occurs on the basis of transfer function between response displacement magnitudes of the pipe and the exciting bottom support motion, there exist no special requirements for the accuracy with which the desired displacement history of the excitation is followed.

The main body of the tests are the earthquake tests, at which a predetermined floor response spectrum shall be followed simultaneously at both load application points. At disposal for this excitation is a displacement history, which was obtained by integration of an artificially generated acceleration history fitted to the desired floor response spectrum. The requirements for the accuracy of the simulation must therefore not be based on the comparison of the specified vs. actual displacement signal (the actually controlled parameter). Instead it will be based on the comparison of the specified vs. actual floor response spectrum of the accelerations at the load application point. This is important, because at high frequencies small deviations of the displacement can lead to significant acceleration deviations.

Fundamentally the controlled displacement magnitude shall be selected in such a manner, that the response spectrum (TRS) of the acceleration at the load application point resulting from the test approaches the desired response spectrum within $\pm 10\%$. This is checked at frequencies spaced by 1/6 octave in the frequency range (2-10 Hz) of interest.

This accuracy shall be satisfied at the SHAM-tests for the 100% load case of each piping configuration. For this purpose, during preliminary tests when only the accelerations at the load application points are recorded (without ZMA measuring technique), the TRS will be determined and the controlled signals changed, if warranted with respect to frequency range. The changed displacement signal, that with 100% loading satisfies the mentioned requirements for a certain configuration, is then retained for all tests with this configuration time wise and is only correspondingly amplified.

5. CALCULATIONS

5.1 Design calculations

5.1.1 Objectives of the design calculations

The primary aim of the design calculations for the SHAM tests was determination of

- suitable excitation points and
- excitation forces including frequency content or time curve,

which are necessary to distinctly exceed the load ranges of a Safe Shutdown Earthquake and the elastic range of the pipe stresses in the VKL system in the HDR.

In addition it was important to specify

- the hydraulic actuator equipment required for this purpose and
- informative measurement locations

for the tests.

Three of the 5 or 7 different support concepts of the VKL system, which were already used in the SHAG tests on the HDR, were considered in the design:

1. flexible HDR system
2. KWU system
3. rigid NRC system

Taking into account the space conditions, excitation in the horizontal direction on the following "fixed points" of the VKL system initially appeared logical and possible:

- Central cover nozzle of the HDU vessel (HDU 704, excitation in z direction, i.e. turned 30° with respect to x)
- Strut H-5 between spherical fitting DF21 and USNRC valve (excitation in x direction),

cf. drawing at top of Figure 5.1-1.

Calculations were likewise made for a further possible excitation point on strut H10 of the NRC support system. As the calculation results revealed that installation of a hydraulic cylinder at this point, which is not a "fixed point" of the flexible HDR system, greatly affects its vibration behavior, this excitation point was not included in further considerations.

Without greater modifications to the experimental plant, the points described above were the only ones which came into consideration for the horizontal installation of hydraulic actuators in the VKL pipe. Without anticipating the calculation results in detail at this point, it proved necessary to select a more suitable excitation point instead of the HDU cover nozzle for reasons of attainable accelerations and stresses. Removal of some pipes in compartment 1.704, which are no longer required for operation of the HDR experimental plant, enabled fitting DF16 (excitation in x direction, cf. Figure 5.1-1, bottom) to be used as a further excitation point.

5.1.2 Calculation models

The SAP model of VKL and HDU shown in Figure 5.1-2, which was taken over from TÜV Rheinland (Ref. 3), was used as basic model for the SHAM design calculations. The model contains all supports of the rigid NRC system used in the SHAG tests. The other two support systems are realized in the computer model by release of the displacement degrees of freedom of the supports removed in each case.

This basic model was suitably modified for the different load cases considered in the course of the design calculations. For example, models were developed, in which the central constraint of the HDU was removed and the HDU was spring mounted, or load cases with and without water filling of the HDU. As will be shown later, extreme requirements are imposed on the excitation system by the heavy weight of the HDU (about 70 t when filled). Hence the case, where the VKL pipes on the HDU were cut off and welded to a light, but rigid frame, was also investigated.

The rigidity of inactive hydraulic cylinders was simulated in the models by rigid springs.

The model had to be augmented by the pipe DR 105 (nominal size 300) between DF 16 and primary steam header for the calculations for the response behavior of the VKL system during excitation at DF 16. The list in Figure 5.1-3 shows the model variations.

5.1.3 Calculations performed

Experience has shown that design calculations with the aims specified in Section 5.1.1 require a large number of calculation runs until the relevant test parameters are determined in an iterative process. Hence, restriction to linear calculations and the application of methods, which minimize the cost of the individual calculation run, are essential. The method of making all calculations in the frequency domain and transforming the results into the time domain was selected for the design calculations for the SHAM test group.

The natural frequencies and forms of vibration were determined in the frequency range up to 20 Hz for the model variations described in Section 5.1.2. Depending on the model and support system these are the first 15 to 19 natural frequencies. The transfer functions between the exciting force and vibration response of the system were set up with these modal parameters. The internal forces (bending and torsional moments) were also initially determined in the frequency domain by complex multiplication of the determined displacement quantities with the system rigidity matrix.

The following load cases were calculated in this way:

Load case I:

Steady harmonic excitation at one point.

The amplitudes of the

- forces
- displacements
- speeds
- accelerations

which must be applied at the excitation point to produce calculated rated stress amplitudes of 500 N/mm^2 (comparison stress according to deformation energy hypothesis) in selected cross-sections of the linear model with assumption of damping of 8% in all modes of the model, were calculated in the frequency range up to 15 Hz.

With this "hard" criterion - exceeding of the yield point by more than a factor of 2 in a linear calculation with simultaneous assumption of relatively high damping values - the aim was to ensure that the requirements on the excitation system derived in this way ensure that the test aims are really fulfilled (see Section 5.1.1).

Examples of the results of these calculations are given in Figure 5.1-5 and 5.1-6 for model L (excitation DF 16) and Figures 5.1-7 and 5.1-8 for model M

(excitation at H5). The excitation locations and the position of the reference cross sections are shown in the diagram in Figure 5.1-4.

Load case II:

Steady harmonic excitation at one point.

The amplitudes of the forces, which must be applied at the excitation point to achieve input accelerations with amplitudes of 10 m/s^2 were calculated in the frequency range up to 15 Hz.

The result of these calculations supplies guide values for the dynamic mass of the system to be excited referred to the excitation point and is important for selection of suitable hydraulic cylinders. However, it is also used for evaluation of the advantages and disadvantages of system modifications. The example of results in Figure 5.1-9 shows that the reduced mass of the HDU without water filling is dynamically effective only at frequencies above 7 Hz.

Load case III:

Transient excitation at one point, earthquake history original.

The force/time curve to be applied to the excitation point to realize a predetermined acceleration/time curve at precisely this point, was calculated. The acceleration/time curve used (see Figure 5.1-10) is an earthquake history curve artificially generated for a given floor response spectrum, which was standardized to a system acceleration of 10 m/s^2 .

Smaller damping values of 4% were assumed for all modes in these calculations to avoid underestimation of the dynamic effects.

Load case IV:

Transient excitation at one point, earthquake history modified.

As shown by the floor response spectrum in Figure 5.1-10, the predetermined original time curve contained the largest vibration proportions at frequencies of 2 to 4 Hz. As the low-frequency accelerations are associated with large displacements, which could not be realized in tests, their proportions were halved; the time curve modified in this way is shown in Figure 5.1-11. The modified floor response spectrum can be considered from the frequency content point of view as a realistic spectrum for a reactor building on firmer subsoil, whereas the original spectrum originates from design calculations for a reactor building on soft soil.

In addition to determination of the required exciter forces to achieve a input acceleration of 10 m/s^2 , the magnitudes required for establishing the measurement locations and ranges were determined for this load case IV, which has prospects of becoming the essential excitation in the planned tests. These are in particular the magnitude and location of the maximum bending and torsional stresses to be expected during the tests. These values were prepared by a graphics post processor as color display. Because of the expense (still) associated with the reproduction of color displays, this report does not contain any examples of these results.

5.1.4 Summary of results

A comprehensive summary of individual results of the design calculations can be found in Refs. 4 and 5. Only the most important conclusions will be described briefly below:

The performance capability of a servohydraulic exciter is limited in the lower frequency range with regard to the displacement amplitude, in the medium range with regard to the velocity amplitude, and in the upper range with regard to the acceleration amplitude. The maximum displacement corresponds to the piston stroke determined by the type of construction. The attainable acceleration depends on the rated force of the cylinder and dynamic mass of the excited system, the rated force being determined by the effective piston area and hydraulic pressure. The attainable piston velocity is dependent on the rated throughflow of the servo valve used and the piston area (and thus, with a predetermined pressure, on the rated throughflow and rated force).

With hydraulic cylinders to have a 250 mm piston stroke - to limit controlling sizes of overall cylinder length and hydrostatic piston bearing - the required piston speeds and rated forces of the exciter are the deciding design parameters. These two parameters then determine the requirement on the servo valve throughflow. Hence a full logarithmic graph of piston speed versus cylinder rated force, in which the family of straight lines with a slope of -1 specifies the required rated throughflow of the associated servo valve, is used to represent the results in Figures 5.1-12 and 5.1-13. Hence the requirements on the exciter system, and thus also its costs, increase from right to left and from bottom to top on this graph. The top righthand corner of the graph represents costs of about one million DM for cylinders and oil supply (for transient excitation of up to 15 sec), which far exceeds the funds available for the excitation system of the project.

Test objective: To exceed the range of elastic material behavior

To establish the requirements on the excitation system in order to distinctly exceed the range of elastic material behavior in the SHAM tests, a "hard" criterion was intentionally selected:

- Rated stresses of over 500 N/mm^2 in a linear calculation with 8% damping in all natural vibration forms with excitation at one point, but
- with steady harmonic excitation (load case I).

The design calculations showed that this criterion cannot be satisfied with excitation at the tip of the HDU within the limits of the graph in Figure 5.1-12, even with flexible mounting of the HDU. On the other hand, in narrow frequency ranges the criterion can be fulfilled both with excitation at H5 and at DF 16 by a cylinder with a rated force of 400 kN and a rated throughflow of at least 1260 l/min (2 x 630 l/min), cf. Figure 5.1-12.

Test objective: To exceed the load range of a Safe Shutdown Earthquake (SSE)

If a quite specific earthquake history is taken as a basis, a fixed relationship exists between maximum acceleration and maximum velocity. Hence the attainable peak acceleration for the modified earthquake history considered as load case IV, can also be plotted on the right as second ordinate in the graph in Figure 5.1-13. The forces required to impose the predetermined acceleration history onto the pipe as excitation have been determined in the design calculations.

If it is taken into account that the dynamic excitation forces are 80% of the rated forces, the straight lines plotted in Figure 5.1-13 with a slope of +1 give the minimum requirements on the rated force of the hydraulic cylinder to enable use of the earthquake history scaled to a predetermined peak acceleration and corresponding to load case IV with the different models (cf. table in Figure 5.1-3). The results reveal that the exciter system selected above (rated force 400 kN, rated throughflow 1260 l/min) should be adequate both for excitation point H5 (model M) and DF 16 (model L) to achieve a peak acceleration of over 60 m/s^2 , i.e. more than 10 times a Safe Shutdown Earthquake with a maximum floor acceleration of 6 m/s^2 . With excitation at the HDU tip, rated cylinder forces of at least 1000 kN and a rated throughflow of about 2000 l/min would be required for this purpose, even with flexible mounting of the HDU (model D).

Measurement locations and predetermined measurement ranges

The reference locations for the accelerations and stresses indicated in Figure 5.1-4 constitute the instrumentation proposal, as it can be derived from the results of the design calculations. The table in Figure 5.1-14 shows the calculated maximum acceleration components in load case IV (earthquake history normalized to 10 m/s^2) at the acceleration reference locations for the two most important models L (excitation DF 16) and M (excitation H5). The table also specifies the maximum values of the displacement components at these points. For derivation of predetermined measurement ranges the calculated values should be multiplied by a factor of about 10 to take into account that an about 6-fold excitation is applied simultaneously at 2 points.

The table in Figure 5.1-15 contains calculation results of the maximum bending and torsional stresses at the stress reference points for the same load cases and models. The stress values were derived from the calculated internal forces at model nodal points by evaluation with the smaller resistance moment of the connected elements. Hence they should be regarded as rated stresses. These values can only serve as guidelines for the local stresses at nozzles, branches, elbows, and also in the regions of load applications.

6. REFERENCES

1. L. Malcher, K.K. Wenzel, C.A. Kot, "Experiences and building behavior during the earthquake tests with a large eccentric mass shaker (SHAG)," Paper No. 1 of the 10th Status Report PHDR, December 1986, Work Report No. 05.27/86 KfK-PHDR
2. M. Steinhilber, H. Idelberger, D. Schrammel, "Vibration behavior of the structure and the mechanical installations during earthquake tests (SHAG)," Paper No. 2 of the 10th Status Report PHDR, December 1986, Work Report 05.27/86 KfK/PHDR
3. Waldner, K., "Blind comparison calculation of the vibration behavior and stressing of the HDR experimental loop with shaker excitation (SHAG)," Cologne, April 1987
4. Steinhilber, H., Störzel, K., "Status of SHAM Test Design Calculations," KfK-NRC-EPRI Planning Meeting on SHAM Tests at HDR, Kahl, April 1987
5. Steinhilber, H., Störzel, K., "Results of SHAM Test Design Calculations," KfK-NRC-EPRI Planning Meeting on SHAM Tests at HDR, Kahl, August 1987

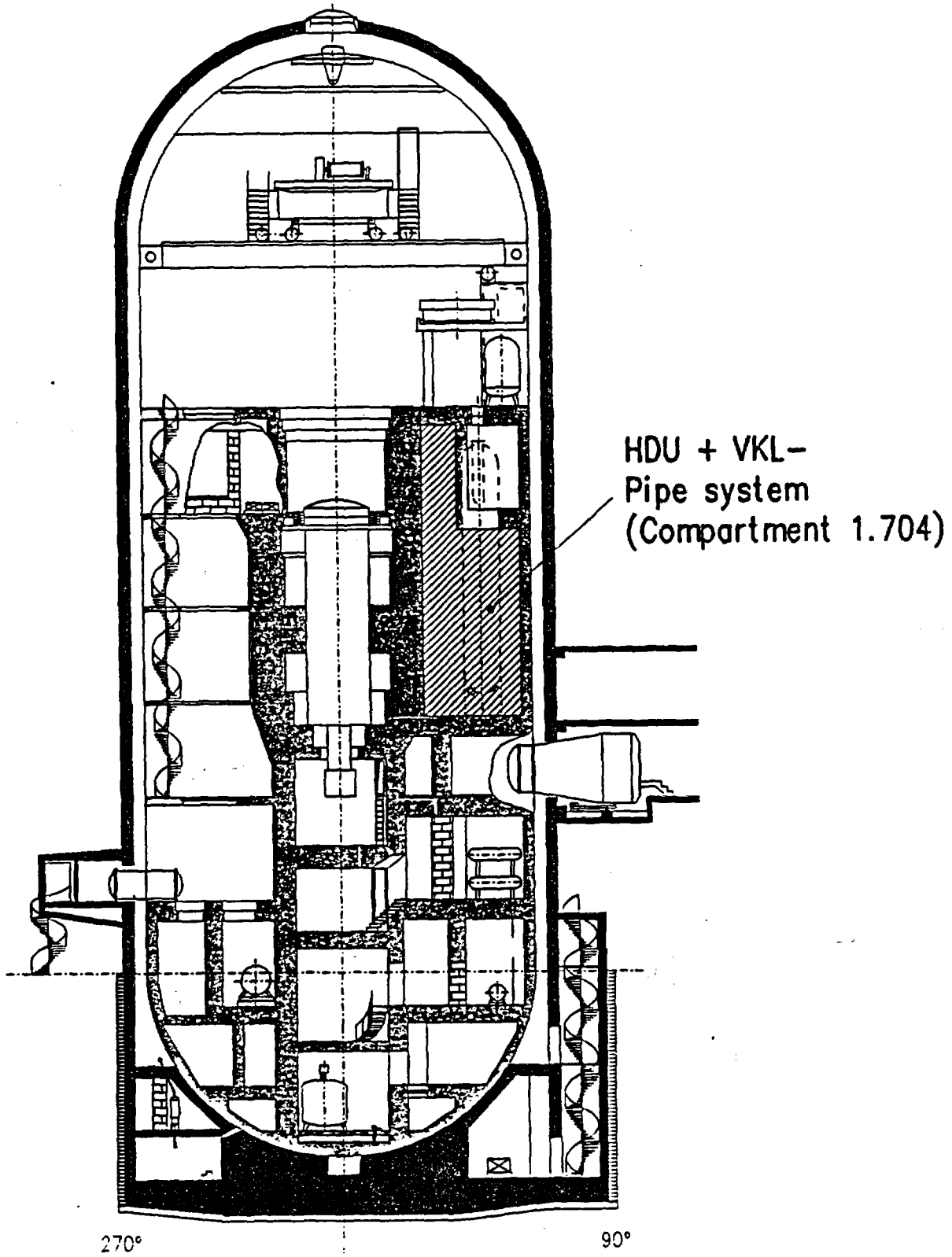


Fig. 2.1-1

HDR-reactor building with HDU and VKL pipe system in compartment 1.704

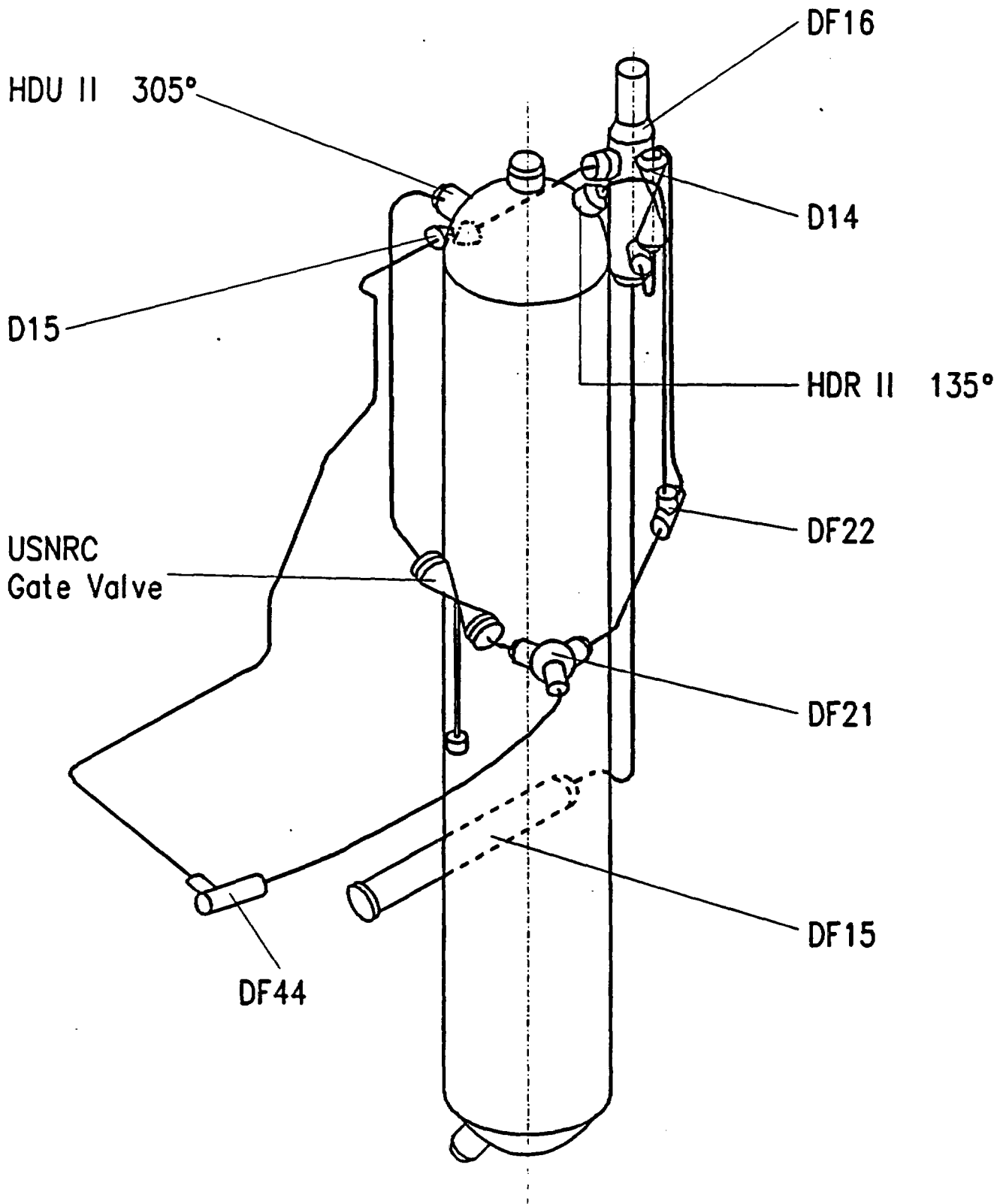


Fig. 2.1-2 HDU and VKL pipe system with components

Pipe designation	Nominal value [DN]	Material	Pipe run		Nominal dimensions [mm]				
					Straight		Bend		
			from	to	Dia	t	Dia	t	R
DR108	200	1.4961	D14	DF16	219.1	14.2	225.7	17.5	305
DR109	125	1.4961	D15	DF16	139.7	8.8	144.1	11	190.5
VN-R23	100	1.4550	DF44)**	D15	114.3	6.1	114.3	8.8	152.5
DR 201	200	1.4550)*	HDU-II 135°	DF21	219.1	14.2	225.7	17.5	305
DR 202	200	1.4550)*	HDU-II 305°	DF21	219.1	14.2	225.7	17.5	305
DR 203	250	1.4550	DF21	DF44)**	273	16	281	20	385
DR 205	200	1.4550	DF22	D14	219.1	14.2	225.7	17.5	305
DR 105	300	1.4961	DF16	DF15	355.6	25	361	28	525

1.4550 X10 CrNiNb 18 9
 1.4961 X8 CrNiNb 16 13
)* 750 mm fabricated from 1.4961
)** DF44 proper fabricated from 1.5415

Fig. 2.1-3

Dimensions and material of the VKL-pipes

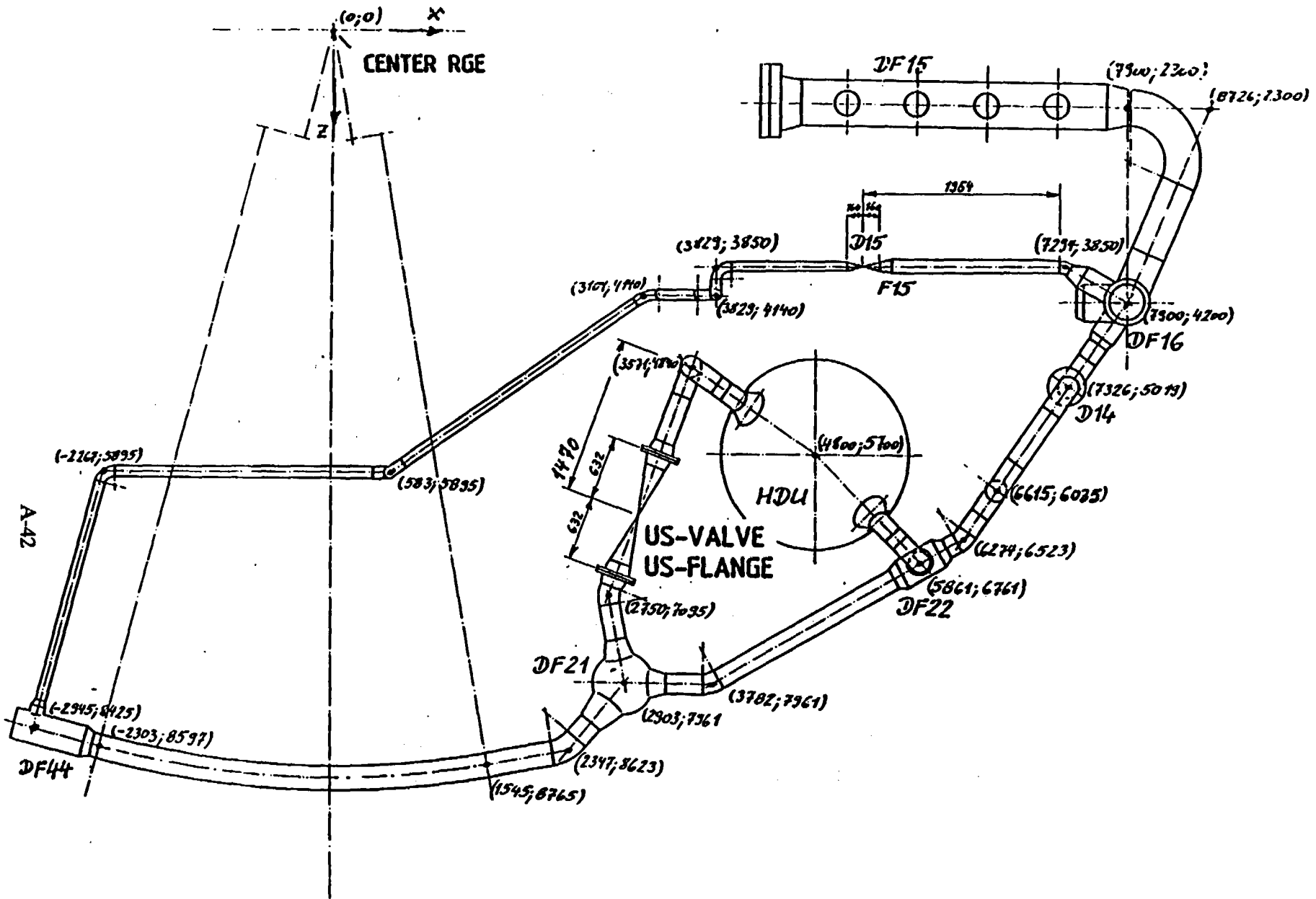


Fig. 2.1-4

VKL dimensions, plan view

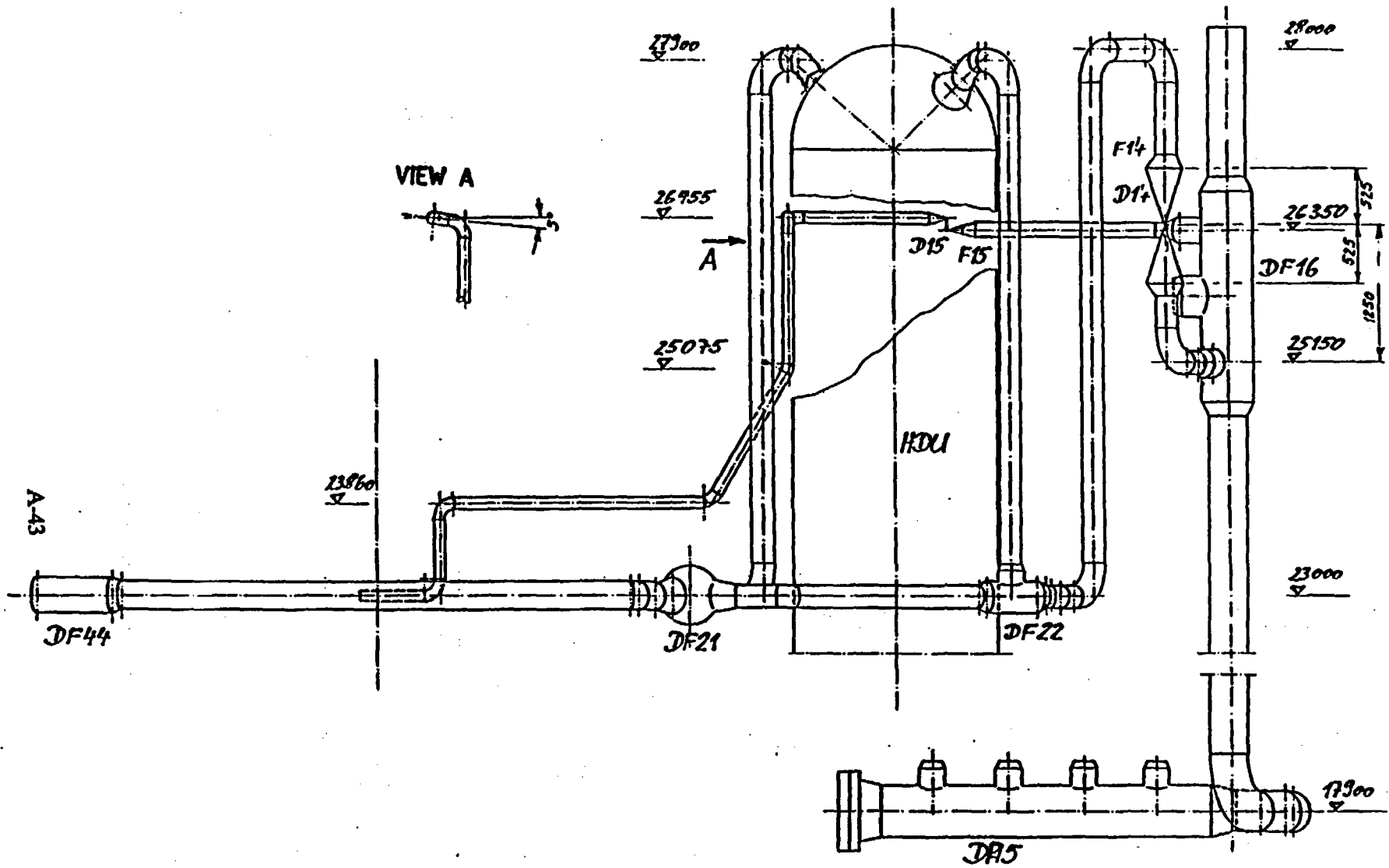


Fig. 2.1-5 VKL dimensions, elevation view

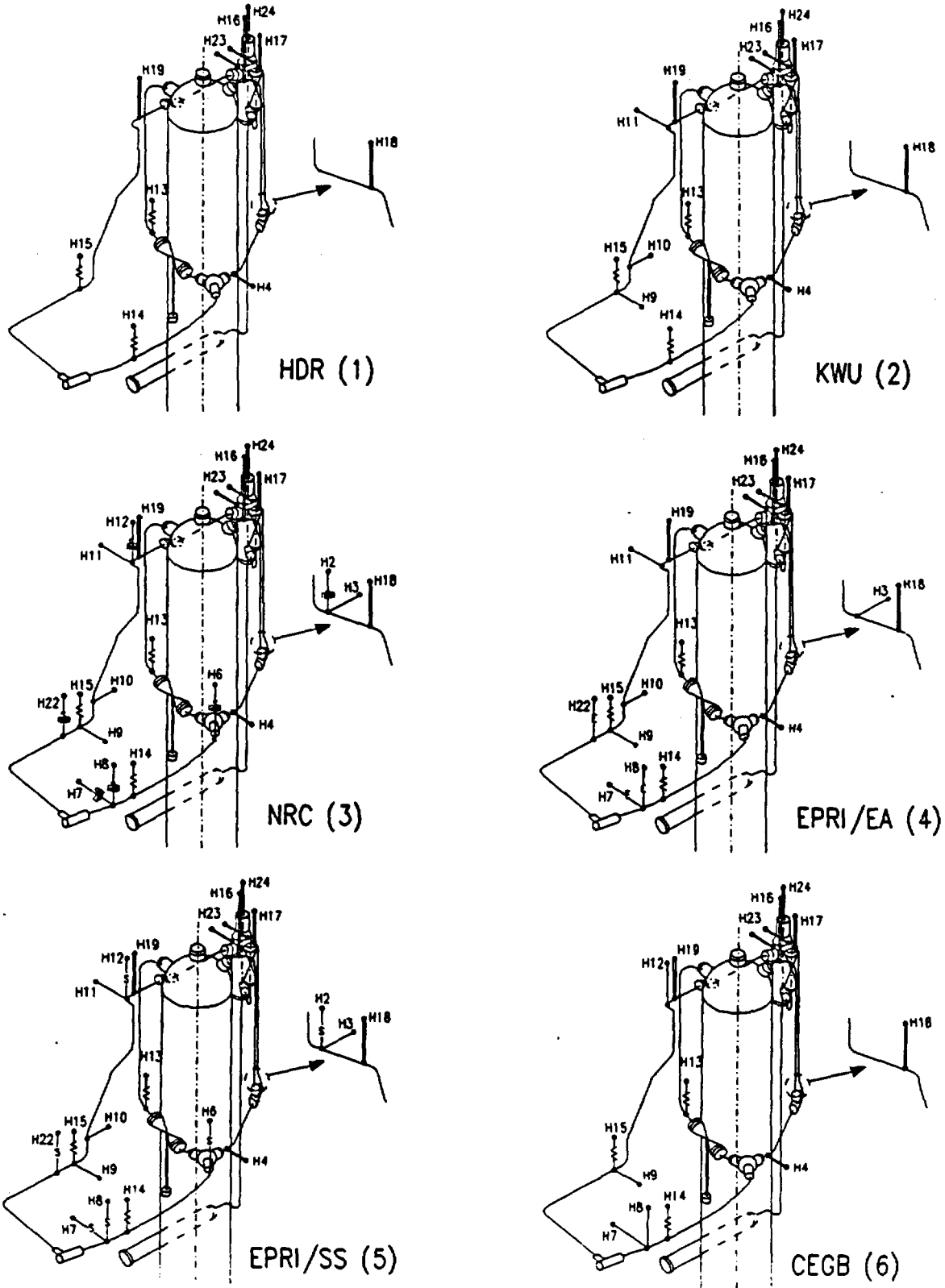


Fig. 2.1-6 Hanger configurations of the VKL pipe systems

HANGER CONFIGURATIONS						
Hang-er No.	1 HDR	2 KWU	3 NRC	4 EPRI/EA	5 EPRI/SS	6 CEGB
2	—	—	Snubber PSA1	—	Seismic stop	—
3	—	—	Strut Size B			—
4	Strut Size 20					
6	—	—	Snubber PSA 1/2	—	Seismic stop	—
7	—	—	Snubber A/D 150	Energy Absorber	Seismic stop	Strut RS-15
8	—	—	Snubber A/D 70	Energy Absorber	Seismic stop	Strut RS-7
9	—	Strut Size B	Strut Size A			Strut RS-7
10	—	Strut Size B	Strut Size A			—
11	—	Strut Size B	Strut Size A			—
12	—	—	Snubber A/D 40	—	Seismic stop	Strut RS-15
22	—	—	Snubber PSA 1/4	Energy Absorber	Seismic stop	—
23	Two Struts 2 x Size 20					

Fig. 2.1-7 Assignment of the dynamic hangers to the different configurations

Hanger No.	Designation	Manufacturer Type Designation	Nominal Load [kN]
9, 10, 11	Strut	ITT Grinell Size A	29
3, 9, 10, 11	Strut	ITT Grinell Size B	6.7
4, 23	Strut	NPS Industries Size 20	149
8, 9	Strut	Carpenter & Paterson RS-7	69
7, 12	Strut	Carpenter & Paterson RS-15	14.7
22	Snubber	Pacific Scientific PSA 1/4	1.6
6	Snubber	Pacific Scientific PSA 1/2	29
2	Snubber	Pacific Scientific PSA 1	6.7
12	Snubber	Anchor Darling A/D 40	
8	Snubber	Anchor Darling A/D 70	
7	Snubber	Anchor Darling A/D 150	
7, 8, 22	Energy Absorber	Bechtel	-
2, 6, 7, 8 12, 22	Seismic Stop	Cloud	-

Fig. 2.1-8

Technical data of dynamic hangers

Hanger No.	Designation	Manufacturer Type Designation	Nominal Load (kN)
13	Spring Hanger	ITT Grinell Size 16	31.69
14	Spring Hanger	ITT Grinell Size 13	12.01
15	Spring Hanger	ITT Grinell Size 6	1.65
16	Constant force Hanger	ITT Grinell GR12, Type 81H-A	8.47
17	Constant force Hanger	ITT Grinell GR22, Type 81H-A	16.38
18	Constant force Hanger	ITT Grinell GR10, Type 81H-A	6.99
19	Constant force Hanger	ITT Grinell GR9, Type 81H-A	4.14
24	Constant force Hanger	ITT Grinell GR21, Type 81H-A	22.51

Fig. 2.1-9

Technical data of dead weight hangers

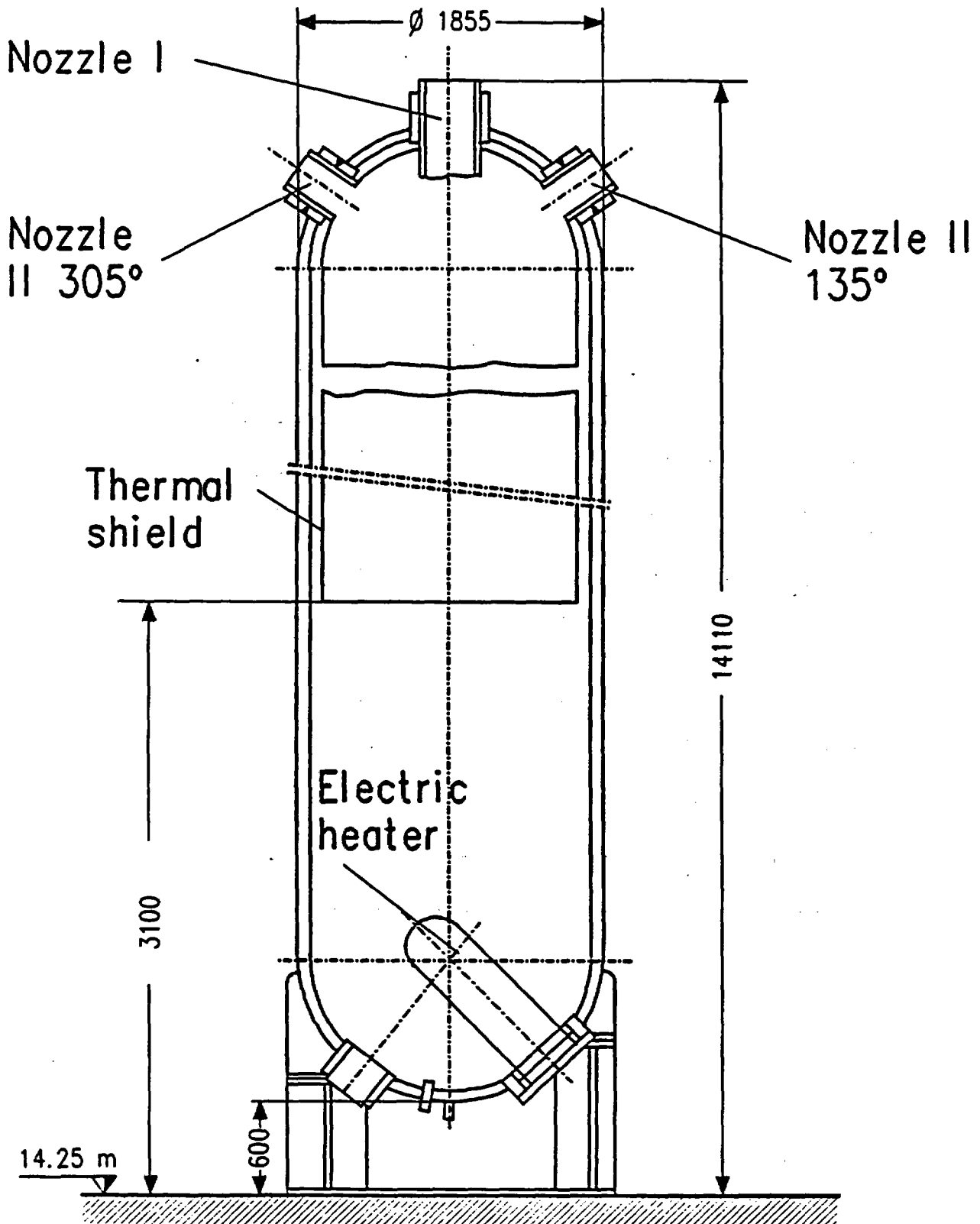
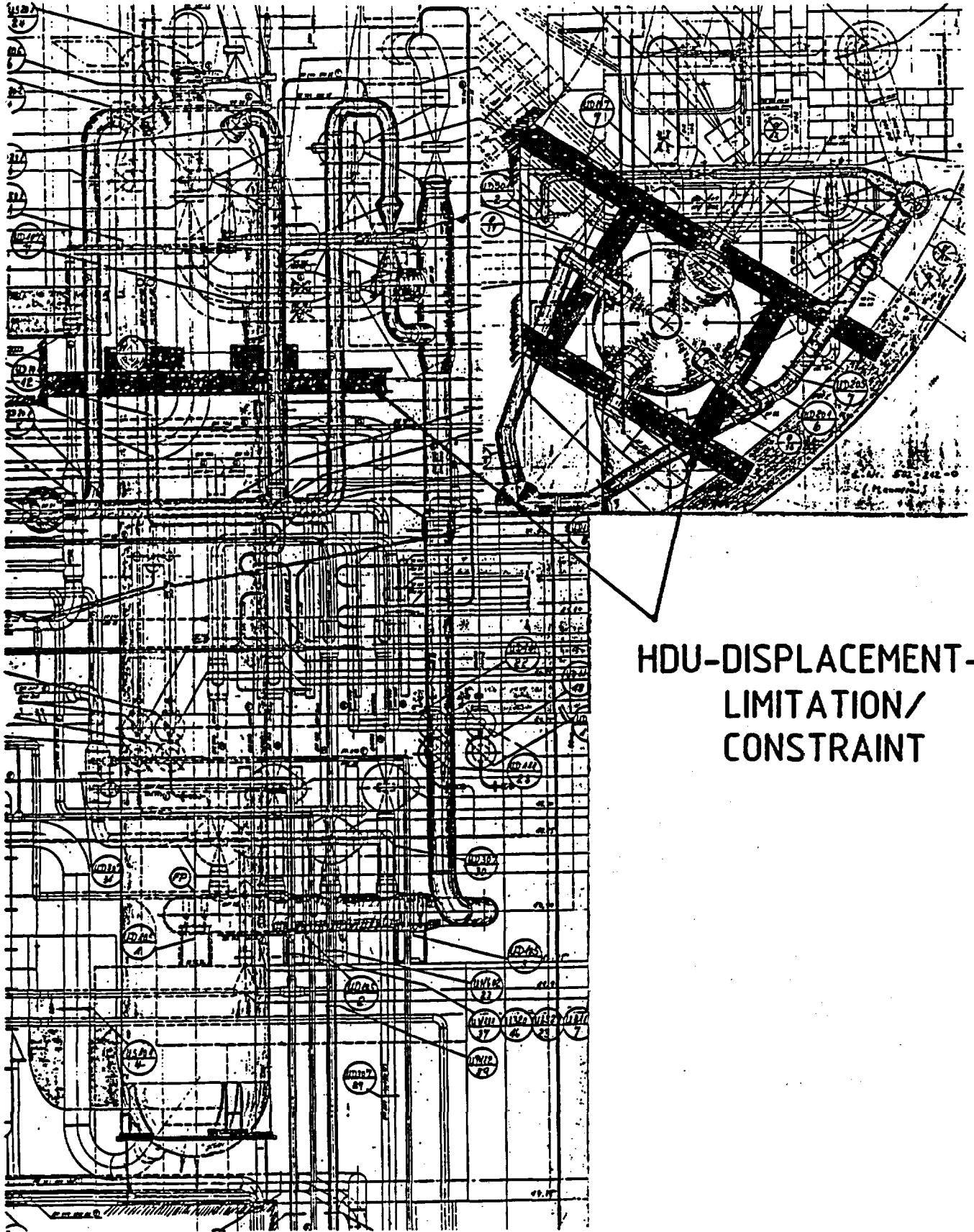


Fig. 2.1-10 Pressurizer (HDU) with VKL, electric heater, and temperature shield

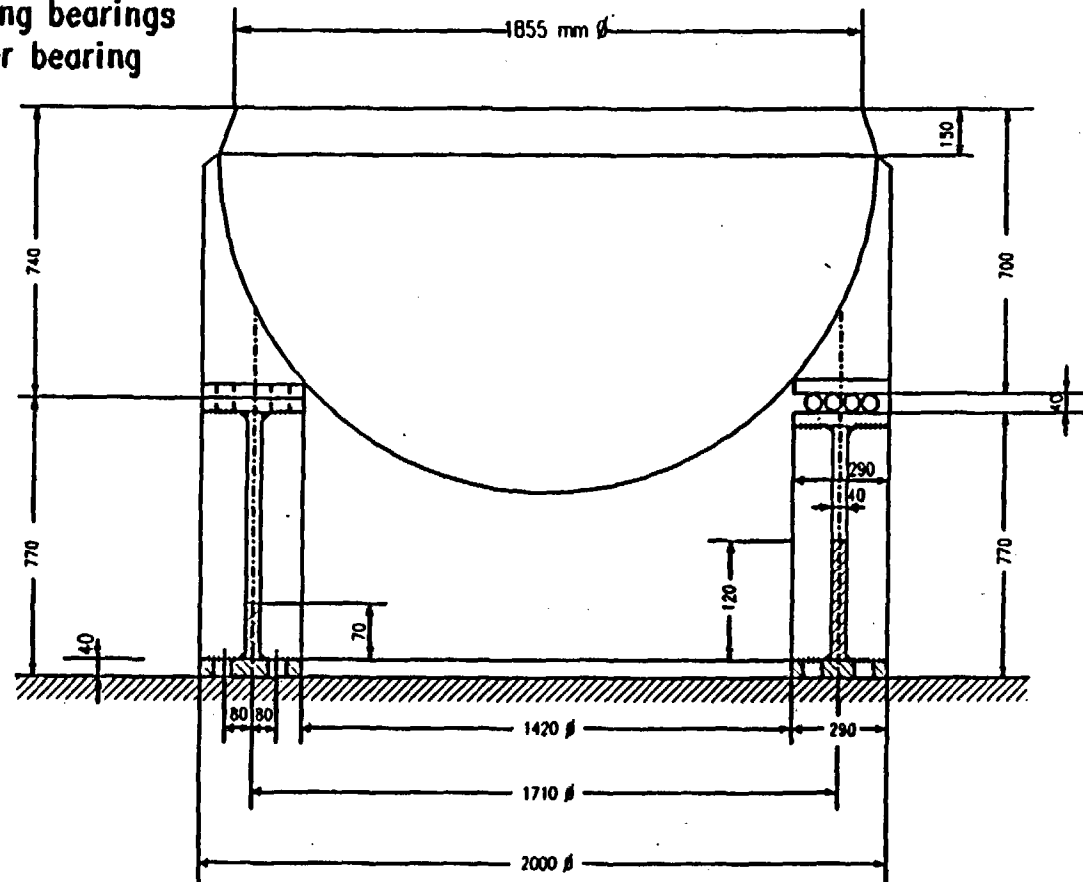


HDU-DISPLACEMENT-
LIMITATION/
CONSTRAINT

Fig. 2.1-11 HDU displacement limitation

Support skirt and assembly stays for superheated steam heat exchanger
H 27 063 d (Detail)

- 4 bearings
- of these:
- 1 fixed bearing
- 2 sliding bearings
- 1 roller bearing



A-50

- A12 -

Fig. 2.1-12

HOU support construction

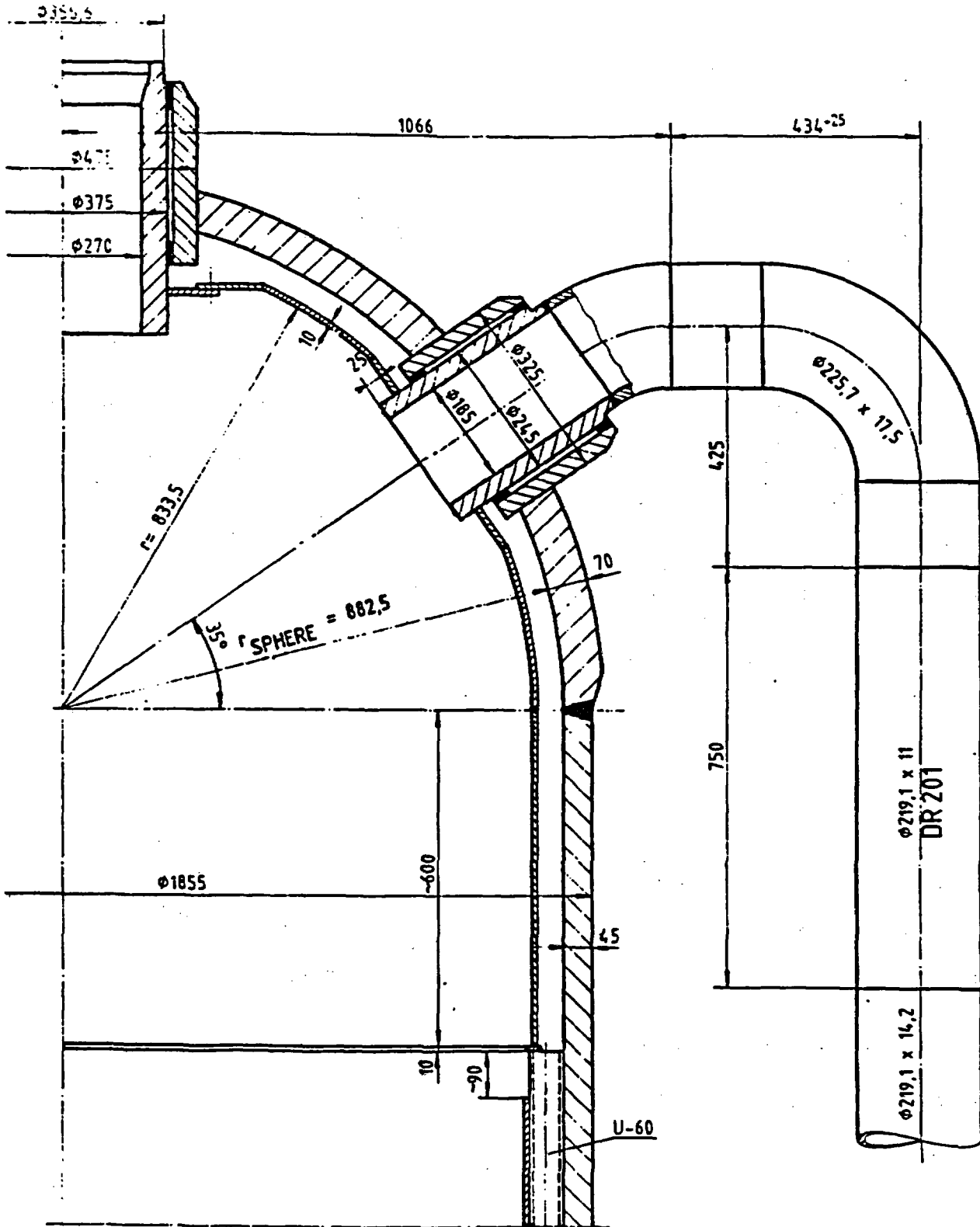
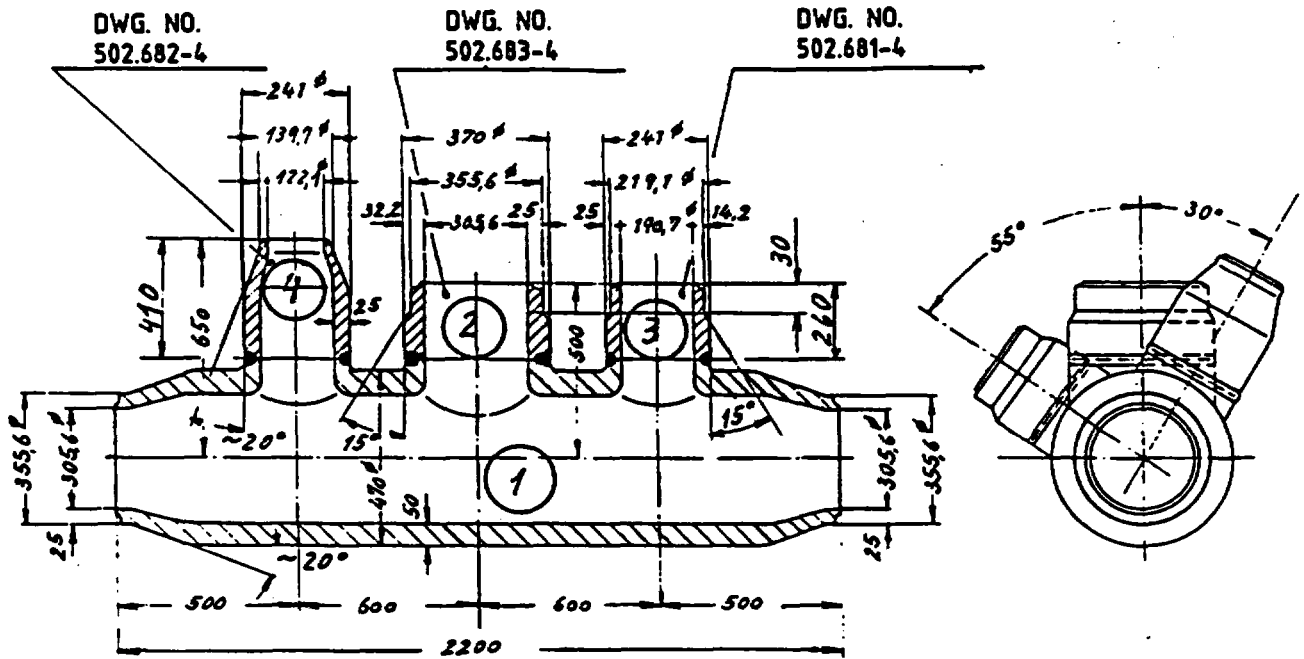


Fig. 2.1-13 Connection of a VKL pipe (DR 201) to HDU cover nozzle II 135



Installation	DR 105	
Material	X 8 Cr Ni Nb 1613	Material No.: 4961
Operating pressure	55 - 80 atmg	Design: 110 atmg
Operating medium	440 - 520 °C	Design: 550 °C
Medium	Primary superheated steam	
Weld joint type	according to work standard 1 required	RN-S2, Form Ar 4
supply with designation	DF 16	
Acceptance	TÜV	

Fig. 2.1-14 Fitting DF 16

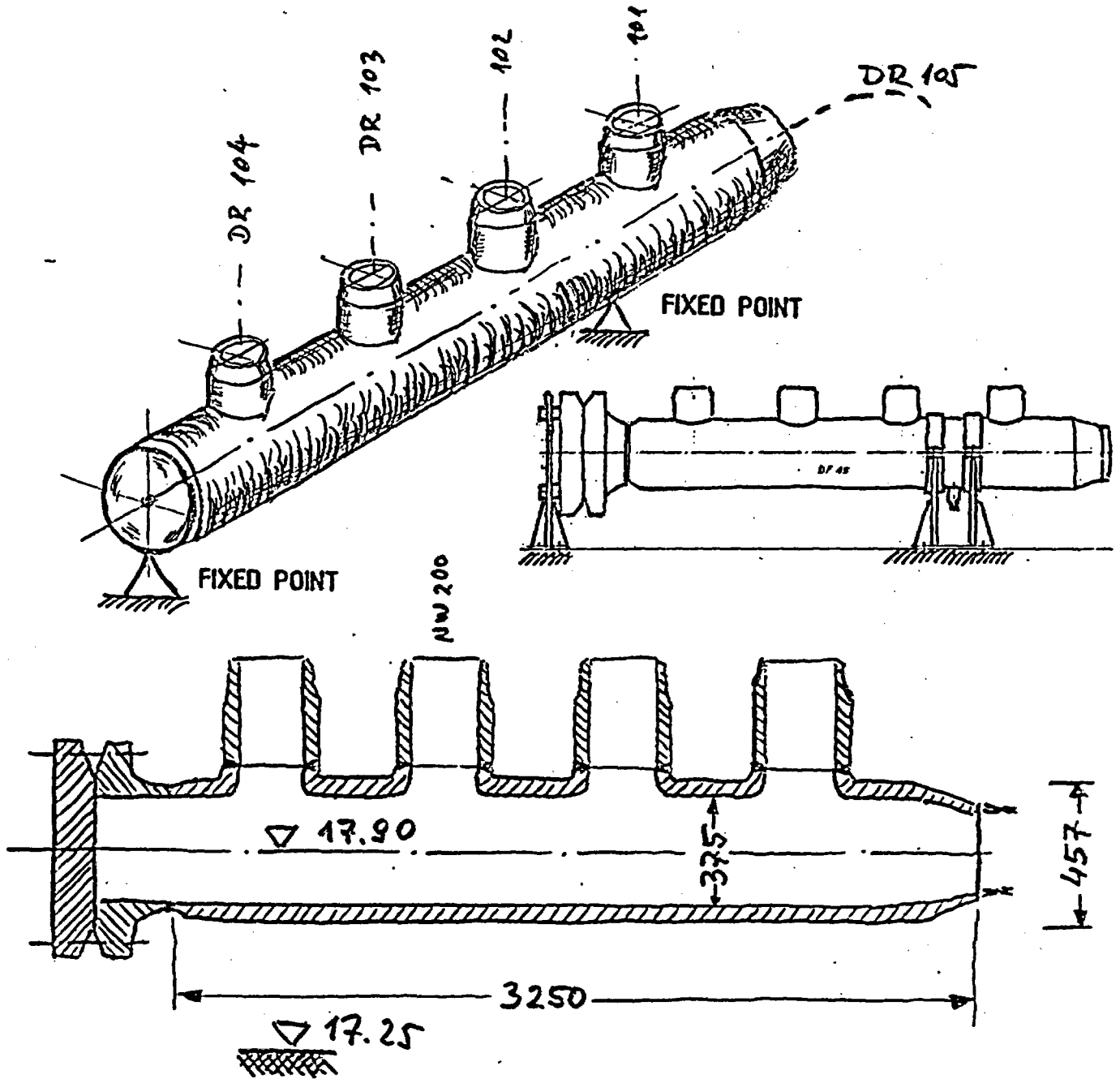


Fig. 2.1-15

Primary steam heater DF 15 (fixed points)

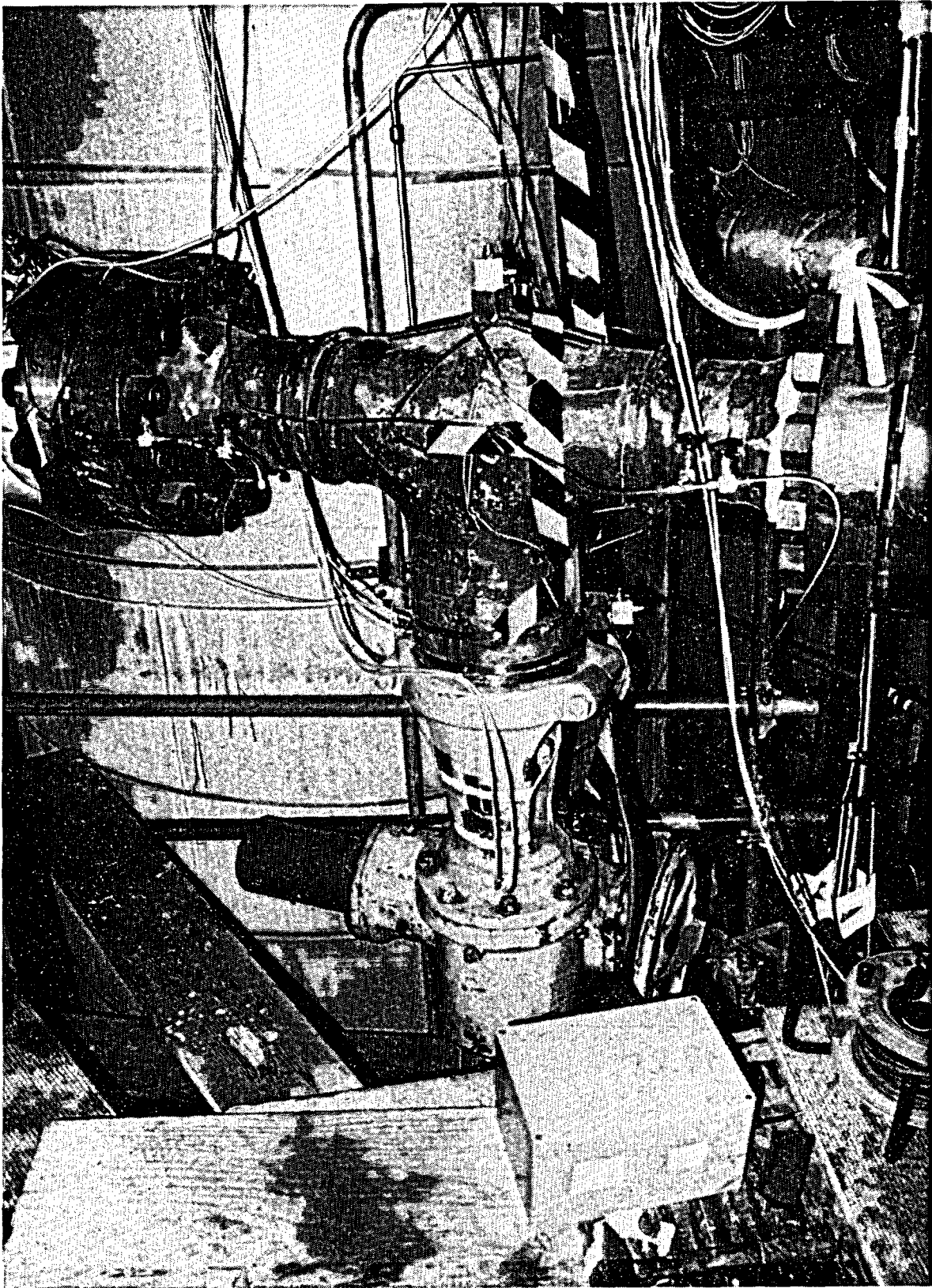


Fig. 2.1-16 Gate Valve From Shippingport Reactor in VKL

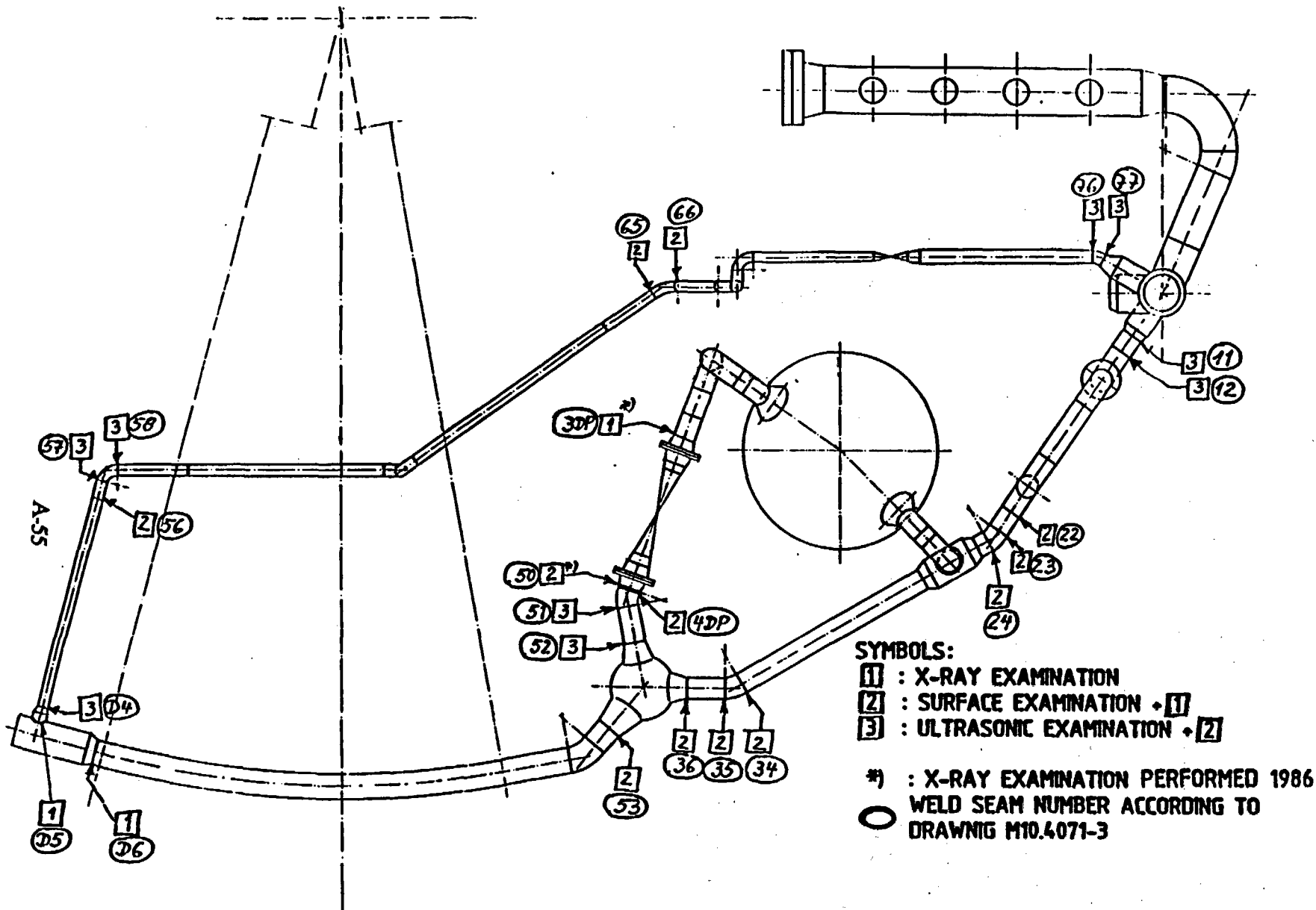


Fig. 2.2-1

Examined weld seams of the VKL, plan view

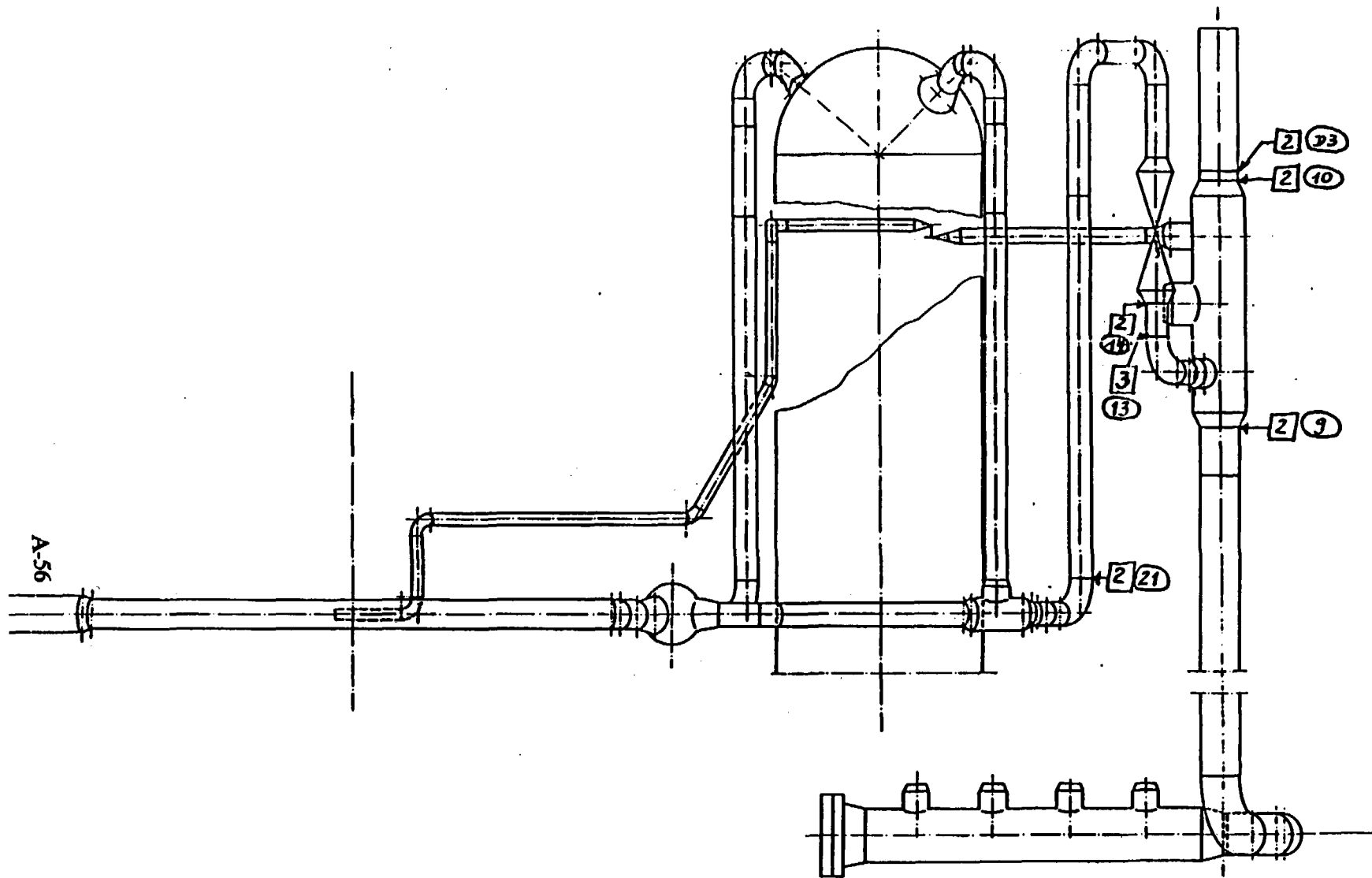
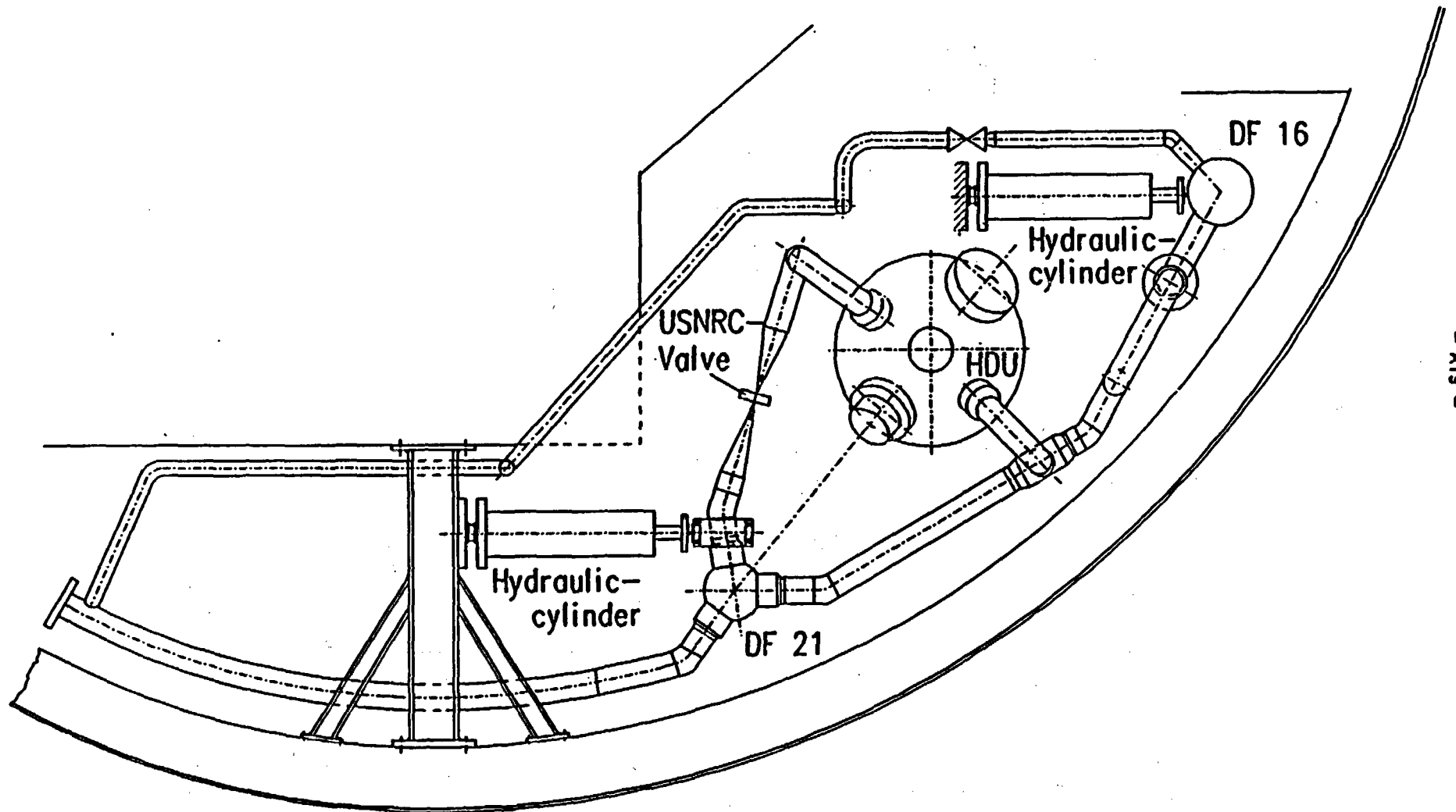


Fig. 2.2-2 Examined weld seams of the VKL, elevation view

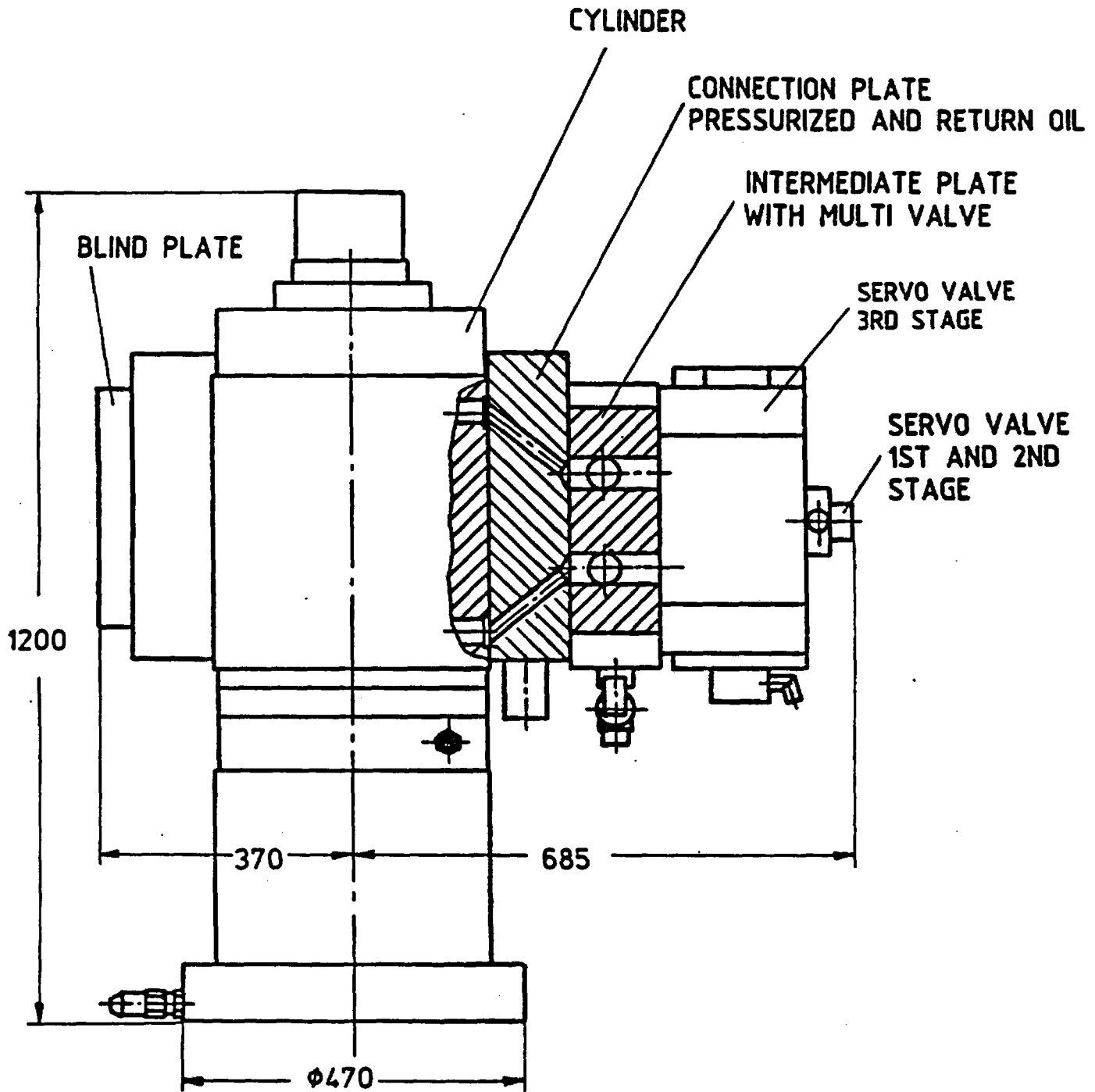
A-57



- 619 -

Fig. 2.3-1

Excitation system of the VKL system



SERVO HYDRAULIC TEST ACTUATOR

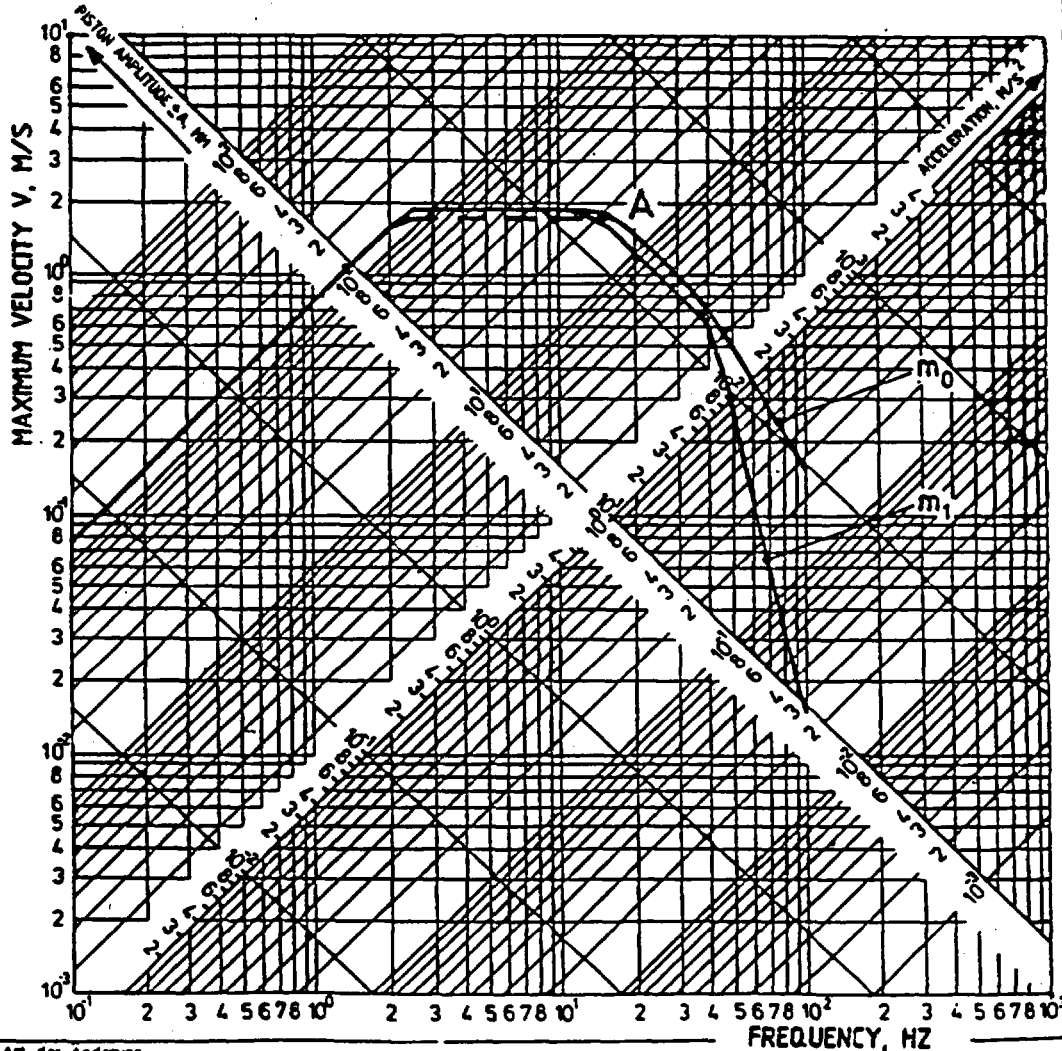
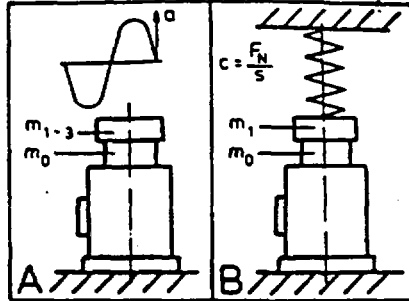
$F_{max} = 400 \text{ kN}$, $s_{max} = \pm 125 \text{ mm}$, $m = 1300 \text{ kg}$

Fig. 2.3-2 Servo-hydraulic test actuator

CYLINDER CHARACTERISTIC DATAS

Rated load	F_N	200 ± 400	kN
Rated stroke	$2 \times s_{max}$	250	mm
Piston area	A	149	cm ²
Piston weight	m_0	92	kg
Additional weight	m_1	2400	kg
	m_2		kg
	m_3		kg
Rated through flow	Q	1000	l/min
Supply pressure	ps	280	bar
Valve type:	SV 1000/9.5		
Pump Unit		1000 l/min	-----
A = no load characteristic curve			
A_m = characteristic curve with additional weights			
$B_{80\%}^n$ = dynamic full load line			

F_N 200 ± 400 kN
 Rated Stroke 250mm
 Typ PLz 600/400NV



Art der Änderung:
 gerechnet: 2.6.87 Hofmann
 Alle Rechte vorbehalten. Verantwortung und
 Haftung an Dritte nicht gestattet. Zusätz-
 liche Bedingungen sind im Schadensfall
 und können strafrechtlich Folgen haben.



Carl Schenck AG

DPP3 268

Fig. 2.3-3

Characteristic curves of the hydraulic actuators

A-60

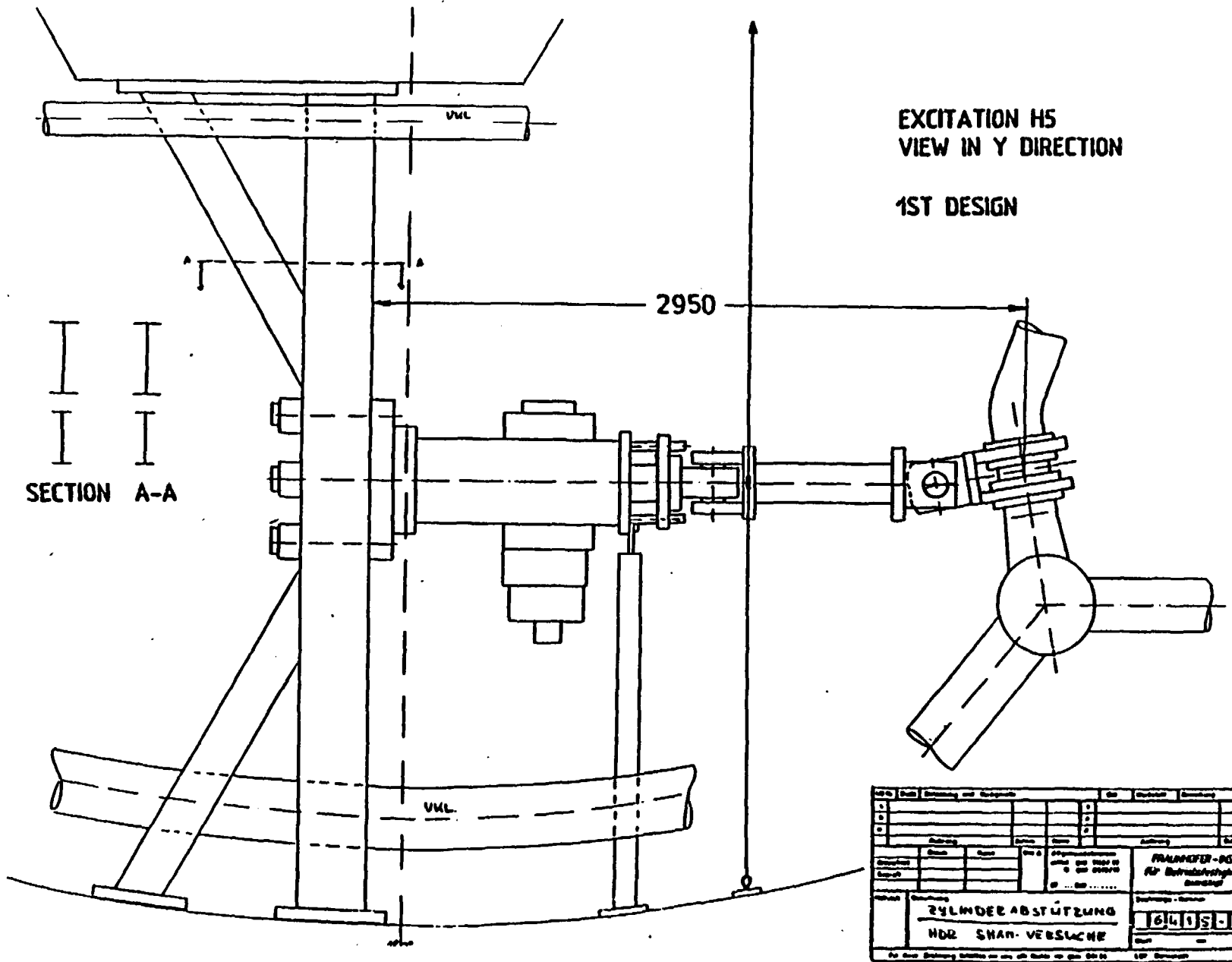
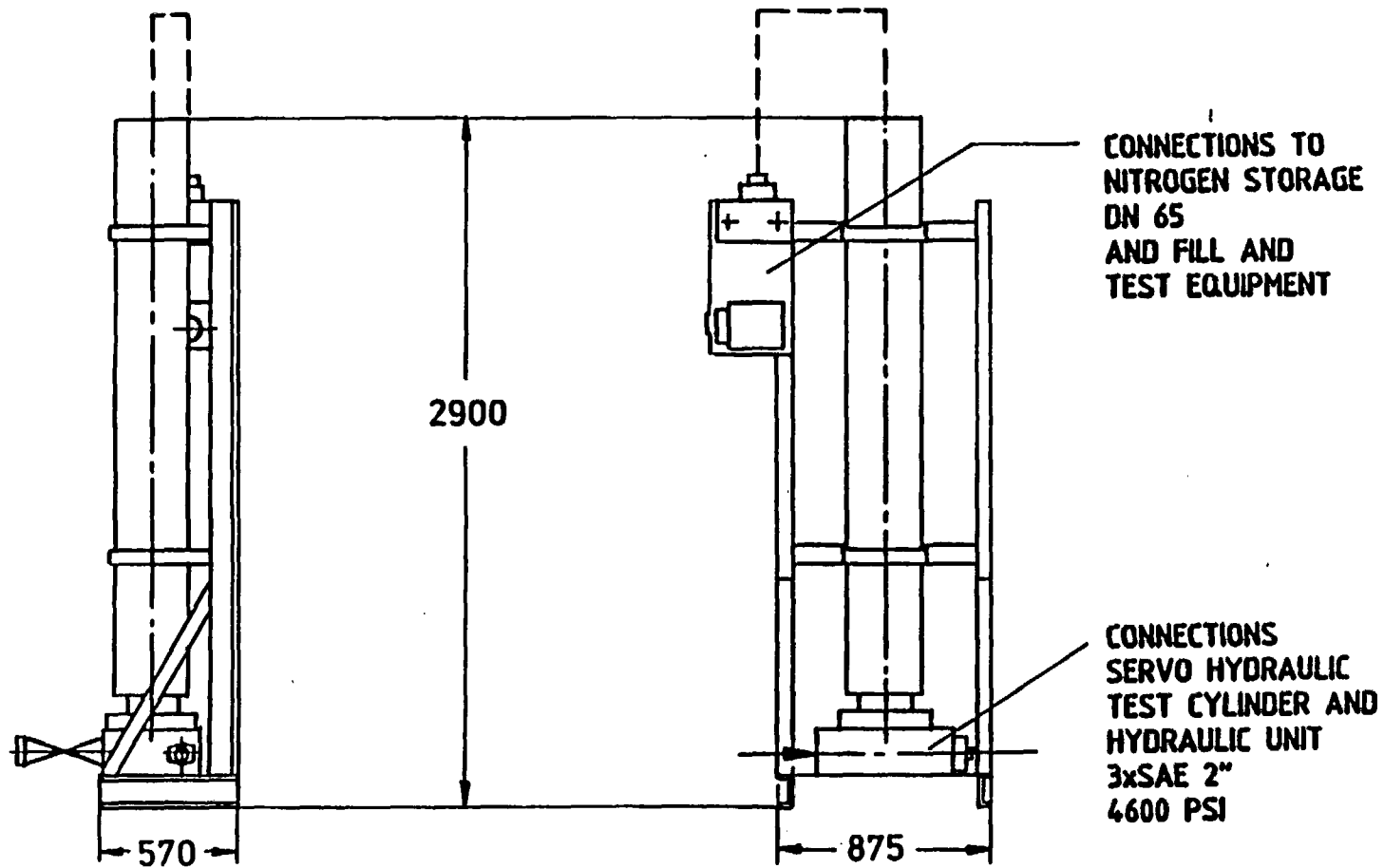


Fig. 2.3-4 Load application H5

A-62



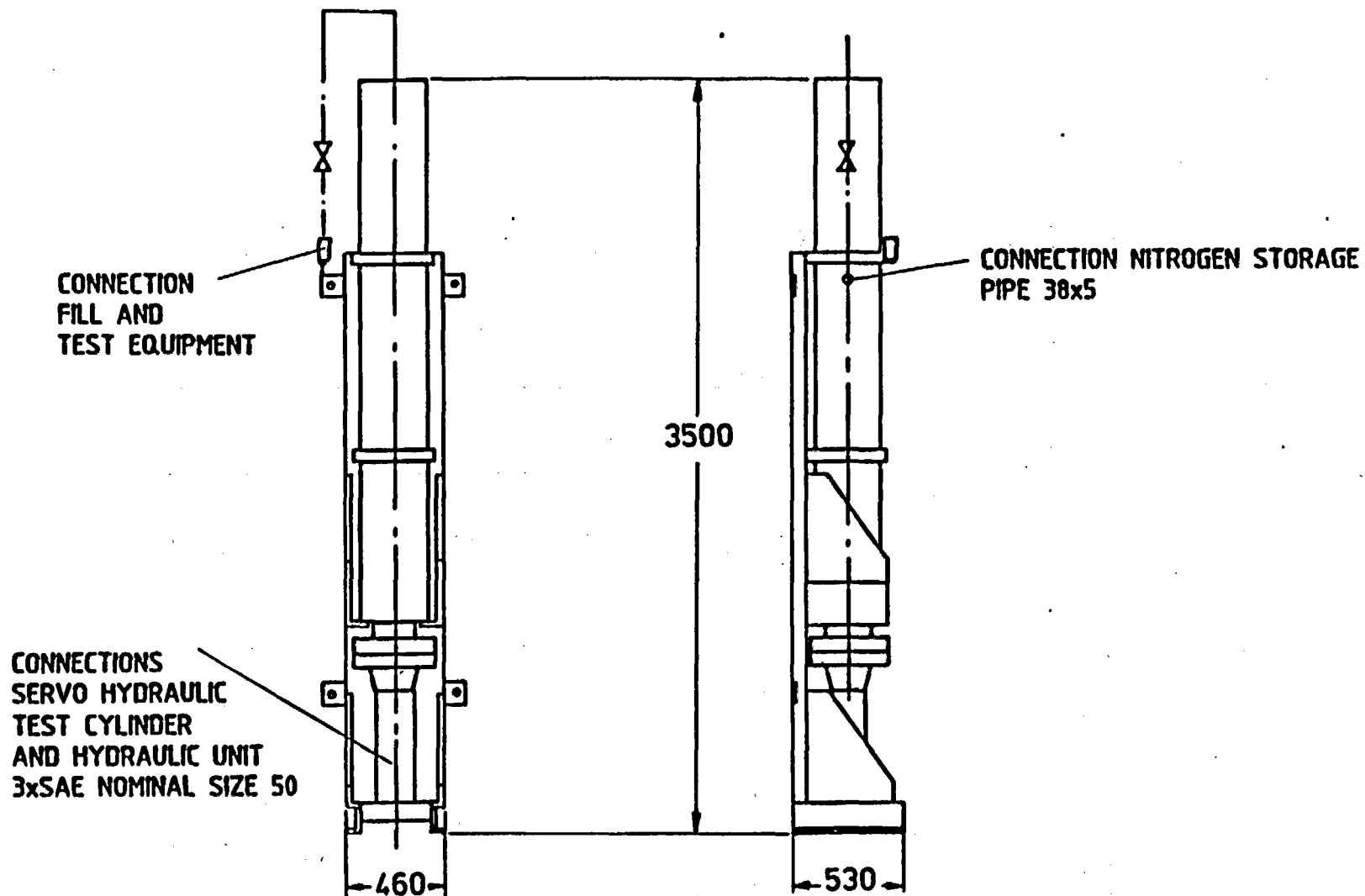
- A24 -

PRESSURIZED OIL STORAGE, $V = 90 \text{ ltr}$, $P_{\text{max}} = 280 \text{ bar}$, $\dot{m} = 50 \text{ ltr/sec}$

Fig. 2.3-6

Pressurized oil storage

A-63



- A25 -

RETURN OIL STORAGE, $V = 100$ ltr, $P_{\max} = 5,8$ bar

Fig. 2.3-7

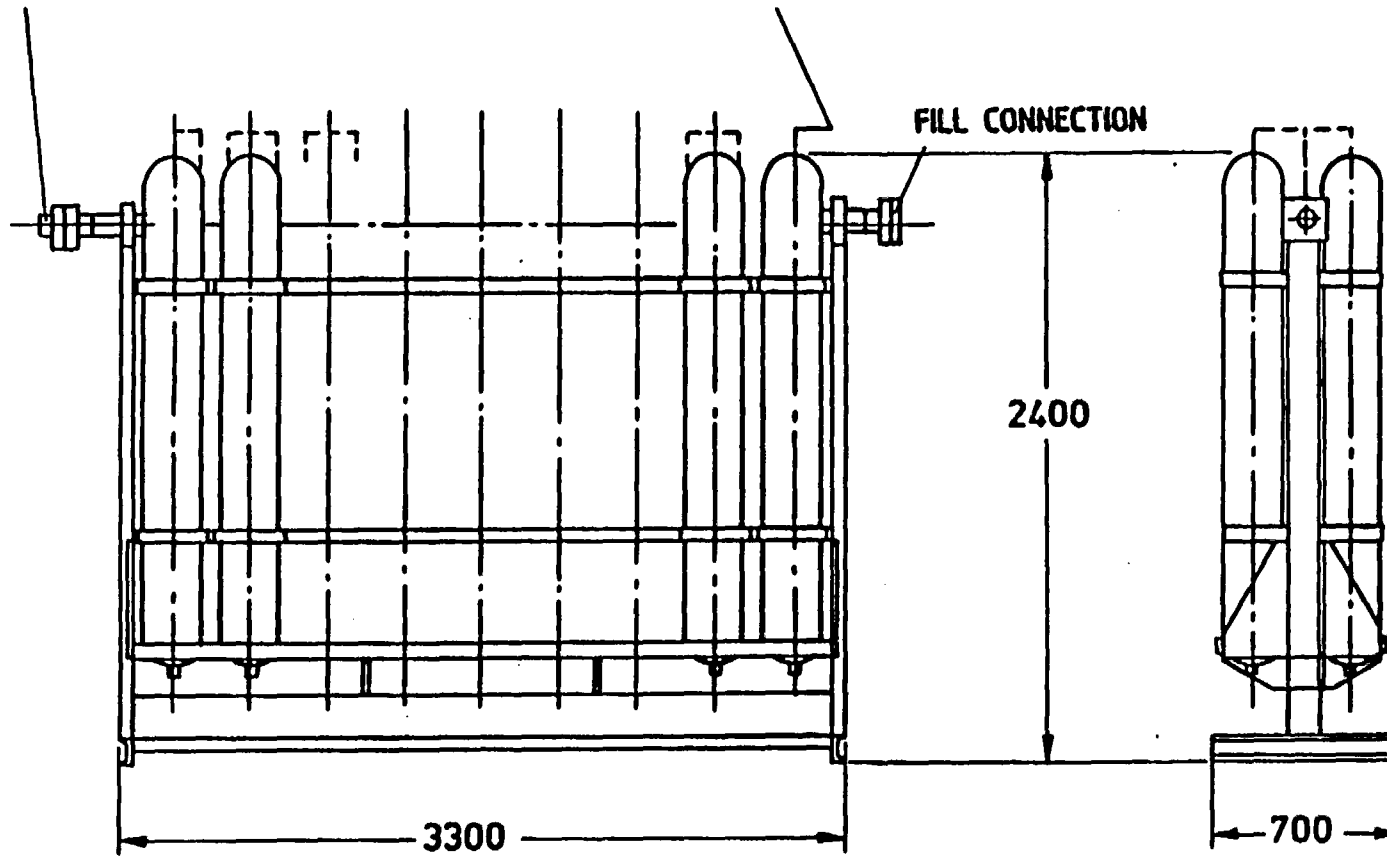
Return oil storage

A-64

CONNECTION PRESSURIZED OIL STORAGE
DN 65

CONNECTION RETURN OIL STORAGE
PIPE 38x5

FILL CONNECTION



- A26 -

NITROGEN STORAGE, $V_P = 890$ ltr , $V_R = 150$ ltr

Fig. 2.3-8

Nitrogen storage

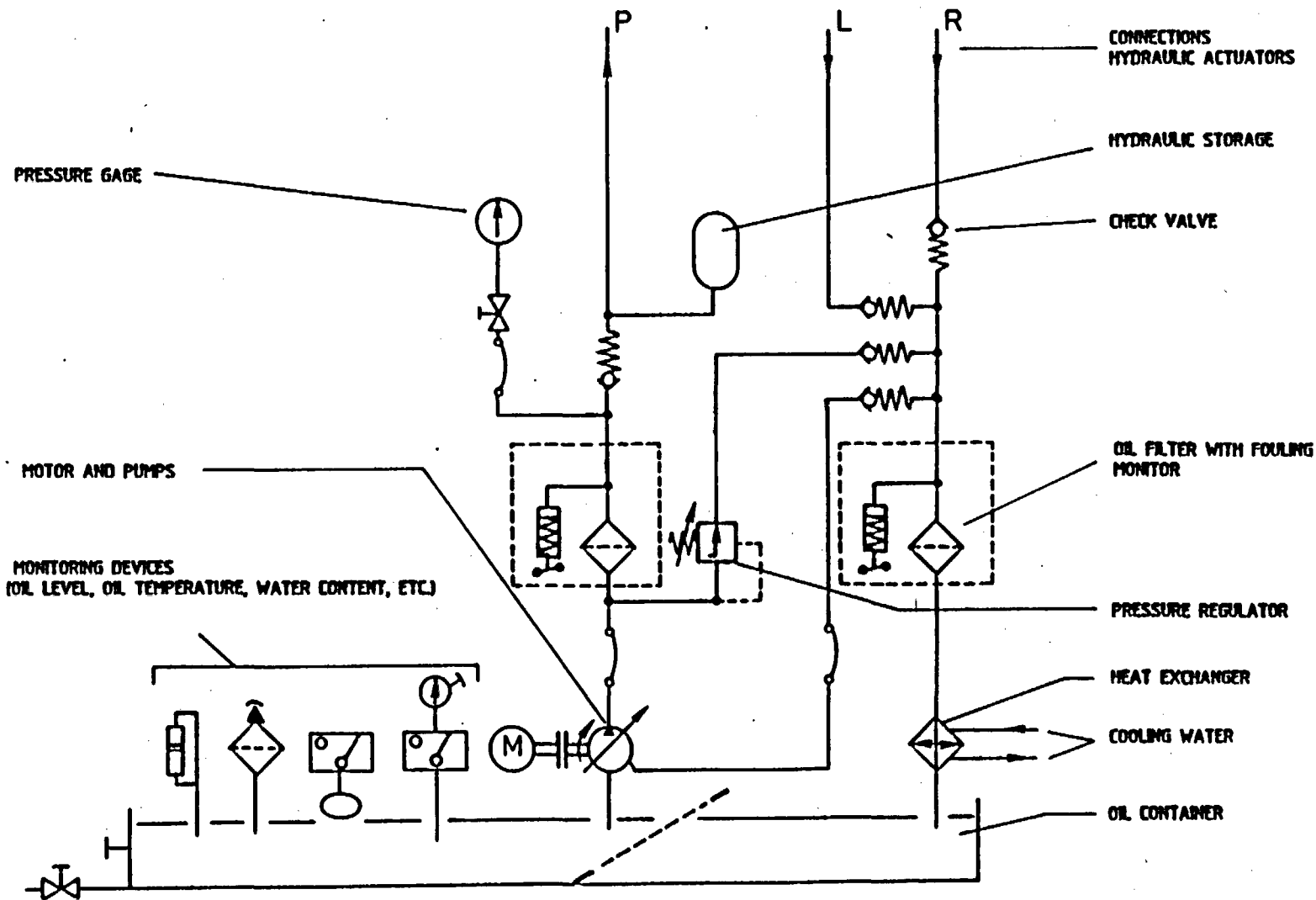


Fig. 2.3-9

Hydraulic unit (Connection diagram)

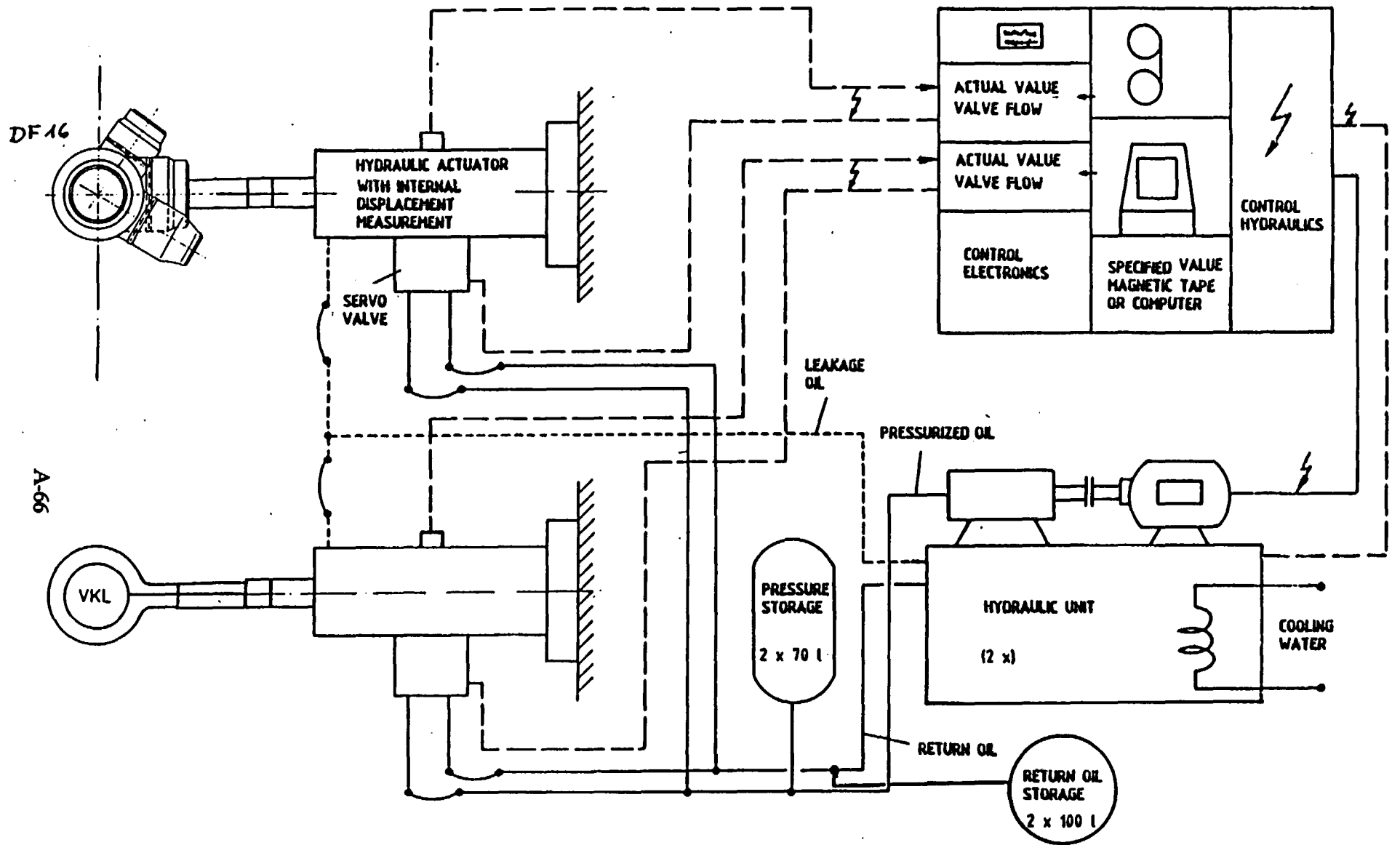


Fig. 2.3-10 Excitation system with hydraulic unit and control electronics (schematic)

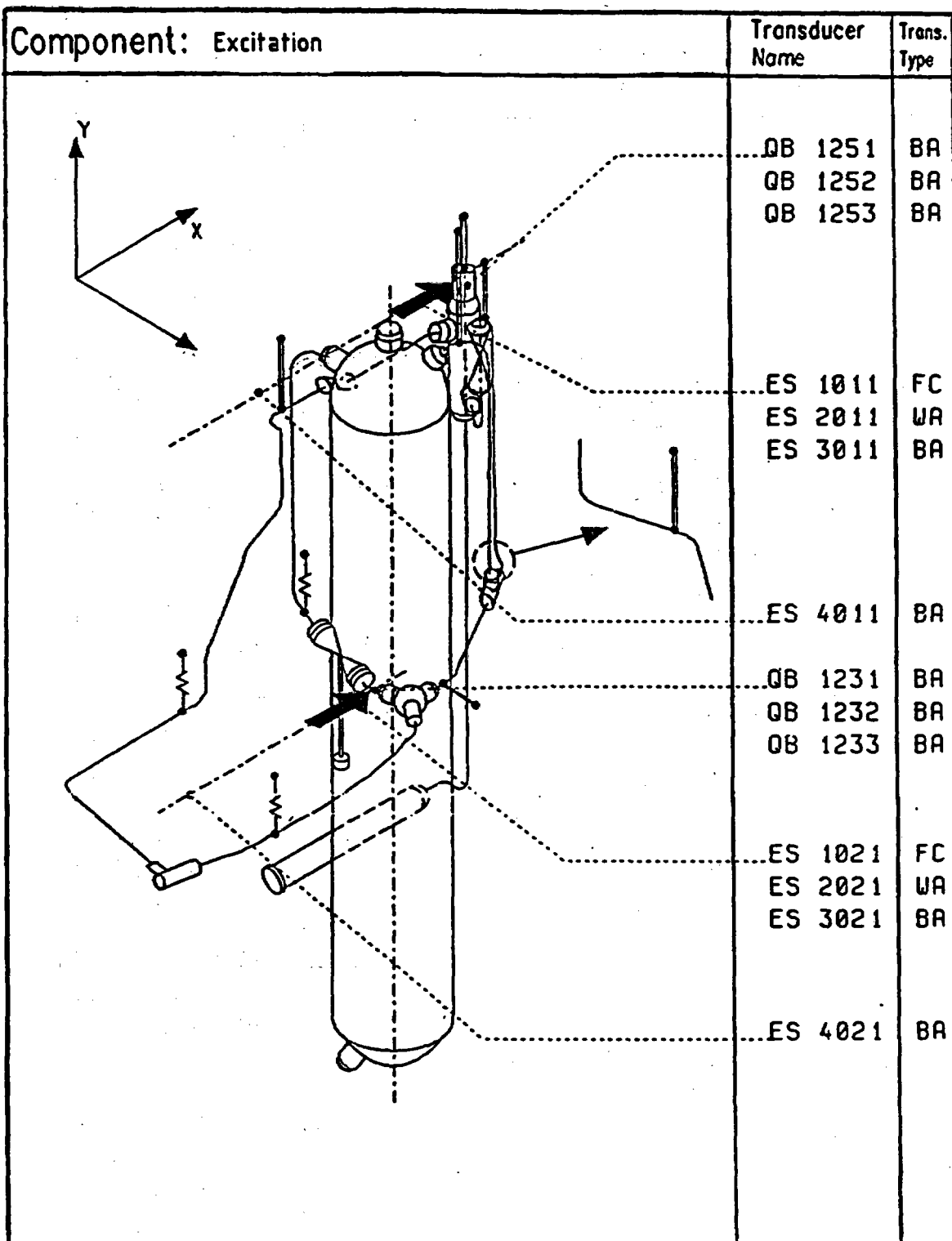


Fig. 3.1-1

Test series: SHAM
Measurement locations plan for T41

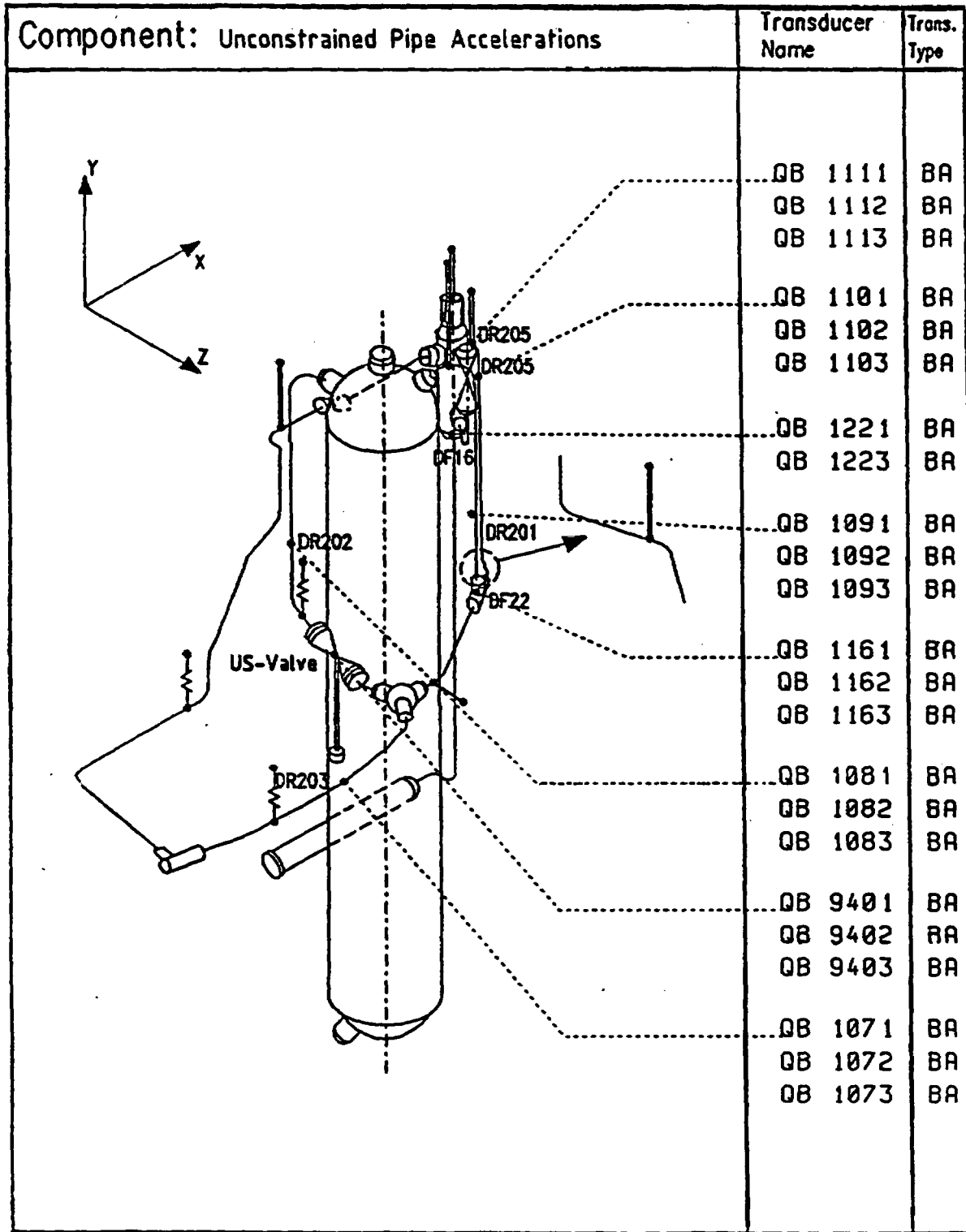


Fig. 3.1-2

Test series: SHAM
Measurement locations plan for T41

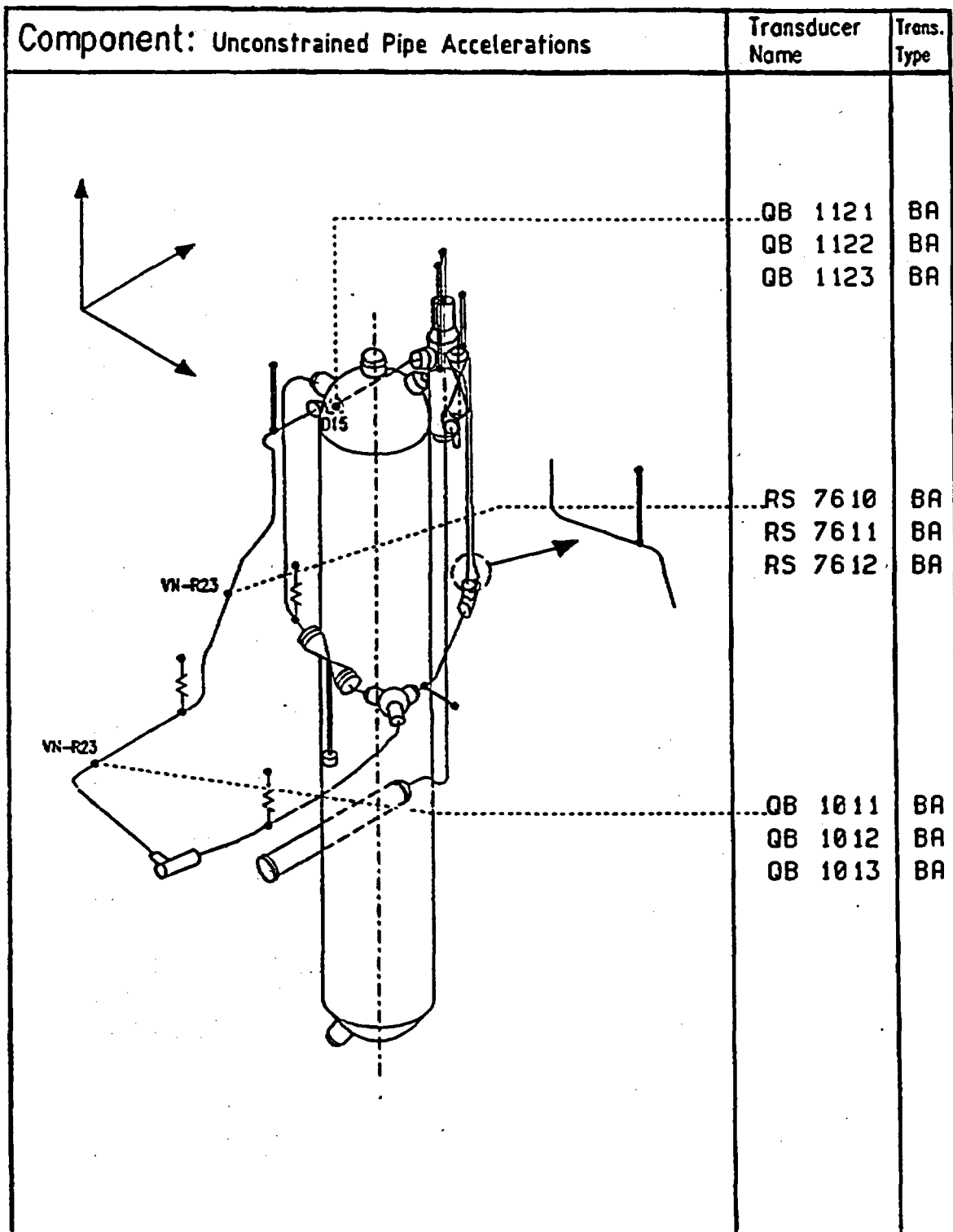


Fig. 3.1-3

Test series: SHAM
Measurement locations plan for T41

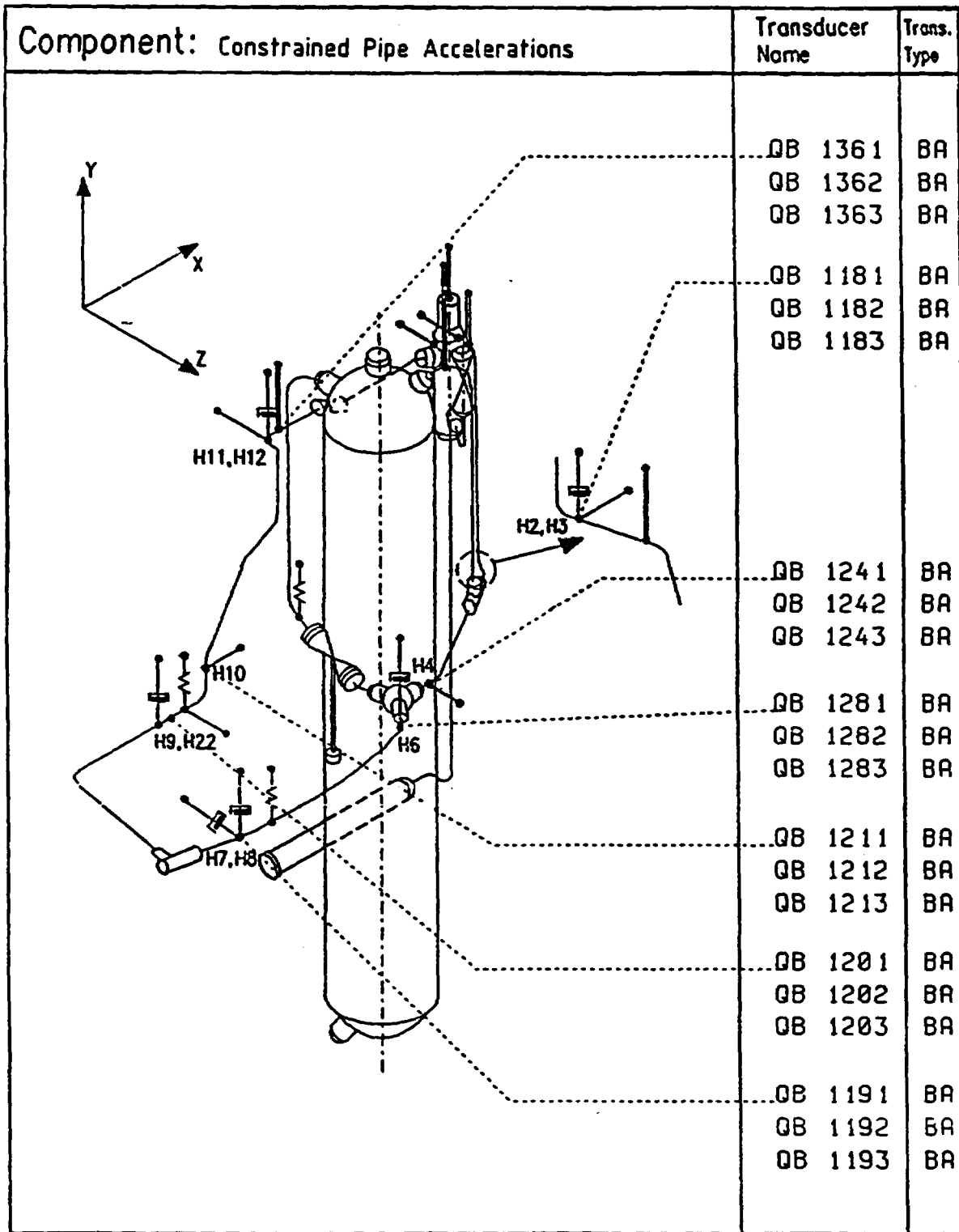


Fig. 3.1-4 Test series: SHAM
Measurement locations plan for T41

Component: Forces at Springhangers and at Permanent struts	Transducer Name	Trans. Type
	QR 1513	FC
	QR 1517	FC
	QR 1243	FC
	UR 7649	FC
	UR 7669	FC
	UR 7659	FC

Fig. 3.1-5 Test series: SHAM
Measurement locations plan for T41

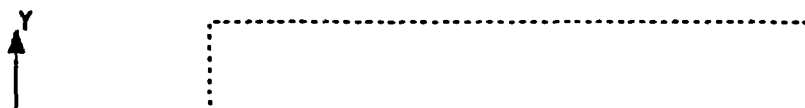


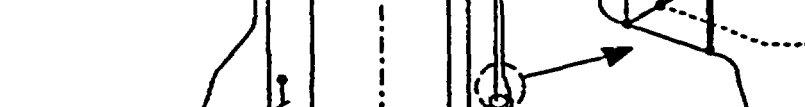






Component: Forces at NRC-Hangers (Snubbers, Struts)	Transducer Name	Trans. Type
	QA 3333	FC
	QA 3342	FC
	QA 3262	FC
	QA 3271	FC
	QA 3321	FC
	QA 3282	FC
	QA 3492	FC
	QA 3313	FC
	QA 3292	FC
	QA 3303	FC

Fig. 3.1-6 Test series: SHAM
Measurement locations plan for T41

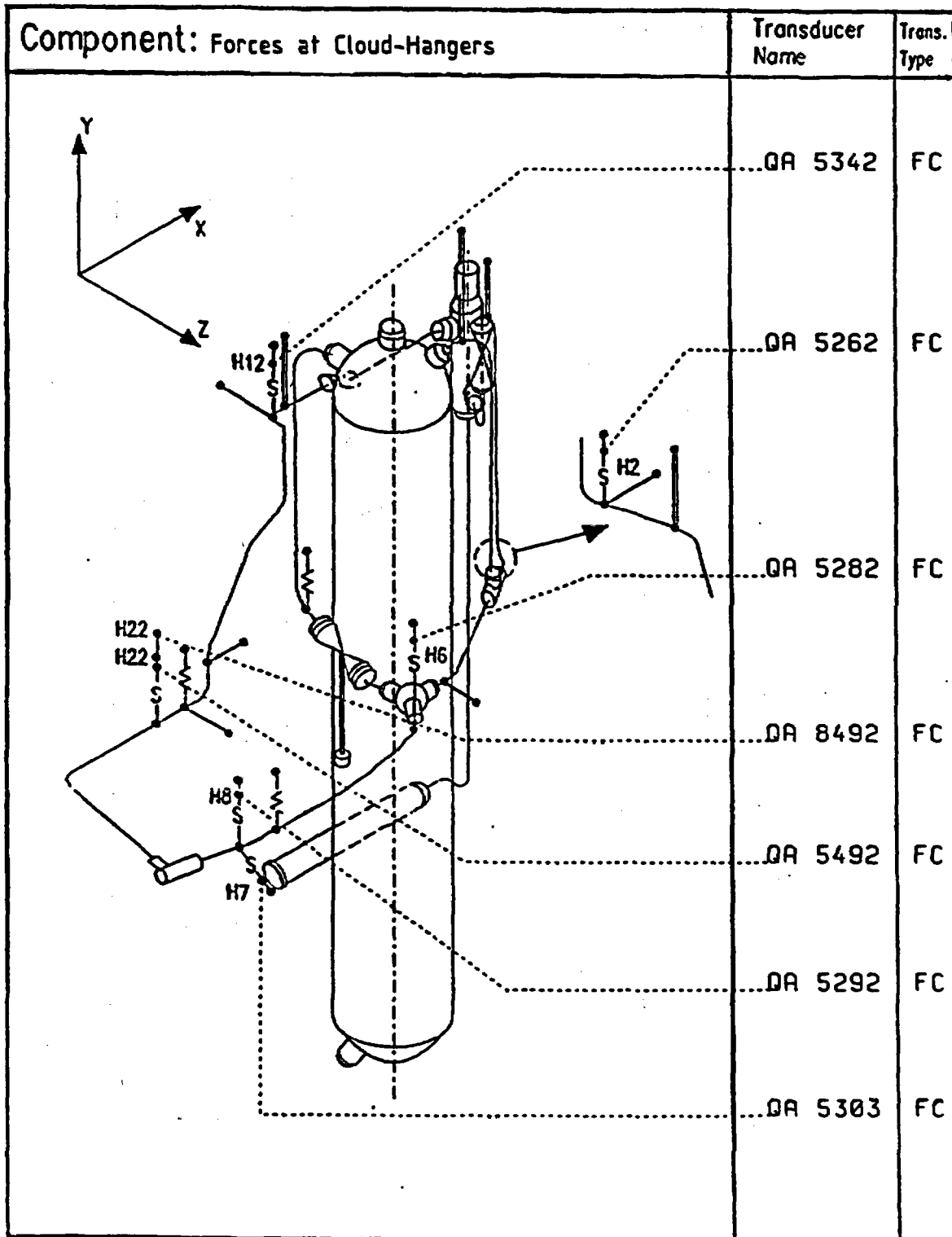


Fig. 3.1-7

Test series: SHAM
 Measurement locations plan for T41

Component: Forces at Bechtel-Hangers	Transducer Name	Trans. Type
<p>The diagram shows a vertical cylindrical component with a central vertical axis. A coordinate system is defined with the Y-axis pointing upwards, the X-axis pointing to the right, and the Z-axis pointing downwards and to the right. Three measurement locations are marked: H22 is located on the upper left side of the cylinder; H8 is located on the lower left side; and H7 is located on the lower right side. Each location is associated with a transducer symbol (a resistor-like symbol with a central dot). Dotted lines connect H22 to QA 4492, H8 to QA 4292, and H7 to QA 4303. A separate detail view on the right shows a close-up of a hanger assembly with a transducer.</p>	<p>QA 4492</p> <p>QA 4292</p> <p>QA 4303</p>	<p>FC</p> <p>FC</p> <p>FC</p>

Fig. 3.1-8

Test series: SHAM
 Measurement locations plan for T41

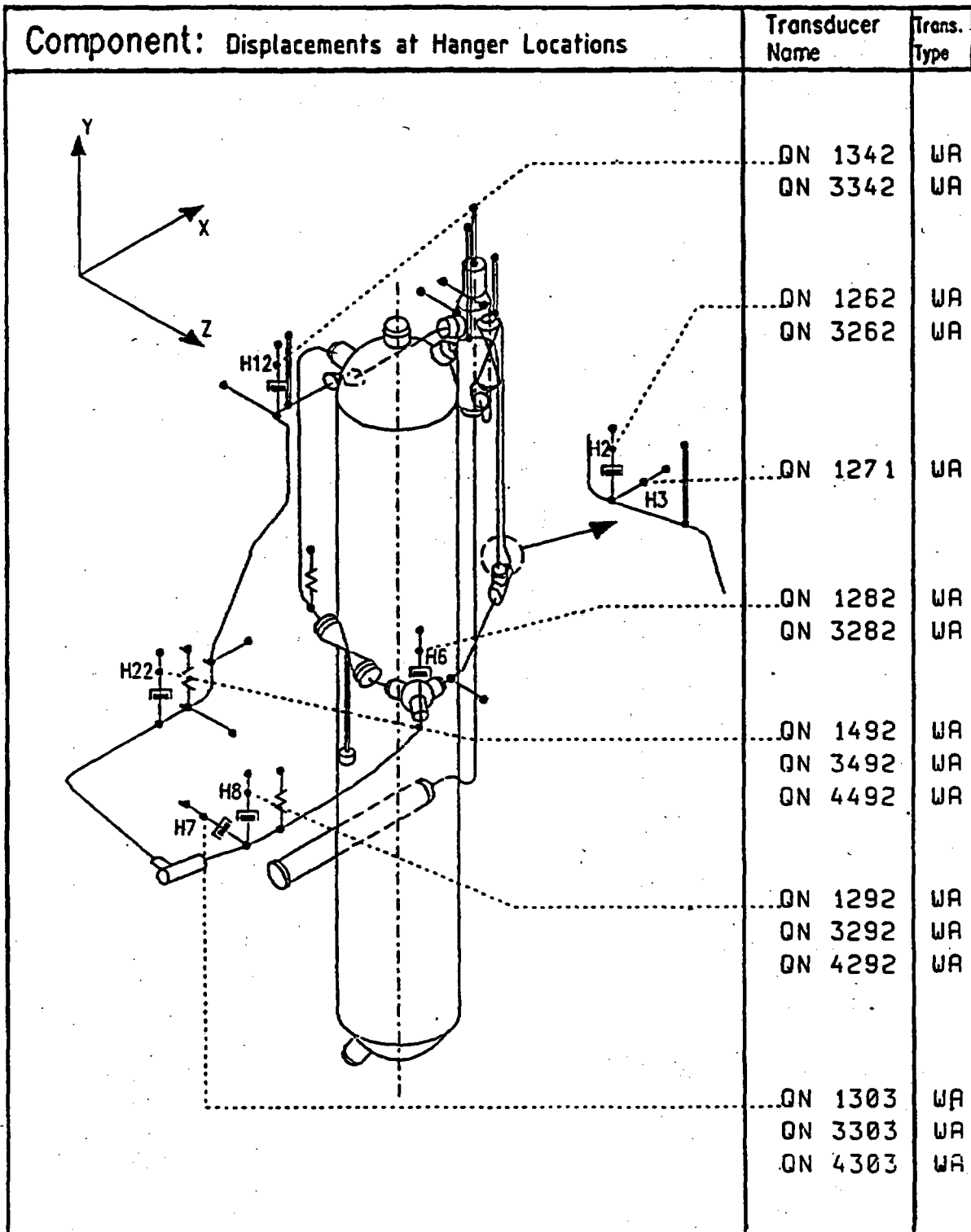


Fig. 3.1-9 Test series: SHAM
Measurement locations plan for T41

Component: Displacements on the Pipes	Transducer Name	Trans. Type
	QN 1221	WA
	QN 1222	WA
	QN 1223	WA
	QN 1351	WA
	QN 1352	WA
	QN 1353	WA
	QN 1011	WA
	QN 1012	WA
	QN 1013	WA

Fig. 3.1-10

Test series: SHAM
Measurement locations plan for T41

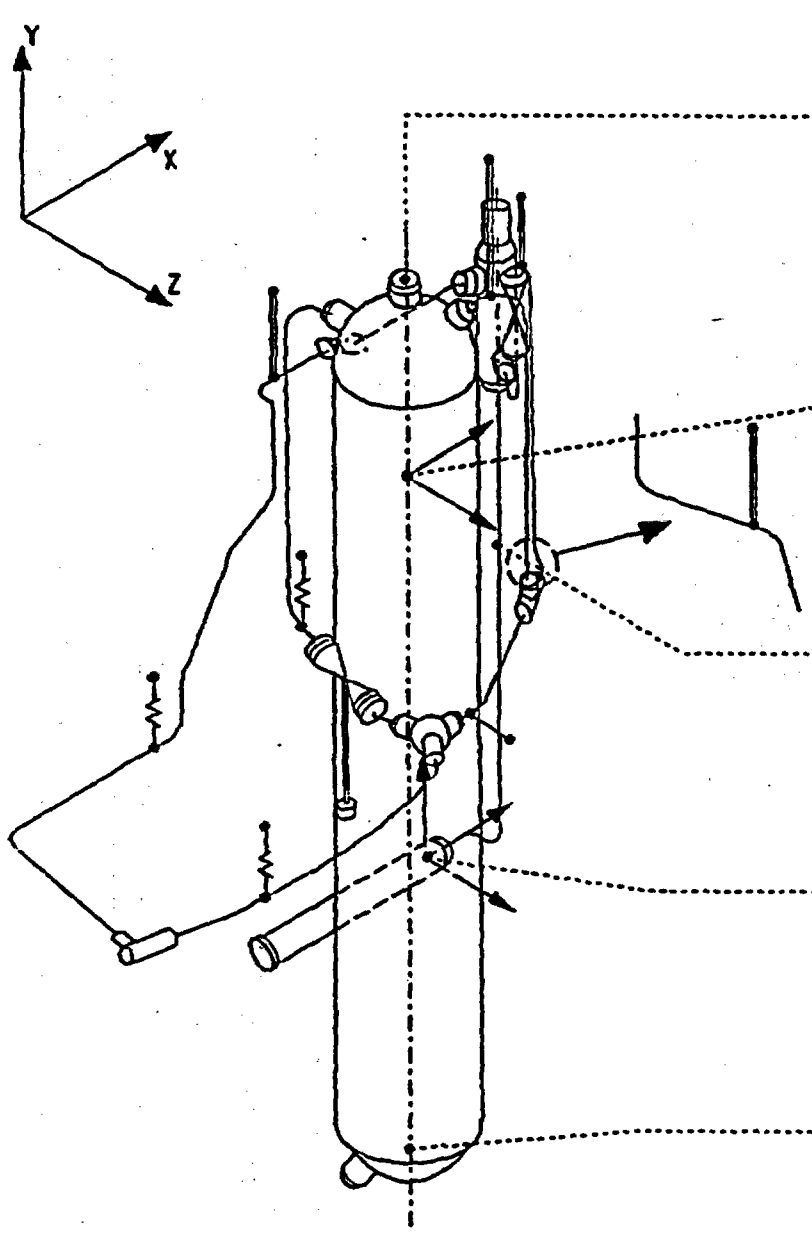
Component: Control of the fixed points	Transducer Name	Trans. Type
	WS 1704	BA
	WS 1705	BA
	WS 1706	BA
	WS 2701	WA
	WS 2703	WA
	RS 6641	BA
	RS 6642	BA
	RS 6643	BA
	RS 6631	BA
	RS 6632	BA
	RS 6633	BA
	WS 3701	BA
	WS 3702	BA
	WS 3703	BA

Fig. 3.1-11

Test series: SHAM
Measurement locations plan for T41

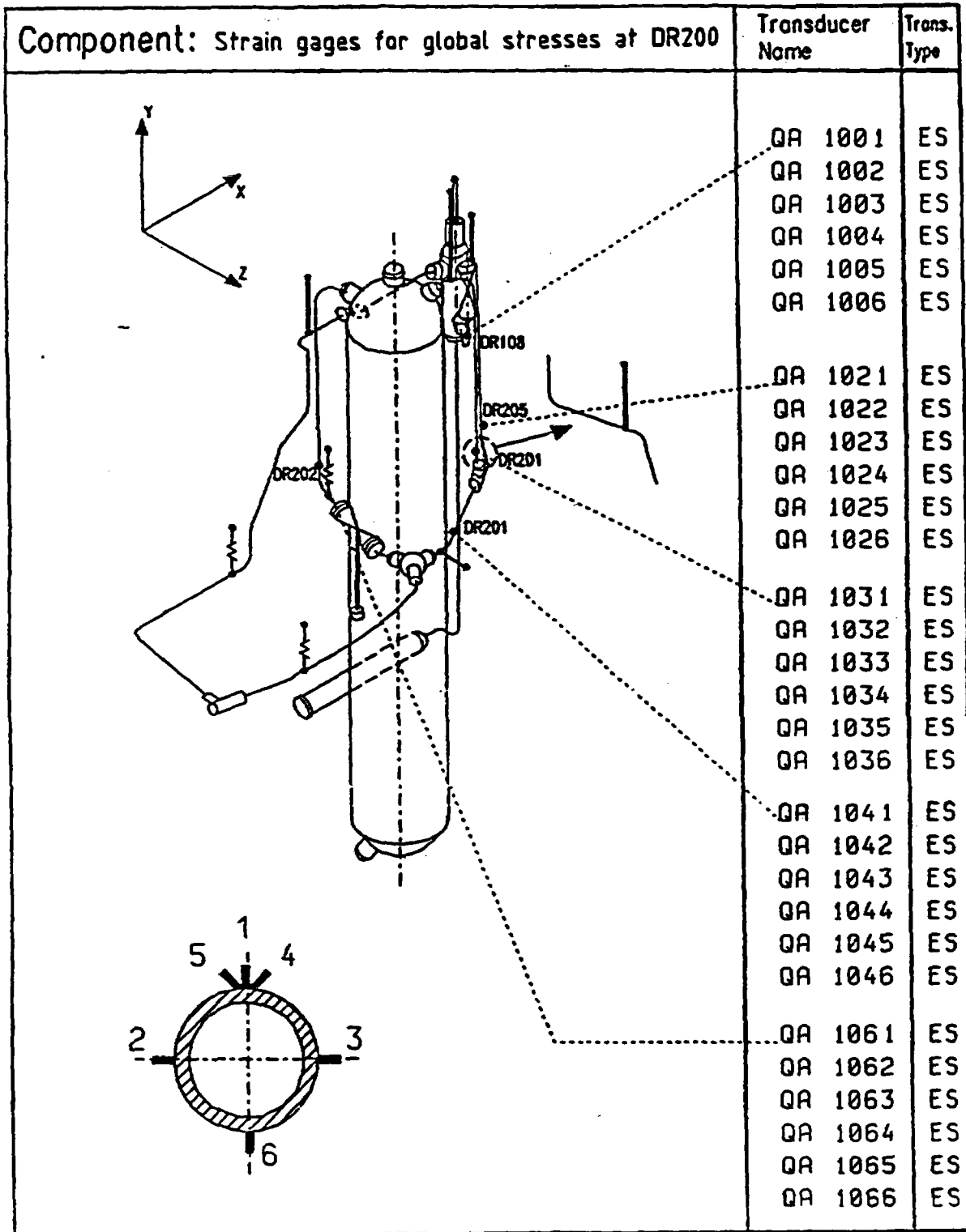


Fig. 3.1-12

Test series: SHAM
Measurement locations plan for T41

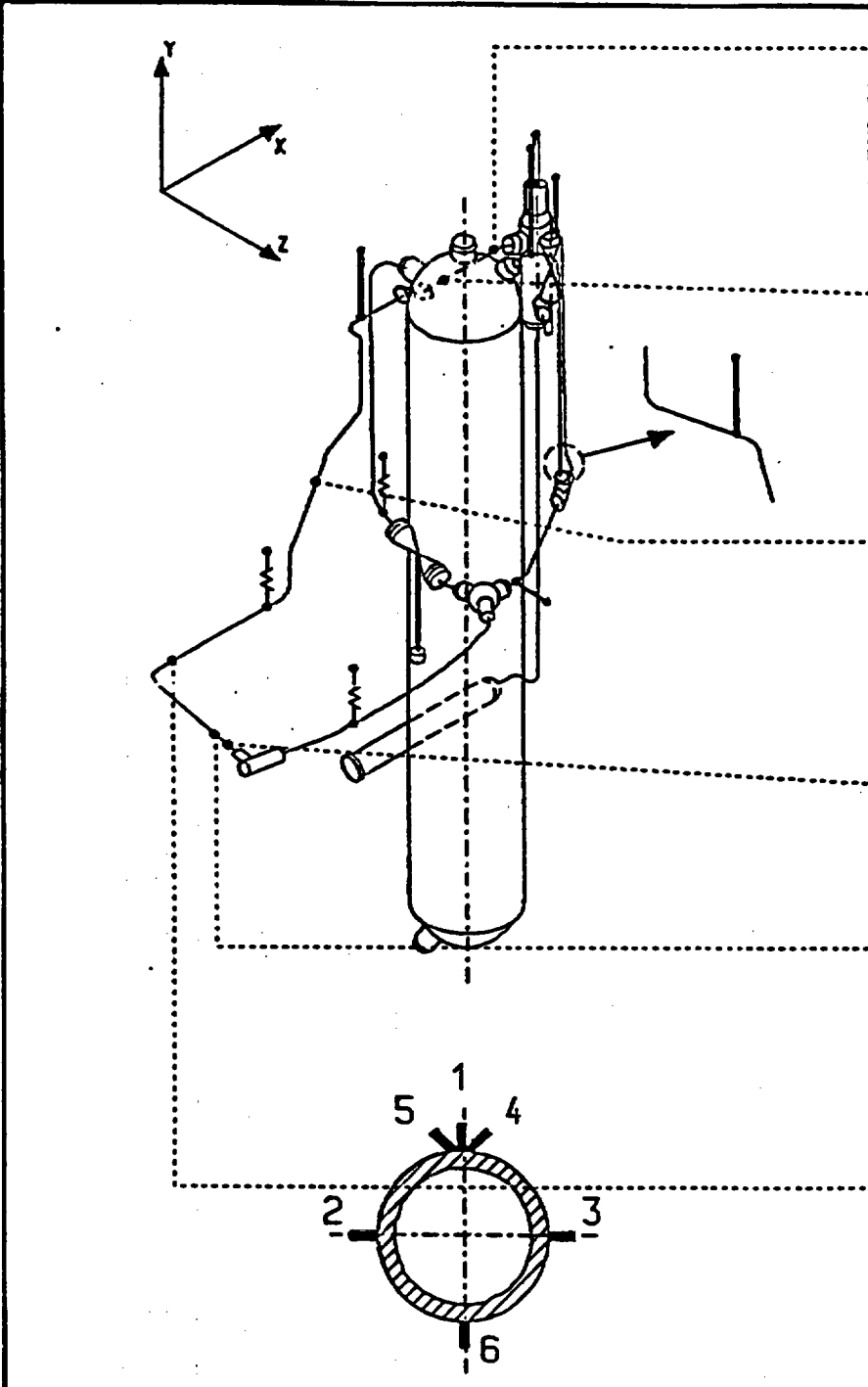
Component: Strain gages for global stresses at VN-R23	Transducer Name	Trans. Type
	RA 7661	ES
	RA 7662	ES
	RA 7663	ES
	RA 7664	ES
	RA 7665	ES
	RA 7666	ES
	RA 7651	ES
	RA 7652	ES
	RA 7653	ES
	RA 7654	ES
	RA 7655	ES
	RA 7656	ES
	RA 7641	ES
	RA 7642	ES
	RA 7643	ES
	RA 7644	ES
	RA 7645	ES
	RA 7646	ES
	RA 7671	ES
	RA 7672	ES
	RA 7673	ES
	RA 7676	ES
	RA 7601	ES
	RA 7602	ES
	RA 7603	ES
	RA 7604	ES
	RA 7605	ES
	RA 7606	ES
	RA 7631	ES
	RA 7632	ES
	RA 7633	ES
	RA 7634	ES
	RA 7635	ES
	RA 7636	ES

Fig. 3.1-13

Test series: SHAM
Measurement locations plan for T41

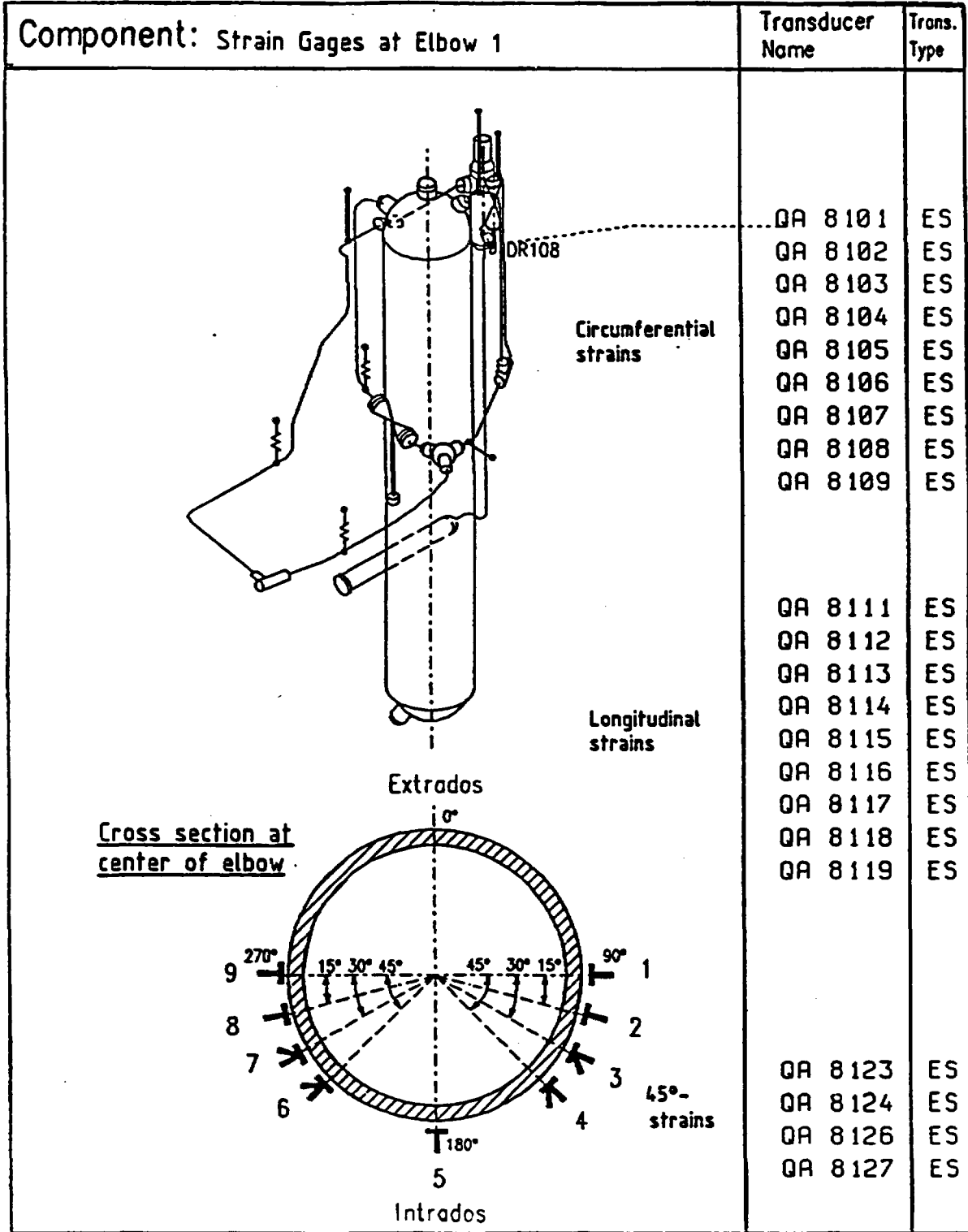


Fig. 3.1-14

Test series: SHAM
Measurement locations plan for T41

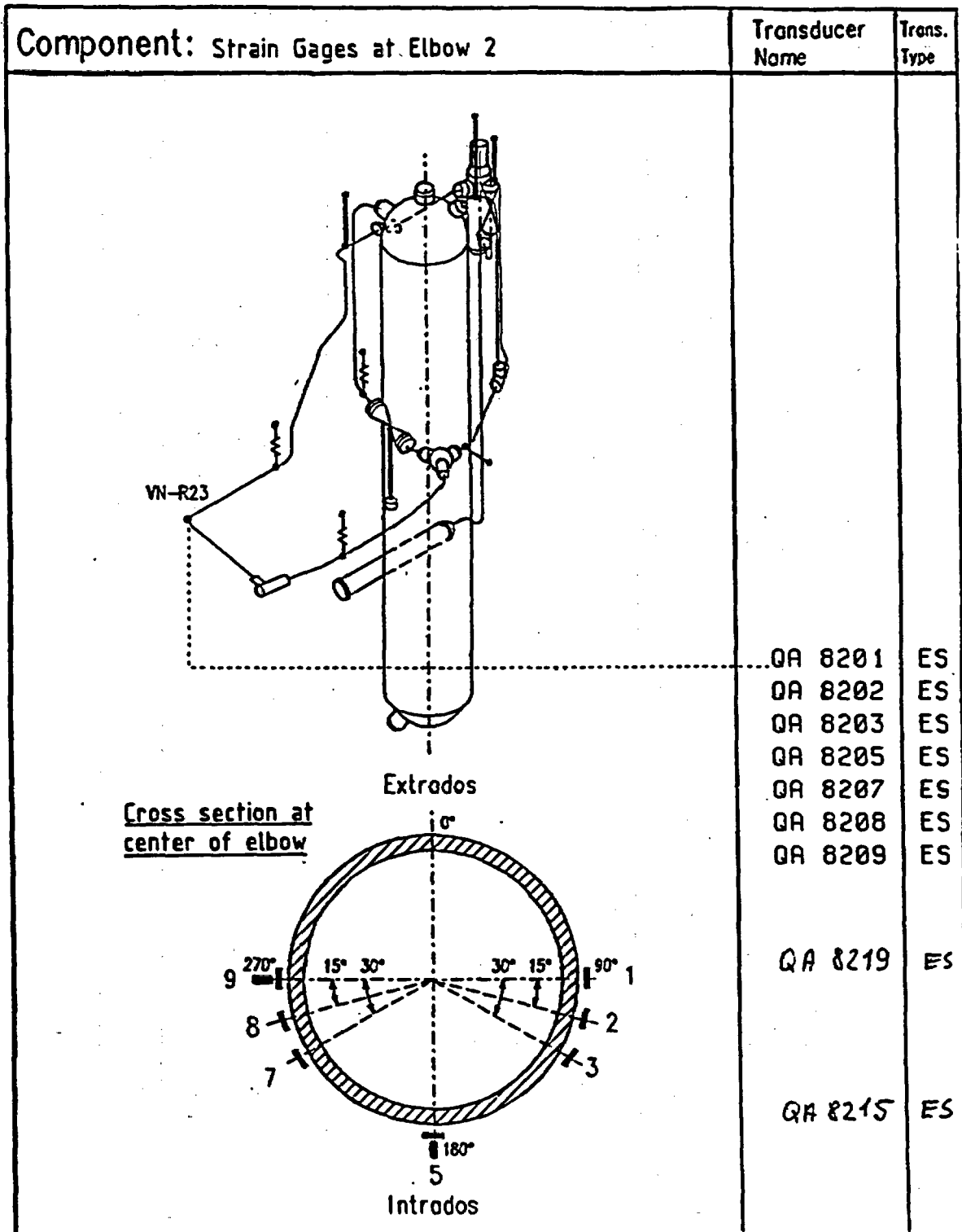


Fig. 3.1-15

Test series: SHAM
 Measurement locations plan for T41

Component: Strain Gages at Elbow 3	Transducer Name	Trans. Type
<p data-bbox="294 1200 538 1272"><u>Cross section at center of elbow</u></p> <p data-bbox="624 1187 740 1219">Extrados</p> <p data-bbox="624 1704 740 1736">Intrados</p>	QA 8301	ES
	QA 8302	ES
	QA 8303	ES
	QA 8305	ES
	QA 8307	ES
	QA 8308	ES
	QA 8309	ES
	QA 8319	ES
	QA 8315	ES

Fig. 3.1-16

Test series: SHAM
 Measurement locations plan for T41

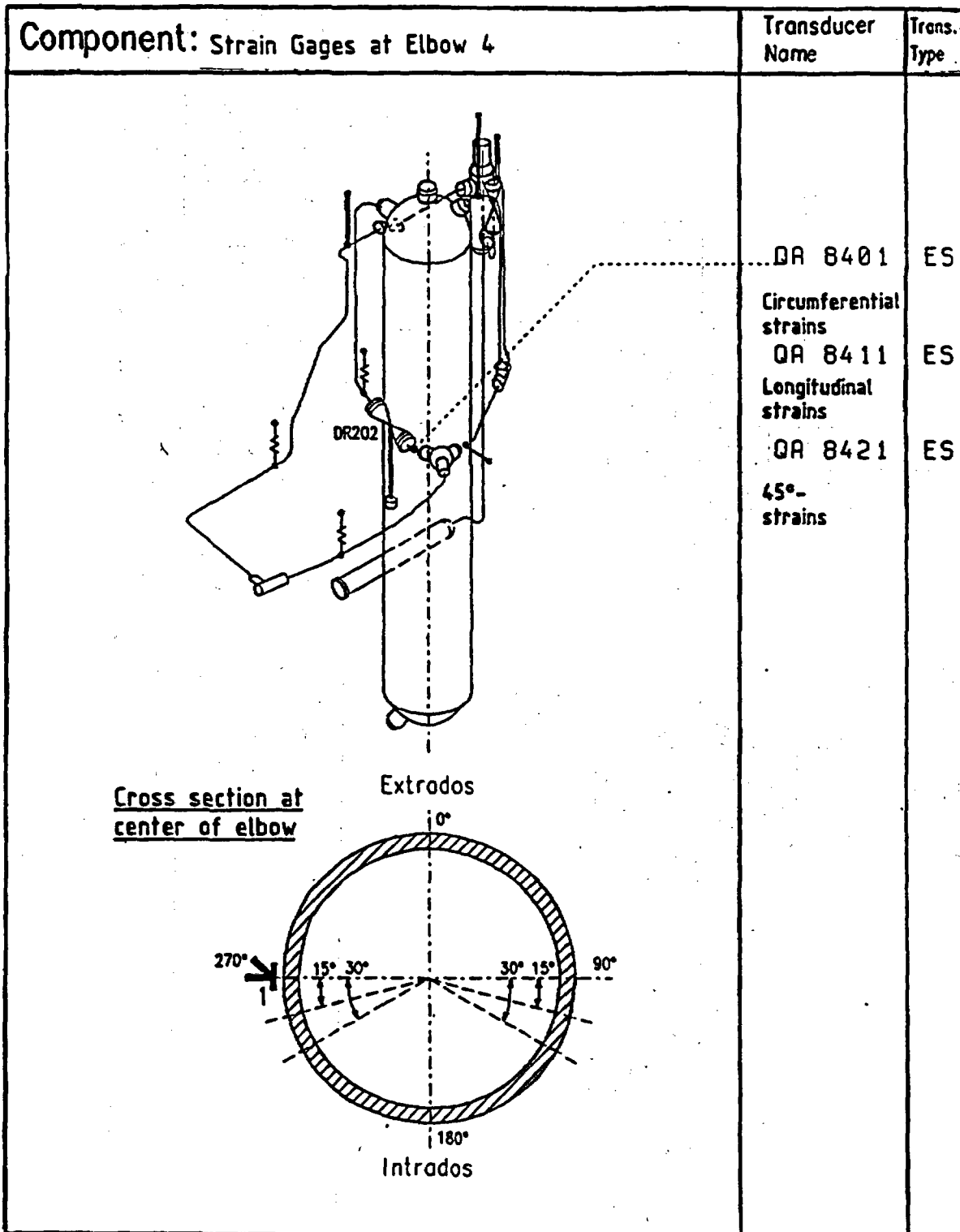


Fig. 3.1-17

Test series: SHAM
Measurement locations plan for T41

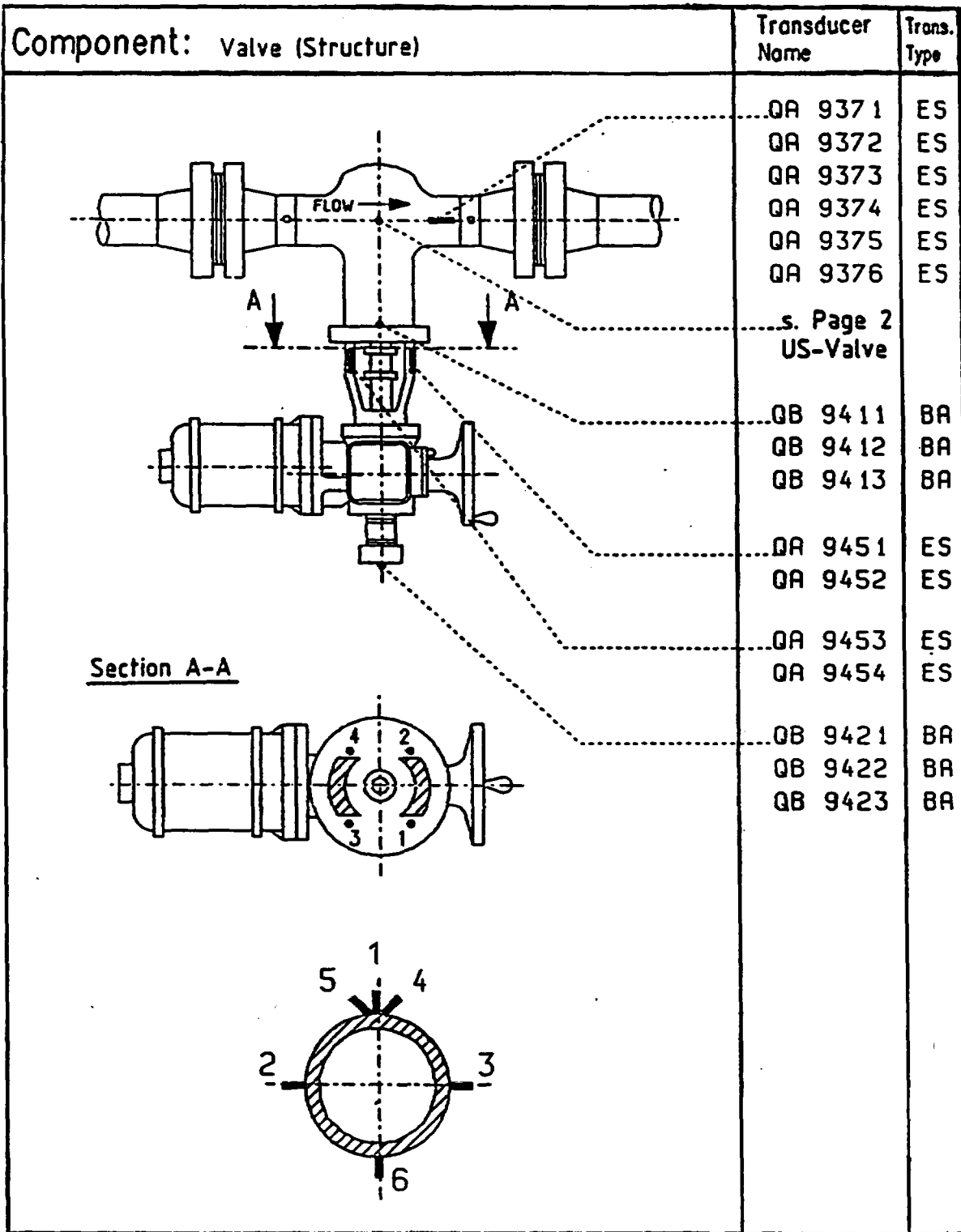


Fig. 3.1-18

Test series: SHAM
Measurement locations plan for T41

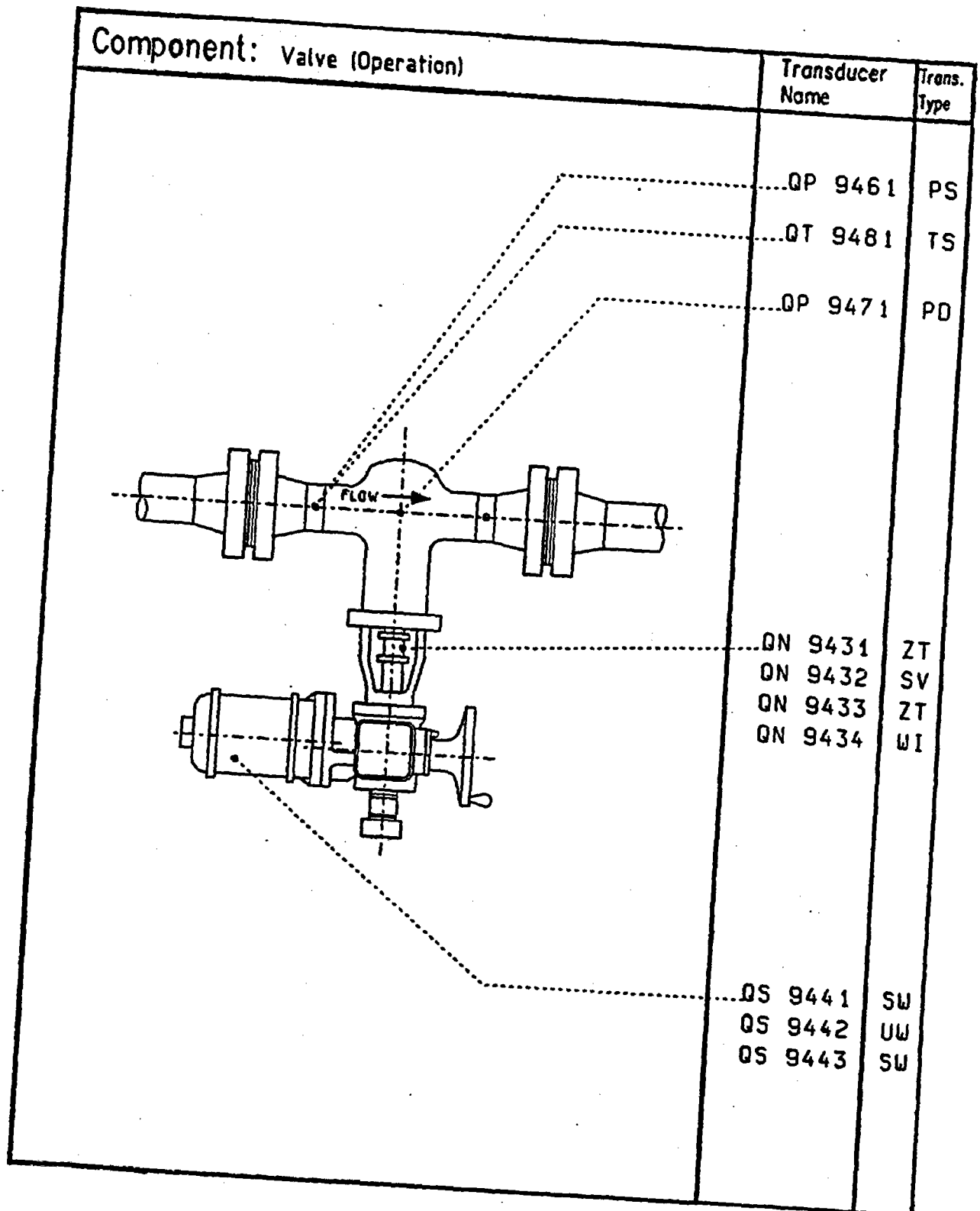


Fig. 3.1-19

Test series: SHAM
 Measurement locations plan for T41

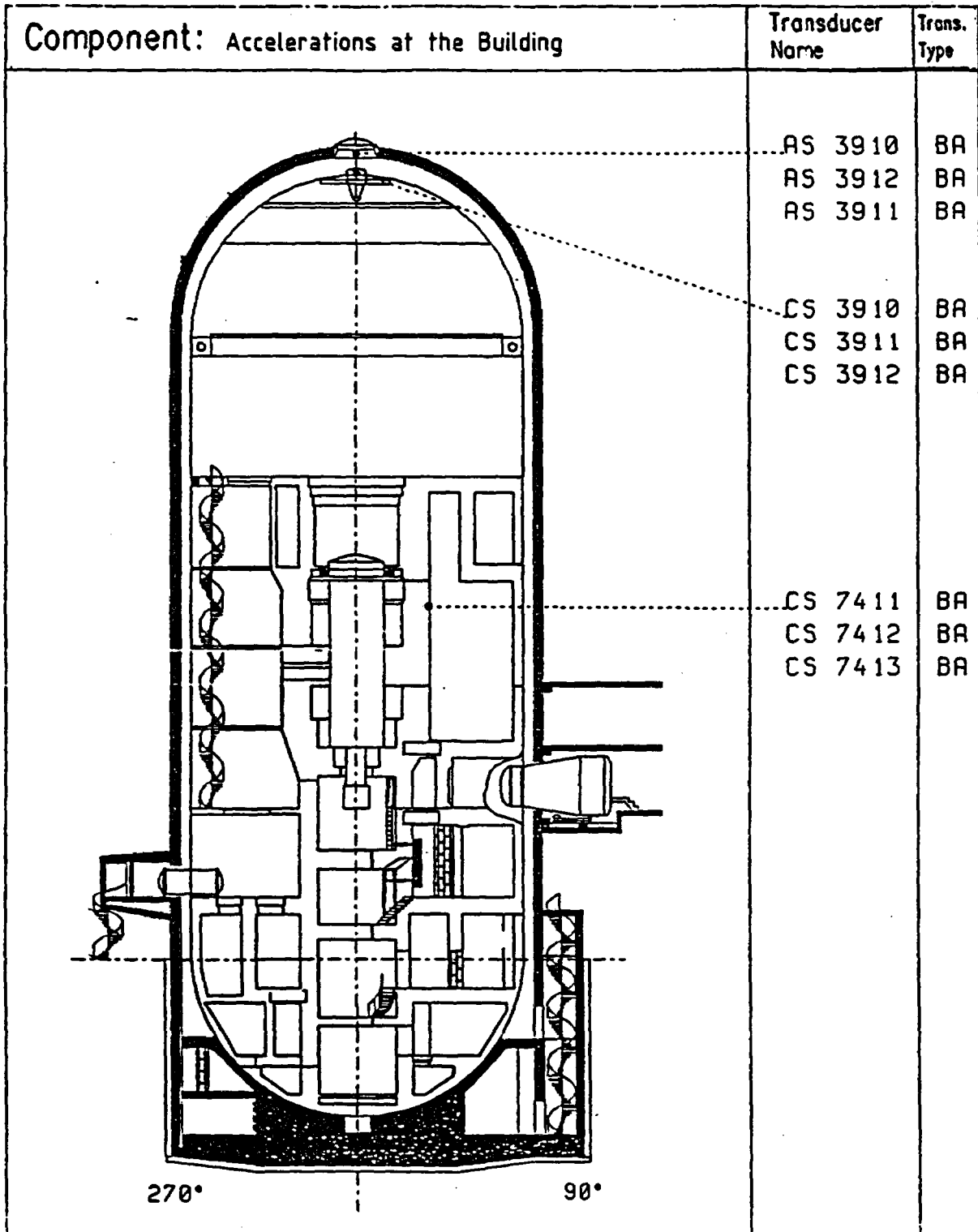


Fig. 3.1-20 Test series: SHAM
Measurement locations plan for T41

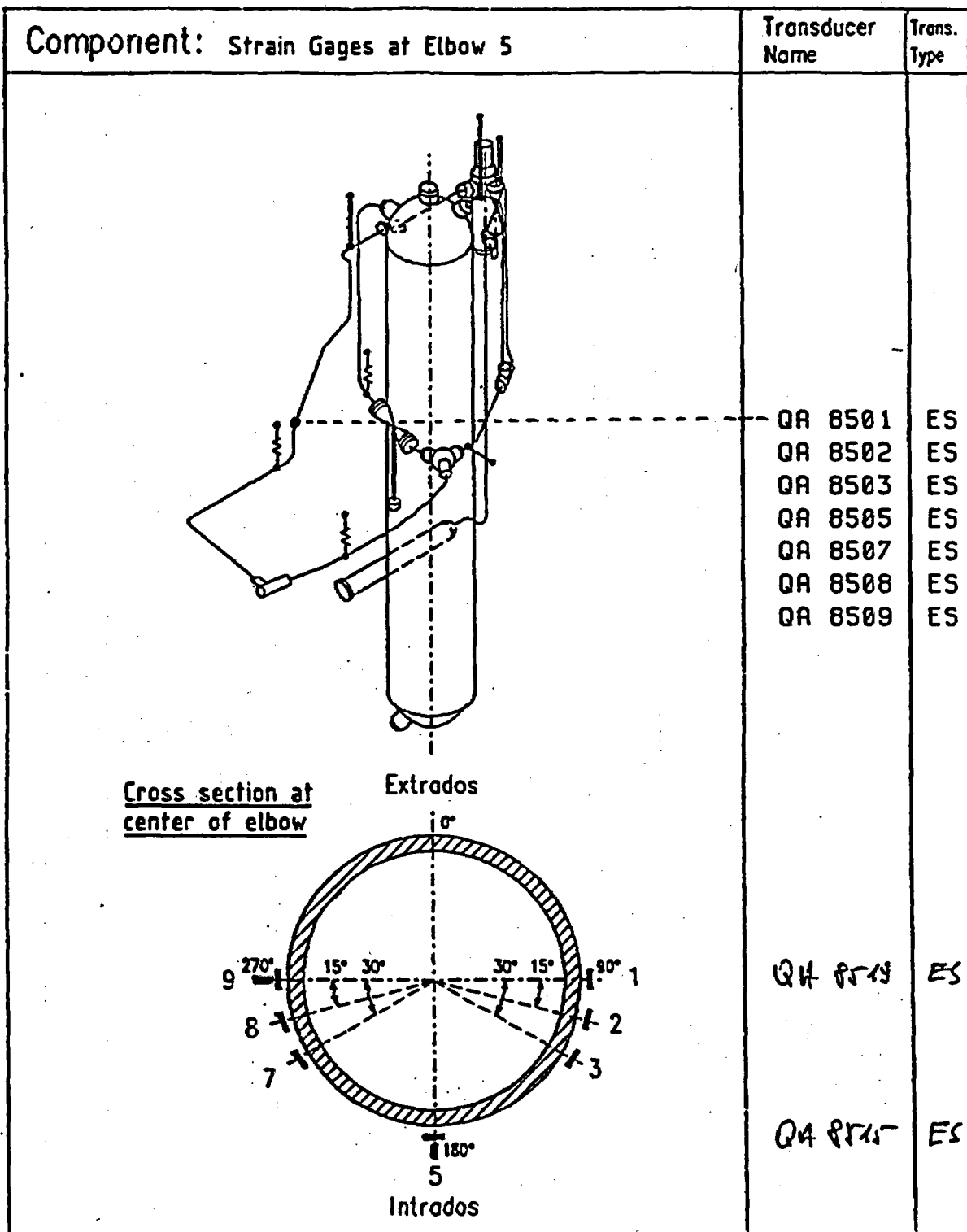


Fig. 3.1-21

Test series: SHAM
Measurement locations plan for T41

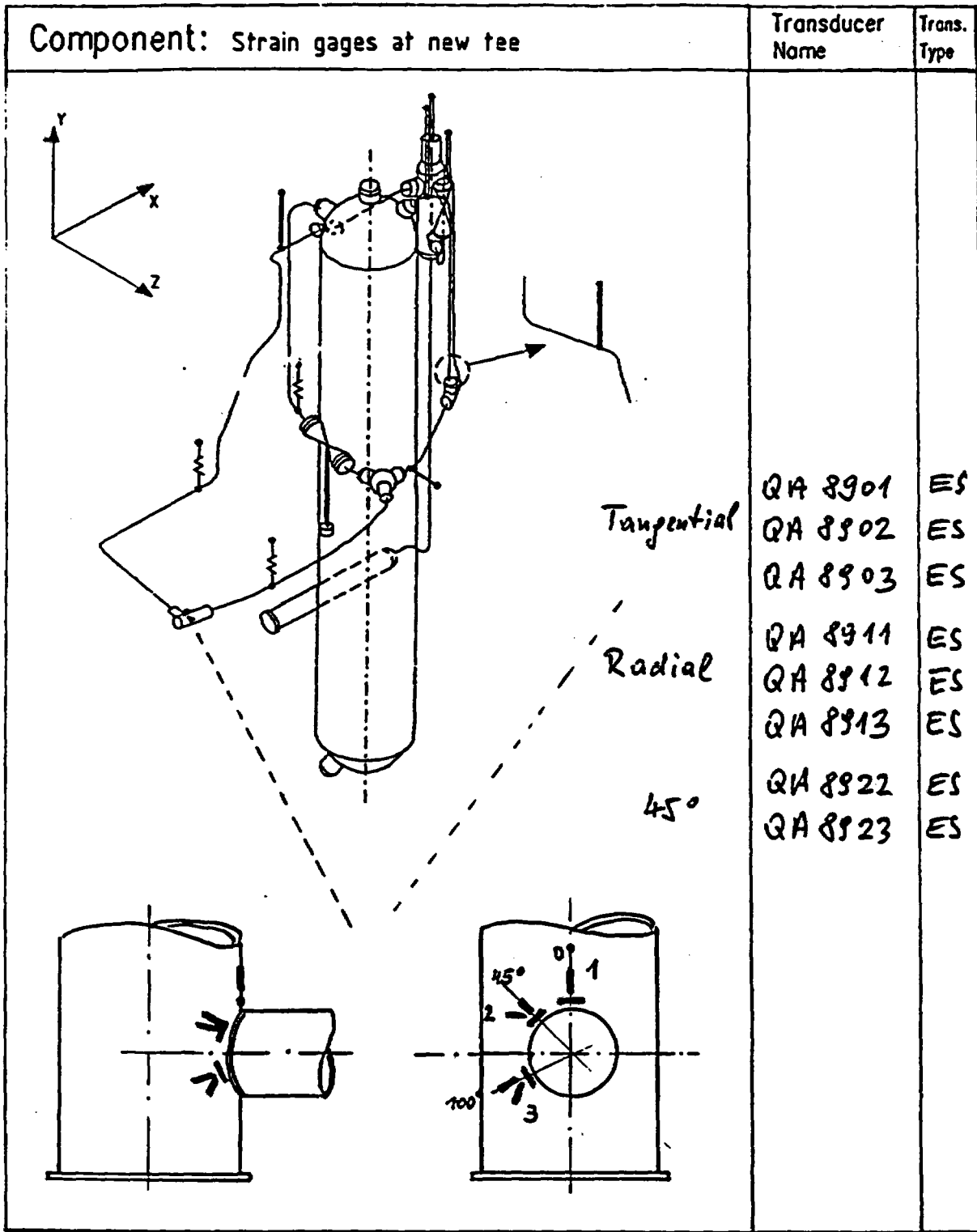


Fig. 3.1-22

Test series: SHAM
Measurement locations plan for T41

	BA	WA	FC	ES	Other
Excitation	10	2	2		1
Pipe accelerations at unconstrained locations	32				
Pipe accelerations at constrained locations	21				
Forces at spring hangers and permanent struts			6		
Forces at NRC hangers			10		
Forces at Bechtel hangers			3		
Forces at Cloud hangers			7		
Displacements at hanger locations		16			
Displacements of the pipes		9			
Control of the fixed points	12	2			
Strain gages for global stresses at DR200				30	
Strain gages for global stresses at VN-R23				34	
Strain gages at elbows				52	
Strain gages at new tee				8	
Unused strain gages available				9	
Valve	6			10	10
Building accelerations	9				
	90	29	28	143	11

Total: 301 Transducers

Date of last correction: 21 March 1988

Fig. 3.1-23 Summarizing survey of measurement locations

***** TRACK 1 *****													
***** EXCITATION ***** MP-S. 1 *****													
ES1011	KN		7.90		27.55		4.20		400		LBF	Genrad	
ES1021	KN		2.80		23.00		7.35		"		LBF	Genrad	
ES2011	MM		7.90		27.55		4.20		150		LBF	Genrad	
ES2021	MM		2.80		23.00		7.35		"		LBF	Genrad	
ES3011	M/S21		7.90		27.55		4.20		100		60g	LBF	Genrad
ES3021	M/S21		2.80		23.00		7.35		"		"	LBF	Genrad
ES4011	M/S21		4.80		27.55		4.20		10		15g	LBF	
ES4021	M/S21		-0.20		23.00		7.35		"		"	LBF	
QB1251	M/S21		7.90		27.55		4.20		200		30g	LBF	
QB1231	M/S21		2.80		23.00		7.35		"		"	LBF	
QB1252	M/S21		7.90		27.55		4.20		50		"	LBF	
QB1253	M/S21		"		"		"		"		"	LBF	
QB1232	M/S21		2.80		23.00		7.35		"		"	LBF	
QB1233	M/S21		"		"		"		"		"	LBF	
XT	1		-		-		-		-			LBF	

Fig. 3.1-24 Measurement locations on ZMA track 1

***** TRACK 2 *****

***** PIPE ACCELERATIONS AT UNCONSTRAINED LOCATIONS ***** MP-S. 2 *****

QB1221	M/S21	7.90	25.15	4.20	200	50g	
QB1223	M/S21	"	"	"	50	10g	
QB1111	M/S21	7.33	27.40	5.02	200	50g	
QB1112	M/S21	"	"	"	50	10g	
QB1113	M/S21	"	"	"	200	50g	
QB1101	M/S21	6.62	27.40	6.04	"	"	
QB1102	M/S21	"	"	"	50	10g	
QB1103	M/S21	"	"	"	200	50g	
QB1161	M/S21	5.86	23.00	6.76	"	"	
QB1162	M/S21	"	"	"	50	10g	
QB1163	M/S21	"	"	"	200	50g	
QB1091	M/S21	5.86	24.60	6.76	"	"	
QB1092	M/S21	"	"	"	50	10g	
QB1093	M/S21	"	"	"	200	50g	
QB1081	M/S21	3.57	24.60	4.84	"	"	
QB1082	M/S21	"	"	"	50	10g	
QB1083	M/S21	"	"	"	200	50g	
QB9401	M/S21	3.07	23.00	6.22	"	100g	NRC
QB9402	M/S21	"	"	"	100	"	NRC
QB9403	M/S21	"	"	"	"	"	NRC
QB1071	M/S21	0.44	23.00	8.46	200	50g	
QB1072	M/S21	"	"	"	100	"	
QB1073	M/S21	"	"	"	"	"	

***** PIPE ACCELERATIONS AT UNCONSTRAINED LOCATIONS ***** MP-S. 3 *****

QB1011	M/S21	-2.15	23.00	5.90	500	100g	
QB1012	M/S21	"	"	"	200	50g	
QB1013	M/S21	"	"	"	"	"	

Fig. 3.1-25

Measurement locations on ZMA track 2

TRACK 3

***** PIPE ACCELERATIONS AT UNCONSTRAINED LOCATIONS ***** MP-S. 3 *****

RS7610	M/S21	3.02	23.86	4.20	500	100g		Genrad
RS7611	M/S21	"	"	"	200	50g		Genrad
RS7612	M/S21	"	"	"	500	100g		Genrad
QB1121	M/S21	5.52	26.35	3.85	200	30g	LBF	
QB1122	M/S21	"	"	"	100	"	LBF	
QB1123	M/S21	"	"	"	200	"	LBF	

***** PIPE ACCELERATIONS AT CONSTRAINED LOCATIONS ***** MP-S. 4 *****

QB1181	M/S21	6.62	23.58	6.04	500	100g	NRC	H-2,3
QB1182	M/S21	"	"	"	"	"	NRC	
QB1183	M/S21	"	"	"	"	"	NRC	
QB1241	M/S21	3.46	23.00	7.96	200	"	NRC	H-4
QB1242	M/S21	"	"	"	100	"		
QB1243	M/S21	"	"	"	"	"		
QB1281	M/S21	2.54	23.00	8.40	200	"		H-6
QB1282	M/S21	"	"	"	500	"	NRC	
QB1283	M/S21	"	"	"	100	"		
QB1191	M/S21	-1.67	23.00	8.77	200	"	NRC	H-7,8
QB1192	M/S21	"	"	"	500	"	NRC	
QB1193	M/S21	"	"	"	"	"	NRC	
QB1201	M/S21	-0.46	23.00	5.90	"	"	NRC	H-9,22
QB1202	M/S21	"	"	"	"	"	NRC	
QB1203	M/S21	"	"	"	"	"	NRC	
QB1211	M/S21	0.58	23.57	5.90	"	"	NRC	H-10
QB1212	M/S21	"	"	"	"	"		
QB1213	M/S21	"	"	"	"	"		
QB1361	M/S21	4.10	26.46	3.85	200	"		H-11,12
QB1362	M/S21	"	"	"	"	"		
QB1363	M/S21	"	"	"	500	"		

Fig. 3.1-26

Measurement locations on ZMA track 3

TRACK 4

***** FORCES AT SPRING HANGERS AND PERMANENT STRUTS * MP-S. 5 ****

QA1513	KN		7.54		26.95		4.20		150		NRC	H-23.1
QA1517	KN		8.26		"		"		"		NRC	H-23.2
QA124J	KN		3.46		23.00		7.96		"		NRC	H-4
UA7649	KN		3.43		23.00		5.22		100			H-13
UA7659	KN		-1.24		23.00		8.88		30			H-14
UA7669	KN		0.32		23.00		5.90		10			H-15

***** FORCES AT NRC HANGERS ***** MP-S. 6 ****

QA3271	KN		6.62		23.91		6.04		100		NRC	H-3
QA3313	KN		0.16		23.00		5.90		50		NRC	H-9
QA3321	KN		0.58		23.57		5.90		"		NRC	H-10
QA3333	KN		4.06		26.46		3.85		"		NRC	H-11
QA3262	KN		6.72		23.24		5.89		100		NRC	H-2
QA3282	KN		2.54		23.00		8.40		"		NRC	H-6
QA3303	KN		-1.58		23.00		8.79		"		NRC	H-7
QA3292	KN		-1.77		23.00		8.74		50		NRC	H-8
QA3492	KN		-1.08		23.00		6.06		"		NRC	H-22
QA3342	KN		4.15		26.46		3.85		"		NRC	H-12

***** FORCES AT CLOUD HANGERS ***** MP-S. 7 ****

QA5262	KN		6.72		23.24		5.89		50		EPRI	H-2
QA5282	KN		2.54		23.00		8.40		"		EPRI	H-6
QA5303	KN		1.58		23.00		8.79		200		EPRI	H-7
QA5292	KN		-1.77		23.00		8.74		100		EPRI	H-8
QA5492	KN		-1.08		23.00		6.06		"		EPRI	H-22
QA8492	KN		-1.08		23.00		6.06		"			H-22
QA5342	KN		4.15		26.46		3.85		"		EPRI	H-12

***** FORCES AT BECHTEL HANGER ***** MP-S. 8 ****

QA4303	KN		-1.58		23.00		8.79		40			H-7
QA4292	KN		-1.77		23.00		8.74		"			H-8
QA4492	KN		-1.08		23.00		6.06		"			H-22

Fig. 3.1-27

Measurement locations on ZMA track 4

TRACK 5

***** DISPLACEMENTS AT HANGER LOCATIONS ***** MP-S. 9 ****

QN1262	MM		6.72		23.24		5.89		300		.53m		H-2
QN1271	MM		6.62		23.91		6.04		300		.60m		H-3
QN1282	MM		2.54		23.00		8.40		300		.66m		H-6
QN1303	MM		-1.58		23.00		8.79		300		.68m		H-7
QN1492	MM		-1.77		23.00		8.74		300		.67m		H-6
QN1492	MM		-1.08		23.00		6.06		300		.46m		H-22
QN1342	MM		4.15		26.46		3.85		300		.46m		H-12
QN3262	MM		6.72		23.24		5.89		3			NRC	H-2
QN3282	MM		2.54		23.00		8.40		3			NRC	H-6
QN3303	MM		-1.58		23.00		8.79		3			NRC	H-7
QN3292	MM		-1.77		23.00		8.74		3			NRC	H-6
QN3492	MM		-1.08		23.00		6.06		3			NRC	H-22
QN3342	MM		4.15		26.46		3.85		3			NRC	H-12
QN4303	MM		-1.58		23.00		8.79		130				H-7
QN4292	MM		-1.77		23.00		8.74		130				H-6
QN4492	MM		-1.08		23.00		6.06		50				H-22

***** DISPLACEMENTS ON THE PIPES ***** MP-S. 10 ****

QN1221	MM		7.90		26.85		4.20		300				
QN1222	MM		"		"		"		"				
QN1223	MM		"		"		"		"				
QN1351	MM		6.37		23.00		6.38		"				
QN1352	MM		"		"		"		"				
QN1353	MM		"		"		"		"				
QN1011	MM		-2.14		23.00		5.90		"				
QN1012	MM		"		"		"		"				
QN1013	MM		"		"		"		"				

Fig. 3.1-28

Measurement locations on ZMA track 5

TRACK 6

***** CONTROL OF THE FIXED POINTS

***** MP-S. 11 ****

RS6641	M/S21	7.90	22.70	4.20	11	10	10g
RS6642	M/S21	"	"	"	11	"	"
RS6643	M/S21	"	"	"	11	"	"
RS6631	M/S21	7.55	17.90	2.30	11	5	"
RS6632	M/S21	"	"	"	11	"	"
RS6633	M/S21	"	"	"	11	"	"
WS1704	M/S21	4.80	28.40	5.70	11	10	"
WS1705	M/S21	"	"	"	11	"	"
WS1706	M/S21	"	"	"	11	"	"
WSJ701	M/S21	4.80	15.00	5.70	11	5	"
WSJ702	M/S21	"	"	"	11	"	"
WSJ703	M/S21	"	"	"	11	"	"
WS2701	MM	5.80	24.50	5.20	11	5	"
WS2703	MM	"	"	"	11	"	"

***** BUILDING ACCELERATIONS

***** MP-S. 20 ****

ASJ910	M/S21	0.00	51.00	0.00	11	1	10g
ASJ912	M/S21	"	"	"	11	"	"
ASJ911	M/S21	"	"	"	11	"	"
CSJ910	M/S21	0.00	50.00	0.00	11	"	"
CSJ911	M/S21	"	"	"	11	"	"
CSJ912	M/S21	"	"	"	11	"	"
CS7411	M/S21?	0.58?	24.22?	5.90?	11	"	"
CS7412	M/S21	"	"	"	11	"	"
CS7413	M/S21	"	"	"	11	"	"

Fig. 3.1-29

Measurement locations on ZMA track 6

TRACK 7

***** STRAIN GAGES FOR GLOBAL STRESSES AT DR200

***** MP-S. 12 *****

QA1001	E-3	7.33	25.61	5.02	3	LBF
QA1002	E-3	"	"	"	"	LBF
QA1003	E-3	"	"	"	"	LBF
QA1004	E-3	"	"	"	"	LBF
QA1005	E-3	"	"	"	"	LBF
QA1006	E-3	"	"	"	"	LBF
QA1021	E-3	6.62	23.71	6.04	"	LBF
QA1022	E-3	"	"	"	"	LBF
QA1023	E-3	"	"	"	"	LBF
QA1024	E-3	"	"	"	"	LBF
QA1025	E-3	"	"	"	"	LBF
QA1026	E-3	"	"	"	"	LBF
QA1031	E-3	5.86	23.75	6.76	"	LBF
QA1032	E-3	"	"	"	"	LBF
QA1033	E-3	"	"	"	"	LBF
QA1034	E-3	"	"	"	"	LBF
QA1035	E-3	"	"	"	"	LBF
QA1036	E-3	"	"	"	"	LBF
QA1041	E-3	4.24	23.00	7.70	"	LBF
QA1042	E-3	"	"	"	"	LBF
QA1043	E-3	"	"	"	"	LBF
QA1044	E-3	"	"	"	"	LBF
QA1045	E-3	"	"	"	"	LBF
QA1046	E-3	"	"	"	"	LBF
QA1061	E-3	3.57	23.76	4.84	"	LBF
QA1062	E-3	"	"	"	"	LBF
QA1063	E-3	"	"	"	"	LBF
QA1064	E-3	"	"	"	"	LBF

Fig. 3.1-30

Measurement locations on ZMA track 7

TRACK 8

***** STRAIN GAGES FOR GLOBAL STRESSES AT DR200

***** MP-S. 12 *****

QA1065	E-J		3.57		23.76		4.84		3		LBF
QA1066	E-J		"		"		"		"		LBF

***** STRAIN GAGES FOR GLOBAL STRESSES AT VN-R23

***** MP-S. 13 *****

RA7671	E-J		-2.86		23.00		8.13		10		LBF
RA7672	E-J		"		"		"		"		LBF
RA7673	E-J		"		"		"		"		LBF
RA7676	E-J		"		"		"		"		LBF
RA7601	E-J		-2.82		23.00		7.96		3		LBF
RA7602	E-J		"		"		"		"		LBF
RA7603	E-J		"		"		"		"		LBF
RA7604	E-J		"		"		"		"		LBF
RA7605	E-J		"		"		"		"		LBF
RA7606	E-J		"		"		"		"		LBF
RA7631	E-J		-1.92		23.00		5.90		"		LBF
RA7632	E-J		"		"		"		"		LBF
RA7633	E-J		"		"		"		"		LBF
RA7634	E-J		"		"		"		"		LBF
RA7635	E-J		"		"		"		"		LBF
RA7636	E-J		"		"		"		"		LBF
RA7641	E-J		2.84		23.86		4.33		"		LBF
RA7642	E-J		"		"		"		"		LBF
RA7643	E-J		"		"		"		"		LBF
RA7644	E-J		"		"		"		"		LBF
RA7645	E-J		"		"		"		"		LBF
RA7646	E-J		"		"		"		"		LBF
RA7651	E-J		5.87		26.35		3.85		"		LBF
RA7652	E-J		"		"		"		"		LBF
RA7653	E-J		"		"		"		"		LBF
RA7654	E-J		"		"		"		"		LBF

Fig. 3.1-31

Measurement locations on ZMA track 8

***** TRACK 9 *****

***** STRAIN GAGES FOR GLOBAL STRESSES AT VN-R23 ***** MP-S. 13 *****

RA7655	E-3	5.87	26.35	3.85	3	LBF
RA7656	E-3	"	"	"	"	LBF
RA7661	E-3	6.96	26.35	3.85	"	LBF
RA7662	E-3	"	"	"	"	LBF
RA7663	E-3	"	"	"	"	LBF
RA7664	E-3	"	"	"	"	LBF
RA7665	E-3	"	"	"	"	LBF
RA7666	E-3	"	"	"	"	LBF

***** STRAIN GAGES AT ELBOW 1 ***** MP-S. 14 *****

QA8101	E-3	7.33	25.15	5.02	10	LBF
QA8102	E-3	"	"	"	"	LBF
QA8103	E-3	"	"	"	"	LBF
QA8104	E-3	"	"	"	"	LBF
QA8105	E-3	"	"	"	"	LBF
QA8106	E-3	"	"	"	"	LBF
QA8107	E-3	"	"	"	"	LBF
QA8108	E-3	"	"	"	"	LBF
QA8109	E-3	"	"	"	"	LBF
QA8111	E-3	"	"	"	"	LBF
QA8112	E-3	"	"	"	"	LBF
QA8113	E-3	"	"	"	"	LBF
QA8114	E-3	"	"	"	"	LBF
QA8115	E-3	"	"	"	"	LBF
QA8116	E-3	"	"	"	"	LBF
QA8117	E-3	"	"	"	"	LBF
QA8118	E-3	"	"	"	"	LBF
QA8119	E-3	"	"	"	"	LBF
QA8123	E-3	"	"	"	"	LBF
QA8124	E-3	"	"	"	"	LBF

Fig. 3.1-32 Measurement locations on ZMA track 9

***** TRACK 10 *****

***** STRAIN GAGES AT ELBOW 1 ***** MP-S. 14 *****

QA8126	E-3		7.33		25.15		5.02		10		LBF
QA8127	E-3		"		"		"		"		LBF

***** STRAIN GAGES AT ELBOW 2 ***** MP-S. 15 *****

QA8201	E-3		-2.27		23.00		5.90		10		LBF
QA8202	E-3		"		"		"		"		LBF
QA8203	E-3		"		"		"		"		LBF
QA8205	E-3		"		"		"		"		LBF
QA8207	E-3		"		"		"		"		LBF
QA8208	E-3		"		"		"		"		LBF
QA8209	E-3		"		"		"		"		LBF
QA8215	E-3		"		"		"		"		LBF
QA8219	E-3		"		"		"		"		LBF

***** STRAIN GAGES AT ELBOW 3 ***** MP-S. 16 *****

QA8301	E-3		7.29		26.35		3.85		10		LBF
QA8302	E-3		"		"		"		"		LBF
QA8303	E-3		"		"		"		"		LBF
QA8305	E-3		"		"		"		"		LBF
QA8307	E-3		"		"		"		"		LBF
QA8308	E-3		"		"		"		"		LBF
QA8309	E-3		"		"		"		"		LBF
QA8315	E-3		"		"		"		"		LBF
QA8319	E-3		"		"		"		"		LBF

***** STRAIN GAGES AT ELBOW 4 ***** MP-S. 17 *****

QA8401	E-3		2.75		23.00		7.10		10		LBF
QA8411	E-3		"		"		"		"		LBF
QA8421	E-3		"		"		"		"		LBF

Fig. 3.1-33 Measurement locations on ZMA track 10

TRACK 11

***** VALVE ***** MP-S. 18 ****

QB9411	M/S21	3.04	?????????	6.30		100		100g	NRC
QB9412	M/S21	"		"		"		"	NRC
QB9413	M/S21	"		"		"		"	NRC
QB9421	M/S21	3.04	?????????	6.30		"		"	NRC
QB9422	M/S21	"		"		"		"	NRC
QB9423	M/S21	"		"		"		"	NRC
QA9371	E-J	?????????	?????????	?????????		1			
QA9372	E-J	"		"		"		"	
QA9373	E-J	"		"		"		"	
QA9374	E-J	"		"		"		"	
QA9375	E-J	"		"		"		"	
QA9376	E-J	"		"		"		"	
QA9451	E-J	"		"		"		"	
QA9452	E-J	"		"		"		"	
QA9453	E-J	"		"		"		"	
QA9454	E-J	"		"		"		"	

***** VALVE ***** MP-S. 19 ****

QP9461	BAR	?????????	?????????	?????????		300			NRC
QP9471	BAR	"		"		"		?????	NRC
QT9481	GRAD	"		"		"		100	NRC
QN9431	V	"		"		"		?????????	NRC
QN9432	MM	"		"		"		"	NRC
QN9433	V	"		"		"		"	NRC
QN9434	V	"		"		"		"	NRC
QS9441	A	"		"		"		50	NRC
QS9442	V	"		"		"		400	NRC
QS9443	A	"		"		"		50	NRC

Fig. 3.1-34 Measurement locations on ZMA track 11

TRACK 12

***** STRAIN GAGES AT ELBOW 5 ***** MP-S. 21 ****

QA8501	E-3		0.58		23.86		5.90		10		LBF
QA8502	E-3		"		"		"		"		LBF
QA8503	E-3		"		"		"		"		LBF
QA8505	E-3		"		"		"		"		LBF
QA8507	E-3		"		"		"		"		LBF
QA8508	E-3		"		"		"		"		LBF
QA8509	E-3		"		"		"		"		LBF
QA8515	E-3		"		"		"		"		LBF
QA8519	E-3		"		"		"		"		LBF

***** STRAIN GAGES AT NEW TEE ***** MP-S. 22 ****

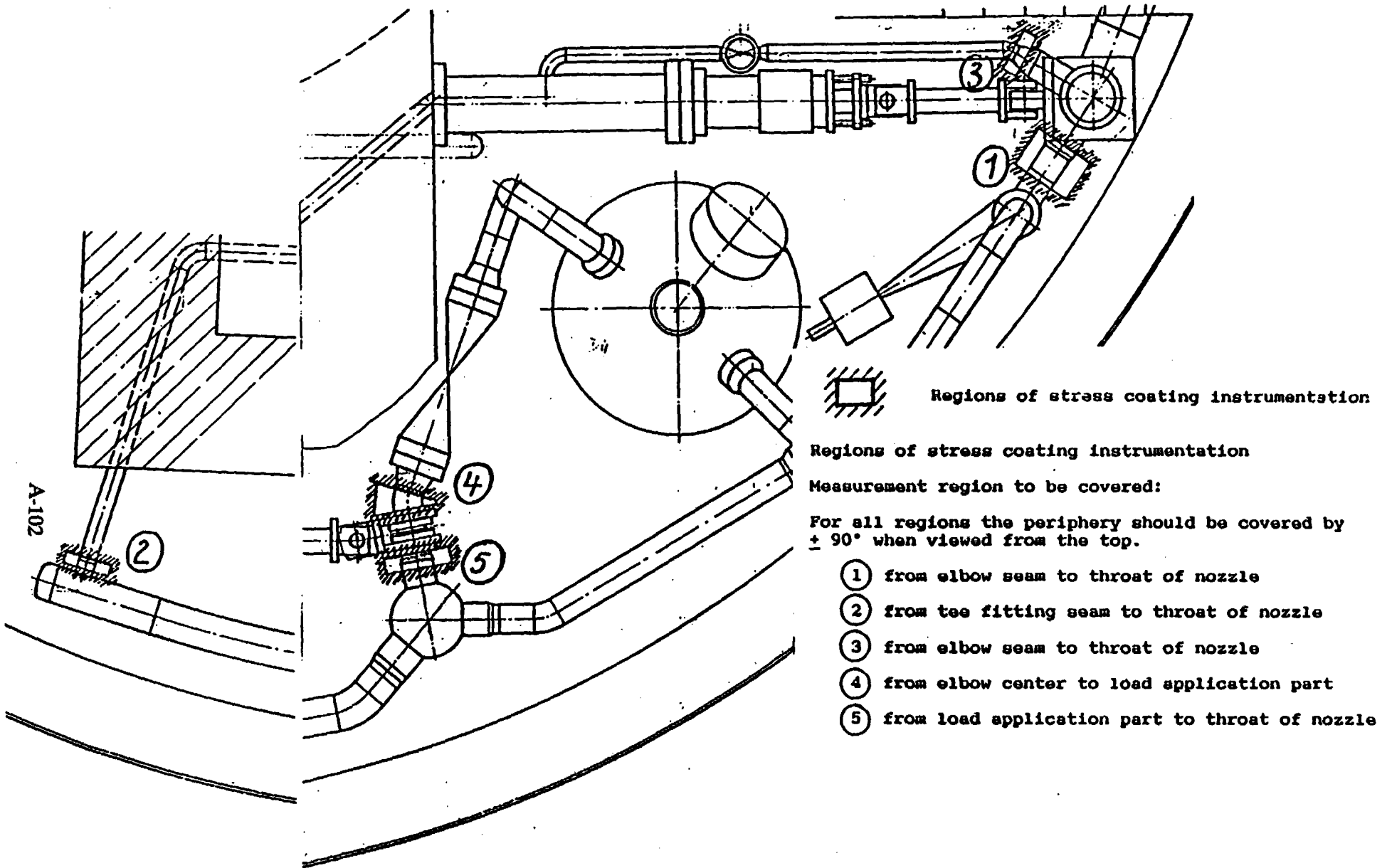
QA8901	E-3		-2.94		23.00		8.28		10		LBF
QA8902	E-3		"		"		"		"		LBF
QA8903	E-3		"		"		"		"		LBF
QA8911	E-3		"		"		"		"		LBF
QA8912	E-3		"		"		"		"		LBF
QA8913	E-3		"		"		"		"		LBF
QA8922	E-3		"		"		"		"		LBF
QA8923	E-3		"		"		"		"		LBF

***** AVAILABLE STRAIN GAGES FOR CRITICAL LOCATIONS *****

QA8081	E-3		offen		offen		offen		10	
QA8082	E-3		offen		offen		offen		10	
QA8083	E-3		offen		offen		offen		10	
QA8084	E-3		offen		offen		offen		10	
QA8085	E-3		offen		offen		offen		10	
QA8086	E-3		offen		offen		offen		10	
QA8087	E-3		offen		offen		offen		10	
QA8088	E-3		offen		offen		offen		10	
QA8089	E-3		offen		offen		offen		10	

Fig. 3.1-35

Measurement locations on ZMA track 12



A-102

Fig. 3.2-1

Stress coating instrumentation

TEST SEQUENCE AND NUMBER	TEST TYPE	CONFIGU- RATION	EXCITATION		
			TYPE	MAGNITUDE % SSE	LOCATION
T41.30.1	Identification	NRC	Random	50	DF16
T41.30.2 OPTIONAL	"	"	"	50	H5
T41.31.1	Earthquake linear	"	HDR-SSE	100	Both
T41.31.2	"	"	"	200	"
T41.40.1	Identification	EPRI/EA	Random	50	DF16
T41.40.2	"	"	"	50	H5
T41.41.1	Earthquake linear	"	HDR-SSE	100	Both
T41.41.2	"	"	"	200	"
T41.41.4	"	"	"	400	"
T41.50.1	Identification	EPRI/SS	Random	50	DF16
T41.50.2	"	"	"	50	H5
T41.51.1	Earthquake linear	"	HDR-SSE	100	Both
T41.51.2	"	"	"	200	"
T41.51.4	"	"	"	400	"
T41.20.1	Identification	KWU	Random	50	DF16
T41.20.2	"	"	"	50	H5
T41.21.1	Earthquake linear	"	HDR-SSE	100	Both
T41.21.2	"	"	"	200	"
T41.21.4 OPTIONAL	"	"	"	400	"
T41.60.1	Identification	CEGB	Random	50	DF16
T41.60.2	"	"	"	50	H5
T41.62.1	Earthquake linear	"	Sizewell-SSE	100	Both
T41.62.2	"	"	"	200	"
T41.62.3	"	"	"	300	"
T41.63.0	"	"	Allsites-SSE	50	"
T41.63.1 OPTIONAL	"	"	"	100	"
T41.72.1 OPTIONAL	Earthquake linear	CEGB-MOD	Sizewell-SSE	100	Both
T41.10.1	Identification	HDR	Random	50	DF16
T41.10.2	"	"	"	50	H5
T41.11.1	Earthquake linear	"	HDR-SSE	100	Both
T41.11.2	"	"	"	200	"
T41.11.4 OPTIONAL	"	"	"	400	"
T41.31.6	Earthquake plastification	NRC	HDR-SSE	600	Both
T41.31.8	"	"	"	800	"
T41.63.2 OPTIONAL	Earthquake plastification	CEGB	Sizewell or Sine	Highest possible	Both
T41.11.6 OPTIONAL	Earthquake plastification	HDR	HDR-SSE	600	Both
T41.11.8 OPTIONAL	"	"	"	800	"

Fig. 4.1-1 Test Matrix and Designations

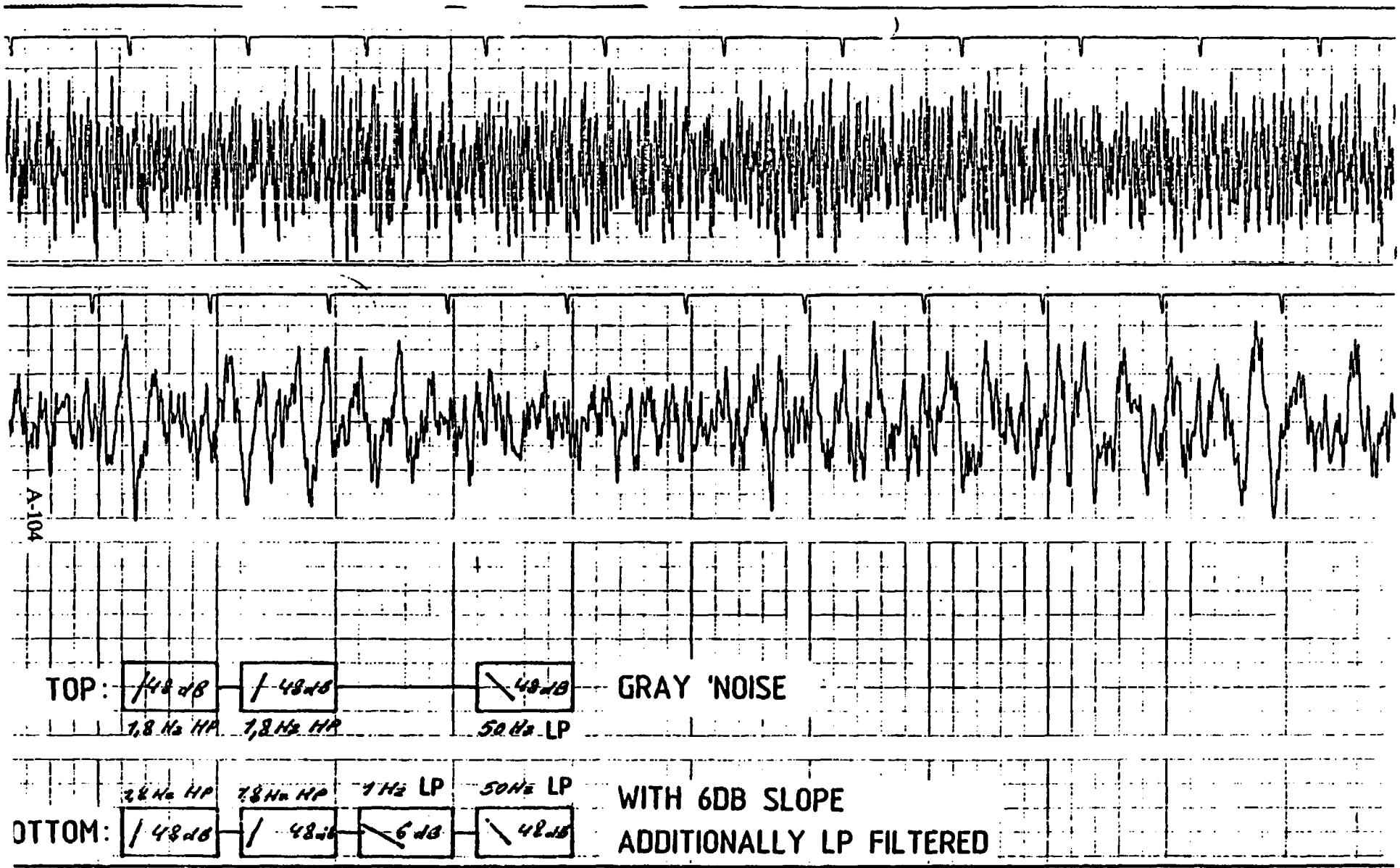


Fig. 4.2-1 Time functions of the random excitation

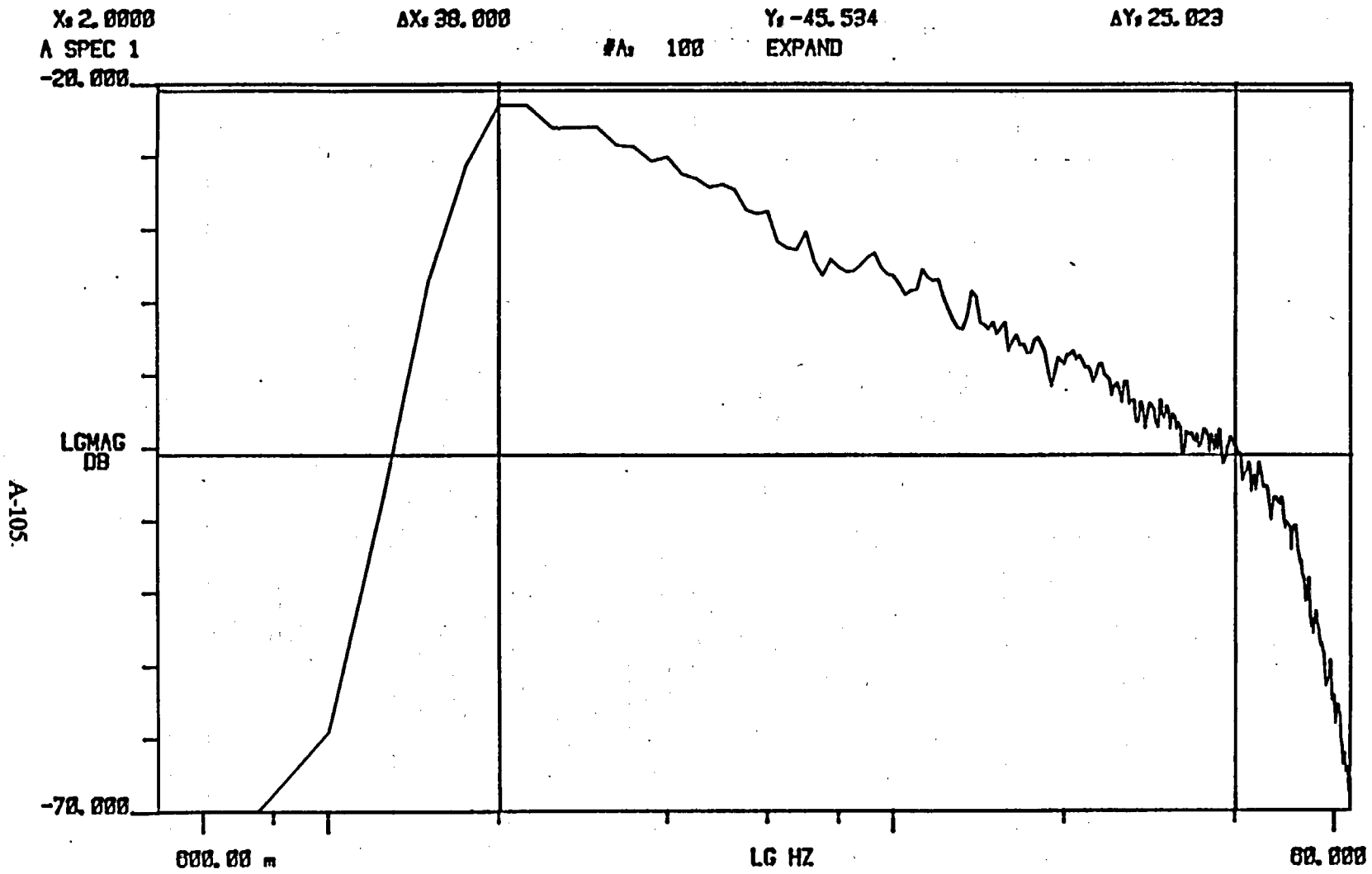
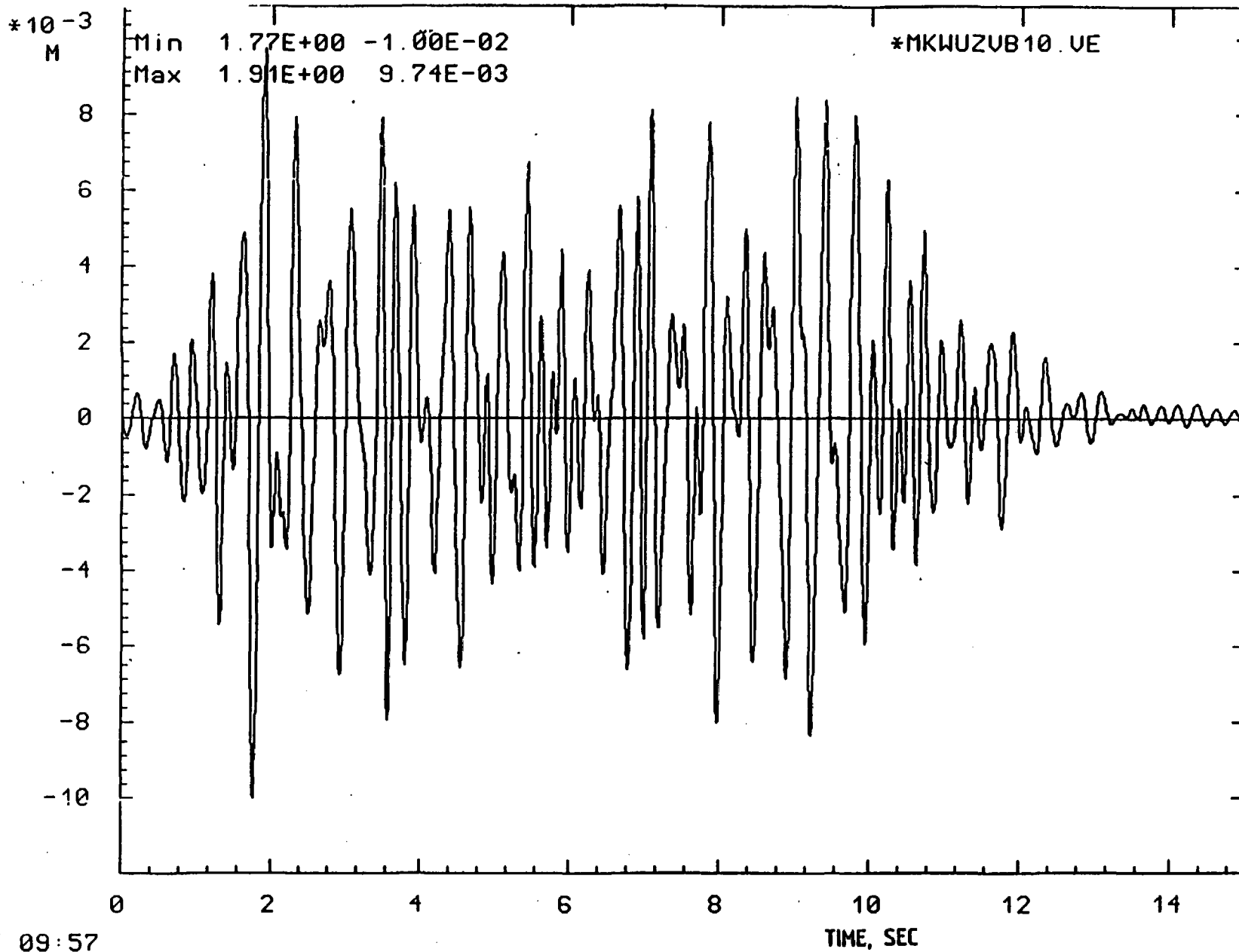


Fig. 4.2-2 Gray noise, additionally filtered with 1 Hz LP

A:106



LBF 09:57

Fig. 4.2-3

Earthquake displacement history for HDR/KWU/NRC/EPRI-configurations

- 89 -

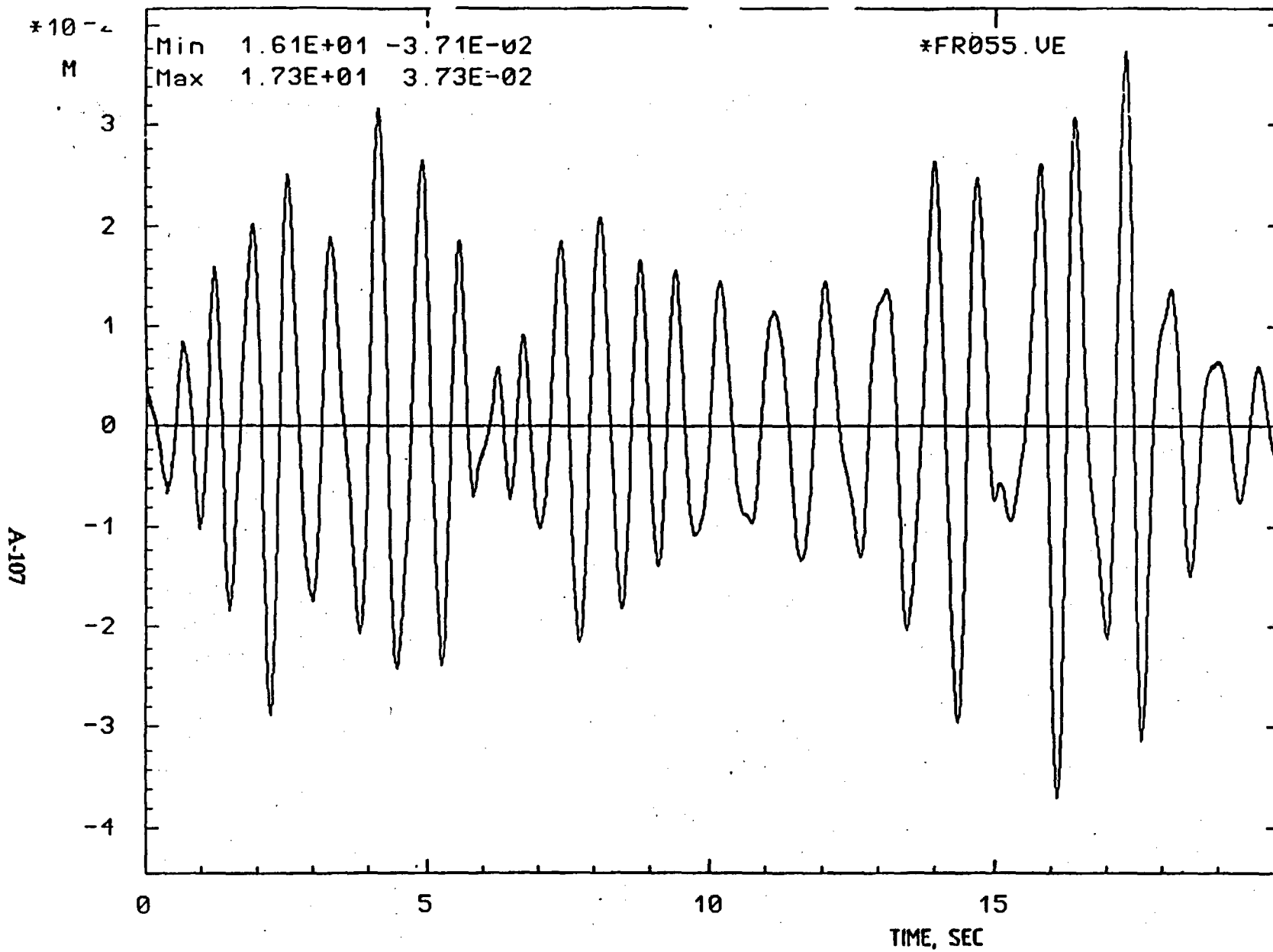
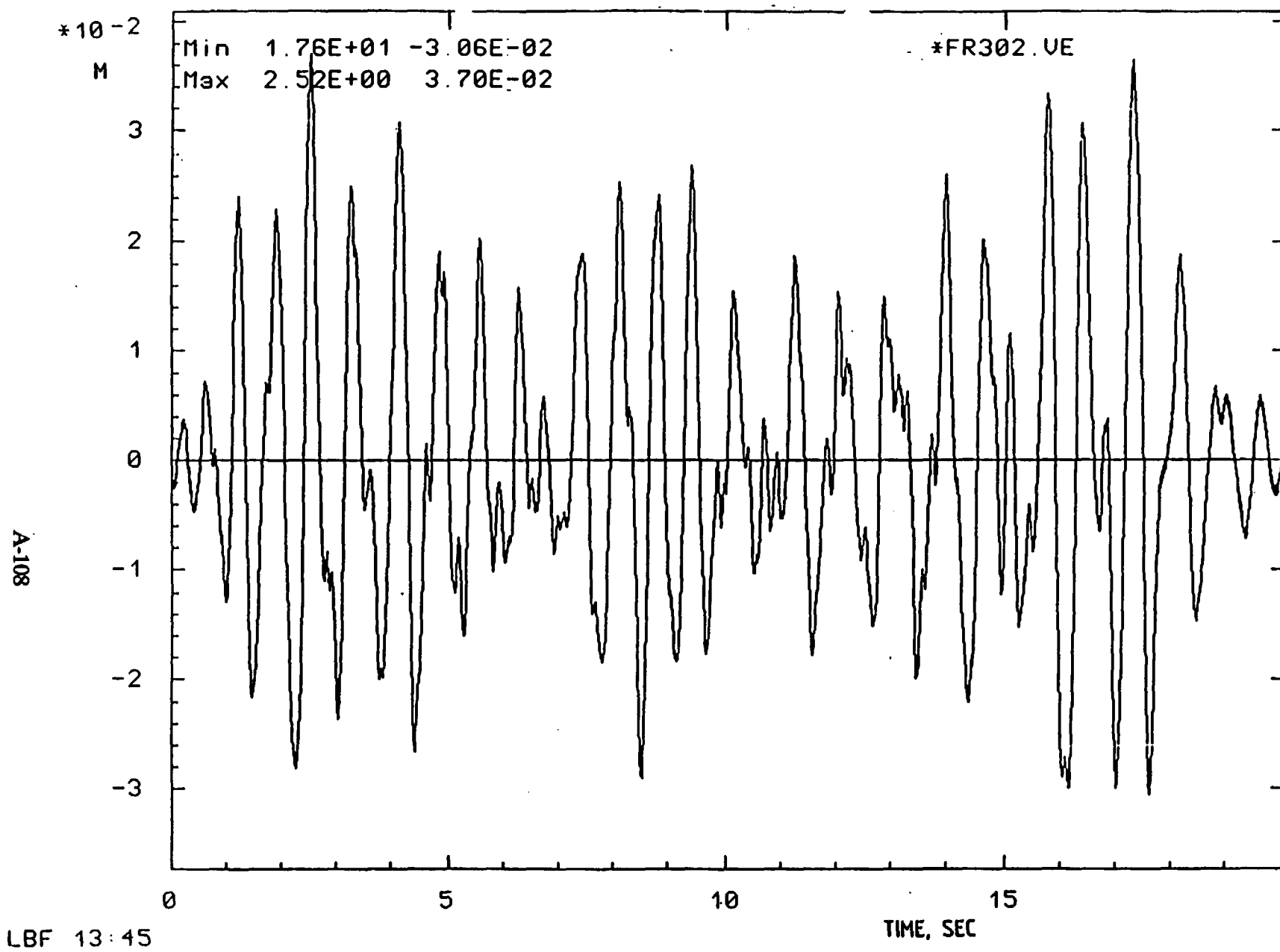


Fig. 4.2-4 Earthquake displacement history for CEGB configuration (Sizewell B)

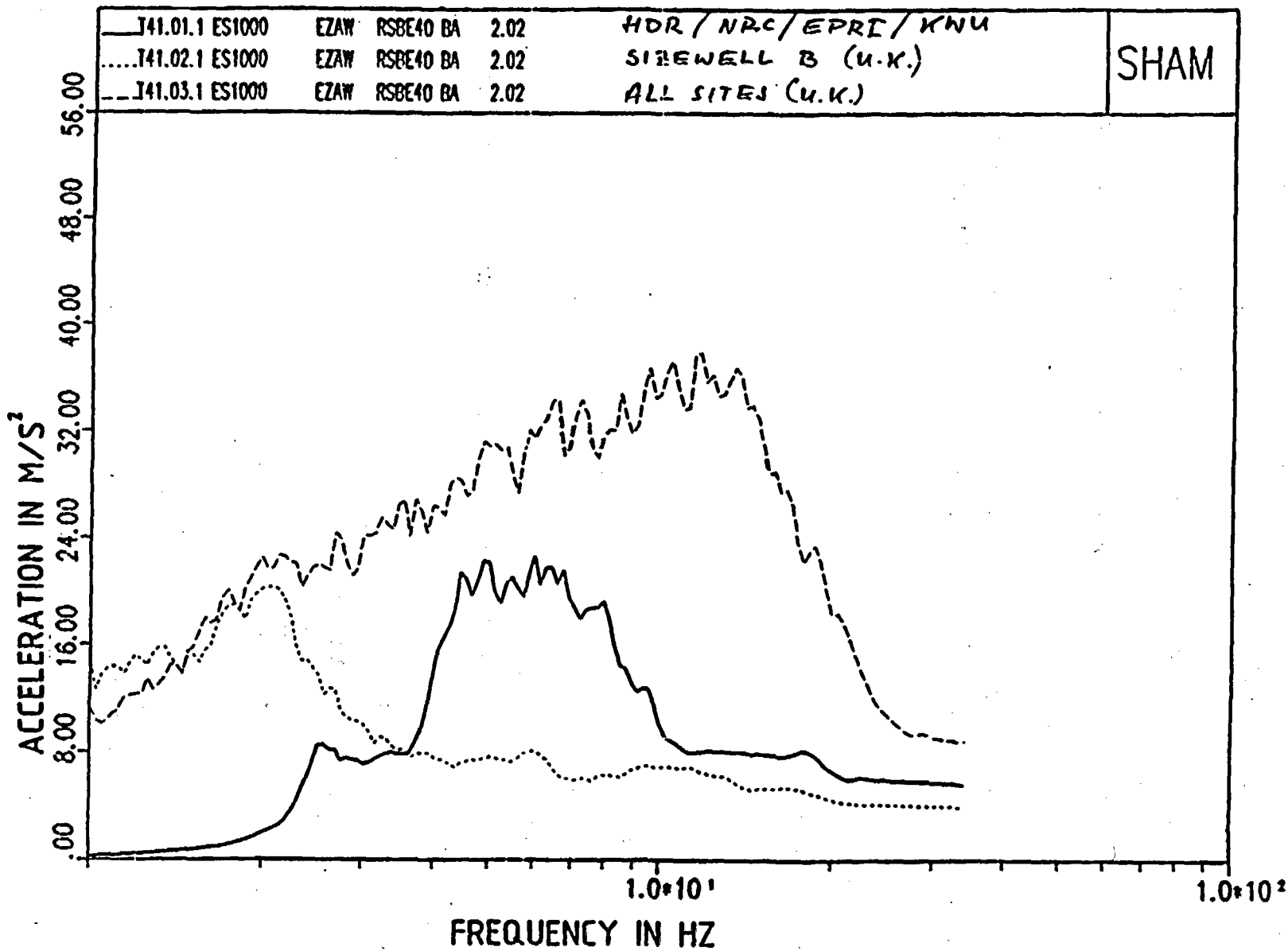


LBF 13:45

Fig. 4.2-5

Earthquake displacement history for CEGB configuration (All sites)

A-109



- A71 -

Fig. 4.2-6

100% SSE Spectra of the earthquake excitations (4% damping)

Recording procedures to be followed by ZMA

For all tests the zero time mark is fixed by the actuation of the trigger (Measurement position XT0001)

Time periods to be established for the ZMA operation:

The various periods are differentiated according to the two different test types

- a) Randöm: for identification (duration of excitation = 120 s)
- b) Earthquake history (Excitation duration = 15 s or 20 s)

Recording periods

- a) -5 s to 200 s
- b) -5 s to 50 s

Data processing periods

- a) -5 s to 150 s
- b) -3 s to 30 s

Time windows for table of extreme values

(during data acquisition a "-1" must be entered instead of the frequency value)

- a) Time window I : -1 s to 0 s
- Time window II : 0 s to 120 s
- Time window III : 148 s to 149 s
- b) Time window I : -1 s to 0 s
- Time window II : 0 s to 20 s
- Time window III : 28 s to 29 s

Plotting periods

- a) -12 s to 120 s with 100 Hz
- 2 s to 20 s with 100 Hz

Fig. 4.2-7 Procedures for ZMA

Procedures for the transient recorder

Tests to be recorded

T41.51.1

T41.51.2

T41.51.4

Measurement locations and filter cutoff frequencies to be used for recording

1 kHz-Filter : XT0001
500 Hz-Filter : QA5262 QA5282 QA5303 QA5292 QA5492 QA5342
QA3262 QA3282 QA3303 QA3292 QA3492 QA3342
QA8492
50 Hz-Filter : ES1011 ES1021

Triggering

The ZMA trigger (XT001) will be used.

Recording periods and scanning rate

The data will be recorded from 1 sec before until approx. 30 s after the trigger. The scanning rate is uniformly 2 kHz.

Time windows for table of extreme values and plotting periods

Identical with the ZMA recording for test type b).

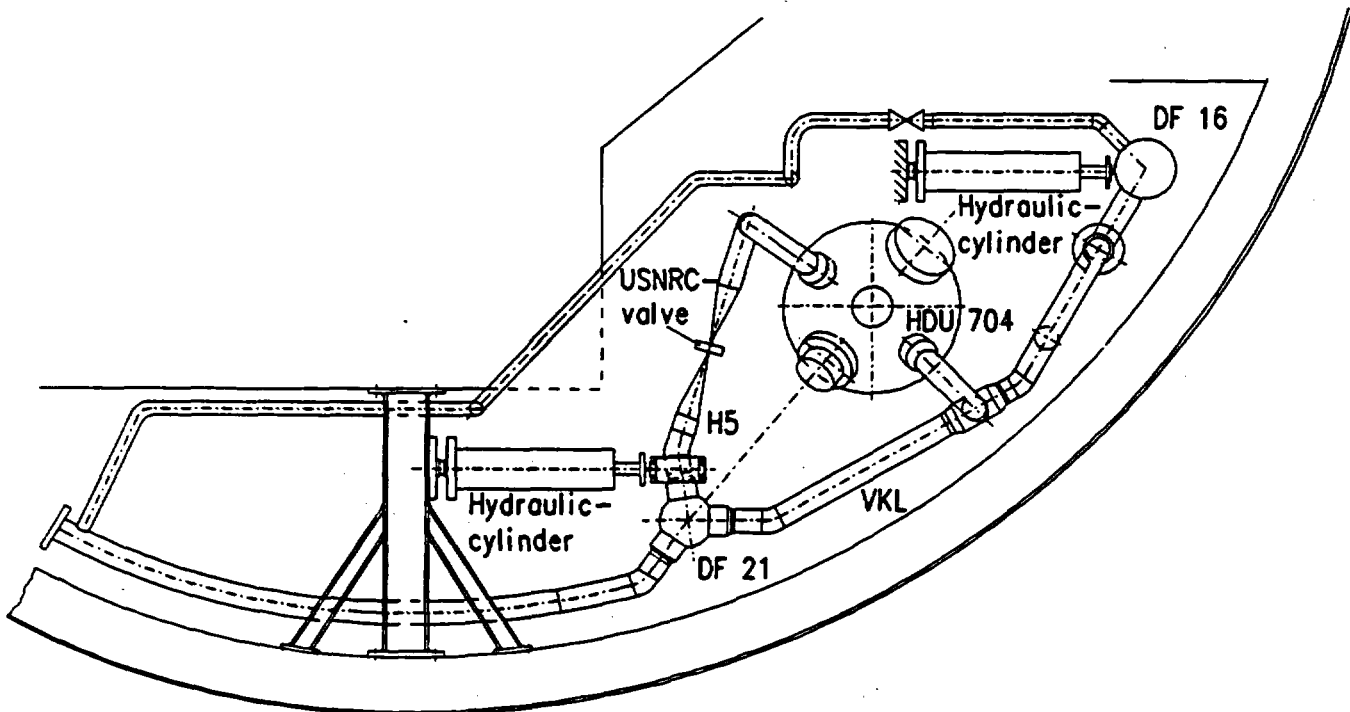
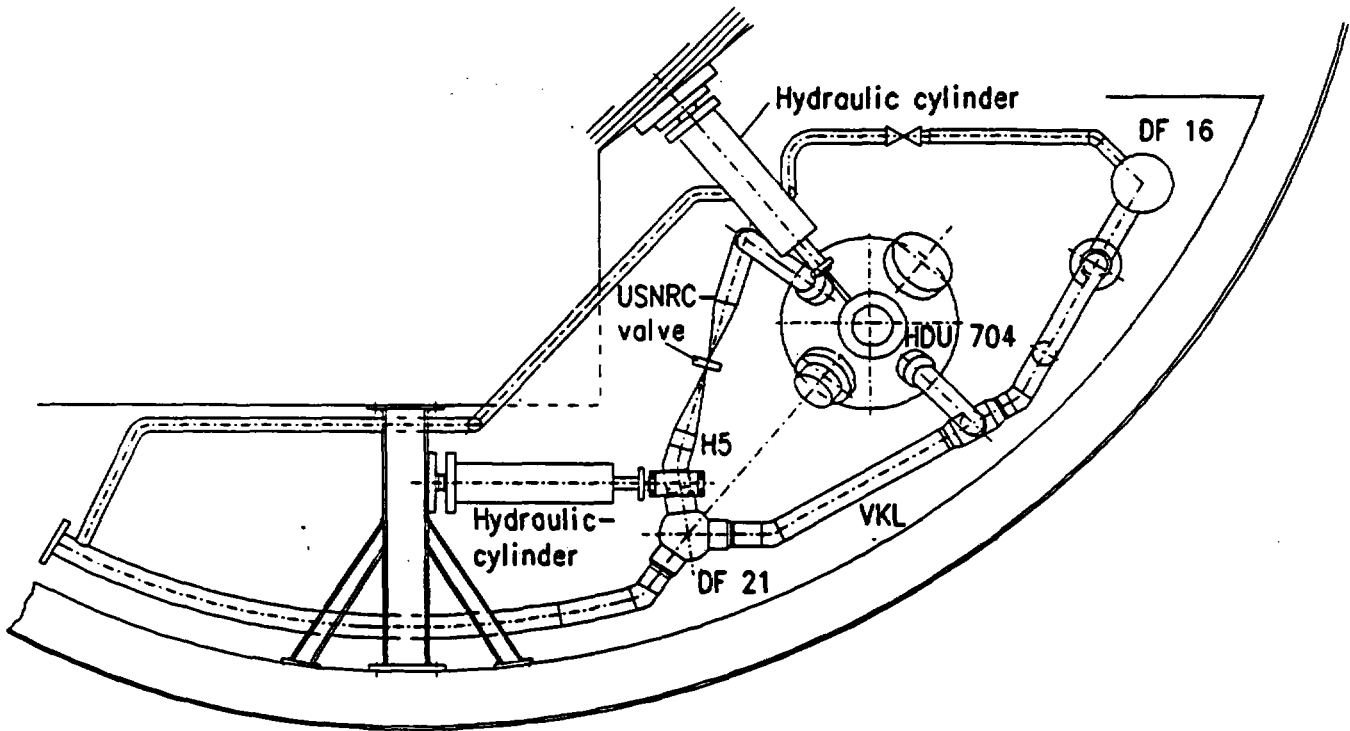


Fig. 5.1-1 Test loop (VKL) with superheated steam heat exchanger (HDU)
Test set-up (plan view)

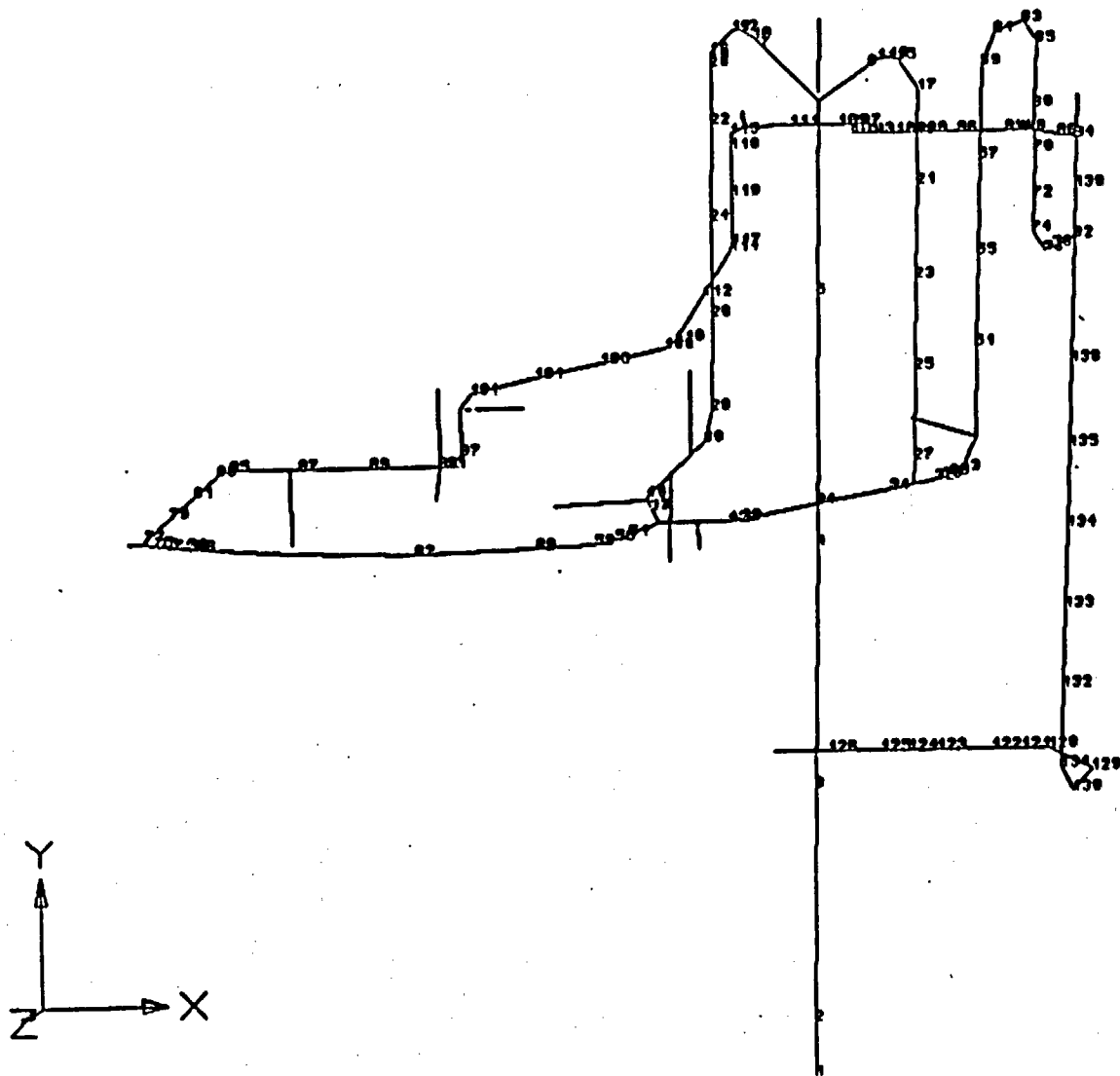


Fig. 5.1-2 Model of the test loop (VKL) with superheated steam heat exchanger (HDU)

Model designation	Load Application		HDU Parameter			VKL modifications
	Location	Direction	Bearing	Water level	Central constraint	
A	HDU 704	Z	stiff	empty	free	Hanger H5 replaced by spring *) Spring with HDU 704 *) as A and B as A as B, H 7 rotated (45° in X-Z plane) as A, HDU separated RI- reinforcement with load application H 5 as G as G Tee fitting with VKL 601 as J, DF 16 unconstrained, DR 105 up to primary steam header connected
B	H 5	X	stiff	empty	free	
C	H 10	X	stiff	empty	free	
D	HDU 704	Z	soft	empty	free	
E	H 5	X	stiff	empty	free	
F	HDU 704	Z	-	-	-	
G	HDU 704	Z	soft	empty	free	
H	H 5	X	stiff	empty	free	
I	H 5	X	soft	empty	free	
J	H 5	X	soft	empty	free	
K	HDU 704	Z	stiff	full	free	
L	DF 16	X	stiff	empty	fixed	
M	H 5	X	stiff	empty	fixed	

*) for simulation of an inactive cylinder

Fig. 5.1-3

Model variations for design calculations

A-115

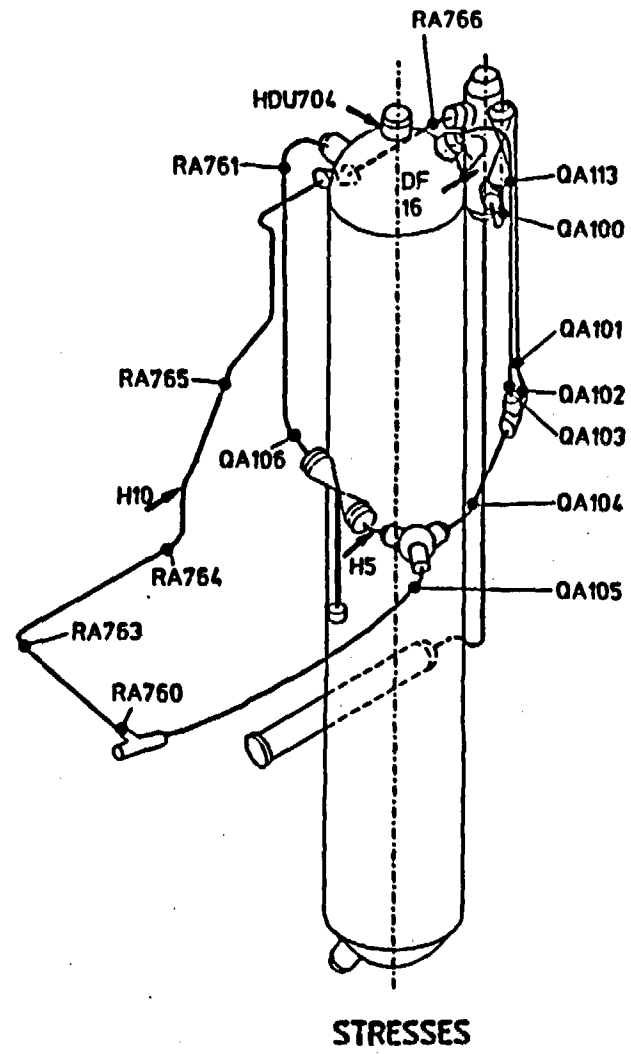
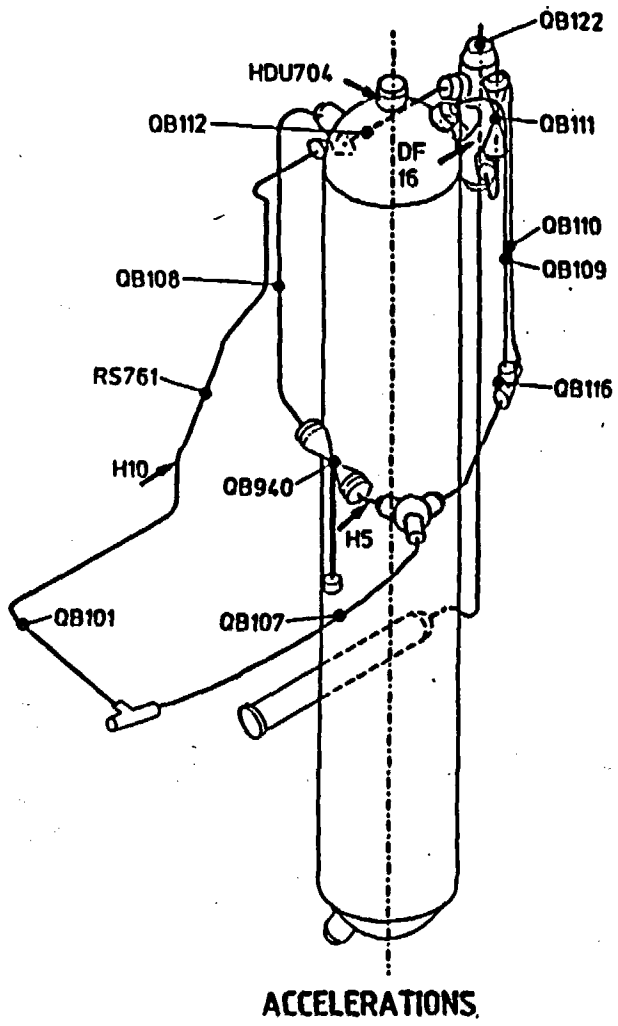
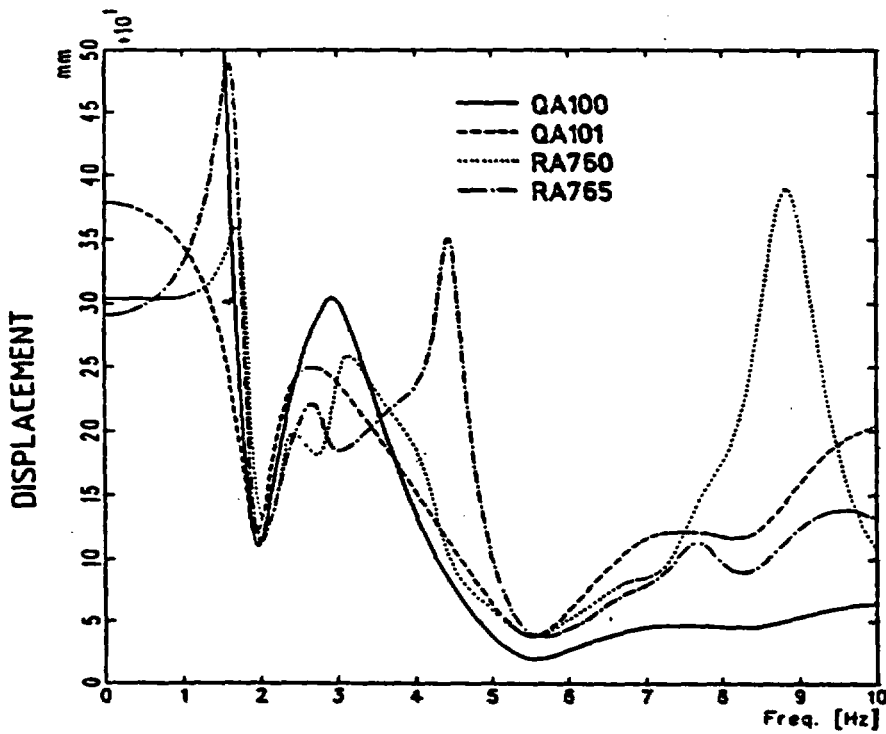
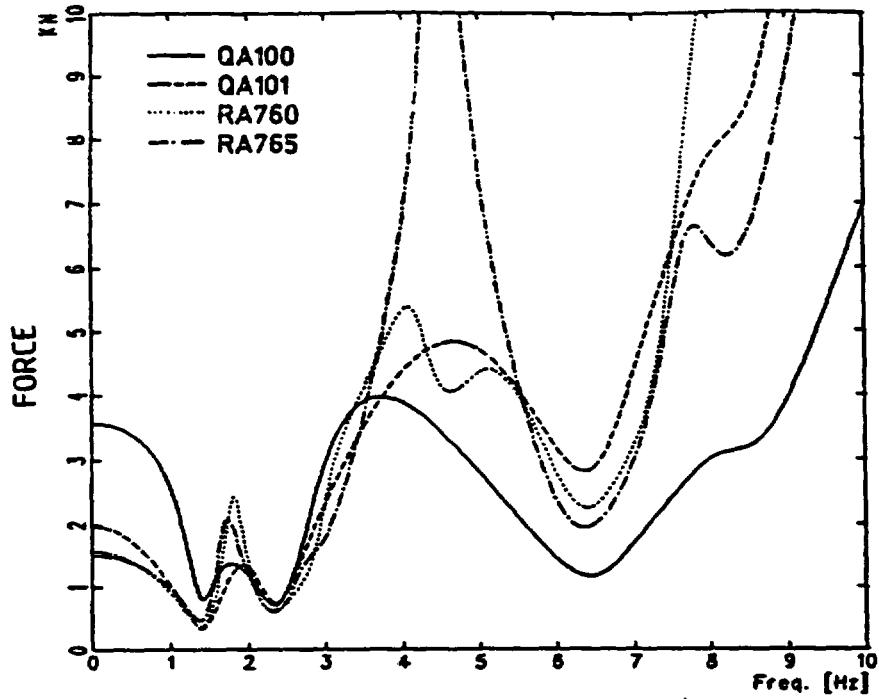


Fig. 5.1-4

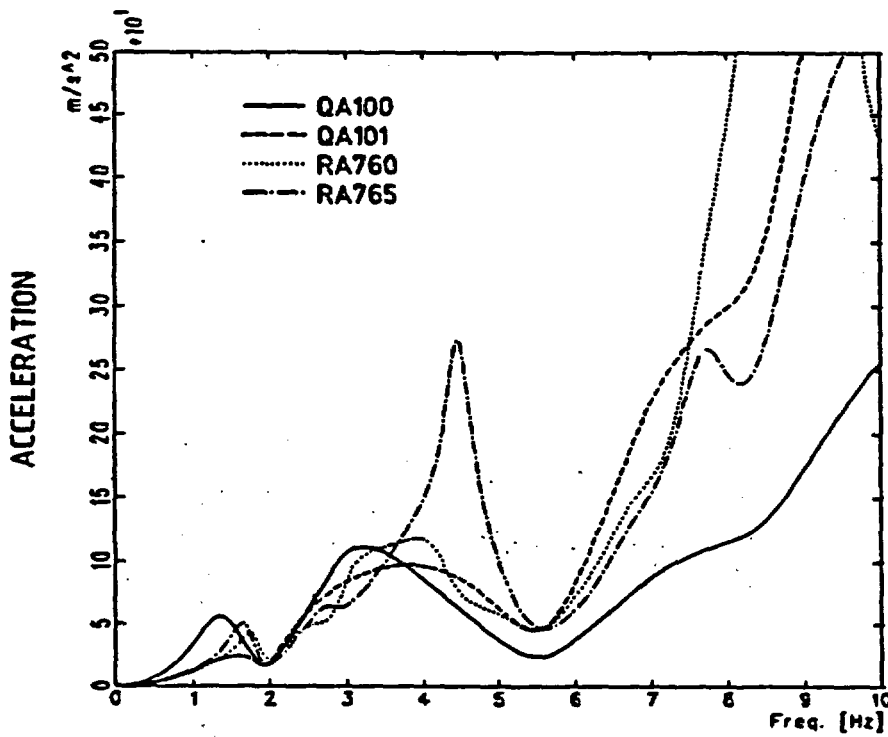
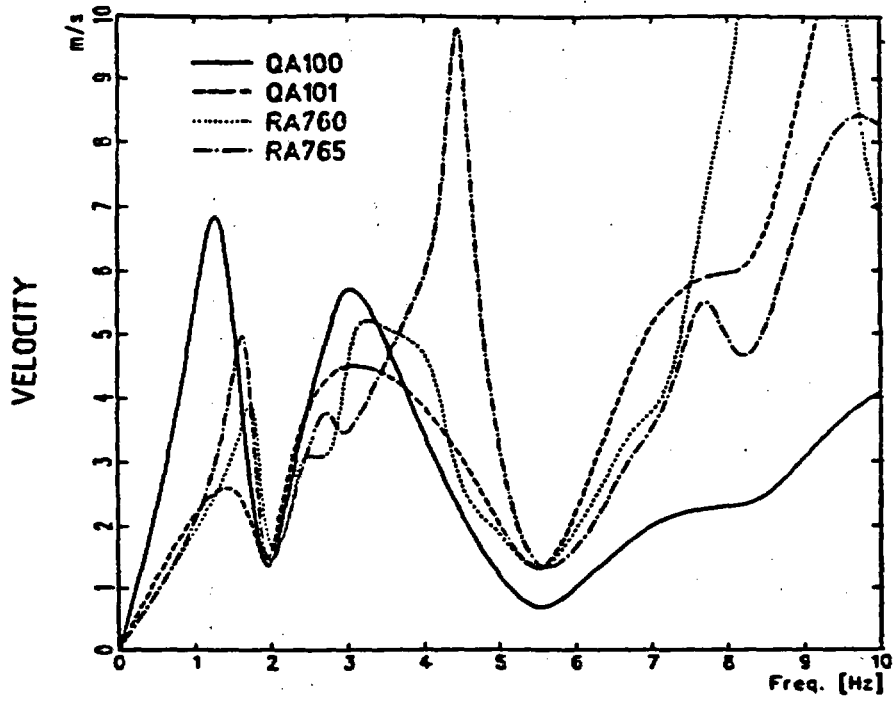
Test loop with the excitation points and reference points considered for accelerations and stresses



LOAD CASE I
MODEL L
EXCITATION POINT: DF16
HANGER CONFIGURATION: HDR

Fig. 5.1-5

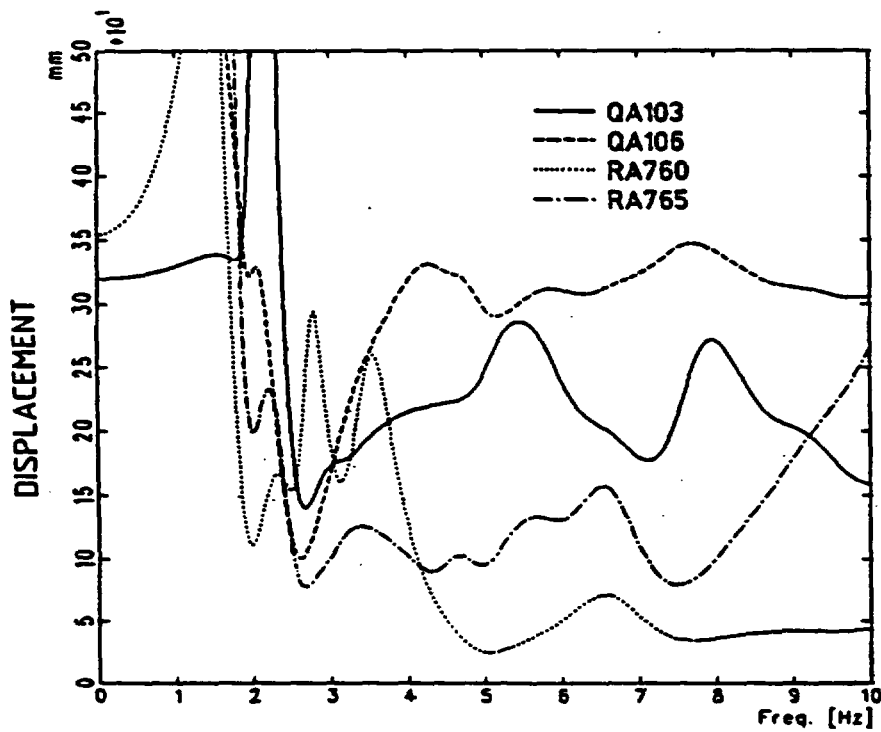
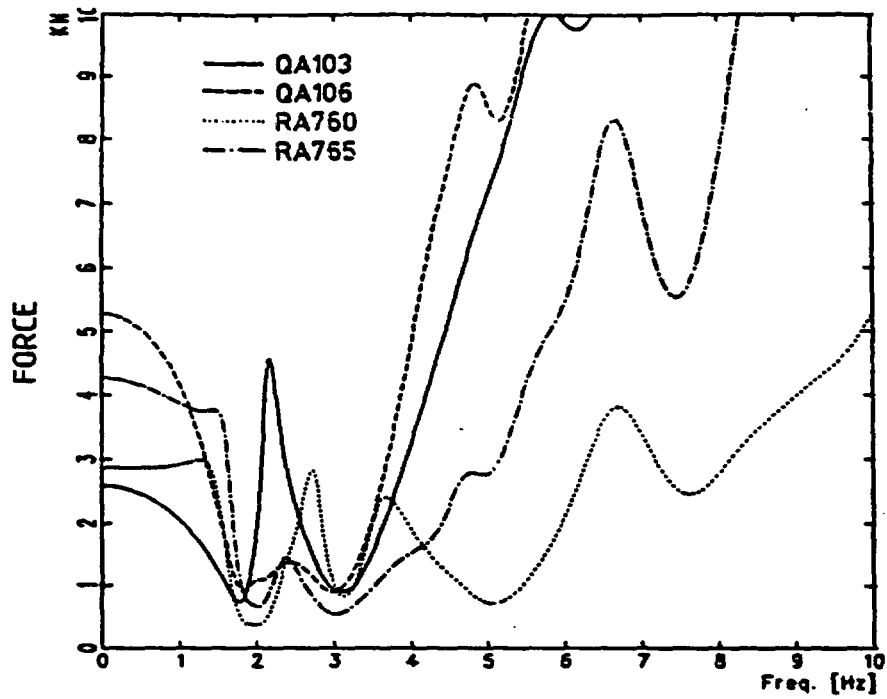
Forces and displacements required at the excitation point to attain a stress of 500 N/mm² at the VKL



LOAD CASE I
MODEL L
EXCITATION POINT: DF16
HANGER CONFIGURATION: HDR

Fig. 5.1-6

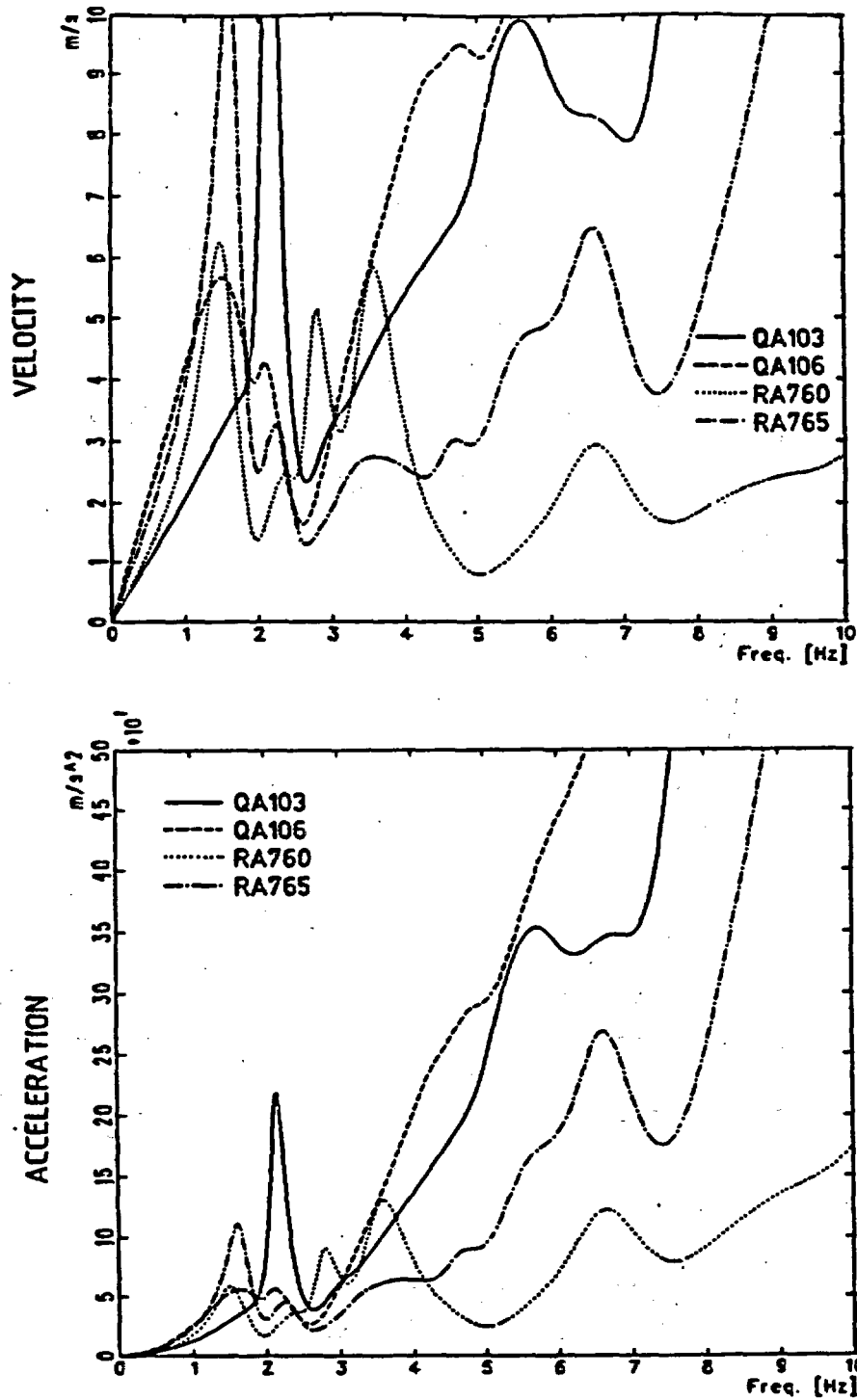
Velocity and acceleration required at the excitation point to attain a stress of 500 N/mm² at the VKL



LOAD CASE I
MODEL M
EXCITATION POINT: H5
HANGER CONFIGURATION: HDR

Fig. 5.1-7

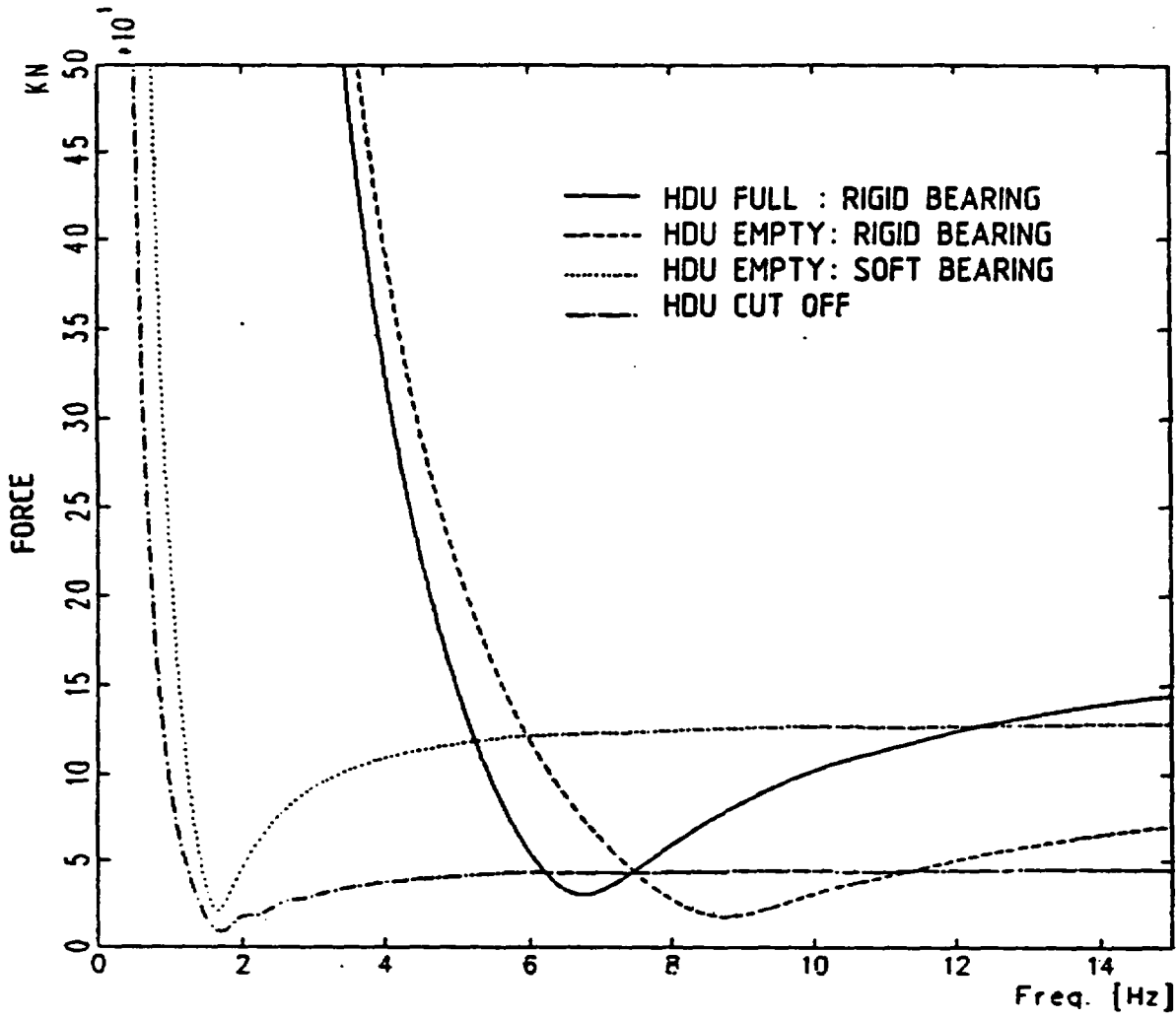
Forces and Displacements required at the excitation point to attain a stress of 500 N/mm² at the VKL



LOAD CASE I
MODEL M
EXCITATION POINT: HS
HANGER CONFIGURATION: HDR

Fig. 5.1-8

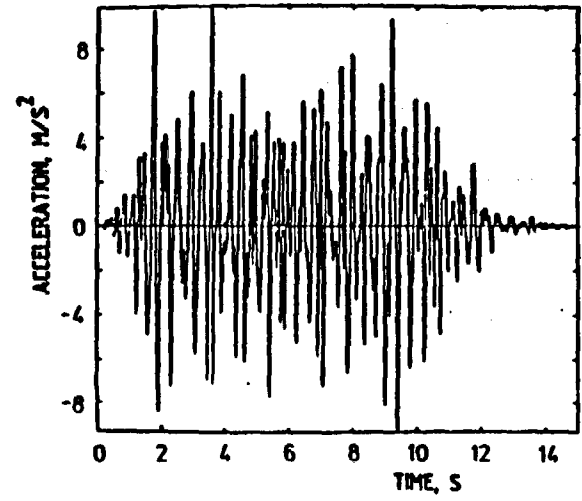
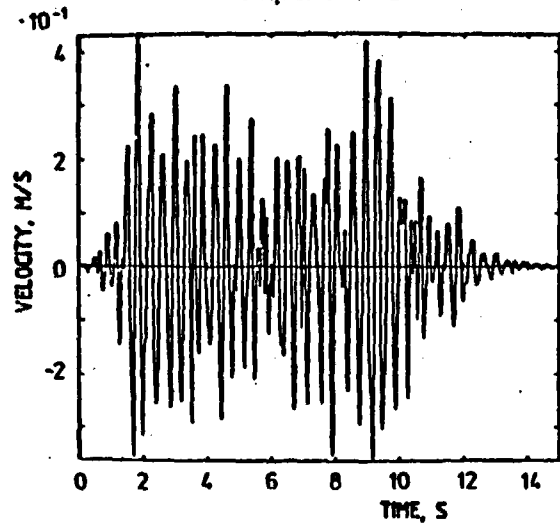
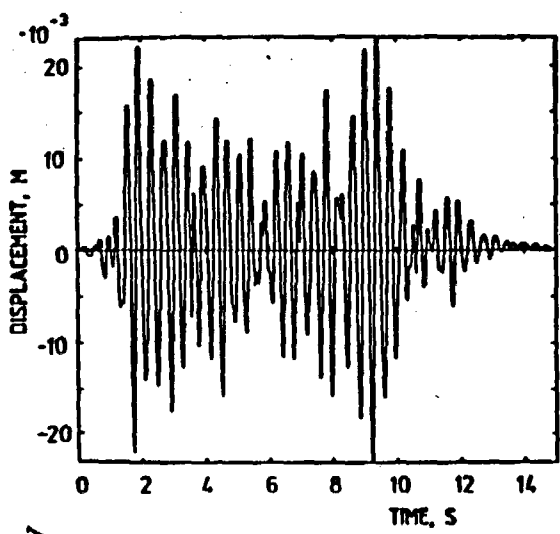
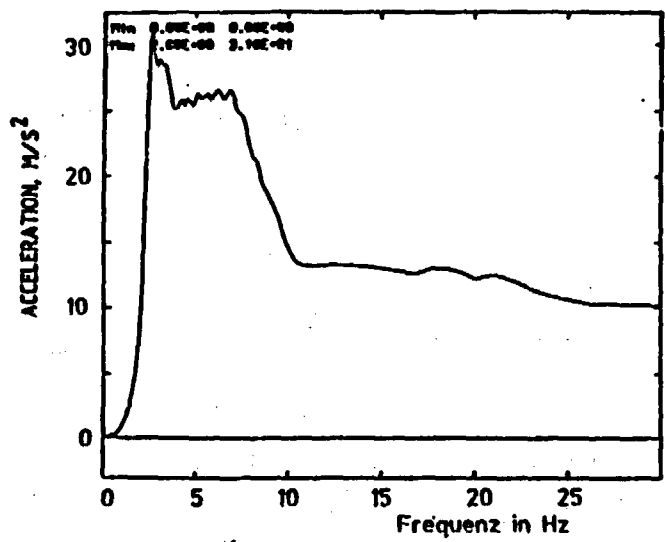
Velocity and acceleration required at the excitation point to attain a stress of 500 N/mm² at the VKL



LOAD CASE II
EXCITATION POINT: HDU 704
HANGER CONFIGURATION: HDR

Fig. 5.1-9

Force required at the excitation point to attain an input acceleration of 10 m/s²



A-121

Fig. 5.1-10 Load case III: Original earthquake history and response spectrum ($D = 7\%$)

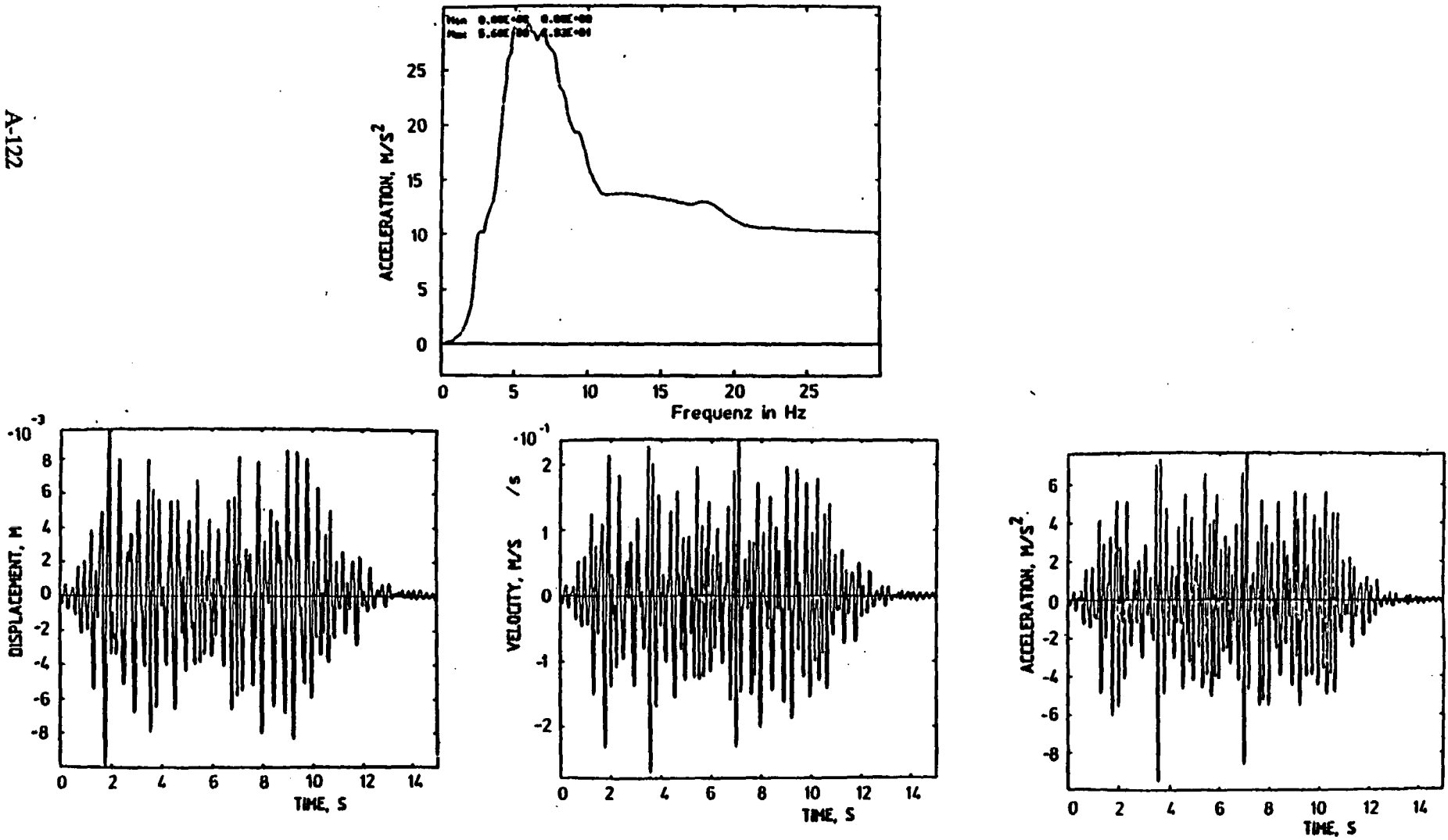
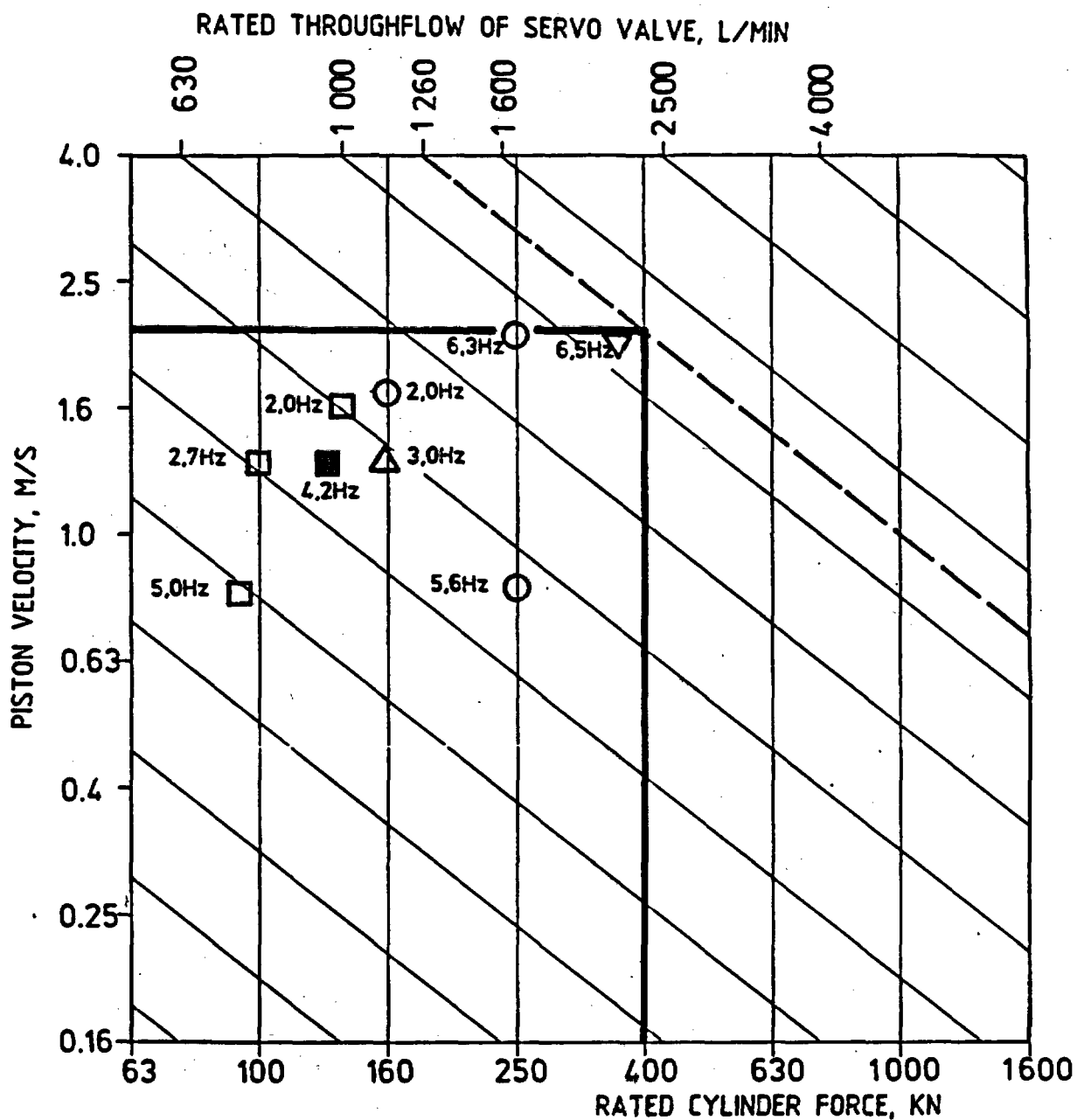


Fig. 5.1-11 Load case IV: Modified earthquake history and response spectrum ($\delta = 7\%$)

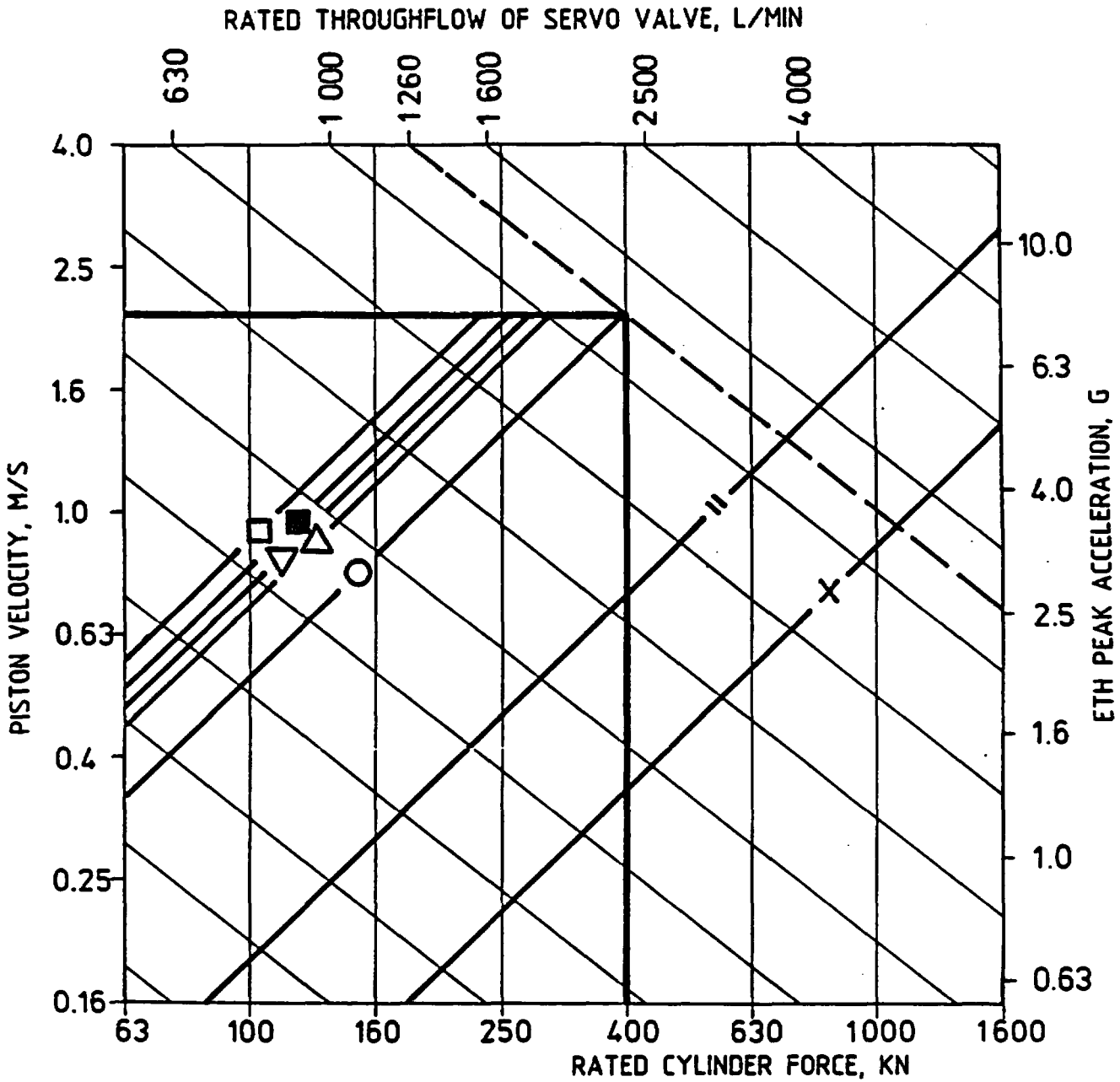


LOAD CASE I STEADY HARMONIC EXCITATION

MODEL	HANGER CONFIGURATIONS			EXCITATION POINT
	HDR	KWU	NRC	
B	■	▲	▼	H5
L	○	-	-	DF16
M	□	-	-	H5

Fig. 5.1-12

Establishment of the excitation system performance: Achievement of the criterion for plasticization at individual frequencies



LOAD CASE IV EARTHQUAKE HISTORY (ETH)

MODEL	HANGER CONFIGURATIONS			EXCITATION POINT
	HDR	KWU	NRC	
A	x	x	x	HDU704
B	■	△	▽	H5
D	"	"	"	HDU704
L	○	-	-	DF16
M	□	-	-	H5

Fig. 5.1-13

Establishment of the excitation system performance:
Attainable peak acceleration with earthquake excitation

Model node no.	Reference Point	H D R / L		H D R / M	
		a m/s ²	d mm	a m/s ²	d mm
23	QB 109	1.1 (z)	0.9 (x)	5.3 (x)	5.0 (x)
24	QB 108	0.8 (x)	0.8 (x)	4.9 (x)	4.6 (x)
29	QB 116	3.2 (z)	2.6 (z)	10.7 (x)	10.3 (x)
36	QB 940	0.6 (x)	0.6 (x)	10.3 (x)	10.0 (x)
46	H 5	0.6 (y)	0.4 (z)	10.0 (x)	10.0 (x)
55	QB 110	14.5 (x)	14.0 (x)	6.7 (x)	6.7 (x)
62	QB 107	1.7 (y)	1.5 (z)	8.9 (x)	18.2 (y)
70	QB 111	15.2 (x)	15.6 (x)	2.4 (z)	4.4 (z)
83	QB 101	10.7 (x)	10.5 (x)	14.6 (x)	20.6 (y)
84	QB 122	10.5 (x)	10.7 (x)	2.0 (z)	3.9 (z)
103	QB 112	10.9 (x)	10.5 (x)	6.6 (z)	8.2 (z)
106	RS 761	12.0 (z)	11.8 (z)	14.6 (x)	19.0 (x)
138	DF 16	10.0 (x)	10.0 (x)	1.9 (z)	3.7 (z)

LOAD CASE IV, NORMALIZED TO $A_{MAX} = 10M/S^2$

HANGER CONFIGURATION HDR

MODEL L: EXCITATION DF-16, X DIRECTION

MODEL M: EXCITATION H5, X DIRECTION

Fig. 5.1-14

Maximum values of acceleration and displacement from design calculation and earthquake history

Model node no.	Reference Point	Model L		Model M	
		σ_B N/mm ²	σ_C N/mm ²	σ_B N/mm ²	σ_C N/mm ²
19	QA 113	4.8	1.7	16.4	2.7
20	RA 761	2.2	1.0	18.6	1.4
27	QA 103	27.5	1.7	26.2	2.7
30	QA 106	3.1	0.6	23.1	11.0
35	QA 102	28.5	20.9	9.2	5.1
38	QA 104	5.4	6.2	18.2	3.9
43	QA 101	22.5	24.8	11.1	5.0
58	QA 105	12.0	0.9	15.4	1.4
74	QA 100	85.9	1.7	16.8	2.2
77	RA 760	53.4	2.9	87.3	6.2
85	RA 763	43.5	3.5	53.0	4.7
92	RA 766	26.9	5.7	47.0	3.4
94	RA 764	14.6	3.9	29.5	4.8
108	RA 765	41.5	3.0	46.1	5.2

LOAD CASE IV, NORMALIZED TO $A_{MAX} = 10M/S^2$

HANGER CONFIGURATION HDR

MODEL L: EXCITATION DF-16, X DIRECTION

MODEL M: EXCITATION H5, X DIRECTION

Fig. 5.1-15

Maximum values of bending and torsional stress from design calculation with earthquake history

Appendix B

Determination of Allowable Stress Values Used on the VKL Piping Analysis for the SHAM Test Series

Appendix B

Determination of Allowable Stress Values Used on the VKL Piping Analysis for the SHAM Test Series

The VKL piping system uses materials designated by DIN Standards 1.4961, 1.5415, and 1.4550. Since detailed material property information needed in the piping analysis was not provided directly, the following procedure was followed to determine equivalent materials listed in the ASME Code:

1. Determine the equivalent material listed in the ASME Code tables by a comparison of chemical analysis data.
2. Obtain the allowable values of S_C and S_H from the appropriate tables in the ASME Code for the equivalent materials.
3. Determine the allowable stress values as defined in the ASME Code, Subsection NC-3600 for Class 2 components.

The following commentary describes the particular details of this process and the results obtained.

The information available from HDR personnel indicated the following chemical analysis for each of the materials:

DIN 1.4961	0.10% C, 0.30 - 0.60% Si, 1.0 - 1.5% Mn, 15.0 - 17.0% Cr, 12.0 - 14.0% Ni
DIN 1.5415	0.12 - 0.20% C, 0.15 - 0.35% Si, 0.50 - 0.80% Mn, 0.04% P (max.), 0.04% S (max.), 0.25 - 0.35% Mo
DIN 1.4550	0.10% C, 1.0% Si, 2.0% Mn, 17.0 - 19.0% Cr, 9.0 - 11.5% Ni.

Reference to Section II (Material Specifications) of the ASME Code shows that the chemical requirements of SA-312, TP316H; S-335, P1; and SA-312, TP312H match the chemical analyses of DIN 1.4961, 1.5415, and 1.4550, respectively. It can be seen that the ASME Code specifications for SA-312, TP316H include 2-3% Mb, which is not specified in the analysis of DIN 1.4961. However, based on the close match of the other chemical content parameters, it was concluded that SA-312, TP316H was the best choice for material properties to be used in the design analysis for the sections of piping fabricated from DIN 1.4961.

Using the procedure described above, the material correlations shown in Table B-1 were determined.

Table B-1. VKL piping material correlations.

DIN designation	ASME Code material
1.4691	SA-312, TP316H
1.5415 ^a	SA-355, P1
1.4550	SA-312, TP321H

a. This material used only in DF44 tee.

The ASME Code Class 2 piping rules require the use of allowable stress values taken at design temperature. Thus, S_h , the basic material allowable at design temperature, can be found in tables in Appendix I of the ASME Code. S_c , the material allowable at room temperature, is also found in these tables.

The basis for establishing allowable stress values is found in Article III-3000 for Class 2 components. Briefly stated, the maximum allowable stress is the least of those listed below:

Carbon steel	Austenitic steel
0.25 S_u (room temperature)	0.25 S_u (room temperature)
0.25 S_u (operating temperature)	0.25 S_u (operating temperature)
0.67 S_y (room temperature)	0.67 S_y (room temperature)
0.67 S_y (operating temperature)	0.90 S_{uy} (operating temperature) but less than or equal to 0.67 S_y (room temperature)

The information included in Table B-2 can be completed using the operating temperature for the VKL piping system of 550°F. No information regarding possible variations of ultimate strength at operating temperatures was obtained for Table B-2.

From the information in Table B-2, we can see that the code allowable values of S_h are based on 0.9 S_y at design temperature (550°F) for the austenitic steels (SA-312, TP316H, and SA-312, TP321H) and 0.25 S_u at room temperature for the carbon steel (SA-335, P1).

For the piping equations in Section NC-3650, the allowable stresses are given as shown in Table B-3.

Table B-2. Material allowable selection matrix-VKL piping system.

Material	$S_y(\text{R.T.})^a$	$S_y(550^\circ\text{F})^b$	Allowable stresses [ksi (MPa)]				S_h	S_c
			$S_u(\text{R.T.})^c$	$.25S_u(\text{R.T.})$	$.67S_y(550^\circ\text{F})$	$.9S_y(\text{R.T.})$		
SA-312, TP316H (1.4691)	30.0 ^d (207)	19.4 ^d (134)	75.0 ^d (517)	18.8 (130)	20.0 (138)	17.5 (121)	17.5 ^d (121)	18.8 ^d (130)
SA-335, P1 (1.5415)	30.0 ^d (207)	24.1 ^d (166)	55.0 ^d (379)	13.8 (95.1)	20.0 (138)	Not applicable	13.8 ^d (95.1)	13.8 ^d (95.1)
SA-312, TP321H (1.4550)	30.0 ^d (207)	18.7 ^d (129)	75.0 ^d (517)	18.8 (130)	20.0 (138)	16.8 (116)	16.8 ^d (116)	18.7 ^d (129)

- a. $S_y(\text{R.T.})$ = Material yield strength at room temperature.
- b. $S_y(550^\circ\text{F})$ = Material yield strength at (550°F).
- c. $S_u(\text{R.T.})$ = Material ultimate strength at room temperature.
- d. From ASME Code, Table I-7.2.

Table B-3. ASME Code Class 2 allowable stress definitions.

Equation	Service level	Allowable ^a
8 (Sustained Loads)	A	1.0 S _h
9 (Occasional Loads)	A, B	1.2 S _h
9 (Occasional Loads)	C	1.8 S _h
9 (Occasional Loads)	D	2.4 S _h
10 (Thermal Loads)	A	1.0 S _a
10a (Anchor Movements)	A	3.0 S _c
11 (Pressure + Sustained + Thermal)	A	1.0 S _h + 1.0 S _a

a. $S_a = f(1.25 S_c + 0.25 S_h)$ where it is assumed $f=1.0$ for this work.

The corresponding ASME Code allowable stress values and the areas of the model to which they apply are shown in Table B-4.

Table B-4. ASME Code allowable stresses used for design analysis.

Model area		Model node		Material	Allowable stresses [ksi (MPa)]				
From	To	From	To		Eq. 8	Eq. 9	Eq. 10	Eq. 11	Eq. 12
D14	DF16	59	68	SA-312, TP316H (1.4691)	17.5 (121)	31.5 (217)	27.9 (192)	56.4 (389)	45.4 (313)
D15	DF16	169	178	SA-312, TP316H (1.4691)	17.5 (121)	31.5 (217)	27.9 (192)	56.4 (389)	45.4 (313)
F44	D15	131	165	SA-335, P1 (1.5415)	13.8 (95.1)	24.8 (171)	20.7 (143)	41.4 (286)	34.5 (238)
HDU (135)	DF21	24	39	SA-312, TP321H (1.4550)	16.8 (116)	30.2 (208)	27.6 (190)	56.1 (387)	44.4 (306)
DF22	DF21	78	83	SA-312, TP321H (1.4550)	16.8 (116)	30.2 (208)	27.6 (190)	56.1 (387)	44.4 (306)
HDU (305)	DF21	88	116	SA-312, TP321H (1.4550)	16.8 (116)	30.2 (208)	27.6 (190)	56.1 (387)	44.4 (306)
DF21	F44	119	130	SA-312, TP321H (1.4550)	16.8 (116)	30.2 (208)	27.6 (190)	56.1 (387)	44.4 (306)
DF22	D14	40	59	SA-312, TP321H (1.4550)	16.8 (116)	30.2 (208)	27.6 (190)	56.1 (387)	44.4 (306)

B-7

NUREG-5646

Appendix B

Appendix C

Power Spectral Density Curves for Selected Points—SHAM Tests T41.81.1, T41.81.2, and T41.81.3

Power Spectral Density Curves for Selected Points— SHAM Tests T41.81.1, T41.81.2, and T41.81.3

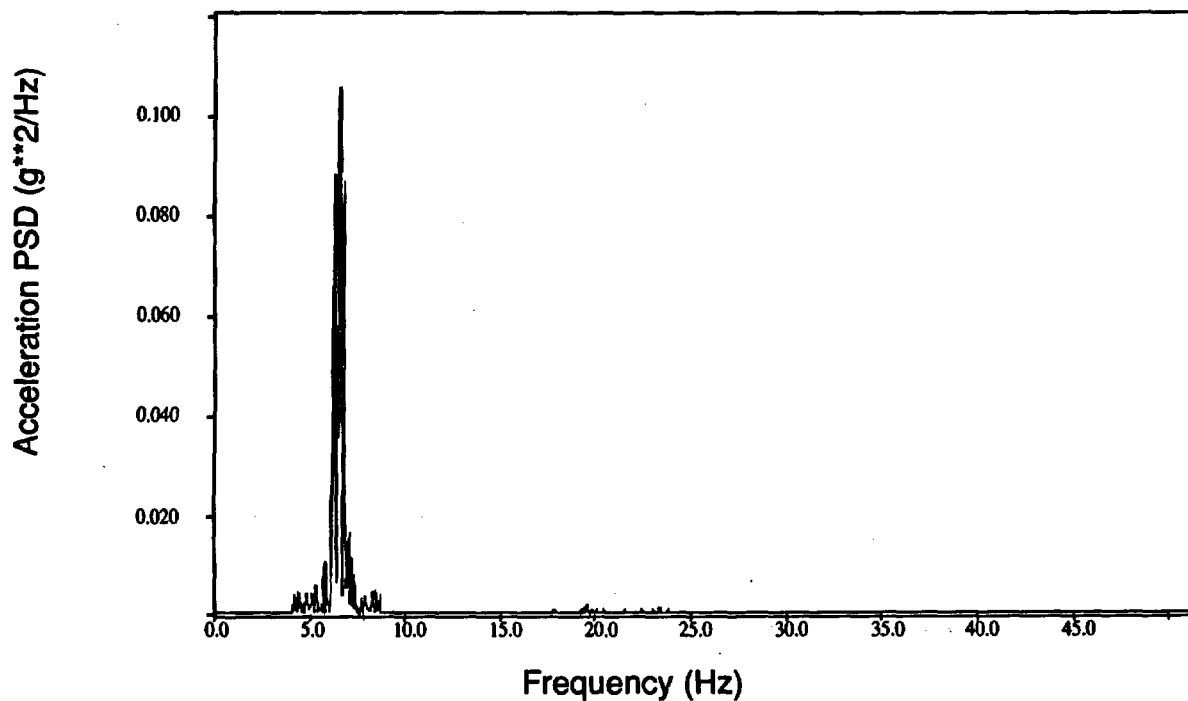


Figure C-1. PSD from QB1101 (Test T41.81.1).

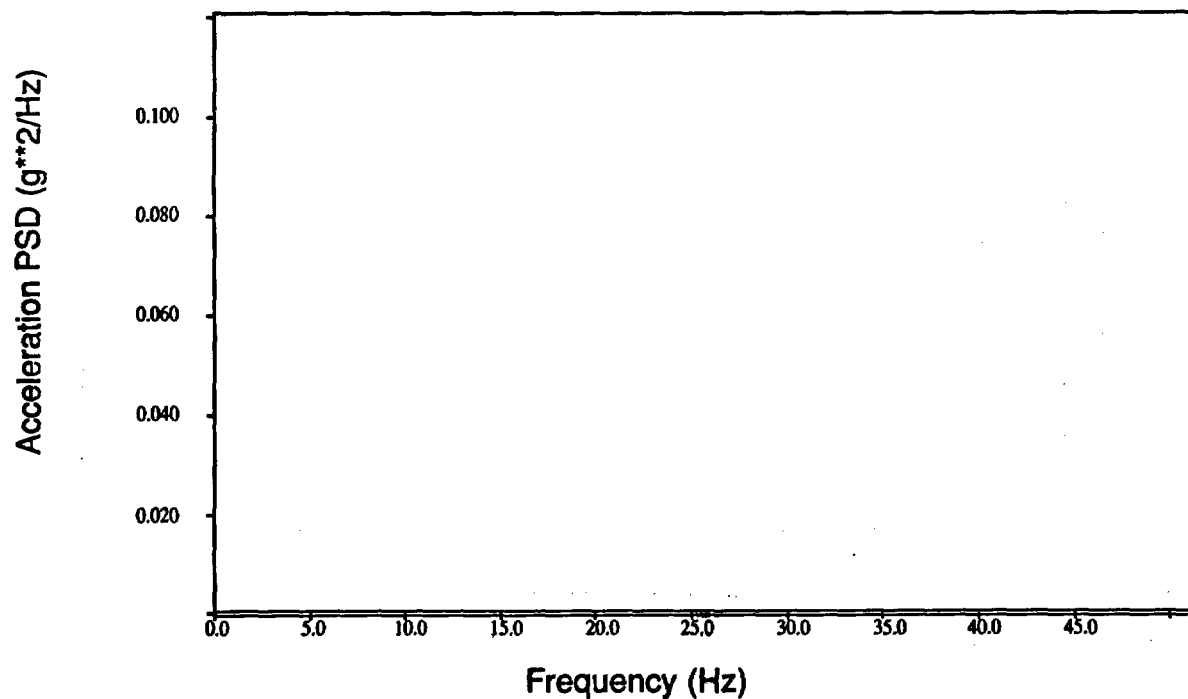


Figure C-2. PSD from QB1102 (Test T41.81.1).

Appendix C

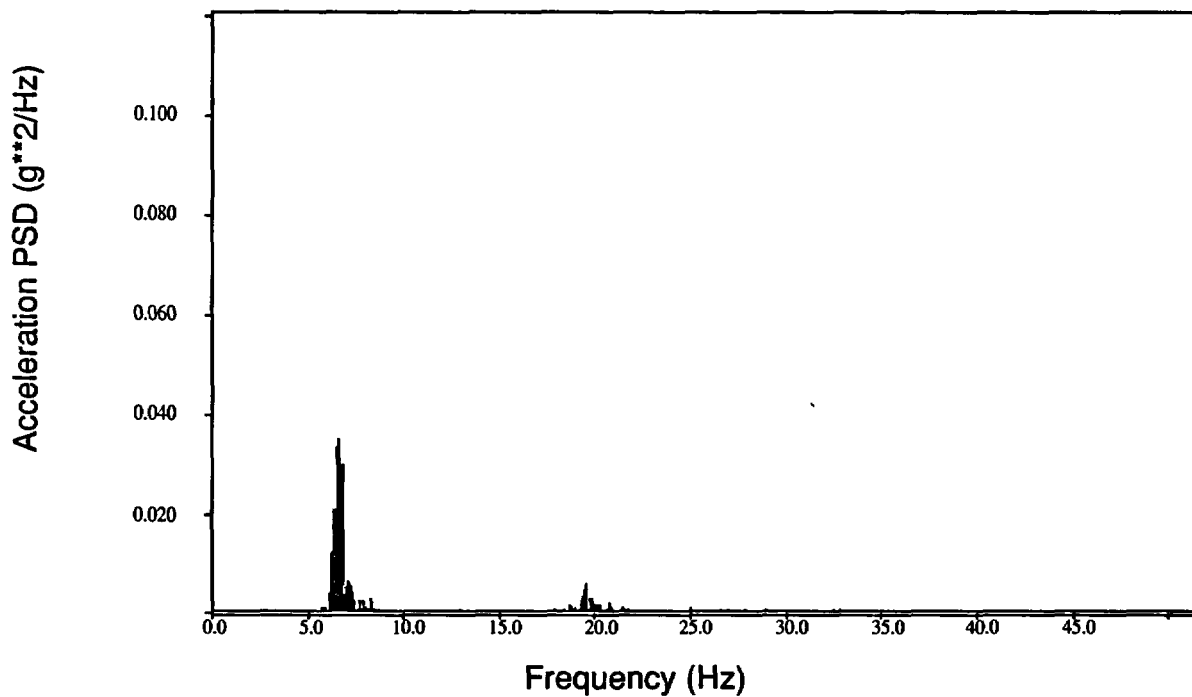


Figure C-3. PSD from QB1103 (Test T41.81.1).

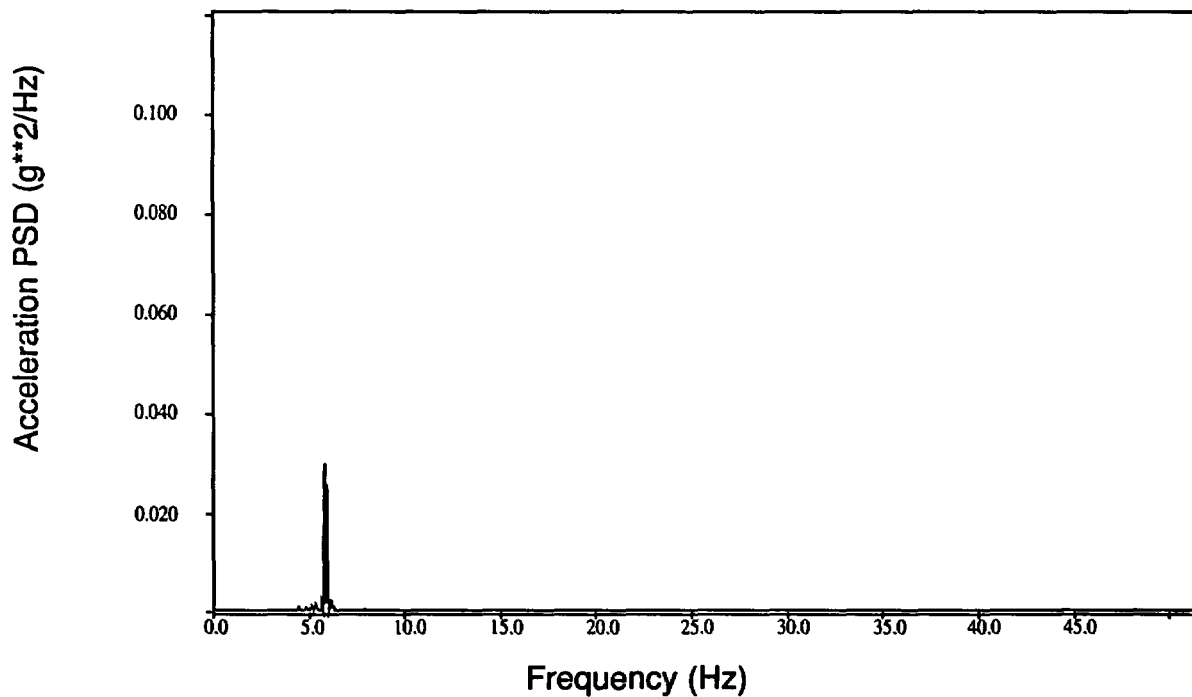


Figure C-4. PSD from RS7610 (Test T41.81.1).

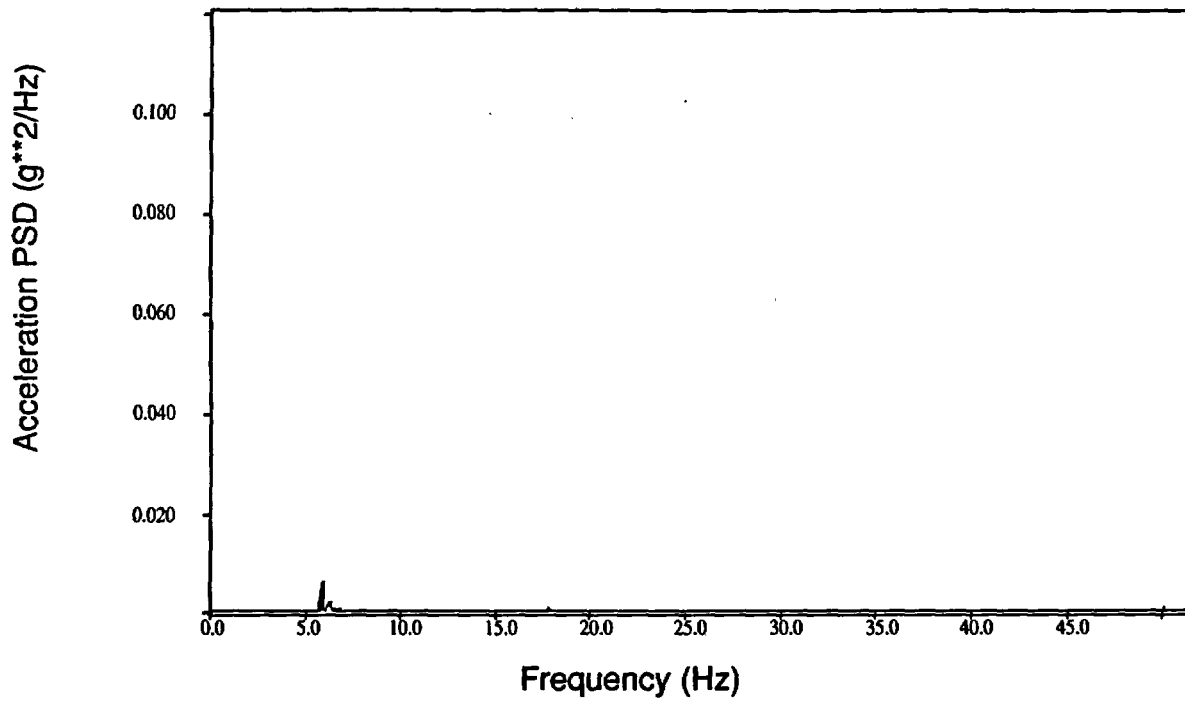


Figure C-5. PSD from RS7611 (Test T41.81.1).

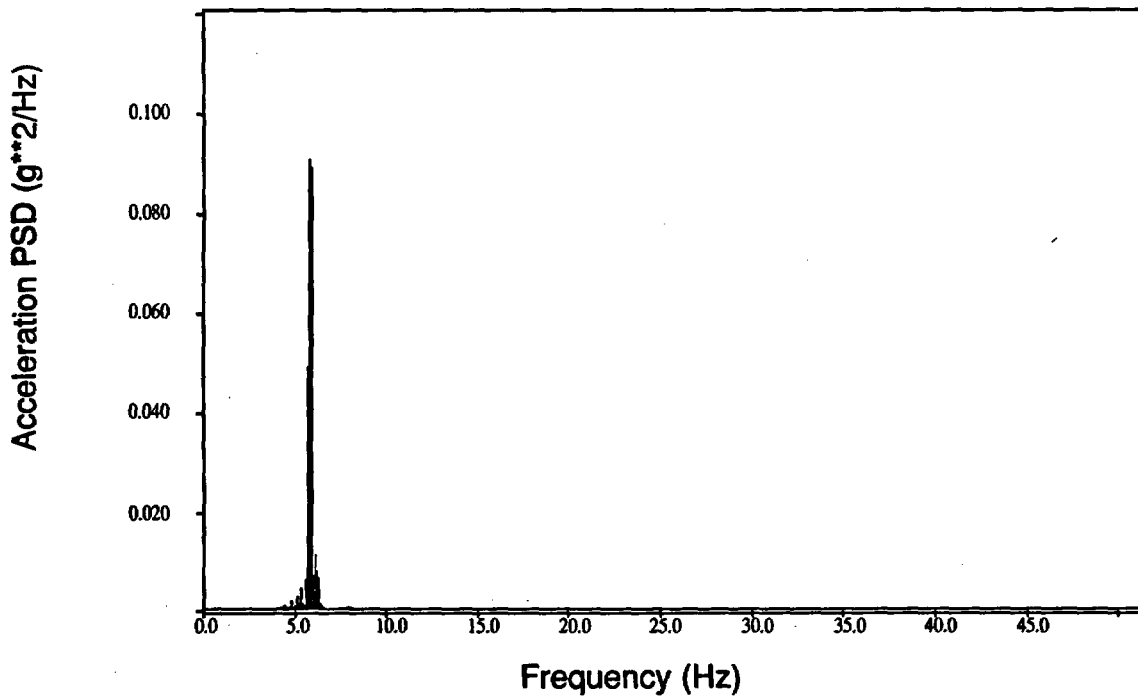


Figure C-6. PSD from RS7612 (Test T41.81.1).

Appendix C

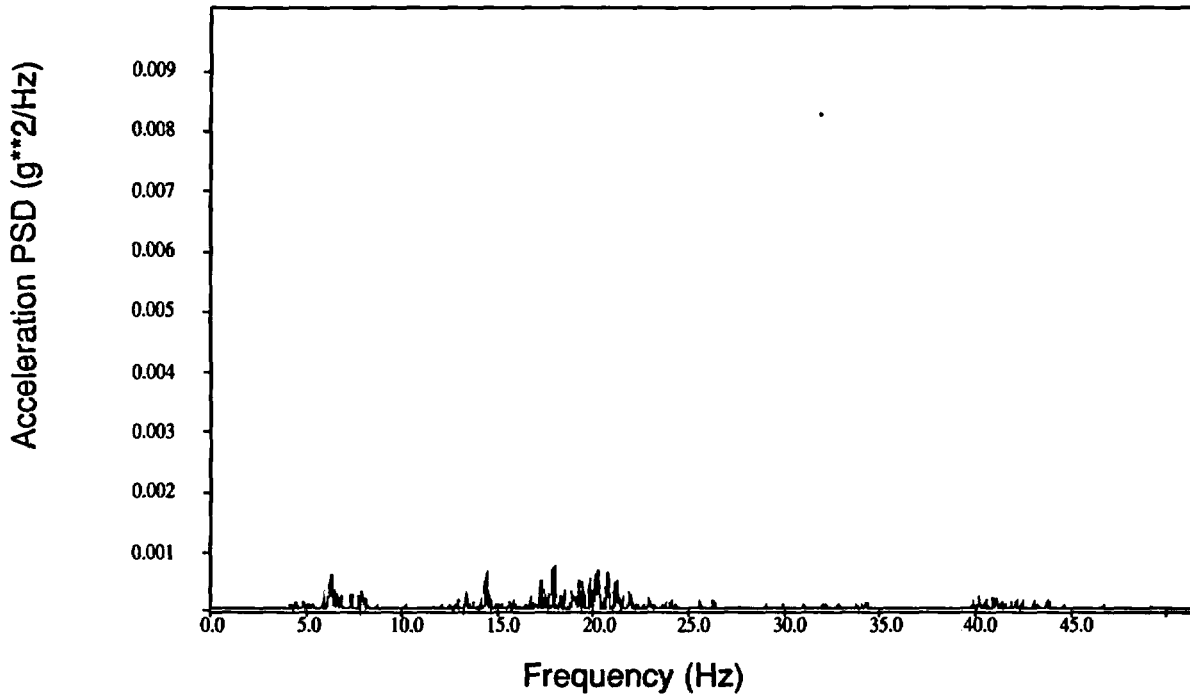


Figure C-7. PSD from QB1011 (Test T41.81.1).

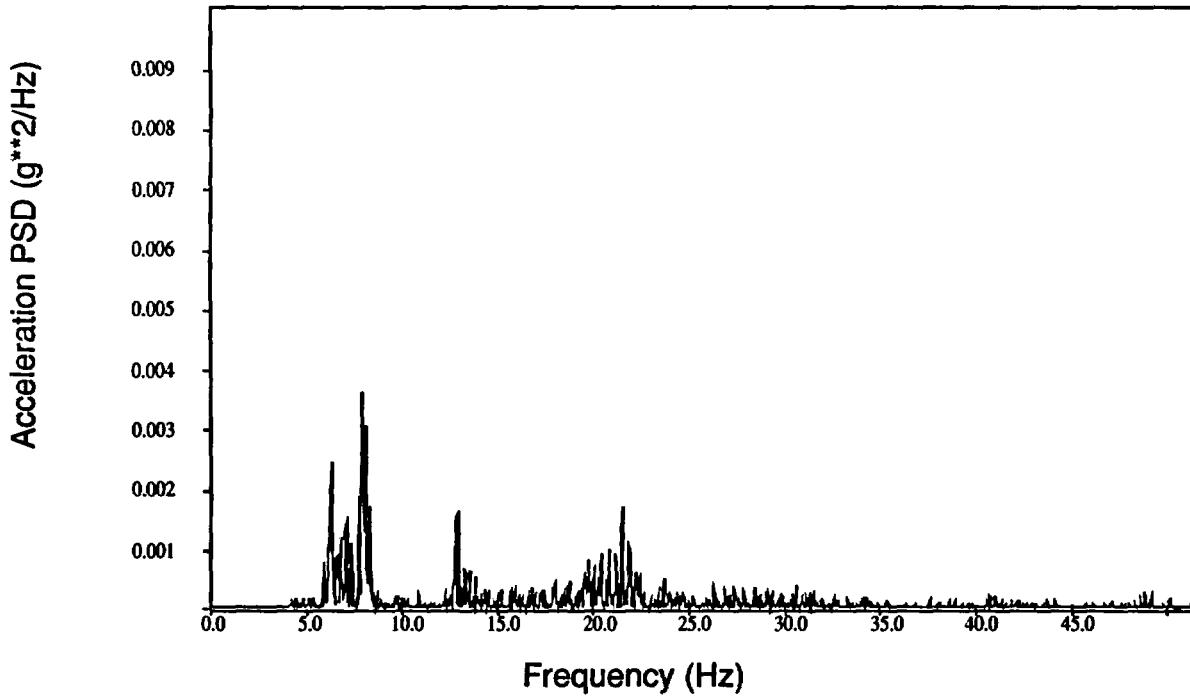


Figure C-8. PSD from QB1012 (Test T41.81.1).

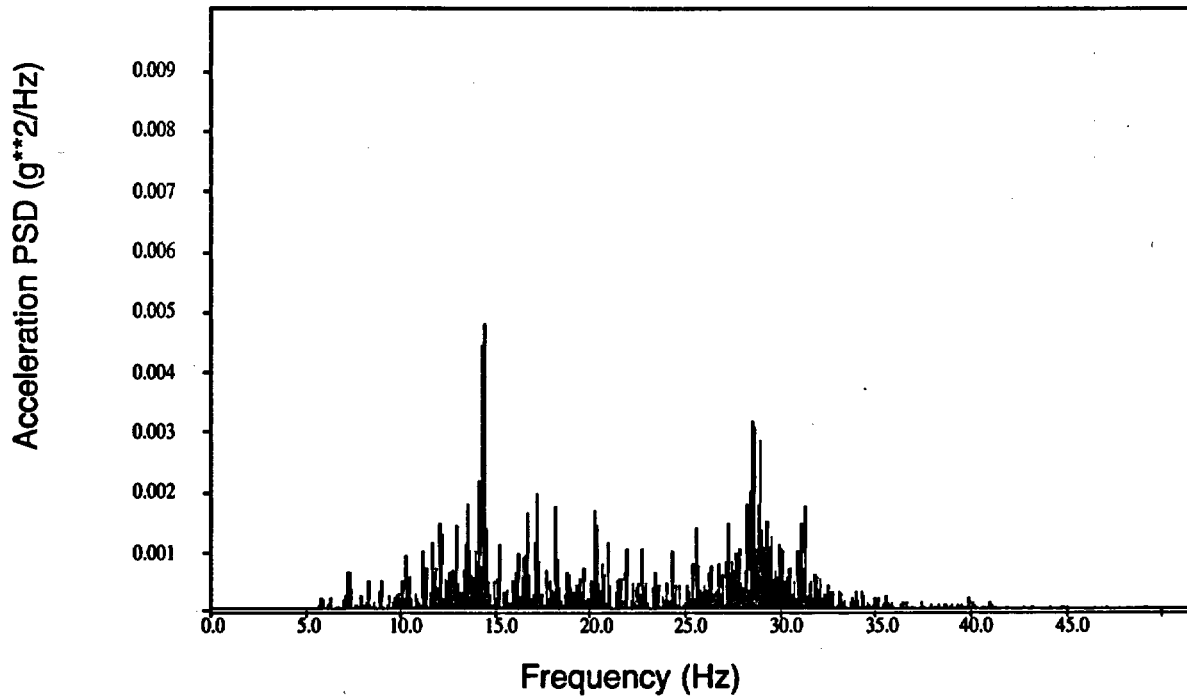


Figure C-9. PSD from QB1013 (Test T41.81.1).

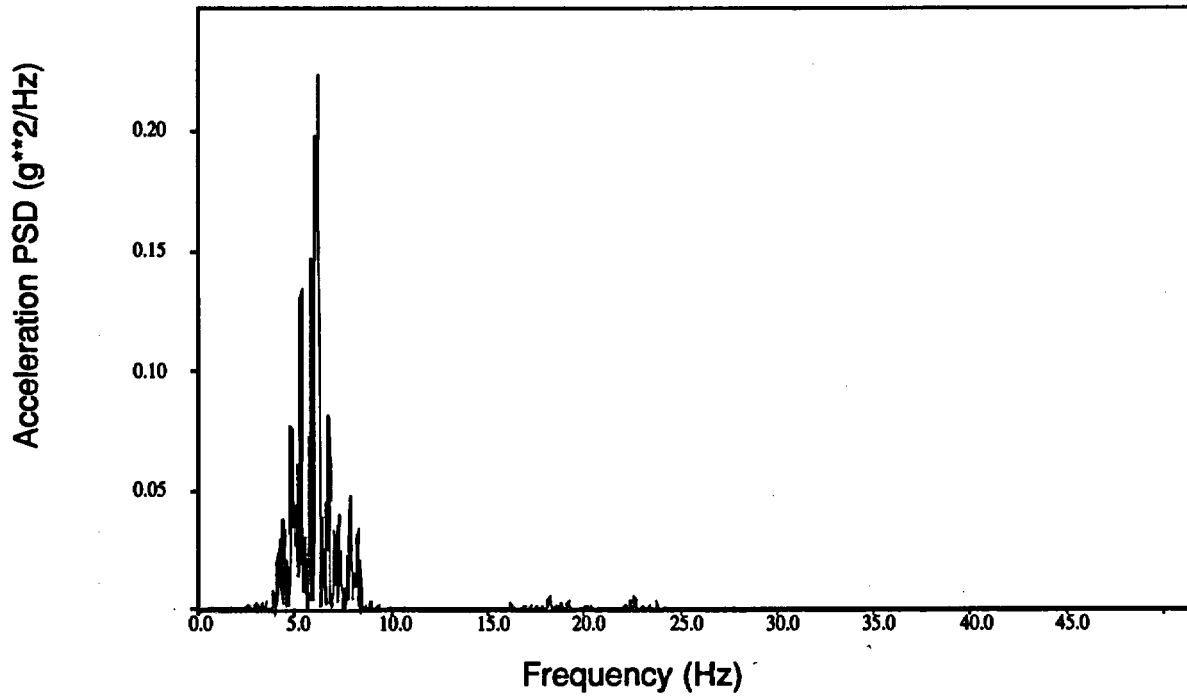


Figure C-10. PSD from QB1101 (Test T41.81.2).

Appendix C

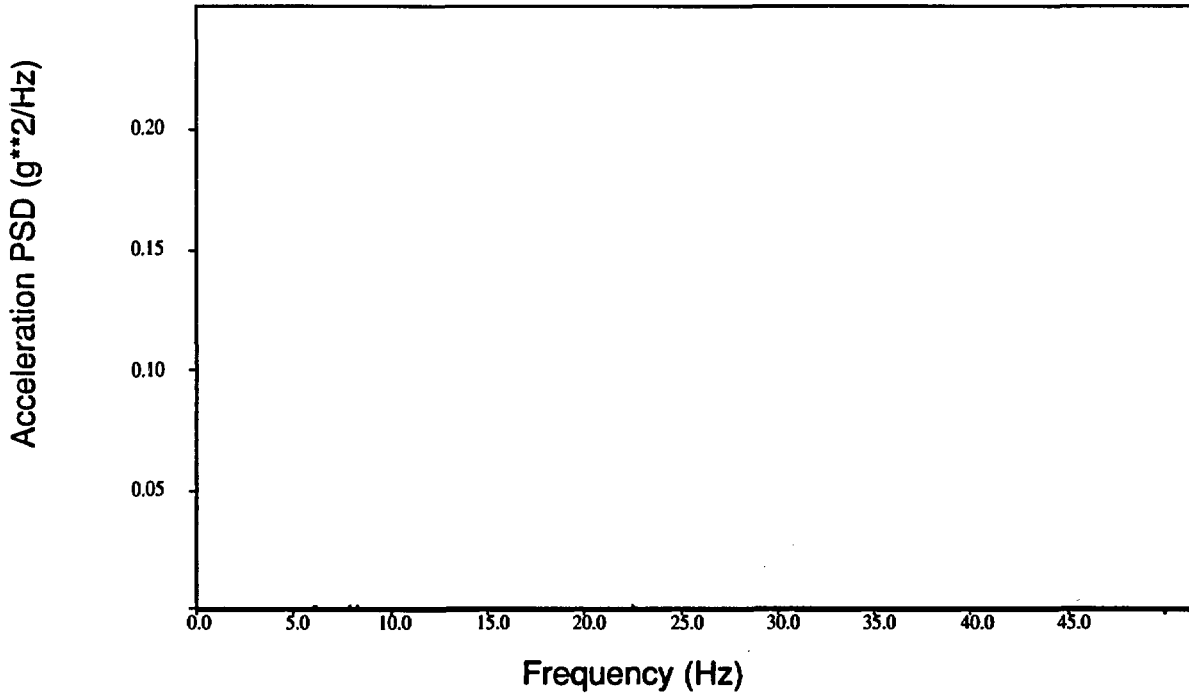


Figure C-11. PSD from QB1102 (Test T41.81.2).

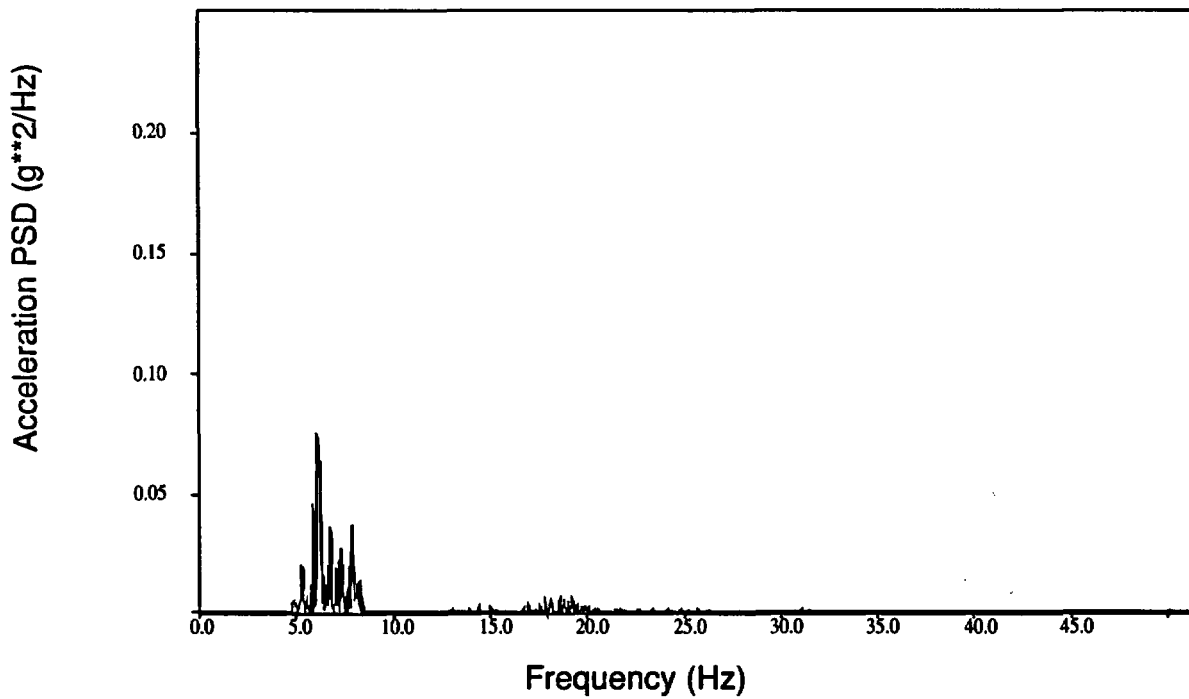


Figure C-12. PSD from QB1103 (Test T41.81.2).

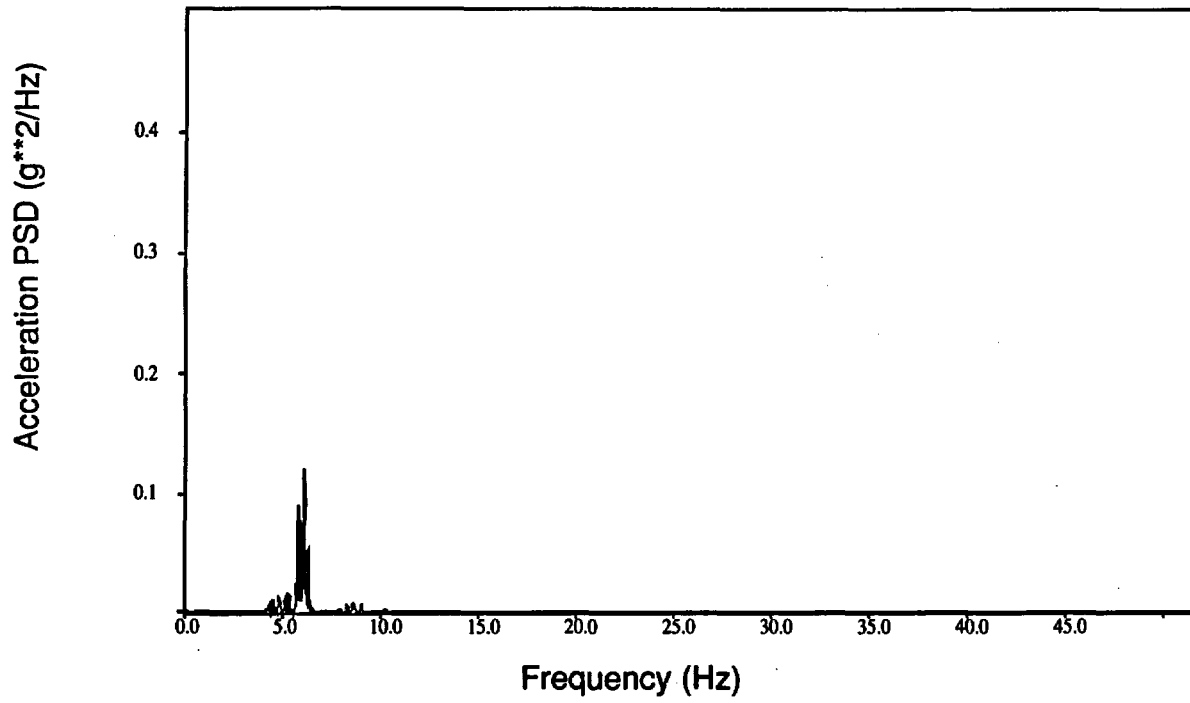


Figure C-13. PSD from RS7610 (Test T41.81.2).

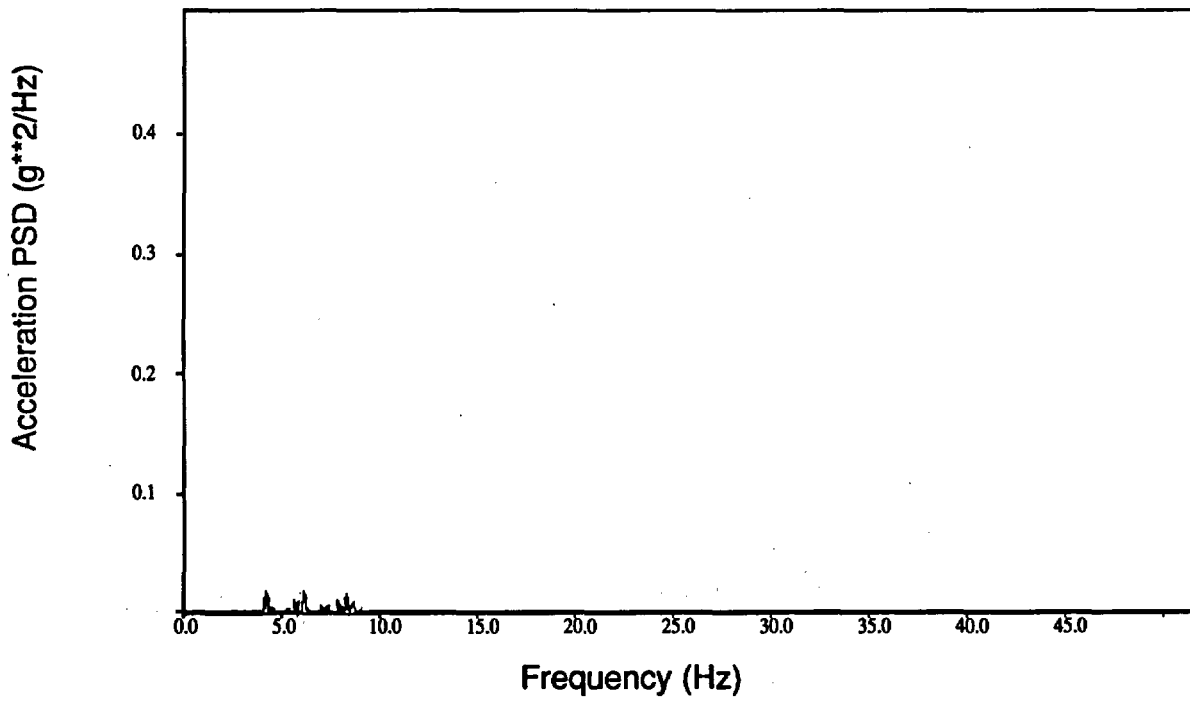


Figure C-14. PSD from RS7611 (Test T41.81.2).

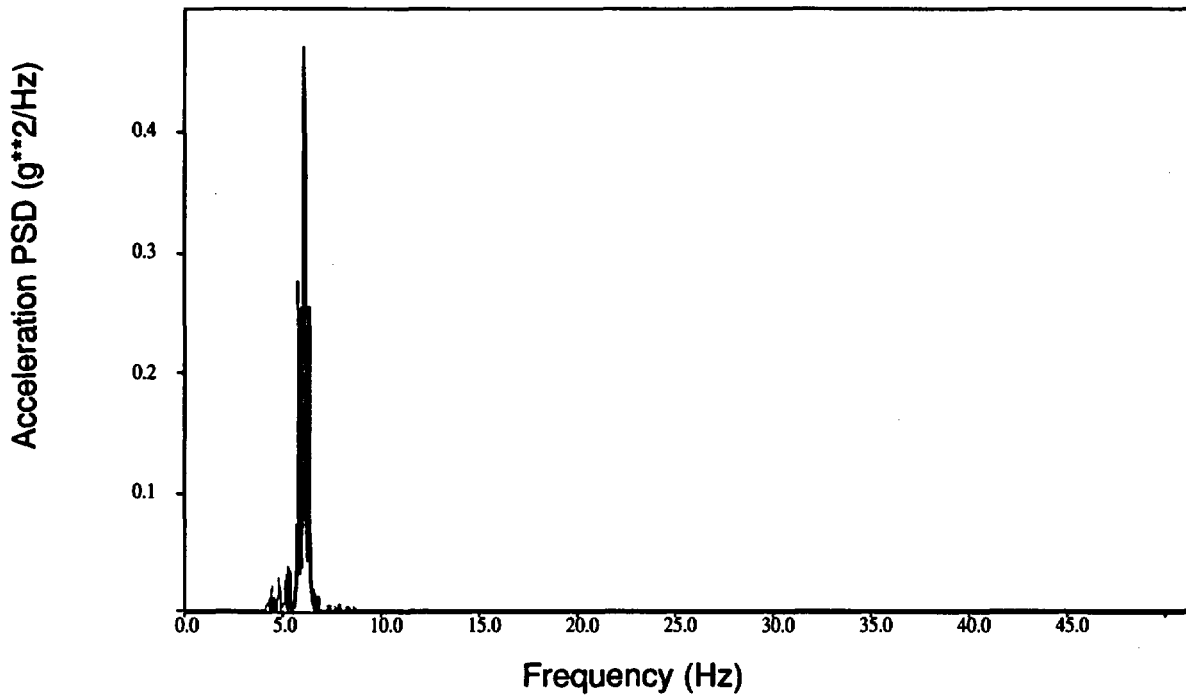


Figure C-15. PSD from RS7612 (Test T41.81.2).

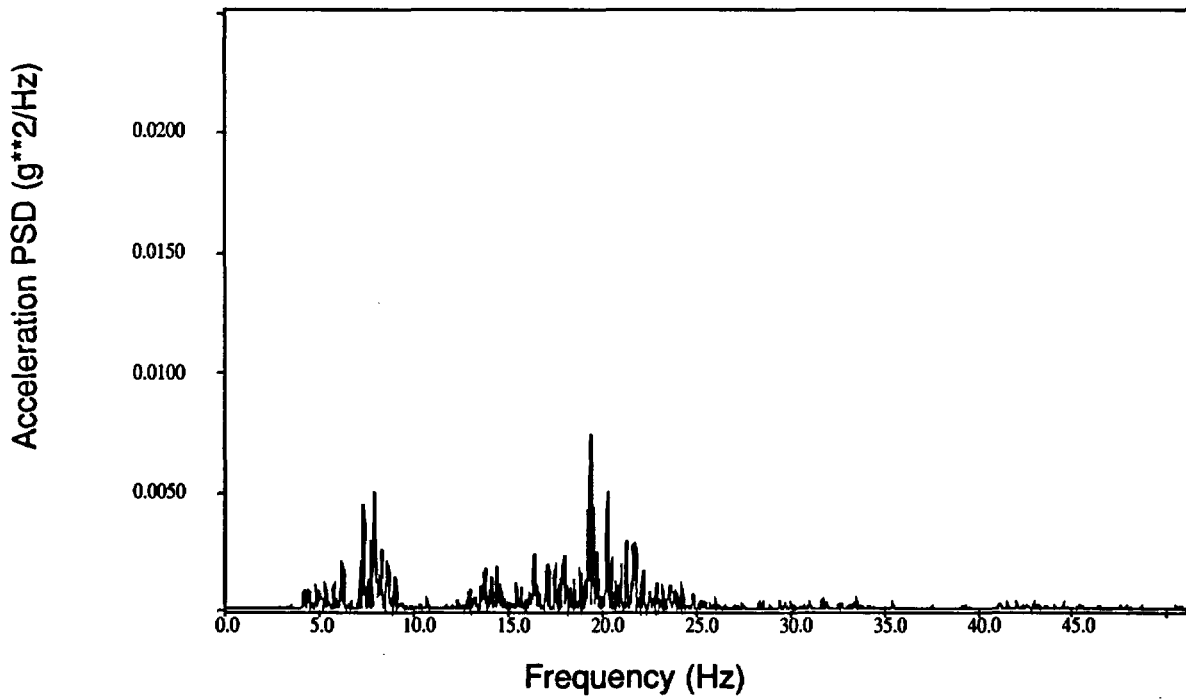


Figure C-16. PSD from QB1011 (Test T41.81.2).

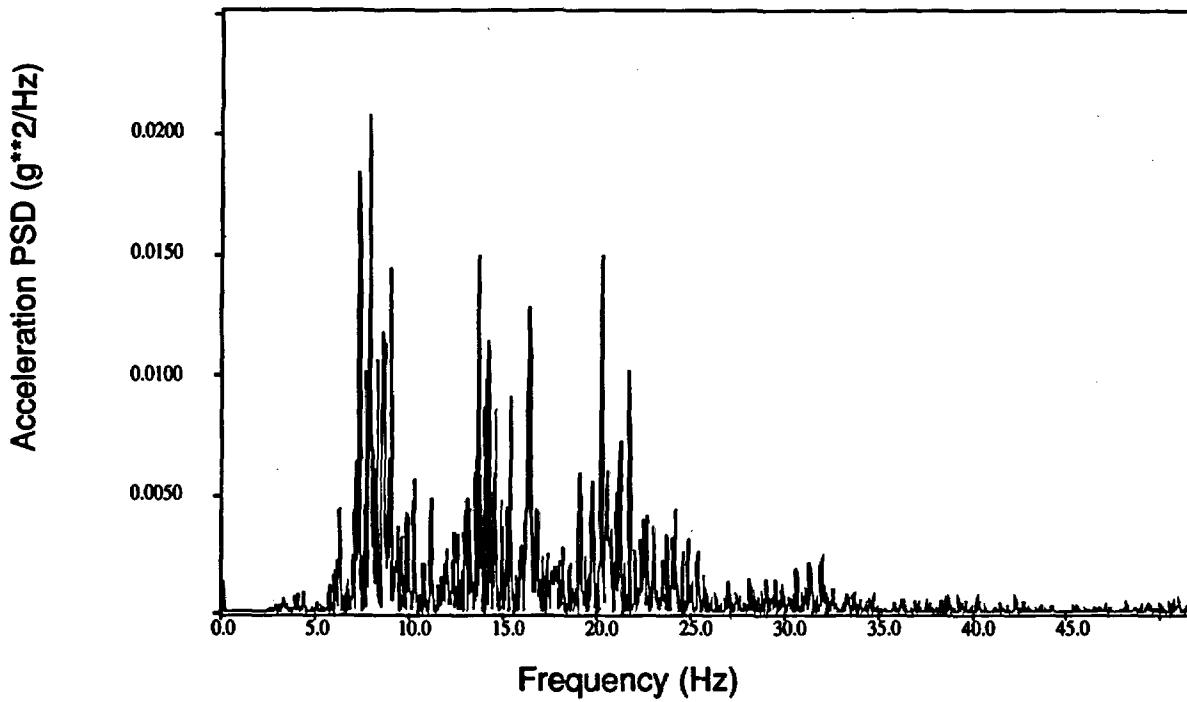


Figure C-17. PSD from QB1012 (Test T41.81.2).

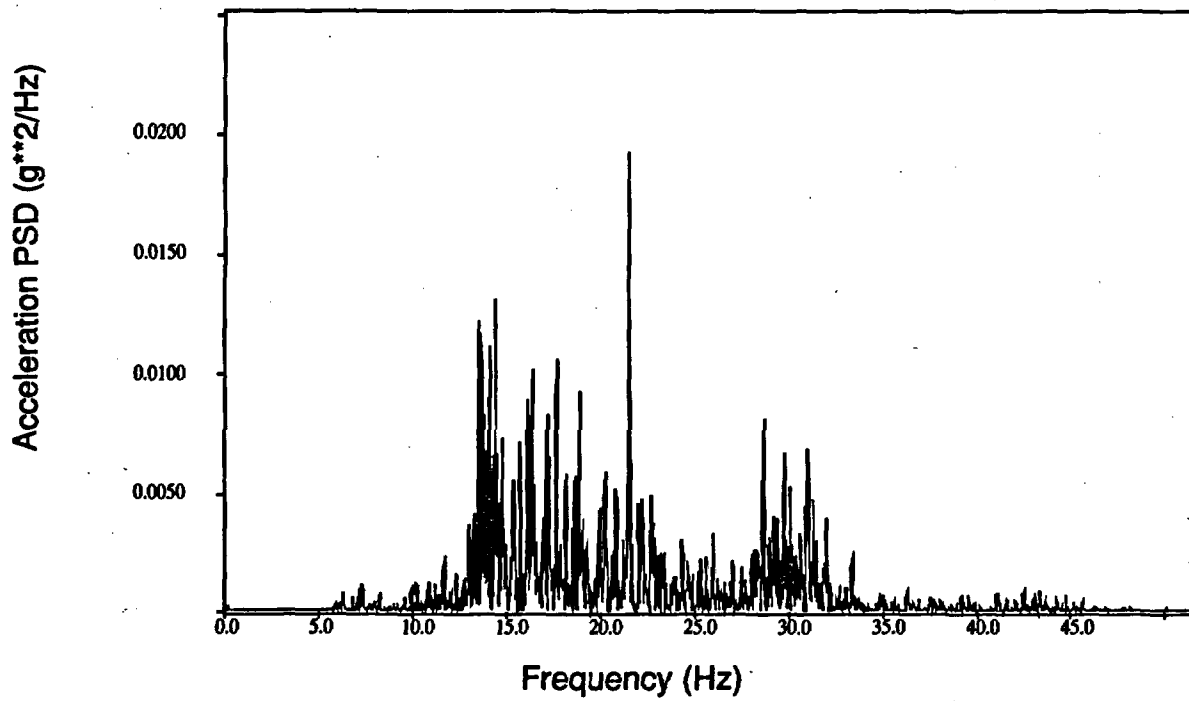


Figure C-18. PSD from QB1013 (Test T41.81.2).

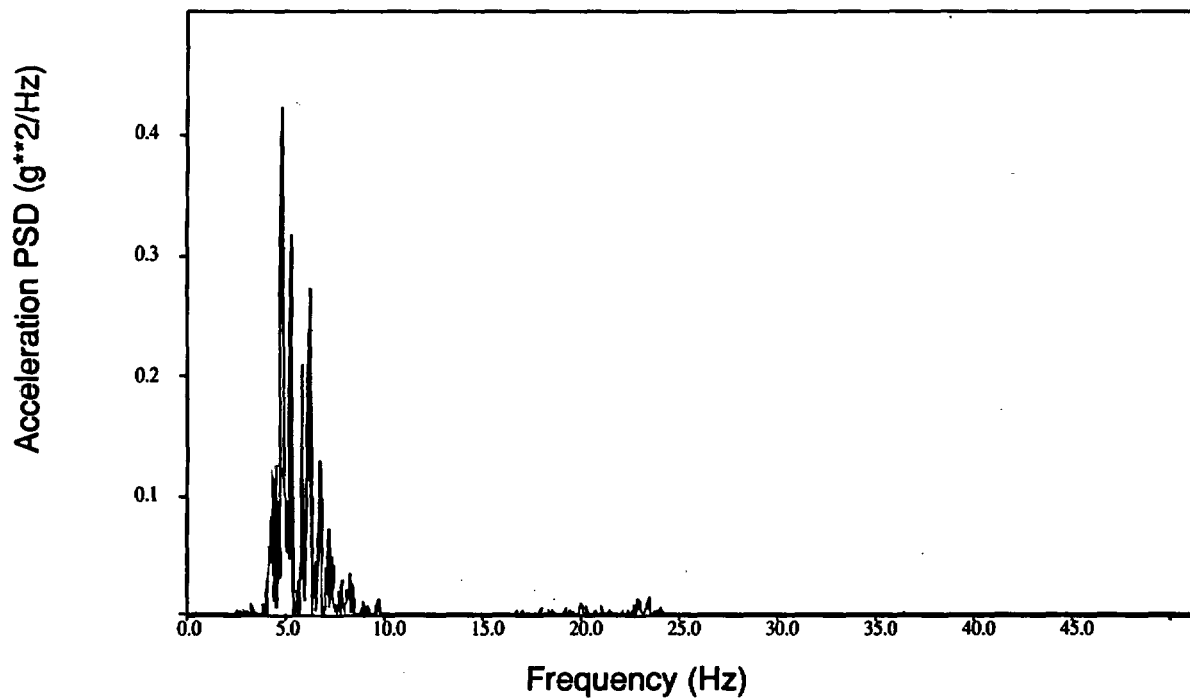


Figure C-19. PSD from QB1101 (Test T41.81.3).

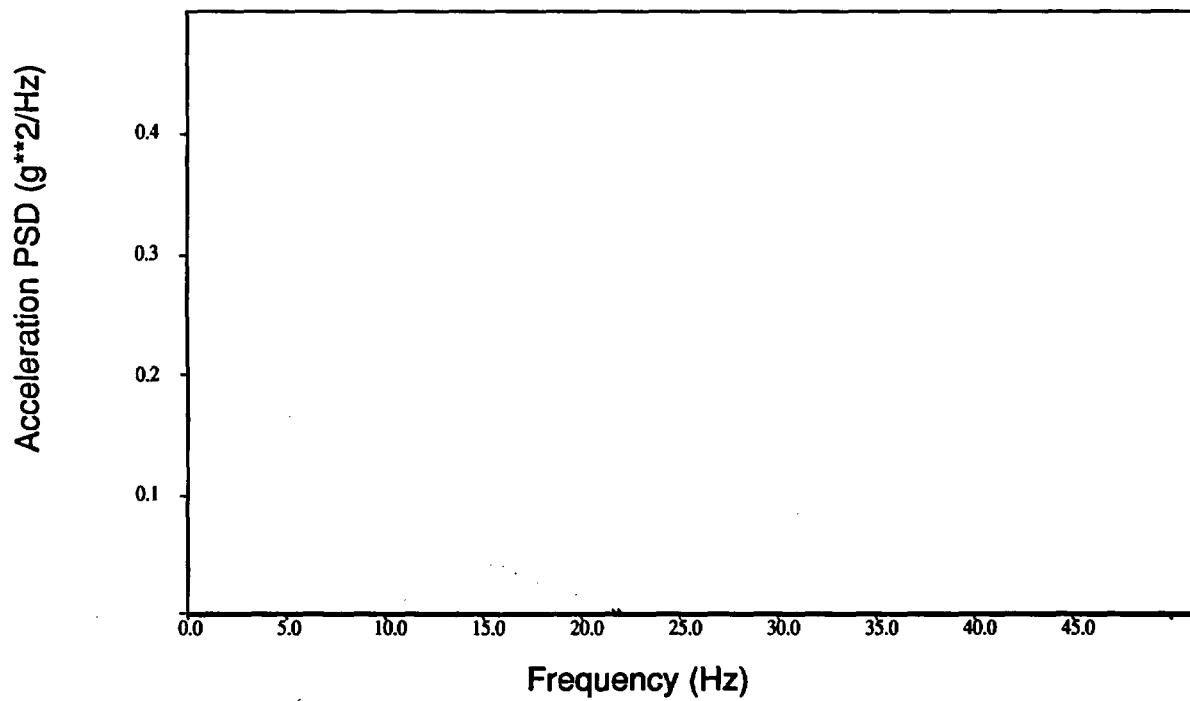


Figure C-20. PSD from QB1102 (Test T41.81.3).

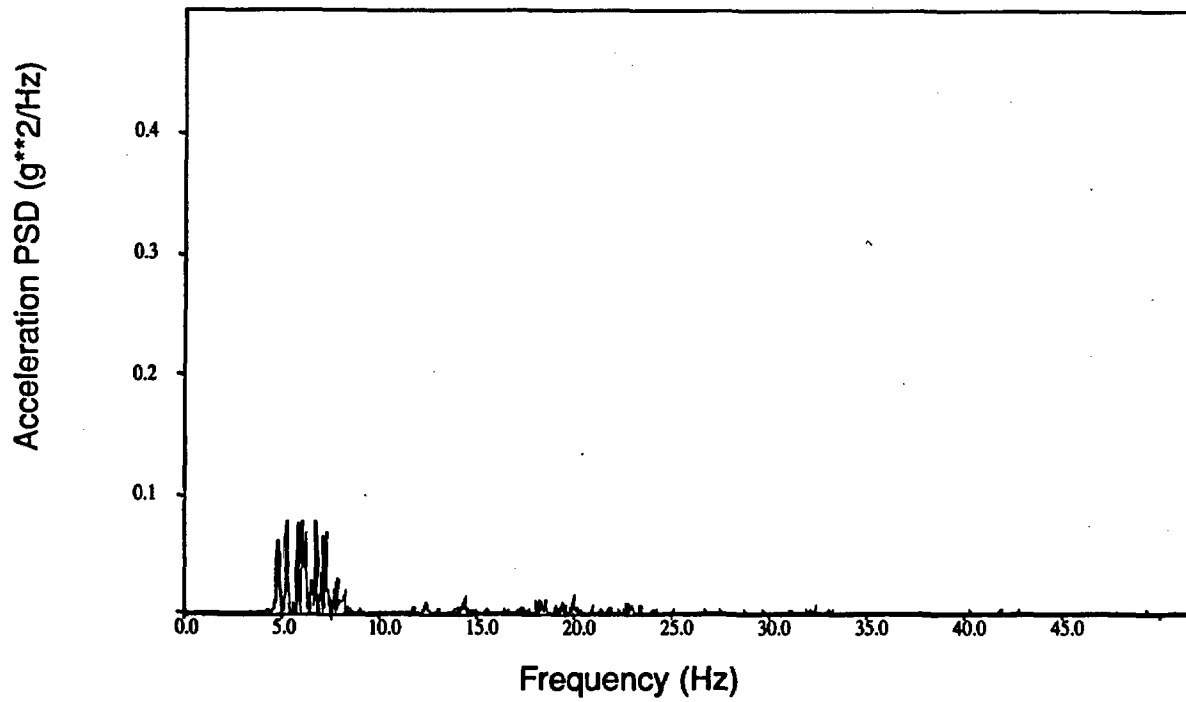


Figure C-21. PSD from QB1103 (Test T41.81.3).

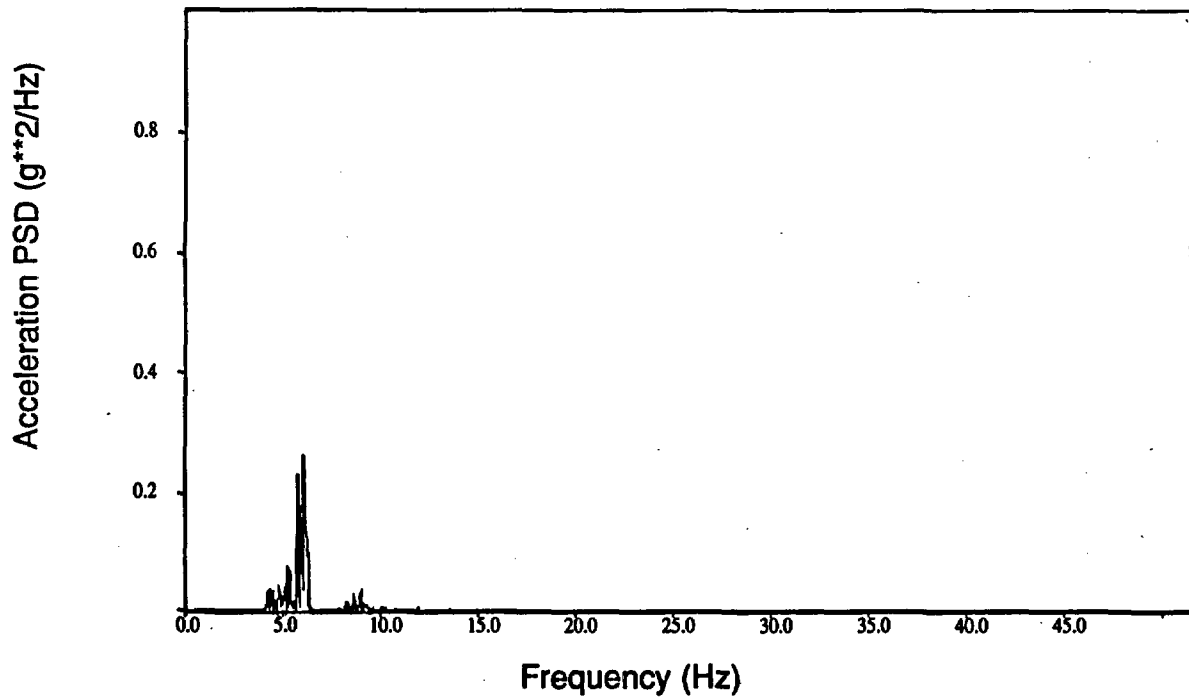


Figure C-22. PSD from RS7610 (Test T41.81.3).

Appendix C

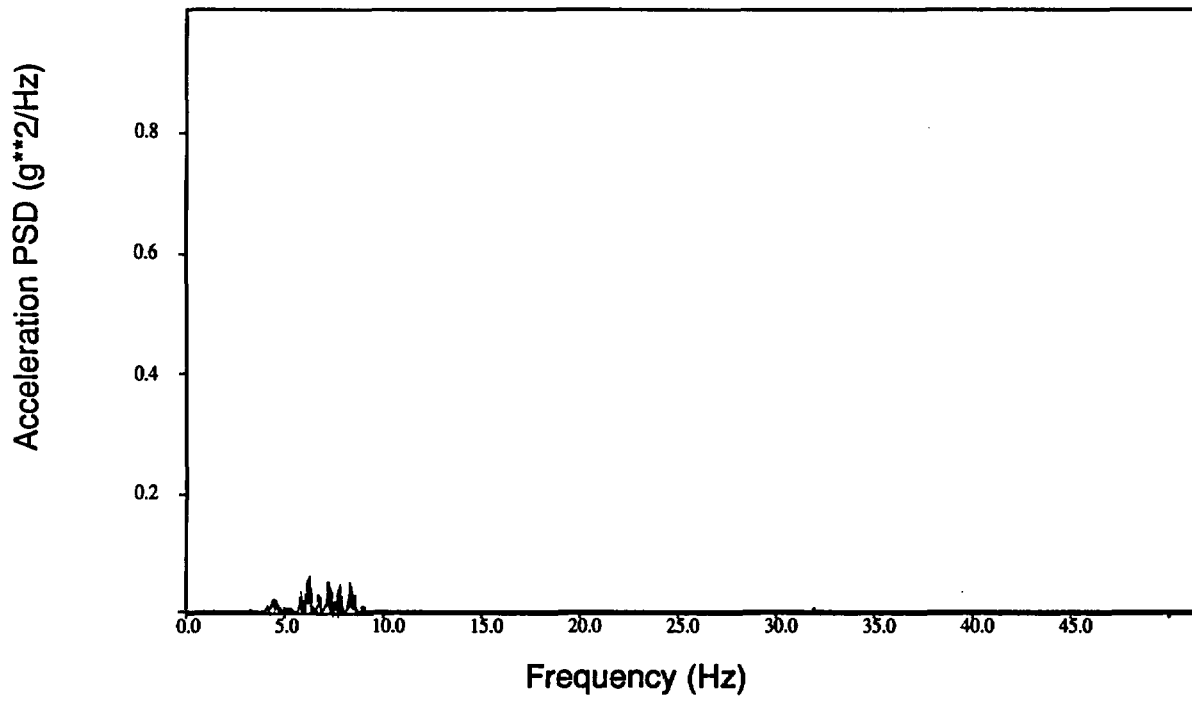


Figure C-23. PSD from RS7611 (Test T41.81.3).

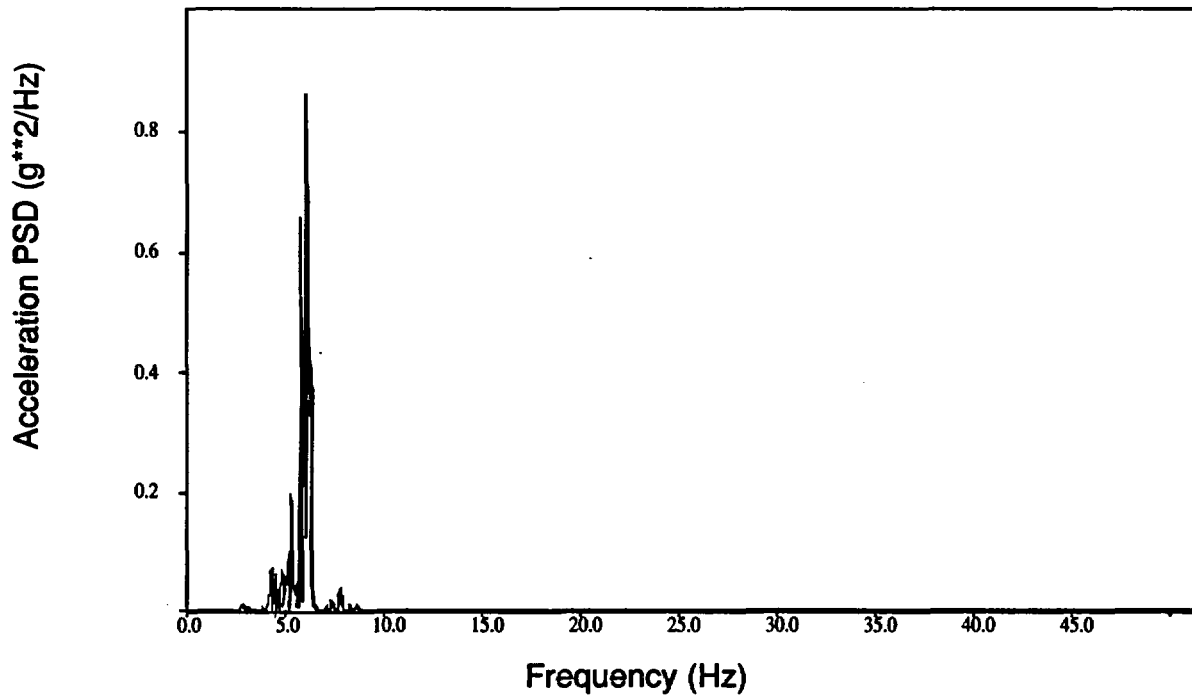


Figure C-24. PSD from RS7612 (Test T41.81.3).

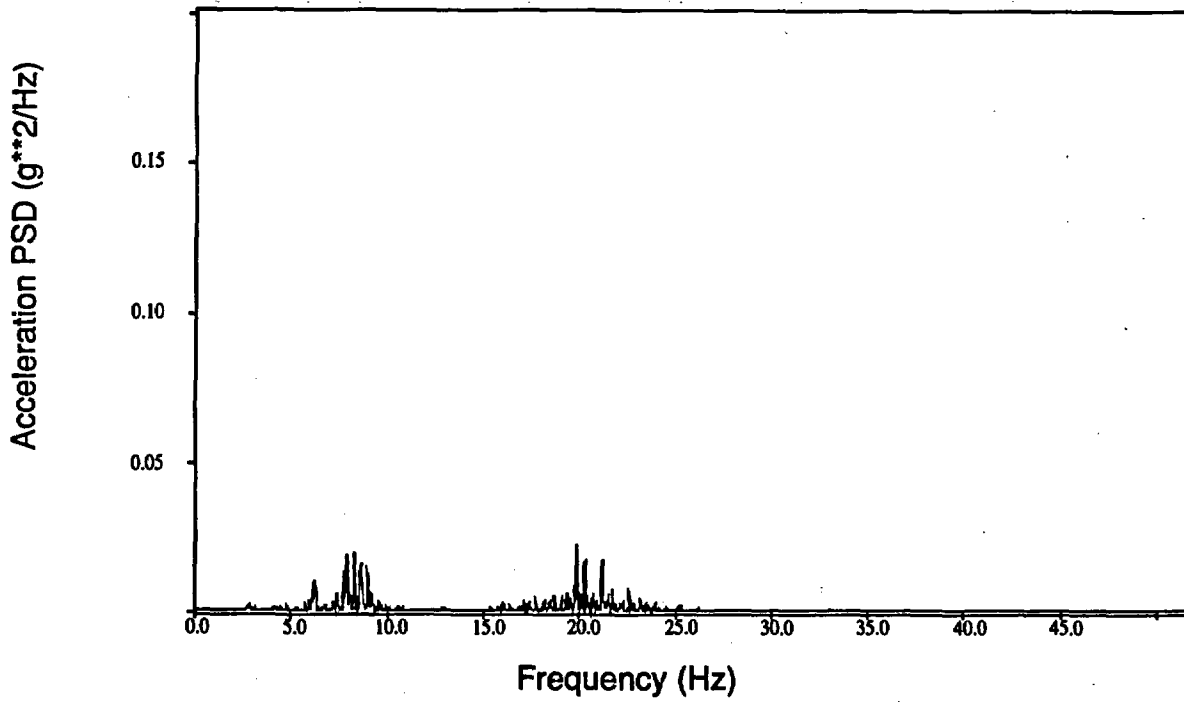


Figure C-25. PSD from QB1011 (Test T41.81.3).

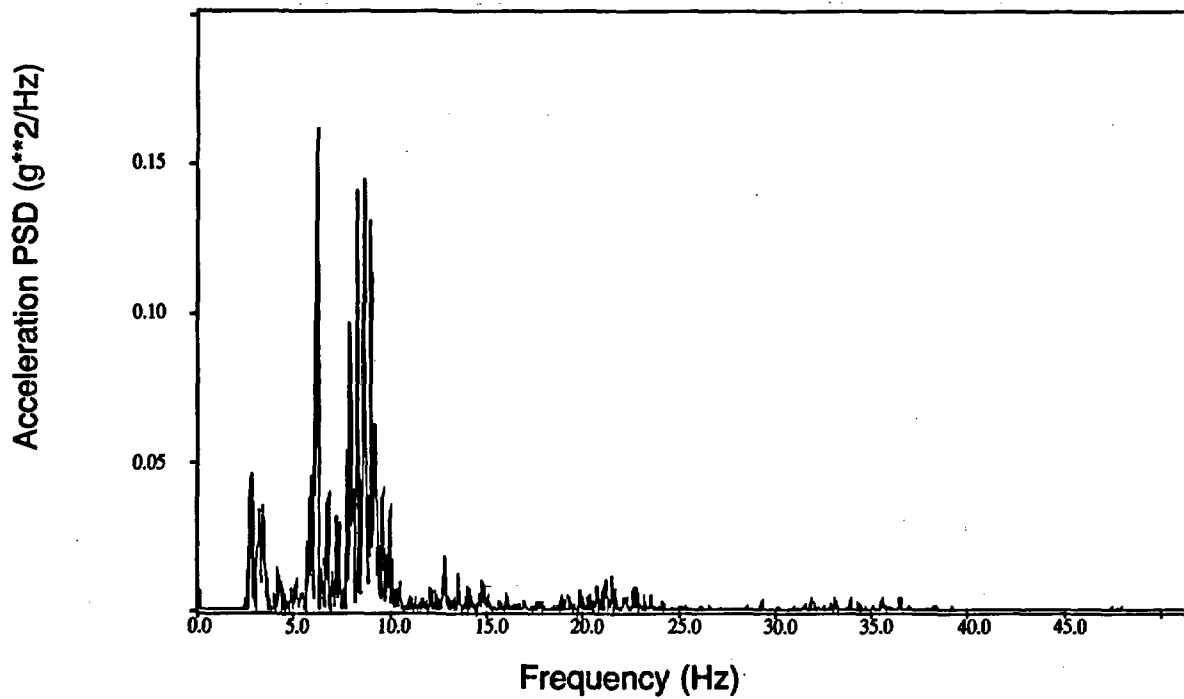


Figure C-26. PSD from QB1012 (Test T41.81.3).

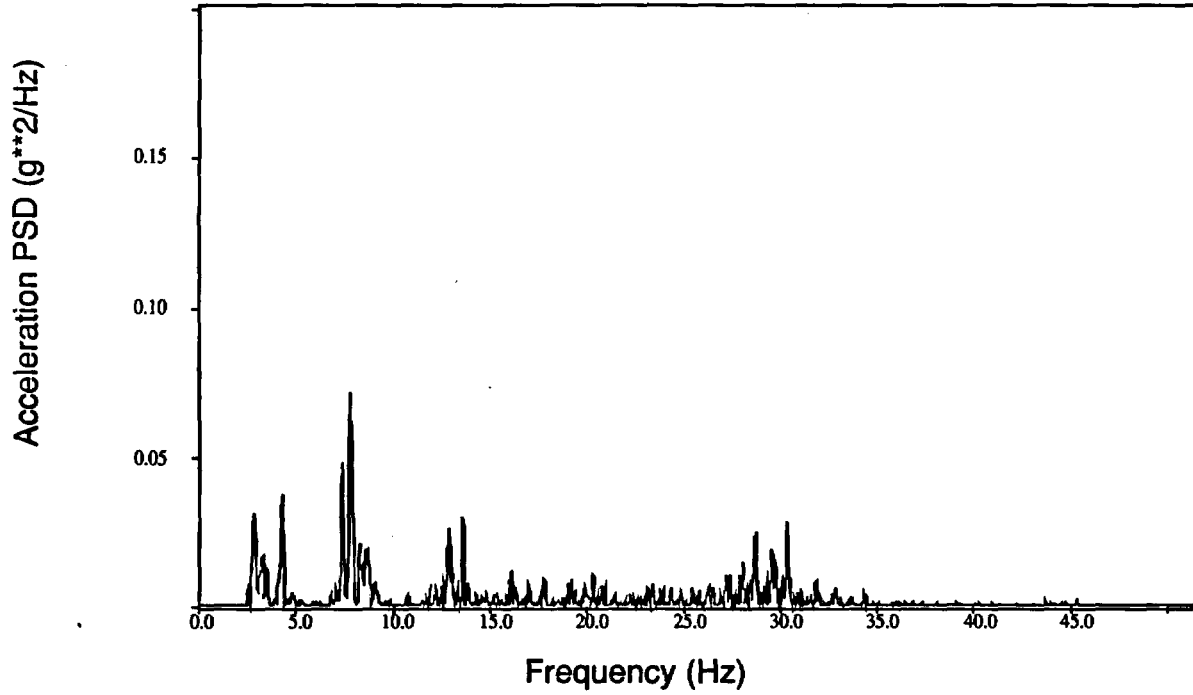


Figure C-27. PSD from QB1013 (Test T41.81.3).

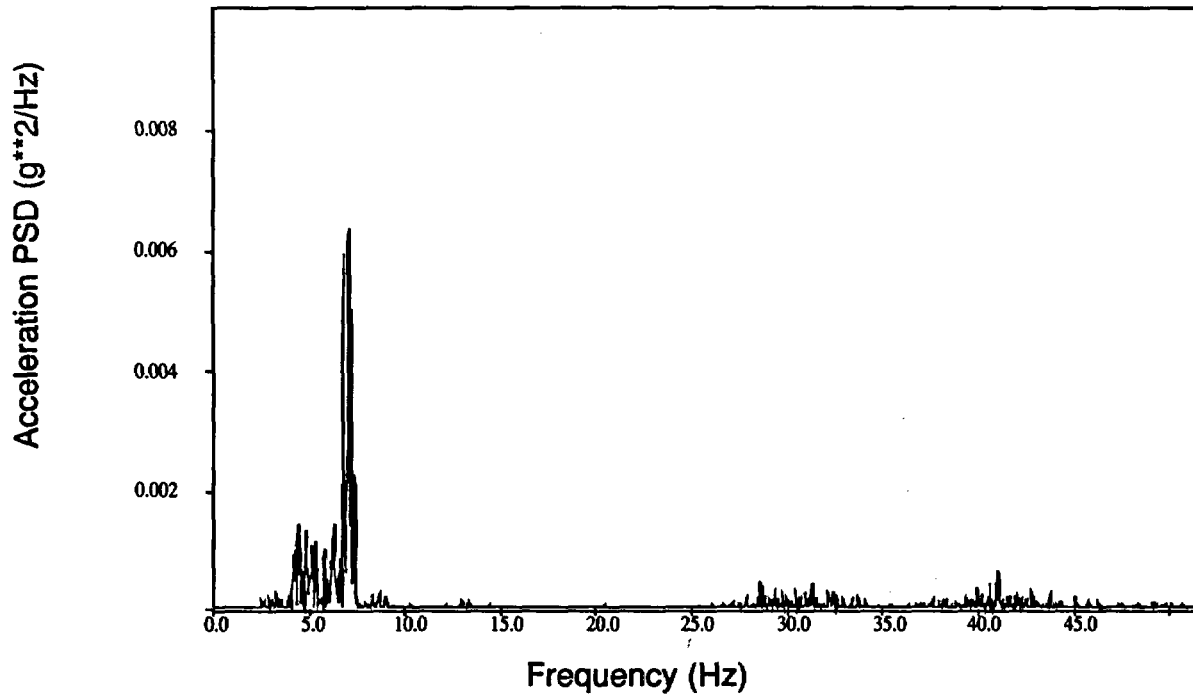


Figure C-28. PSD from gate valve body, X direction, QB9401 (Test T41.81.1).

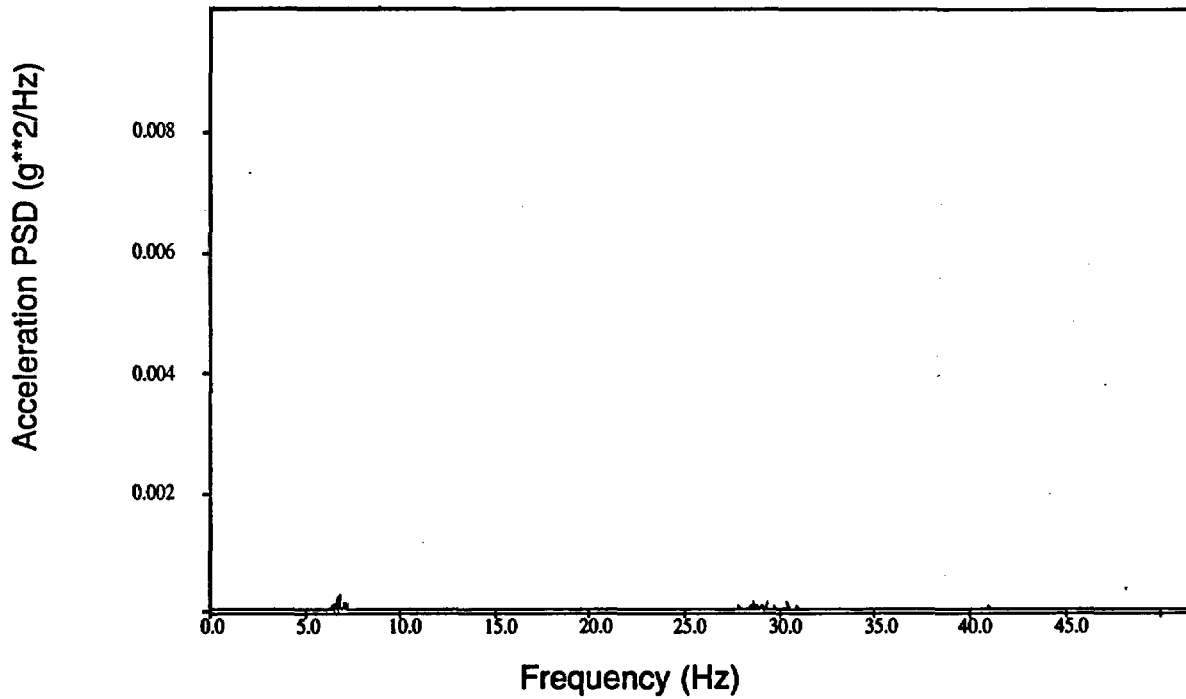


Figure C-29. PSD from gate valve body, Y direction, QB9402 (Test T41.81.1).

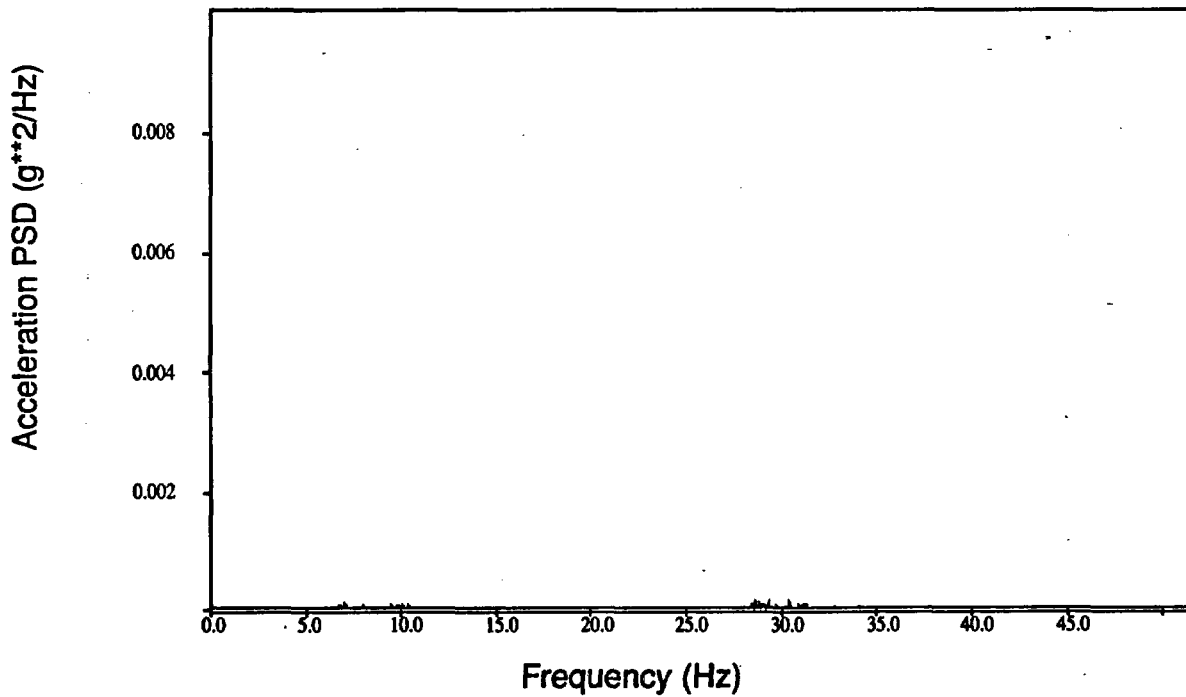


Figure C-30. PSD from gate valve body, Z direction, QB9403 (Test T41.81.1).

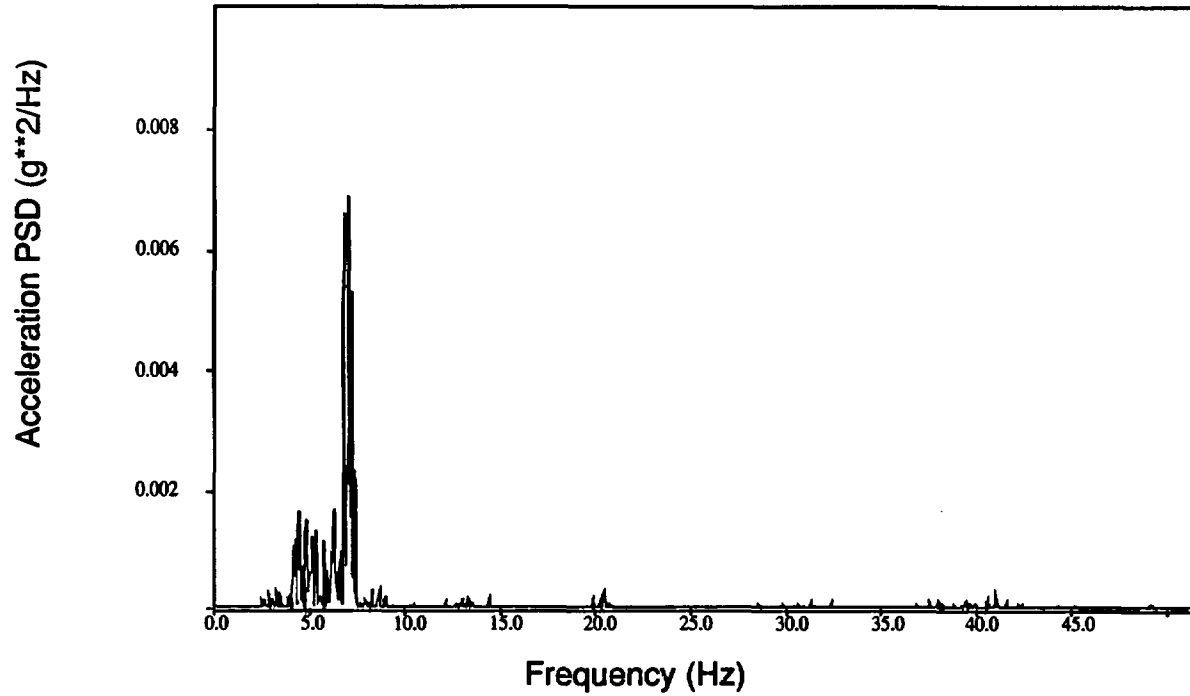


Figure C-31. PSD from gate valve c.g., X direction, QB9411 (Test T41.81.1).

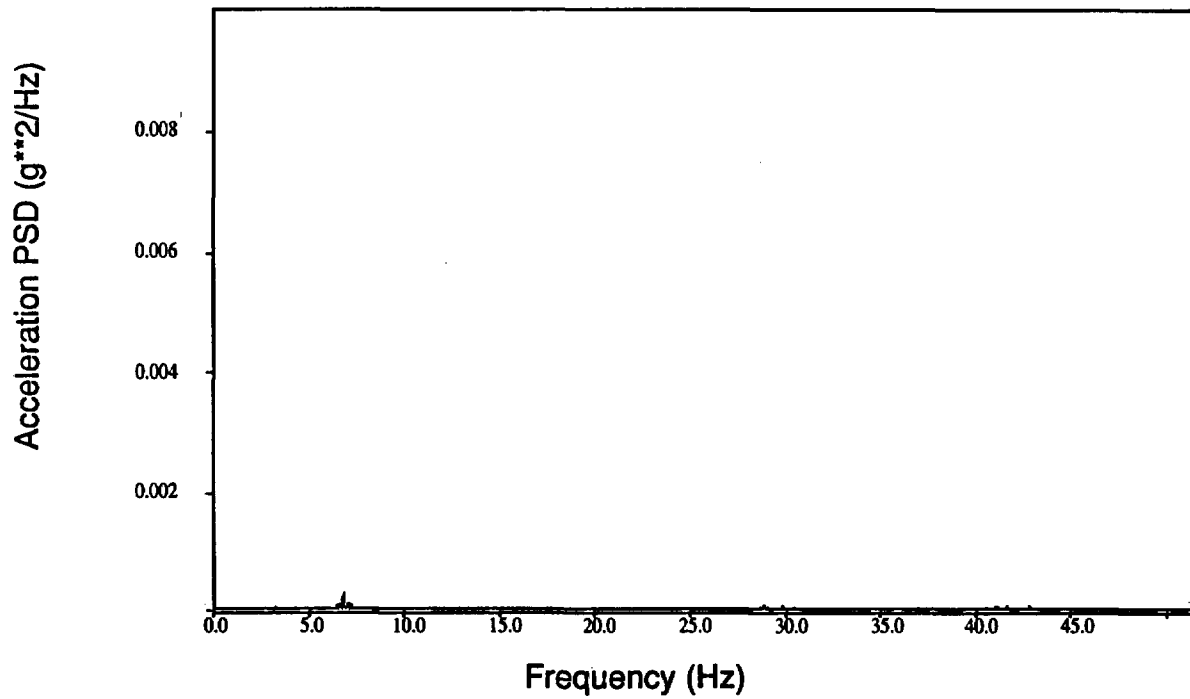


Figure C-32. PSD from gate valve c.g., Y direction, QB9412 (Test T41.81.1).

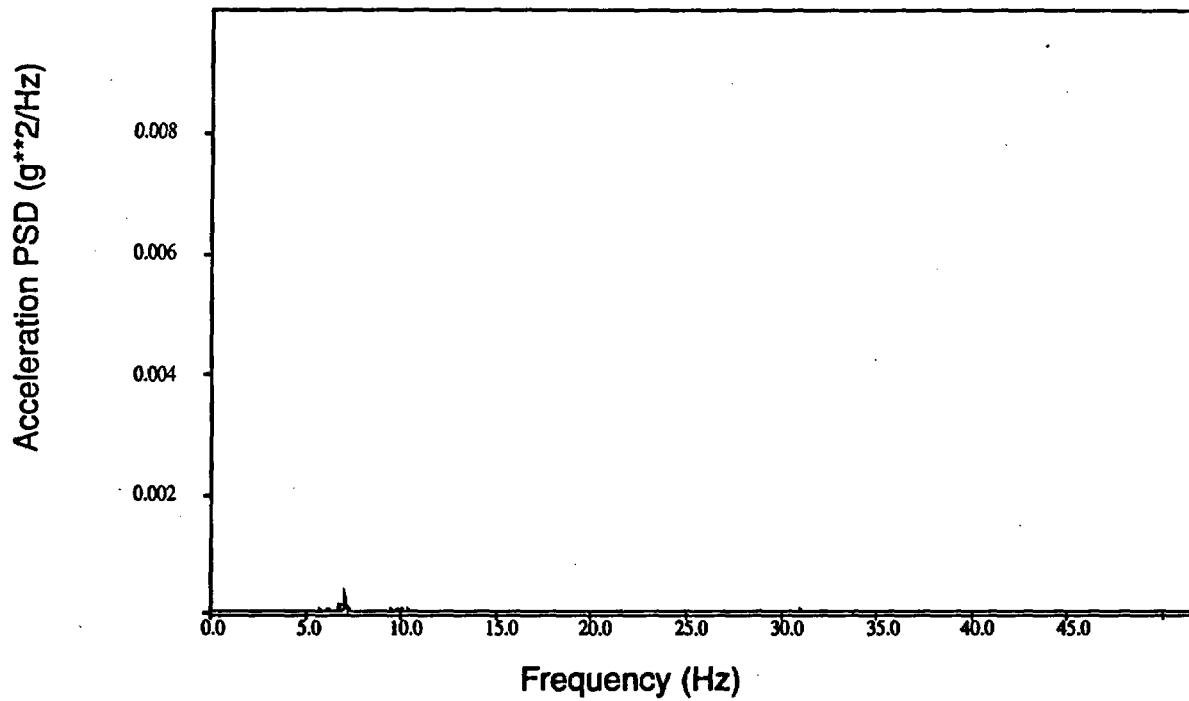


Figure C-33. PSD from gate valve c.g., Z direction, QB9413 (Test T41.81.1).

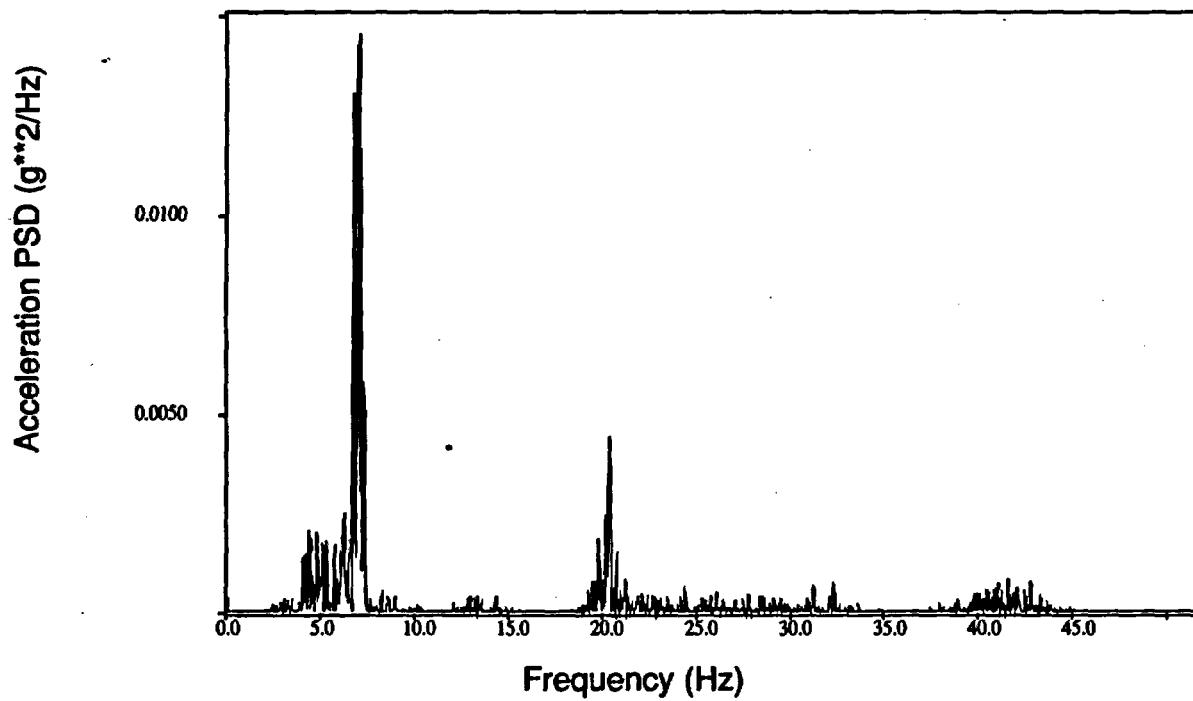


Figure C-34. PSD from gate valve operator, X direction, QB9421 (Test T41.81.1).

Appendix C

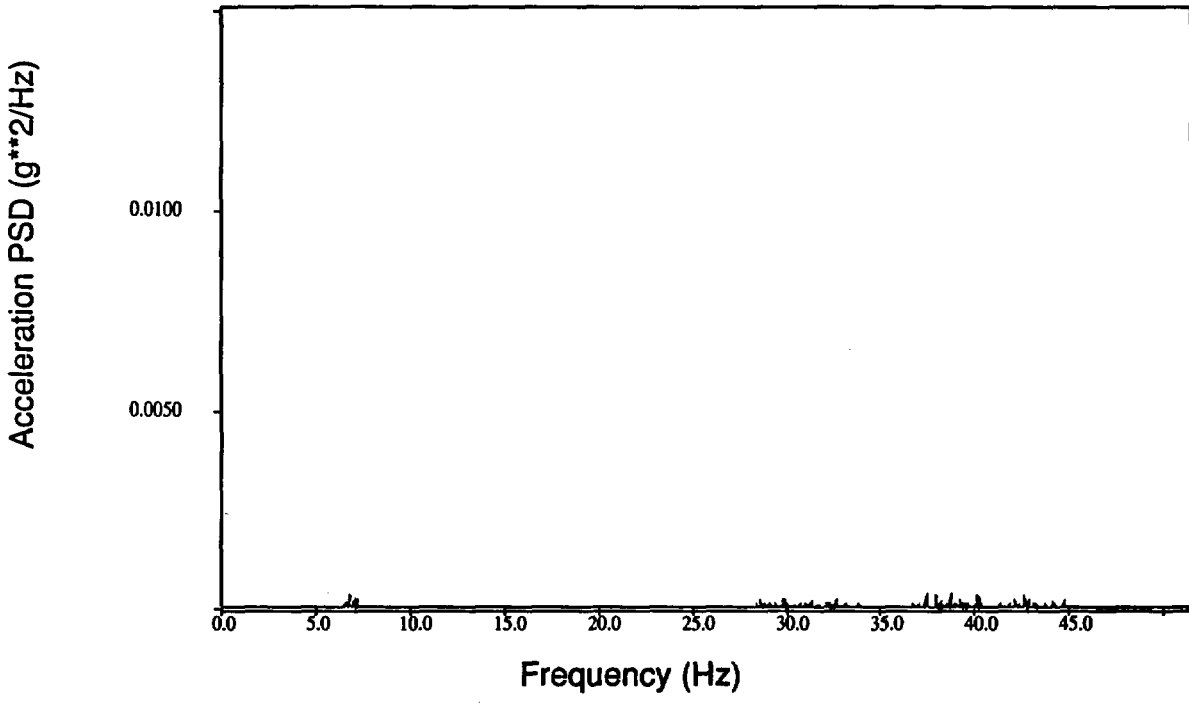


Figure C-35. PSD from gate valve operator, Y direction, QB9422 (Test T41.81.1).

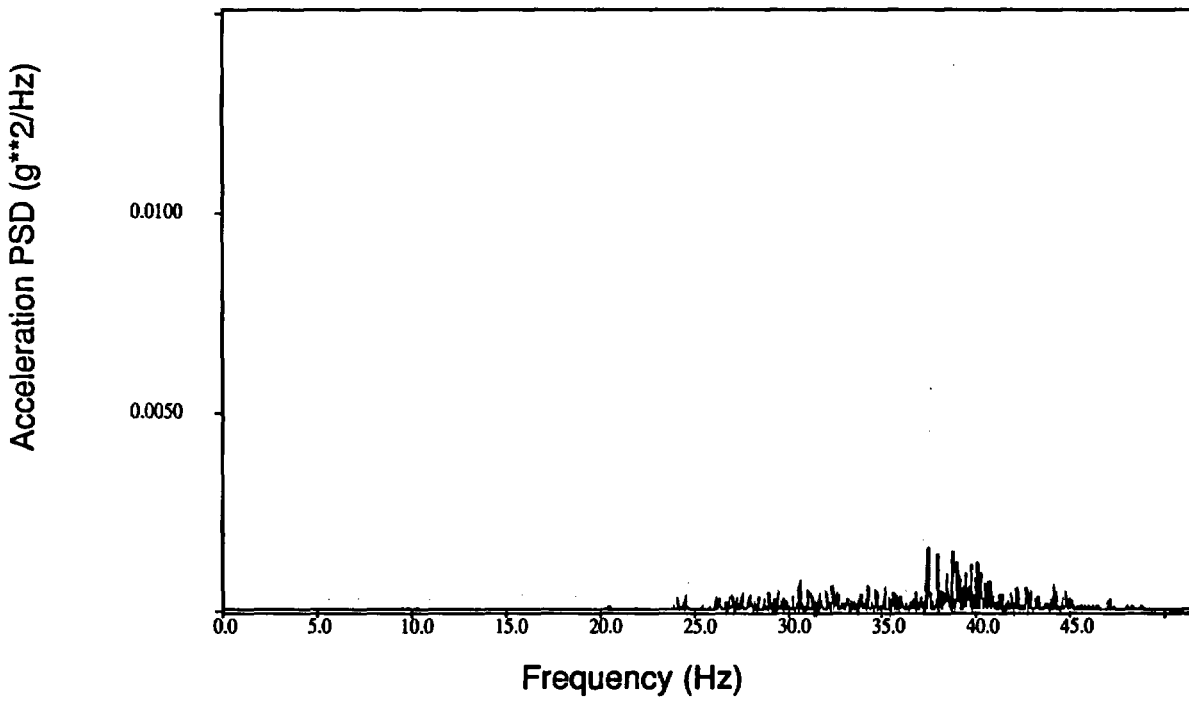


Figure C-36. PSD from gate valve operator, Z direction, QB9423 (Test T41.81.1).

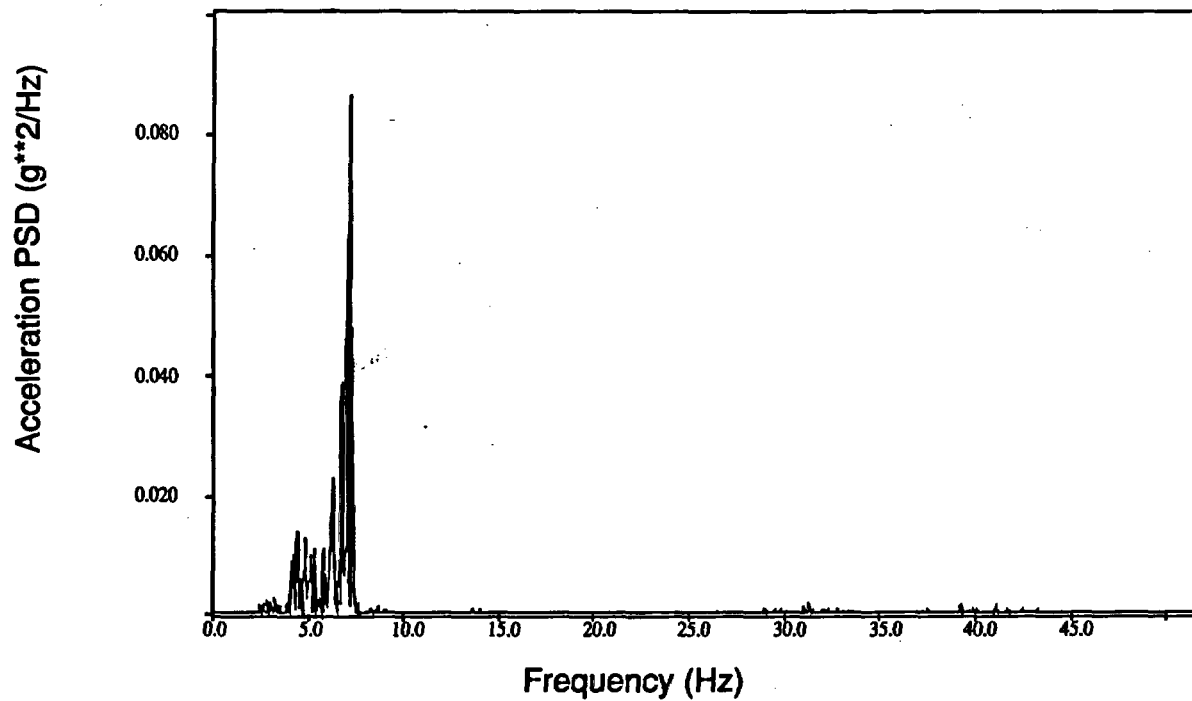


Figure C-37. PSD from gate valve body, X direction, QB9401 (Test T41.81.2).

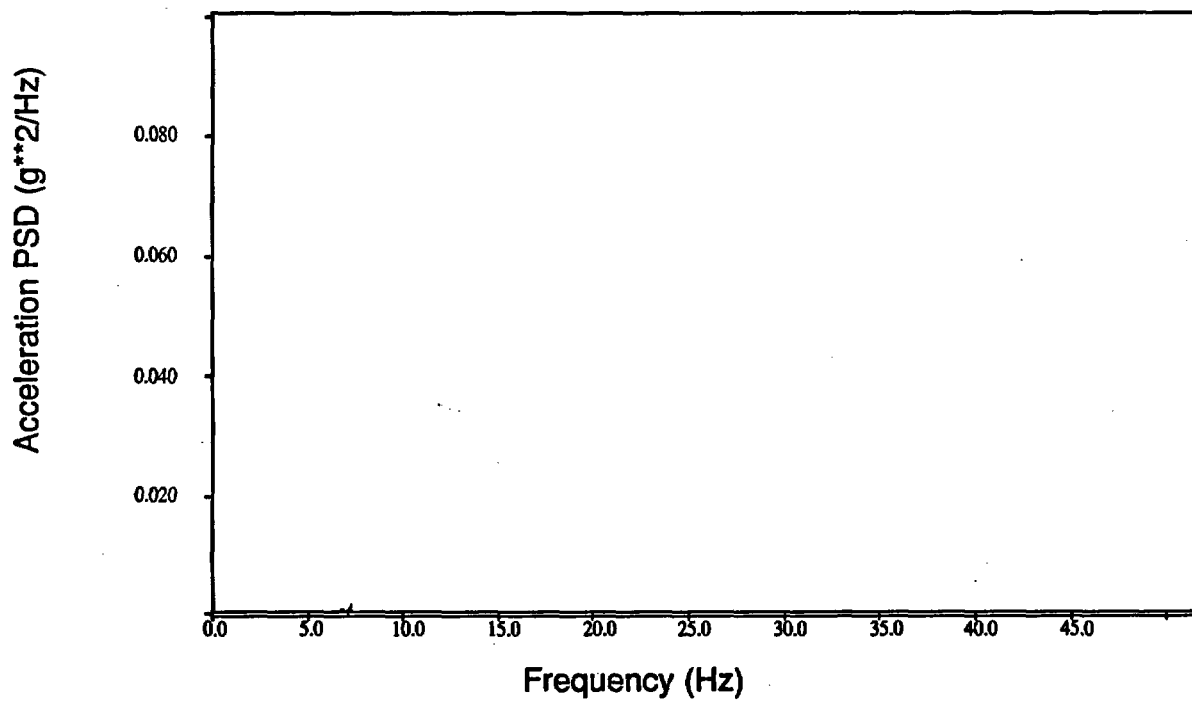


Figure C-38. PSD from gate valve body, Y direction, QB9401 (Test T41.81.2).

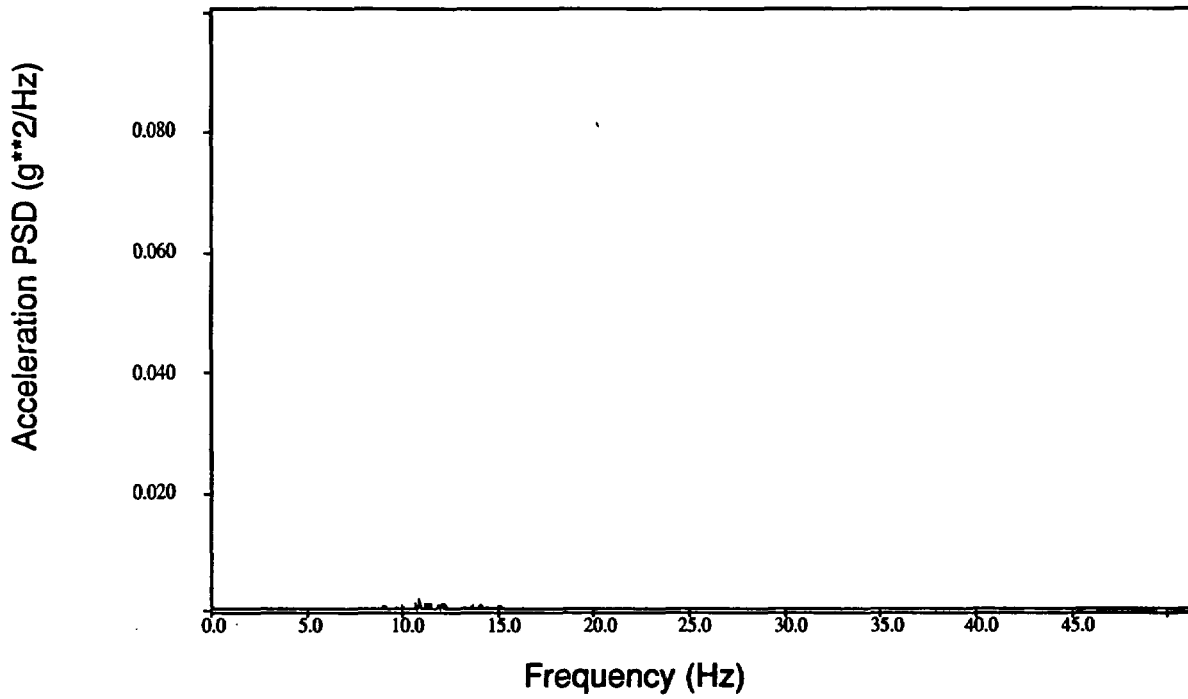


Figure C-39. PSD from gate valve body, Z direction, QB9403 (Test T41.81.2).

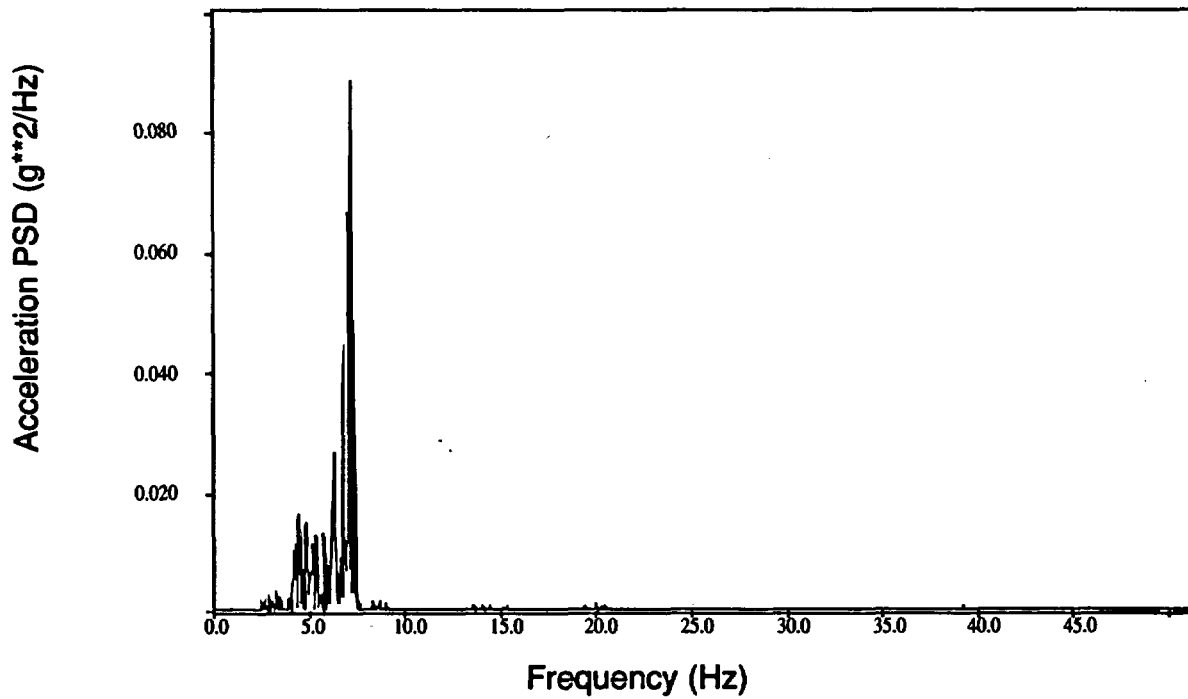


Figure C-40. SD from gate valve c.g., X direction, QB9411 (Test T41.81.2).

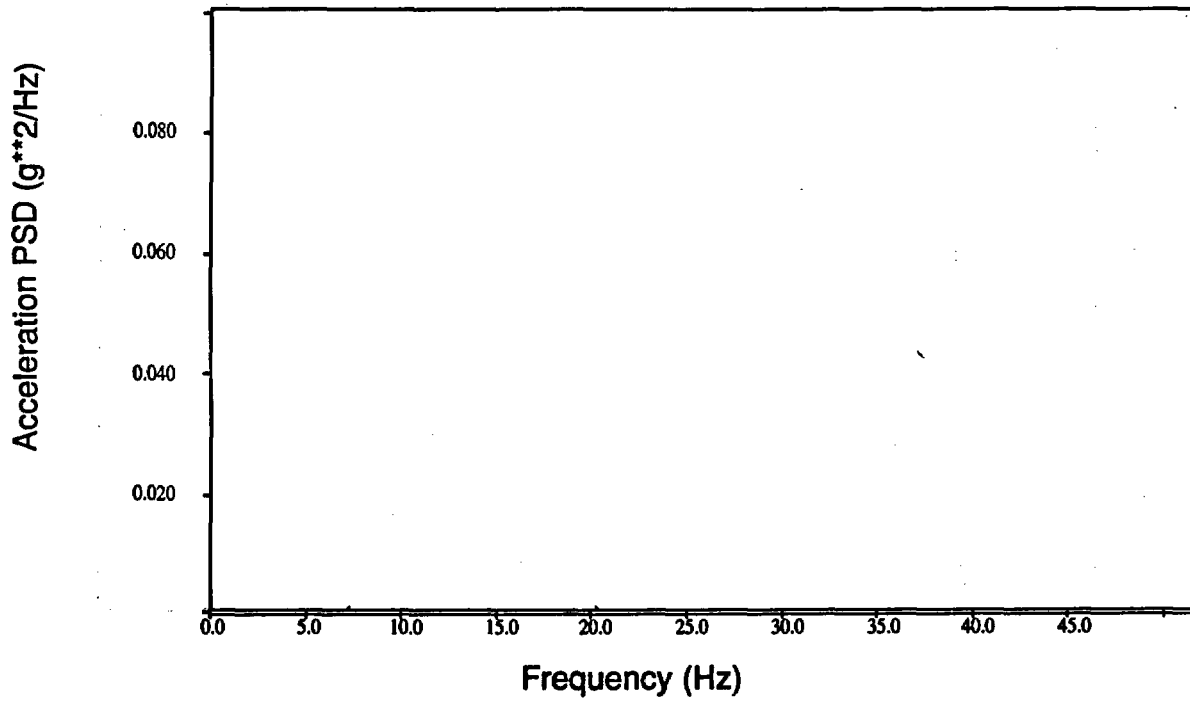


Figure C-41. PSD from gate valve c.g., Y direction, QB9412 (Test T41.81.2).

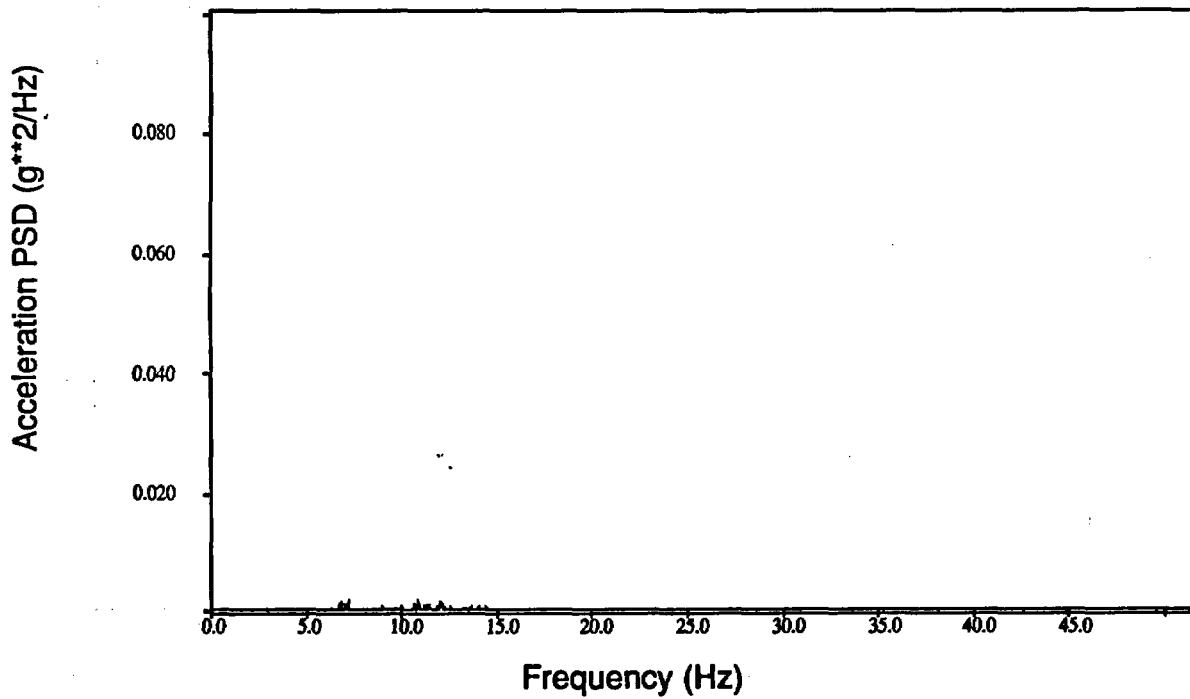


Figure C-42. PSD from gate valve c.g., Z direction, QB9413 (Test T41.81.2).

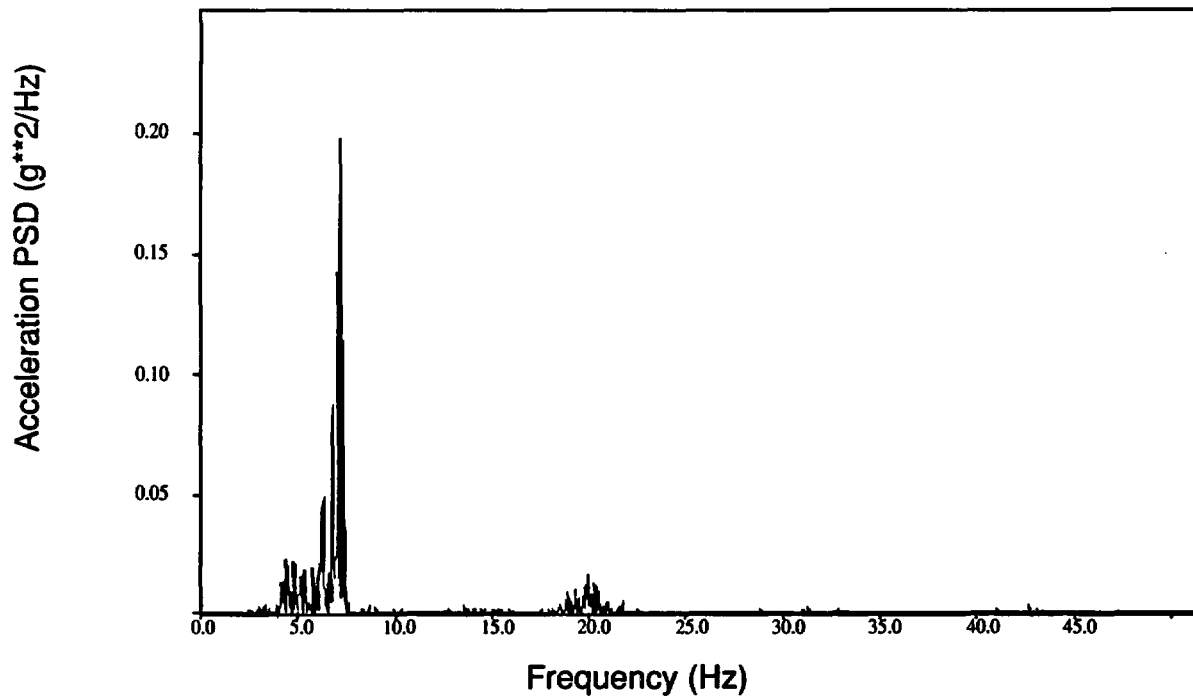


Figure C-43. PSD from gate valve operator, X direction, QB9421 (Test T41.81.2).

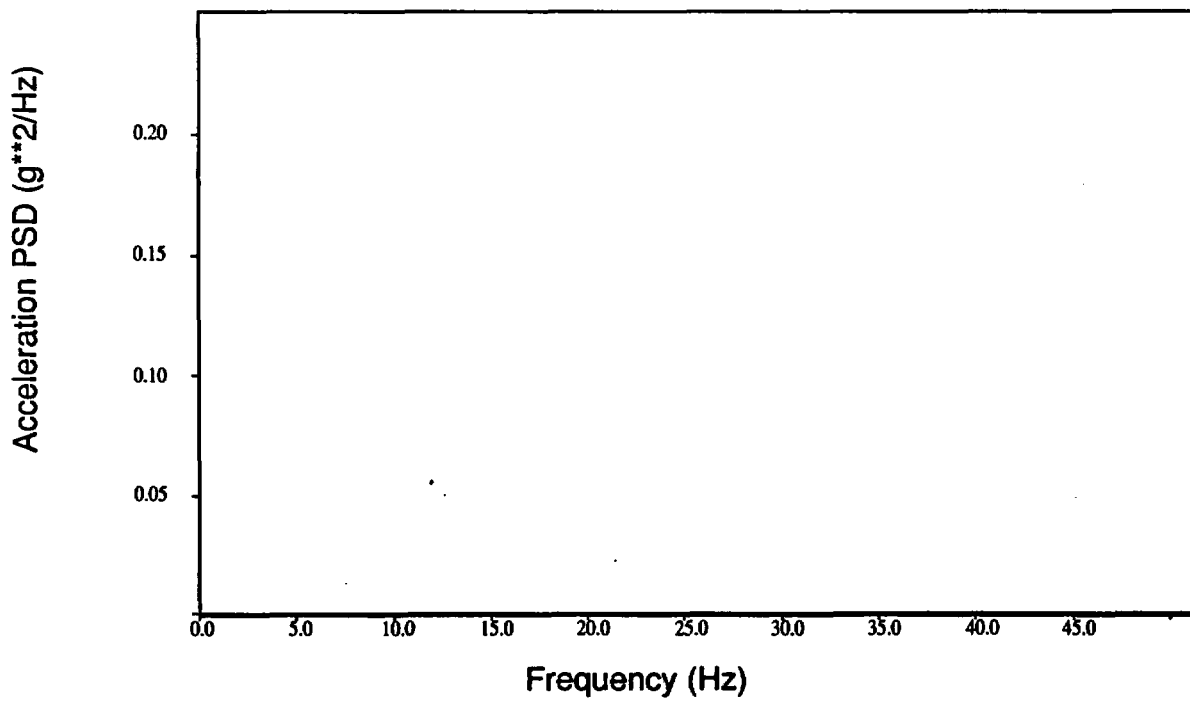


Figure C-44. PSD from gate valve operator, Y direction, QB9422 (Test T41.81.2).

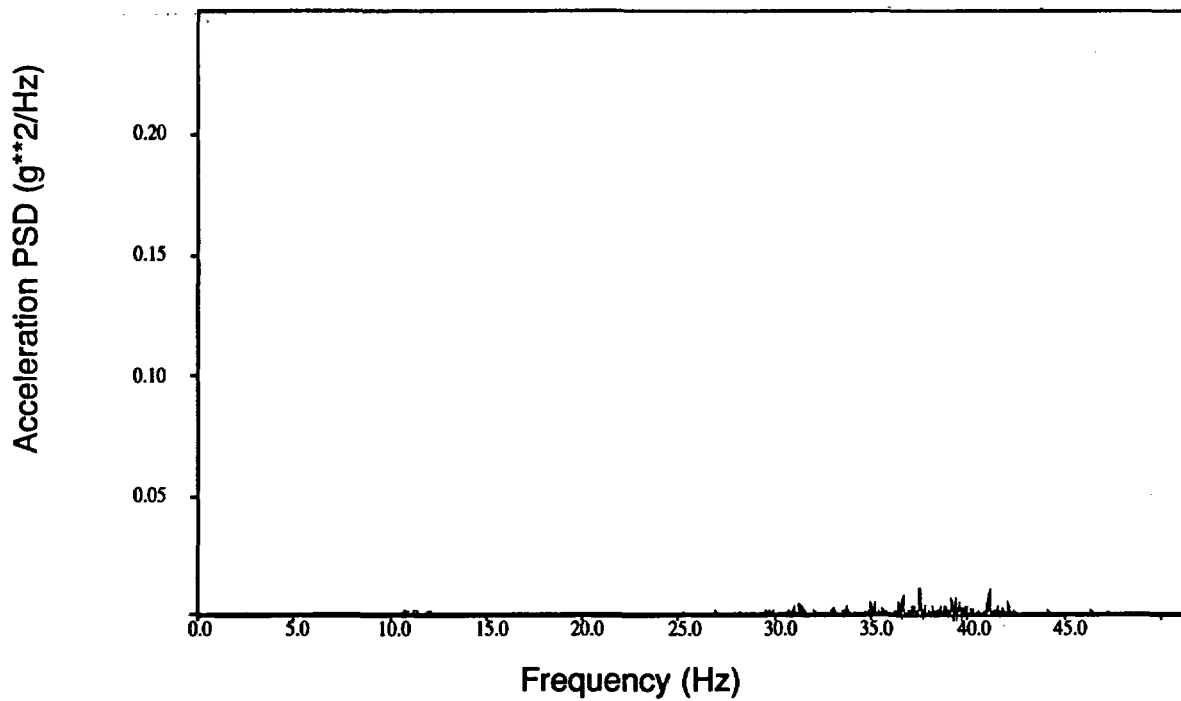


Figure C-45. PSD from gate valve operator, Z direction, QB9423 (Test T41.81.2).

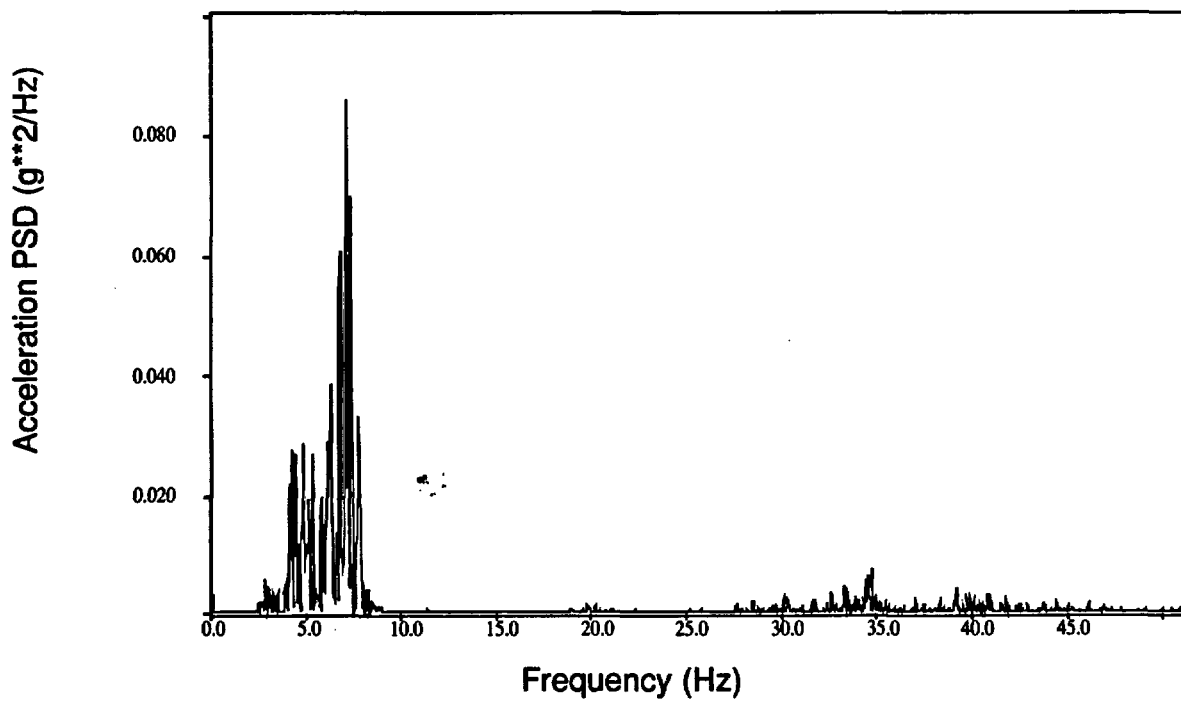


Figure C-46. PSD from gate valve body, X direction, QB9401 (Test T41.81.3).

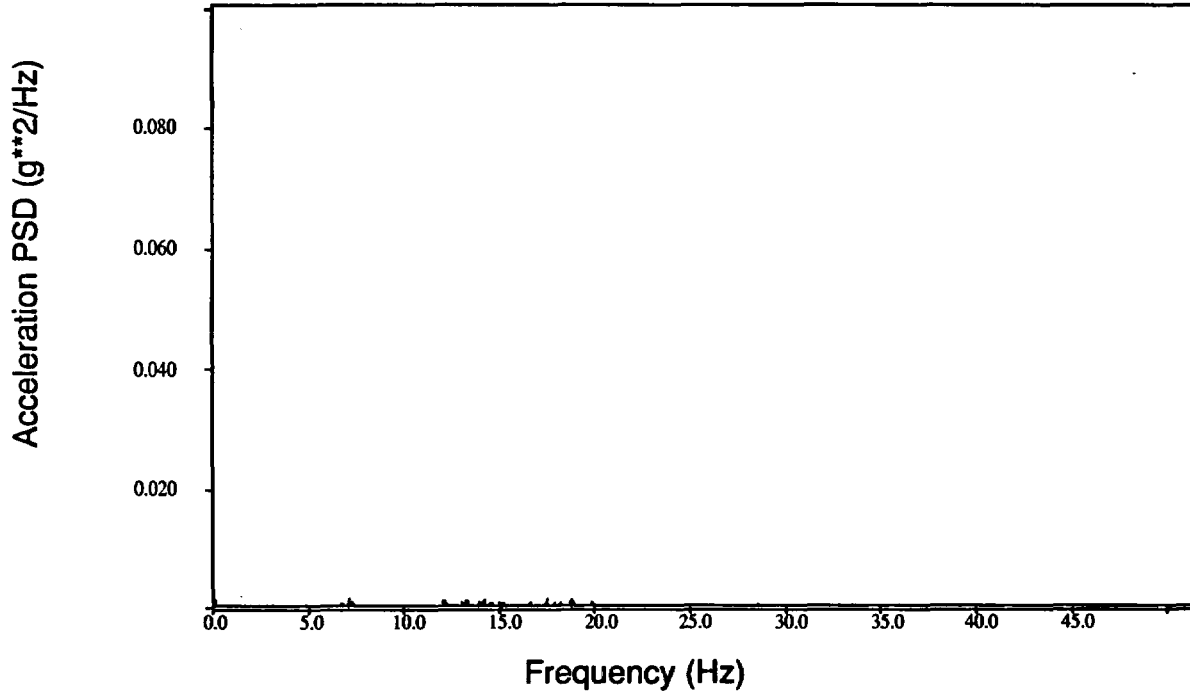


Figure C-47. PSD from gate valve body, Y direction, QB9402 (Test T41.81.3).

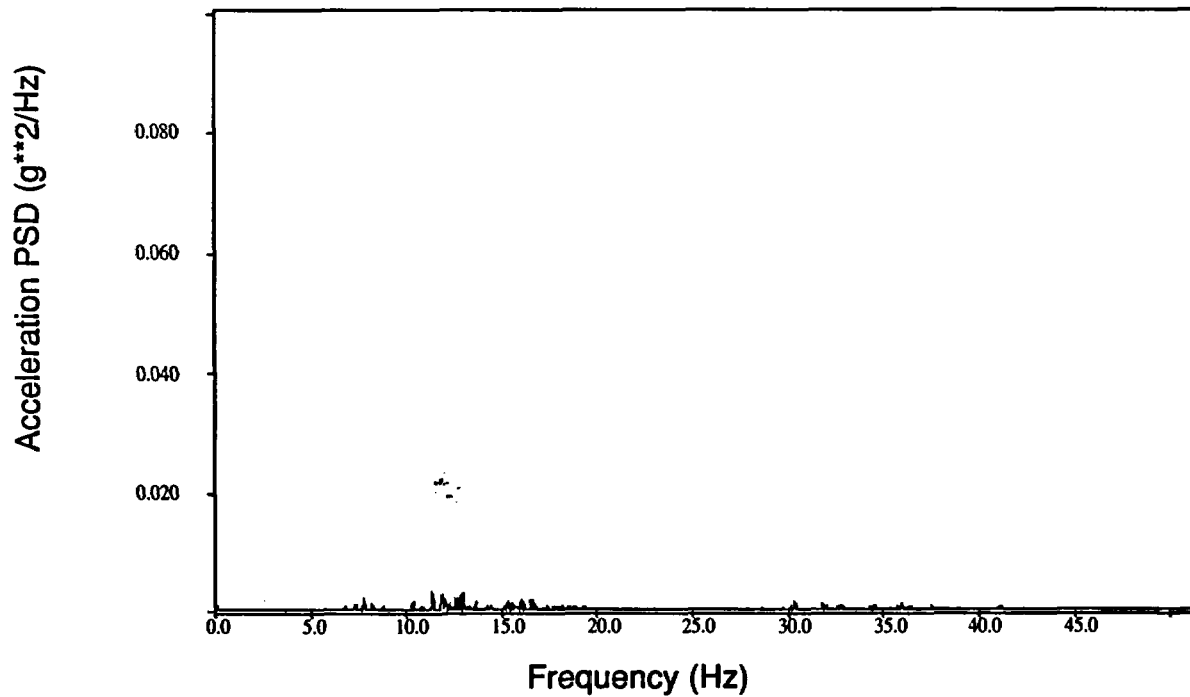


Figure C-48. PSD from gate valve body, Z direction, QB9403 (Test T41.81.3).

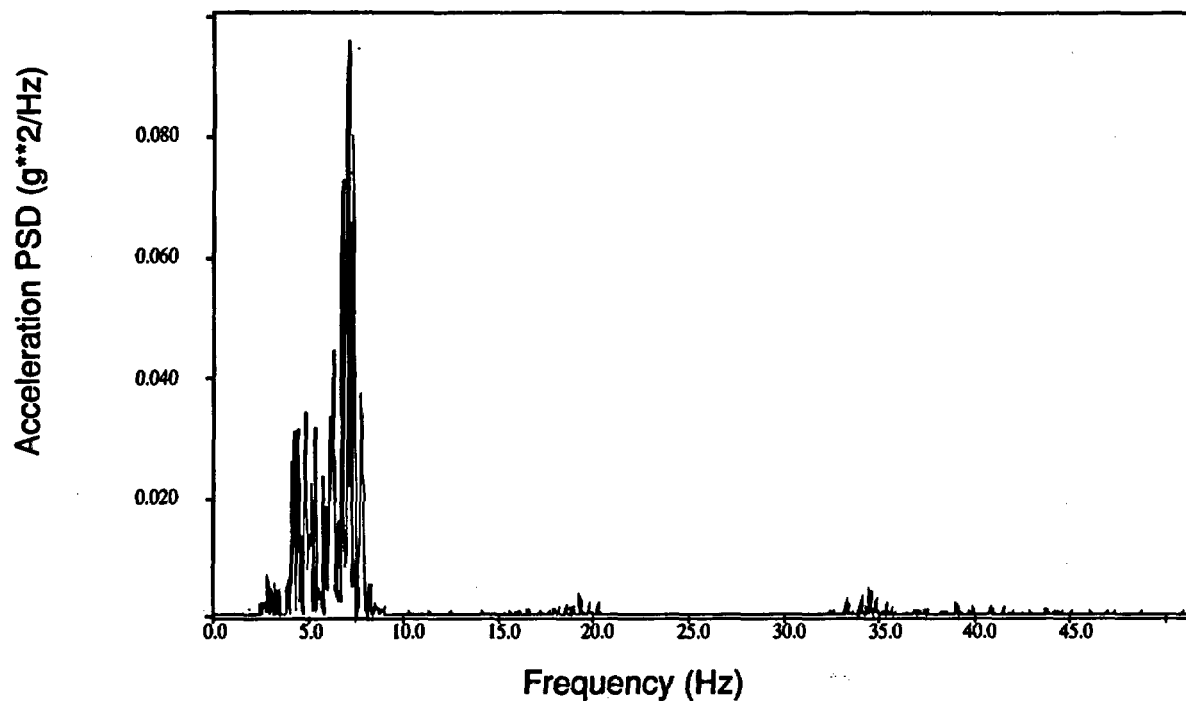


Figure C-49. PSD from gate valve c.g., X direction, QB9411 (Test T41.81.3).

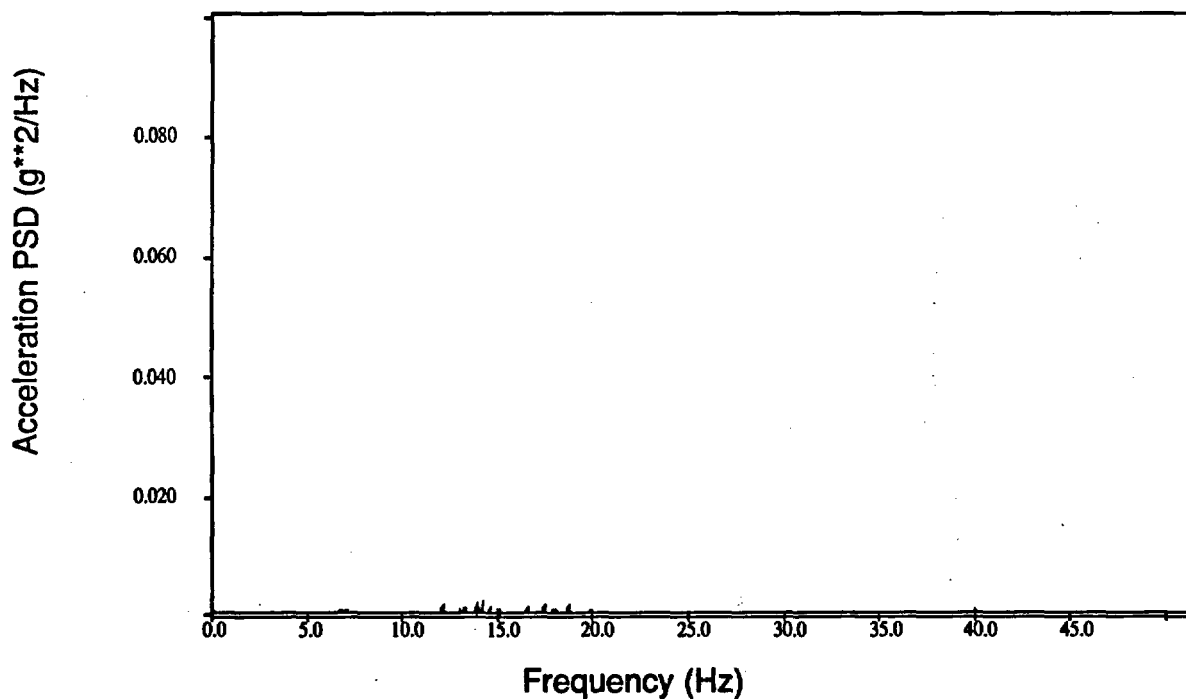


Figure C-50. PSD from gate valve c.g., Y direction, QB9412 (Test T41.81.3).

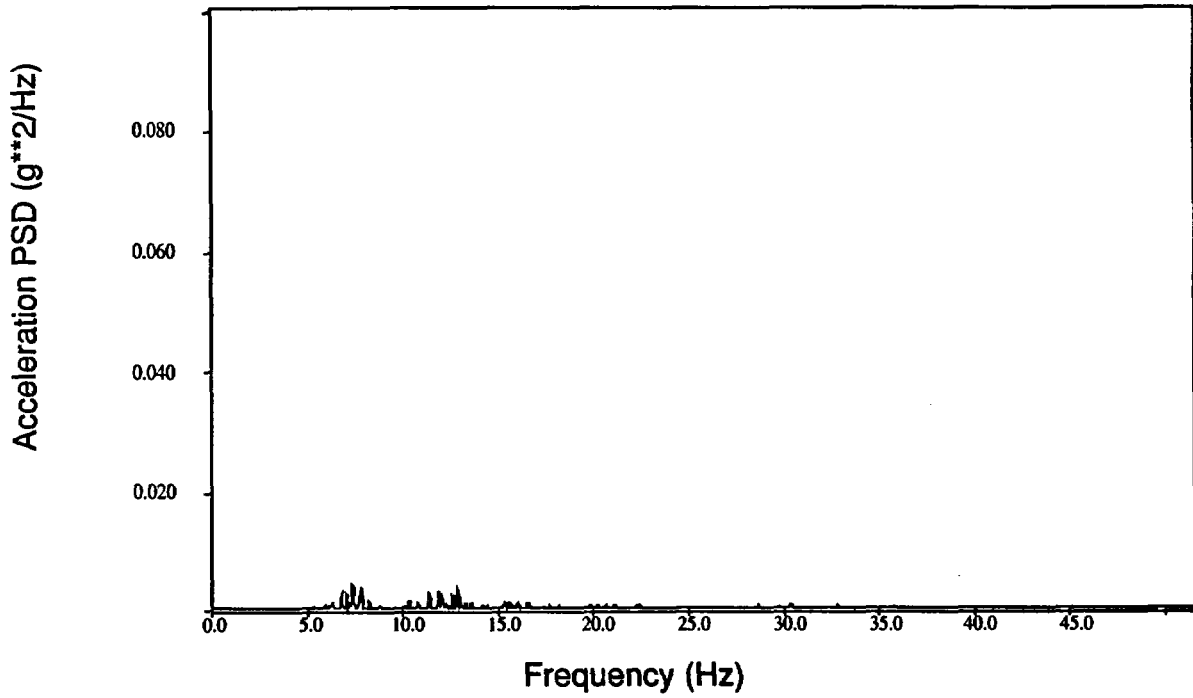


Figure C-51. PSD from gate valve c.g., Z direction, QB9413 (Test T41.81.3).

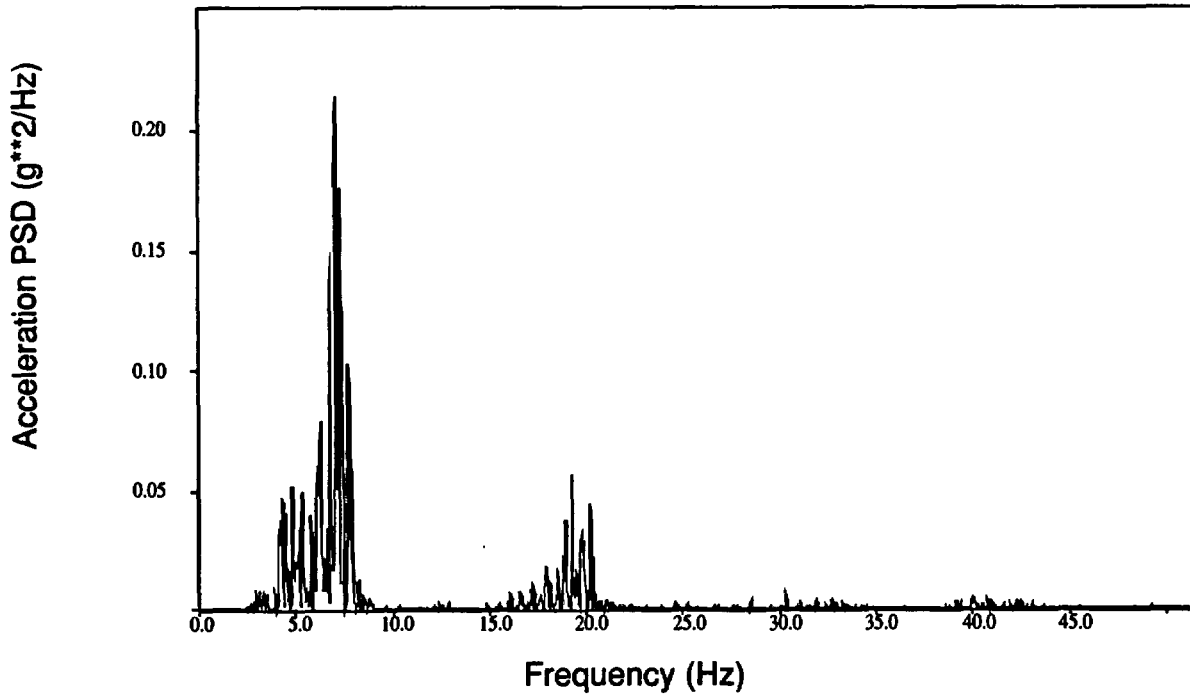


Figure C-52. PSD from gate valve operator, X direction, QB9421 (Test T41.81.3).

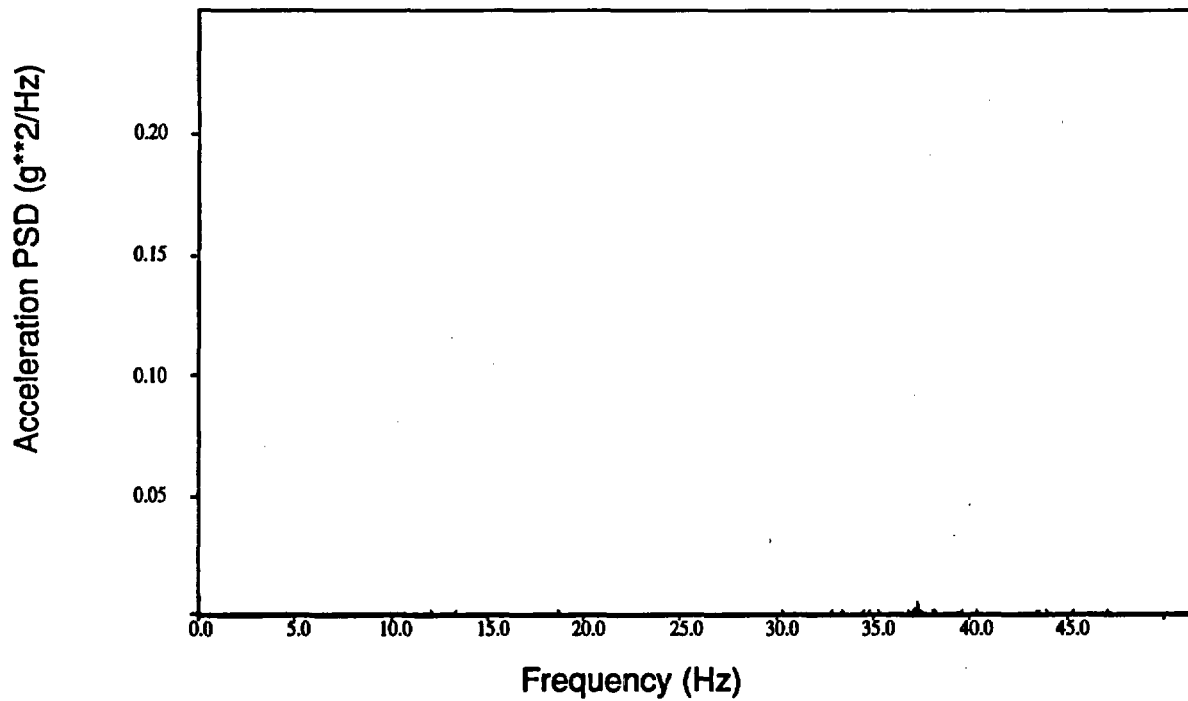


Figure C-53. PSD from gate valve operator, Y direction, QB9422 (Test T41.81.3).

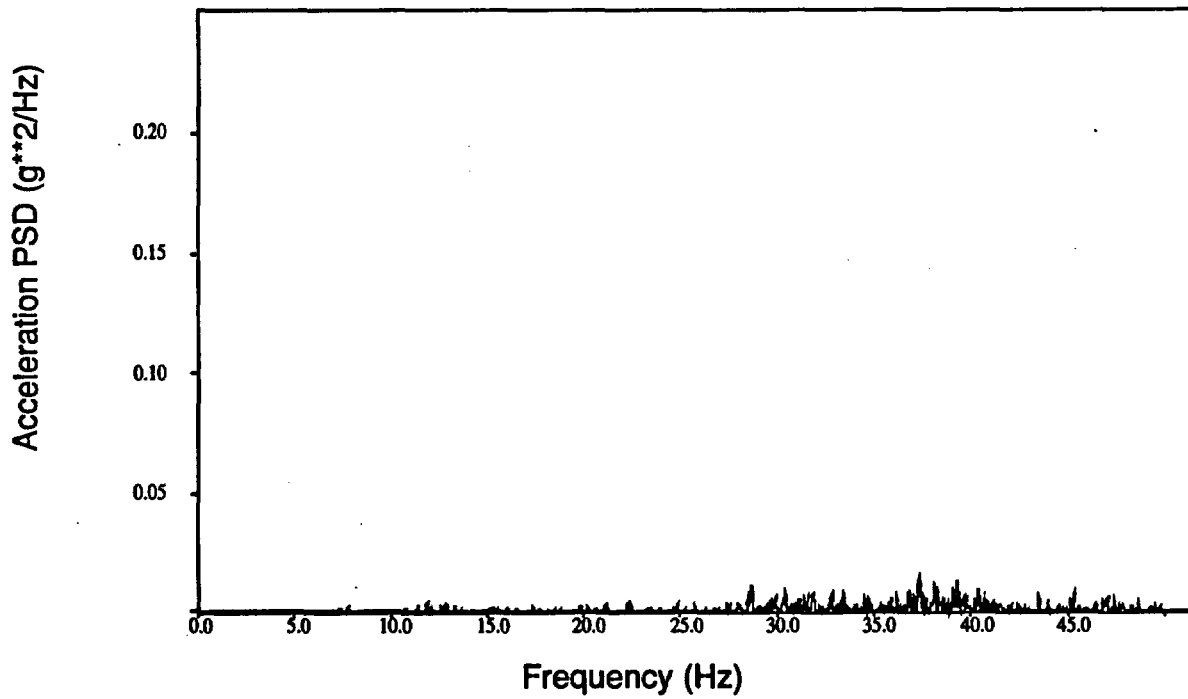


Figure C-54. PSD from gate valve operator, Z direction, QB9423 (Test T41.81.3).

NRC FORM 335 (2-89) NRCM 1102, 3201, 3202	U.S. NUCLEAR REGULATORY COMMISSION BIBLIOGRAPHIC DATA SHEET <i>(See instructions on the reverse)</i>	1. REPORT NUMBER (Assigned by NRC, Add Vol., Supp., Rev., and Addendum Numbers, if any.) NUREG/CR-5646 EGG-2655				
2. TITLE AND SUBTITLE Piping System Response During High-Level Simulated Seismic Tests at the Heissdampfreaktor Facility (SHAM Test Series)		3. DATE REPORT PUBLISHED <table border="1" style="width: 100%;"> <tr> <td style="text-align: center;">MONTH</td> <td style="text-align: center;">YEAR</td> </tr> <tr> <td style="text-align: center;">July</td> <td style="text-align: center;">1992</td> </tr> </table>	MONTH	YEAR	July	1992
MONTH	YEAR					
July	1992					
5. AUTHOR(S) R. Steele, Jr. M. E. Nitzel		4. FIN OR GRANT NUMBER A6857 6. TYPE OF REPORT Technical 7. PERIOD COVERED <i>(inclusive Dates)</i>				
8. PERFORMING ORGANIZATION - NAME AND ADDRESS <i>(If NRC, provide Division, Office or Region, U.S. Nuclear Regulatory Commission, and mailing address; if contractor, provide name and mailing address.)</i> Idaho National Engineering Laboratory EG&G Idaho, Inc. P.O. Box 1625 Idaho Falls, Idaho 83415						
9. SPONSORING ORGANIZATION - NAME AND ADDRESS <i>(If NRC, type "Same as above". If contractor, provide NRC Division, Office or Region, U.S. Nuclear Regulatory Commission, and mailing address.)</i> Division of Engineering Office of Nuclear Regulatory Research U.S. Nuclear Regulatory Commission Washington, D.C. 20555						
10. SUPPLEMENTARY NOTES						
11. ABSTRACT <i>(200 words or less)</i> <p>The SHAM seismic research program studied the effects of increasing levels of seismic excitation on a full-scale, in situ nuclear piping system containing a naturally aged United States (U.S.) 8-in. motor-operated gate valve. The program was conducted by Kernforschungszentrum Karlsruhe at the Heissdampfreaktor near Frankfurt, Germany. Participants included the United States, Germany, and England. Fifty-one experiments were conducted, with the piping supported by six different piping support systems, including a typical stiff U.S. piping support system of snubbers and rigid struts. This report specifically addresses the tests conducted with the U.S. system. The piping system withstood large displacements caused by overload snubber failures and local piping strains. Although some limit switch chatter was observed, the motor operator and valve functioned smoothly throughout the tests. The results indicate that sufficient safety margins exist when commonly accepted design methods are applied and that piping systems will likely maintain their pressure boundary in the presence of severe loading and the loss of multiple supports.</p>						
12. KEY WORDS/DESCRIPTORS <i>(List words or phrases that will assist researchers in locating the report.)</i> Seismic, Heissdampfreaktor Facility Motor-operated gate valve Stiff piping support system		13. AVAILABILITY STATEMENT Unlimited 14. SECURITY CLASSIFICATION <i>(This Page)</i> Unclassified <i>(This Report)</i> Unclassified 15. NUMBER OF PAGES 16. PRICE				

THIS DOCUMENT WAS PRINTED USING RECYCLED PAPER

**UNITED STATES
NUCLEAR REGULATORY COMMISSION
WASHINGTON, D.C. 20555-0001**

**OFFICIAL BUSINESS
PENALTY FOR PRIVATE USE, \$300**

**SPECIAL FOURTH-CLASS RATE
POSTAGE AND FEES PAID
USNRC
PERMIT NO. G-67**